

OPTIMAL RISK-BASED DESIGN OF HYDRAULIC STRUCTURES

by

Yeou-Koung Tung
and
Larry W. Mays

Bureau of Engineering Research
Center for Research in Water Resources

and

Department of Civil Engineering

FINAL REPORT

Sponsored by

National Science Foundation
Research Initiation Grant ENG 78-05449

CRWR - 171

August 1980

FOREWORD

This report is the completion report for National Science Foundation Research Institution Grant NSF-ENG 78-05449 entitled, "Optimal Risk Based Design of Water Resources Engineering Projects." The support of the National Science Foundation for this research is gratefully acknowledged. This report is essentially the same as the doctoral thesis of Yeou-Koung Tung which has the same title as this report. Appreciation is extended to Quentin W. Martin of the Texas Department of Water Resources and to Leo R. Beard, Paul A. Jensen, Randy Machemehl, and Carl Morris of The University of Texas at Austin, all of whom have reviewed this material and given their critical comments. Special thanks are due to Mrs. Carol Sellers of the Center for Research in Water Resources at The University of Texas for her patient, painstaking typing of this report.

Other publications which resulted from work associated with this research project are the following:

1. Mays, L.W., "Optimal Design of Culverts Under Uncertainties," Journal of the Hydraulics Division, ASCE, Vol. 105, No. HY5, pp. 443-460, May 1979.
2. Tung, Y.K. and Mays, L.W., "Risk Analysis for Hydraulic Design," Journal of the Hydraulics Division, ASCE, Vol. 106, No. HY5, pp. 893-913, May 1980.
3. Tung, Y.K. and Mays, L.W., "Generalized Skew Coefficients for Flood Frequency Analysis," Water Resources Bulletin, American Water Resources Association (in press).
4. Tung, Y.K., "Optimal Risk-Based Design of Hydraulic Structures," Ph.D. Thesis, Department of Civil Engineering, The University of Texas at Austin, Austin, Texas, August 1980.

The following papers have been submitted for review on the respective journals:

1. Tung, Y.K. and Mays, L.W., "Reducing Hydrologic Parameter Uncertainty," submitted to the Journal of the Water Resources Planning and Management Division, ASCE.
2. Tung, Y.K. and Mays, L.W., "Risk and Reliability Models for Flood Levee Design," submitted to Water Resources Research, AGU.
3. Tung, Y.K. and Mays, L.W., "Optimal Risk Based Design of Flood Levee Systems, submitted to Water Resources Research, AGU.

The following oral presentations have been given that relate to this work:

1. Optimal Risk-Based Design of Water Resource Projects, paper presented at the International Symposium on Risk and Reliability in Water Resources, University of Waterloo, Waterloo, Ontario, Canada, June 26-28, 1978.
2. Urban Hydraulic Structure Design: Risk and Reliability Analysis, with Y-K. Tung, paper presented at the 1978 Fall Annual Meeting of the American Geophysical Union in San Francisco, California, December 7, 1978.
3. Risk Based Design of Hydraulic Structures, with Y.K. Tung, paper presented at the Texas Section, American Society of Civil Engineers, Texas A & M University, October 5, 1979.
4. Flood Flow Frequency: Where Do We Go From Here, invited speaker for panel discussion at American Water Resources Association Symposium on Flood Plain Problems - Planning and Management, Austin, Texas, December 7, 1979.

The excellent research facilities at The University of Texas, in particular the Department of Civil Engineering, the Center for Research in Water Resources, and the Computation Center also made this research effort possible.

ABSTRACT

OPTIMAL RISK-BASED DESIGN OF
HYDRAULIC STRUCTURES

Yeou-Koung Tung
and
Larry W. Mays

In the design of water resource engineering projects there exist many uncertainties in addition to the conventionally considered hydrologic uncertainty due to the randomness in flood and rainfall frequency. Uncertainties are also contributed from many other sources such as hydraulics, economics, structural, etc. A general framework for evaluating the risk and reliability of water resource engineering projects is developed which takes into account the uncertain features involved in both hydrologic and hydraulic aspects and parameter uncertainties. In most water resource engineering projects the evaluation of risk is limited to the consideration of the inherent hydrologic uncertainty while the hydrologic model and parameter uncertainties and the hydraulic uncertainties are ignored. This report illustrates that ignoring these additional uncertainties can lead to serious underestimates of the associated risks and consequently, underestimate the associated economic losses and safety hazard.

First-order analysis is used to estimate the uncertainty of deterministic hydraulic models which have uncertain parameters. The first-order analysis

of uncertainty enables the estimation of the mean and variance of the capacity of hydraulic structures. An example of developing the risk evaluation procedure by considering the inherent hydrologic uncertainty and hydraulic uncertainties for culvert design is presented. Both static reliability models, which consider single loading application to hydraulic structures, and time-dependent (dynamic) reliability models, which consider the random nature of the loading, are developed.

Furthermore, a new methodology for treating (minimizing) the hydrologic parameter uncertainty is developed that uses generalized parameter (mean, standard deviation, and skewness) values from a weighting between sample and regional hydrologic information. Weights are defined as a function of the variances of the sample parameters and regionalized parameters. The methodology uses either of two non-parametric statistical techniques, the jackknife or the bootstrap, to determine variances of the sample parameters, and regression analysis is used to determine variances of the sample parameters. The hydrologic model uncertainty is treated using a weighting procedure by assigning a weight to various probability models considered. The weight is determined by applying Bayes theorem, to compute the posterior probability of the model for a given prior probability of the model. The generalized parameter estimates described above, and the observations of sample data are both used. By doing so a composite probability model can be developed to define risk and reliability which reduces the uncertainty of adopting the probability model. The application is made considering all the hydrologic and the hydraulic uncertainties to define

the risk-safety factor relationship for levee design considering both the static and the time-dependent cases.

The methods for analyzing the uncertainty of the hydrologic and hydraulic aspects are incorporated in optimization procedures to design the hydraulic structures to minimize total expected costs. Dynamic programming (DP) and discrete differential dynamic programming (DDDP) are used in a model to minimize the total annual expected cost for a levee system, taking into account the tradeoff between installation cost and expected damage cost.

TABLE OF CONTENTS

	<u>Page</u>
FOREWORD	iv
ABSTRACT	v
LIST OF TABLES	xi
LIST OF FIGURES	xv
1. INTRODUCTION	1
1.1 Preliminaries	1
1.2 Existence of Uncertainties	4
1.3 Previous Considerations of Uncertainty	7
1.4 Definition of Risk and Reliability	10
1.5 Safety Factors	11
1.6 Purpose of the Research	15
1.7 The Scope of and Limitation of the Research	17
1.8 Overview of Research Results	19
2. RISK ANALYSIS FOR DESIGN	22
2.1 Introduction	22
2.2 Analysis of Hydraulic Uncertainties	23
2.3 Static Risk and Reliability	27
2.4 Example for Culvert Design (Static Reliability Model)	30
2.5 Dynamic or Time-Dependent Reliability	43
2.6 Example for Culvert Design (Time-Dependent Model)	48
2.7 Need for Expanded Model	49
3. HYDROLOGIC UNCERTAINTIES	
3.1 Introduction	57
3.2 Hydrologic Parameter Uncertainties	58
3.2.1 Hydrologic Parameters for Frequency Analysis	58
3.2.2 Review of Previous Works on Parameter Uncertainty	60
3.2.3 Weighted Parameter Estimates	65
3.2.4 Variance of Sample Estimates	67
3.2.4.1 Jackknife Method	67
3.2.4.2 Bootstrap Method	68
3.2.5 Applications of Jackknife and Bootstrap	69
3.2.6 Variance of Regional Estimators	93
3.2.6.1 Regressional Analysis	93
3.2.6.2 Regression Analysis Study for a Southwest Region	99

3.2.7	Illustration of Procedure for Minimizing Hydrologic Parameter Uncertainty	104
3.3	Hydrologic Model Uncertainty	122
3.3.1	Review of Model Selection Techniques	122
3.3.2	Philosophy of Proposed Method	127
4.	RISK AND RELIABILITY MODELS FOR FLOOD LEVEE DESIGN	131
4.1	Introduction	131
4.2	Analysis of Hydraulic Uncertainties	133
4.3	Analysis of Hydrologic Uncertainties	143
4.4	Development of Static and Time-Dependent Risk-Safety Factor Curves	150
4.5	Discussion	177
5.	OPTIMAL RISK-BASED DESIGN OF LEVEE SYSTEM	180
5.1	Problem Statement	180
5.2	Assumptions and Constraints	182
5.3	Optimization Techniques	187
5.3.1	Linear Programming	187
5.3.2	Dynamic Programming	187
5.3.3	Nonlinear Programming	190
5.3.4	Selection of Optimization Technique	191
5.4	Dynamic Programming Technique	191
5.4.1	Objective Function	192
5.4.2	System Components	197
5.4.2.1	Stages	197
5.4.2.2	Stages	198
5.4.2.3	Decisions	200
5.4.2.4	Transition Function	202
5.4.3	DP Optimization Procedure	204
5.4.4	Limitations of DP Approach	207
5.5	Discrete Differential Dynamic Programming (DDDP) Approach	209
6.	RISK CONSIDERATIONS AND ECONOMIC IMPLICATIONS	218
6.1	Introduction	218
6.2	Example	219
6.3	Effect of Design Philosophy	224
6.4	Effect of Loading Distribution	233
7.	SUMMARY AND CONCLUSION	239
7.1	Summary	239
7.2	Conclusion	242
7.3	Suggestions for Further Study	245
7.4	Final Comments	248

LIST OF REFERENCES	250
APPENDIX	
A. REGRESSION ANALYSIS FOR REGIONAL STREAMFLOW CHARACTERISTICS IN THE CENTRAL AND EAST PART OF TEXAS	256
B. FIRST-ORDER ANALYSIS TO DETERMINE THE MEAN AND COEFFICIENT OF VARIATION OF THE LEVEE CAPACITY BY THE AREA-SLOPE METHOD	297
C. VARIOUS STATIC RELIABILITY MODELS	306
D. USER'S MANUAL FOR COMPUTER PROGRAM "RECVLT"	312
E. LISTING OF COMPUTER PROGRAM FOR GENERATING RISK-SAFETY FACTOR RELATIONSHIPS FOR HIGHWAY CULVERTS - "RECVLT"	319
F. USER'S MANUAL FOR COMPUTER PROGRAM "RELEVEE"	338
G. LISTING OF COMPUTER PROGRAM FOR GENERATING RISK-SAFETY FACTOR RELATIONSHIP FOR FLOOD LEVEES - "RELEVEE"	346
H. USER'S MANUAL FOR COMPUTER PROGRAM "LEVOPT"	362
I. LISTING OF COMPUTER PROGRAM FOR OPTIMAL RISK-BASED FLOOD LEVEE DESIGN - "LEVOPT"	373
VITA	

LIST OF TABLES

		<u>Page</u>
Table 2.1	Result of Regression Analysis in Culvert Design	42
Table 3.1a	Annual Maximum Series for Mill Creek near Los Molinos, California	71
Table 3.1b	Annual Maximum Series for Greenbrier River at Alderson, West Virginia	72
Table 3.2	Standard Errors of the Sample Statistics for Mill Creek	73
Table 3.3	Standard Error of the Sample Statistics for the Greenbrier River	73
Table 3.4	Skew Weights for the Methods	76
Table 3.5	Root-Mean Square Error of Frequency Factor, N=10	81
Table 3.6	Root-Mean Square Error of Frequency Factor, N=30	82
Table 3.7	Root-Mean Square Error of Frequency Factor, N=50	83
Table 3.8	Root-Mean Square Error of Frequency Factor, N=70	84
Table 3.9	Comparison of Root-Mean Square Error of Frequency Factor K_T for Bootstrap Method With and Without Normality Assumption on the Bootstrap Samples	92
Table 3.10	Statistics of Regression Equations for Regional Parameter Estimates	103
Table 3.11	Basin Characteristics for Streamflow Gaging Stations Tested	106
Table 3.12	ERR_1 and ERR_2 for Station 8022500	111
Table 3.13	ERR_1 and ERR_2 for Station 8030500	111
Table 3.14	ERR_1 and ERR_2 for Station 8033500	111
Table 3.15	ERR_1 and ERR_2 for Station 805700	112
Table 3.16	ERR_1 and ERR_2 for Station 8096500	112
Table 3.17	Percentage of Cases in Flood Flow Frequency Analysis for One Method is Better Than the Other Based on the Error Criteria ERR_1	114

LIST OF TABLES

		<u>Page</u>
Table 3.18	Percentage of Cases in Flood Flow Frequency Analysis for One Method is Better Than the Other Based on the Error Criteria ERR_2	114
Table 3.19	Variance of Sample and Regional Parameter Estimates and Weight for Station 8022500	116
Table 3.20	Variance of Sample and Regional Parameter Estimates and Weight for Station 8030500	117
Table 3.21	Variance of Sample and Regional Parameter Estimates and Weight for Station 8033500	118
Table 3.22	Variance of Sample and Regional Parameter Estimates and Weight for Station 8057000	119
Table 3.23	Variance of Sample and Regional Parameter Estimates and Weight for Station 8096500	120
Table 4.1	Annual Maximum Series for Guadalupe River near Victoria, Texas	134
Table 4.2	Means, Tolerances, and Distribution of Hydraulic Variables in the Levee Design	144
Table 4.3	Sample Hydraulic Data for a Levee Height and Encroachment Width	145
Table 4.4	Physiographic and Meteorologic Characteristics for Guadalupe River near Victoria, Texas	146
Table 4.5	Parameter Estimates, Variances and Weights for Victoria Data	148
Table 4.6	Posterior Probability of the Loading Distribution Models	149
Table 4.7	Comparison of Overall Risk and Inherent Hydrologic Risk	178
Table 6.1	Uncertain Characteristics of Hydraulic Variables, Length, and Unit Land Cost of Each Channel Reach in Levee Design	221

LIST OF TABLES

		<u>Page</u>
Table 6.2	Hypothetical Relationship Between the Volume of Water, the Flood Stage, and the Flood Damage Cost	222
Table 6.3	Computer Time (in Seconds) Required to Execute the 3-Stage DP Problem with Different Sizes of State Space and Various Risk Considerations Using Log-Pearson III Loading Distribution	225
Table 6.4	The Minimum Total Annual Cost and Its Component Costs for Various Risk Considerations Using Log-Pearson III Loading Distribution	228
Table 6.5	Optimal Levee Layout and Design for Various Risk Considerations Using Log-Pearson Type III Loading Distribution	229
Table 6.6	Safety Factor Associated with the Optimal Levee Design in Each Reach for Various Risk Considerations Using Log-Pearson Type III Loading Distribution	231
Table 6.7	The Annual Expected Damage Costs Associated with the Given Optimal Design for the Other Risk Options Considered When the Log-Pearson III Loading Distribution is Used	231
Table 6.8	The Minimum Annual Total Expected Cost and Its Component Costs Using Various Loading Distributions and Different Risk Considerations	234
Table 6.9	Optimal Levee Layout and Design for Various Risk Considerations and Different Loading Distributions Obtained by DDDP Approach	235
Table A.1	List of Streamflow Gaging Stations in Southwestern United States Used for Regression Study	257
Table A.2	Basin Characteristics for Each Streamflow Gaging Station in Southwestern United States Used for Regression Study	260
Table A.3	Streamflow Characteristics for Each Gaging Station in Southwestern United States Used for Regression Study	264

LIST OF TABLES

		<u>Page</u>
Table A.4	Regression Results for Mean of Streamflows, \bar{Z}_r	267
Table A.5	Regression Results for Standard Deviation of Streamflows, S_{Z_r}	282
Table A.6	Regression Results for Skewness of Streamflow, G_{Z_r}	286
Table A.7	Regression Results for Mean of Log-transformed Streamflow, \bar{Y}_r	289
Table A.8	Regression Results for Standard Deviation of Log-transformed Streamflow, S_{Y_r}	292
Table A.9	Regression Results for Skewness of Log-transformed Streamflow G_{Y_r}	294

LIST OF FIGURES

		<u>Page</u>
Figure 1.1	Load-Resistance Interference (Kapur and Lamberson, 1977)	12
Figure 2.1	Triangular Distribution	33
Figure 2.2	Sensitivity of Risk-Safety Factor Relationship with Respect to Different Values of S_n	38
Figure 2.3	Risk-Safety Factor Curves for Culvert Design (Static Reliability Model)	39
Figure 2.4	Risk vs. Return Period with Different Safety Factor for Culvert Design (Static Reliability Model)	40
Figure 2.5	Risk-Safety Factor Curves for Culvert Design Based on Return Period 10 Years (Time-Dependent Reliability Model)	50
Figure 2.6	Risk-Safety Factor Curves for Culvert Design Based on Return Period 15 Years (Time-Dependent Reliability Model)	51
Figure 2.7	Risk-Safety Factor Curves for Culvert Design Based on Return Period 20 Years (Time-Dependent Reliability Model)	52
Figure 2.8	Risk-Safety Factor Curves for Culvert Design Based on Return Period 25 Years (Time-Dependent Reliability Model)	53
Figure 2.9	Risk-Safety Factor Curves for Culvert Design Based on Return Period 30 Years (Time-Dependent Reliability Model)	54
Figure 2.10	Risk-Safety Factor Curves for Culvert Design Based on Return Period 50 Years (Time-Dependent Reliability Model)	55
Figure 3.1	Generalized Skew Coefficient Map (W.R.C. 1976)	62
Figure 3.2	Comparison of Root-Mean Square Errors of K_T Using the W.R.C. Method for Different Sample Size	85

LIST OF FIGURES

		<u>Page</u>
Figure 3.3	Comparison of Root-Mean Square Errors of K_T Using the Jackknife Method for Different Sample Size	86
Figure 3.4	Root-Mean Square Errors of K_T Using Different Methods for Sample Size $N=10$	87
Figure 3.5	Foot-Mean Square Errors of K_T Using Different Methods for Sample Size $N=30$	88
Figure 3.6	Root-Mean Square Errors of K_T Using Different Methods for Sample Size $N=50$	89
Figure 3.7	Root-Mean Square Errors of K_T Using Different Methods for Sample Size $N=70$	90
Figure 3.8	Mallows' C_p Statistic vs. Number of Independent Variables in Regression Model	98
Figure 3.9	Location of Streamflow Gaging Stations Selected in Texas for Regression Study	101
Figure 4.1	Cross-sectional Configuration of Rivers	136
Figure 4.2	Idealization of River Cross-section	137
Figure 4.3	Statistics of Five Simple Distributions	142
Figure 4.4	Static Risk-Safety Factor Curves for Levee Design Using Normal Loading Distribution	152
Figure 4.5	Static Risk-Safety Curves for Levee Design Using Lognormal Loading Distribution	153
Figure 4.6	Static-Risk-Safety Factor Curves for Levee Design Using Gumbel Loading Distribution	154
Figure 4.7	Static Risk-Safety Factor Curves for Levee Design Using Pearson III Loading Distribution	155
Figure 4.8	Static Risk-Safety Factor Curves for Levee Design Using Log-Pearson III Loading Distribution	156

LIST OF FIGURES

		<u>Page</u>
Figure 4.9	Time-Dependent Risk-Safety Factor Curves for Levee Design Using Normal Loading Distribution Based on $T_r = 100$ Years	157
Figure 4.10	Time-Dependent Risk-Safety Factor Curves for Levee Design Using Lognormal Loading Distribution Based on $T_r = 100$ Years	158
Figure 4.11	Time-Dependent Risk-Safety Factor Curves for Levee Design Using Gumbel Loading Distribution Based on $T_r = 100$ Years	159
Figure 4.12	Time-Dependent Risk-Safety Factor Curves for Levee Design Using Pearson III Loading Distribution Based on $T_r = 100$ Years	160
Figure 4.13	Time-Dependent Risk-Safety Factor Curves for Levee Design Using Log-Pearson III Loading Distribution Based on $T_r = 100$ Years	161
Figure 4.14	Time-Dependent Risk-Safety Factor Curves for Levee Design Using Normal Loading Distribution Based on $T_r = 200$ Years	162
Figure 4.15	Time-Dependent Risk-Safety Factor Curves for Levee Design Using Lognormal Loading Distribution Based on $T_r = 200$ Years	163
Figure 4.16	Time-Dependent Risk-Safety Factor Curves for Levee Design Using Gumbel Loading Distribution Based on $T_r = 200$ Years	164
Figure 4.17	Time-Dependent Risk-Safety Factor Curves for Levee Design Using Pearson III Loading Distribution Based on $T_r = 200$ Years	165
Figure 4.18	Time-Dependent Risk-Safety Factor Curves for Levee Design Using Log-Pearson III Loading Distribution Based on $T_r = 200$ Years	166
Figure 4.19	Time-Dependent Risk-Safety Factor Curves for Levee Design Using Normal Loading Distribution Based on $T_r = 500$ Years	167

LIST OF FIGURES

		<u>Page</u>
Figure 4.20	Time-Dependent Risk-Safety Factor Curves for Levee Design Using Lognormal Loading Distribution Based on $T_r=500$ Years	168
Figure 4.21	Time-Dependent Risk-Safety Factor Curves for Levee Design Using Gumbel Loading Distribution Based on $T_r=500$ Years	169
Figure 4.22	Time-Dependent Risk-Safety Factor Curves for Levee Design Using Pearson III Loading Distribution Based on $T_r=500$ Years	170
Figure 4.23	Time-Dependent Risk-Safety Factor Curves for Levee Design Using Log-Pearson III Loading Distribution Based on $T_r=500$ Years	171
Figure 4.24	Static Risk-Safety Factor Curves for Levee Design Using a Composite Probability Model for Loading	173
Figure 4.25	Time-Dependent Risk-Safety Factor Curves for Levee Design Using a Composite Probability Model for Loading Based on $T_r=100$ Years	174
Figure 4.26	Time-Dependent Risk-Safety Factor Curves for Levee Design Using a Composite Probability Model for Loading Based on $T_r=200$ Years	175
Figure 4.27	Time-Dependent Risk-Safety Factor Curves for Levee Design Using a Composite Probability Model for Loading Based on $T_r=500$ Years	176
Figure 5.1	Configuration of Levee Section	183
Figure 5.2	Schematic Diagram for Calculating Annual Expected Damage Cost	195
Figure 5.3	Channel Reach Configuration and Levee Layout	199
Figure 5.4	State Space for a Two Dimensional Problem	201
Figure 5.5	Transition Relationship Between Input State, Output State, and Decision Variable for Encroachment Width of Levees	203

LIST OF FIGURES

		<u>Page</u>
Figure 5.6	Flow Chart of DP Approach for Serial Levee Systems	208
Figure 5.7	Schematic Diagram for Corridor and Trial Trajectory in DDDP Applied to Serial Levee System	212
Figure 5.8	Flow Chart of DDDP Approach for Serial Levee Systems	216
Figure 6.1	Hypothesized Triangular Inflow Hydrograph	223
Figure 6.2	Computer Time vs. Number of States in DP Approach for Levee Problem	226
Figure 6.3	Optimal Levee Design Using DDDP Technique for Log-Pearson Type III Loading Distribution with Different Design Philosophies	232
Figure 6.4	Optimal Levee Design Using DDDP for Different Loading Models with IRISK = 2	237
Figure A.1	Probability Plot of Standardized Residuals	266
Figure A.2	Standardized Residuals vs. Predicted \bar{Z}_r	269
Figure A.3	Residuals (e_1) vs. Percentage of Surface Storage (S_t)	270
Figure A.4	Residuals (e_1) vs. Main Channel Slope (S_ℓ)	271
Figure A.5	Residuals (e_1) vs. Average Annual Thunderstorm Days (N_t)	272
Figure A.6	Probability Plot of Standardized Residuals	273
Figure A.7	Standardized Residuals vs. Predicted $\ln(\bar{Z}_r)$	275
Figure A.8	Residuals (e_2) vs. Log-transformed Drainage Area, $\ln(A_d)$	276
Figure A.9	Residuals (e_2) vs. Log-transformed Main Channel Slope, $\ln(S)$	277

LIST OF FIGURES

	<u>Page</u>
Figure A.10 Residuals (e_2) vs. Log-transformed Surface Storage, $\ln(S_t)$	279
Figure A.11 Mallows' C_p Statistic vs. Number of Independent Variables P in Regression Model	280

CHAPTER 1

INTRODUCTION

1.1 PRELIMINARIES

Hydraulic structures are designed with reference to some natural events that could be imposed on the structure during its expected service life. This involves hydrologic determination of the magnitude of a design event, which is a design flood or rainfall event. In principle the design event can be characterized by an annual exceedance probability or by its reciprocal, the design return period. Any design event which is selected can be expressed either by its magnitude or by its return period, since these two quantities must be directly related by a probability distribution. The engineer's basic task in the design procedure is to determine the "best" design considering the return period of the design event as the basic variable. This return period has economic, social, legal, and engineering consequences that are often overlooked in the design process.

Conventionally, the return period is so determined that the many associated risks are either ignored or not mentioned and consequently, the result often leads to misleading conclusions or decisions. For instance, the current practice of designing highway culverts and storm sewers by selecting a rainfall or flood for a given return period without specifying the associated risks often causes unnecessary misunderstandings. Knowledge of the many

associated risks is essential in estimating the expected damages to properties and inconvenience to the public because of flooding or improper functioning of a hydraulic structure over its expected service life.

The return period design method has as its background a large amount of practical engineering experience. However, the fact that the method has been so widely used suggests to many engineers the possibility that the return periods presented in design manuals may reflect some approximate nonanalytical correspondence with optimal economic design. This is truly misleading especially to the inexperienced, young engineer. The existing conventional return period design method fails to account explicitly for the cost interaction of the project components so that a proper trade-off analysis between potential damages and project costs is not performed in determining the design.

Existing return period design methods also fail to systematically account for the many uncertainties in design. The existence of uncertainties in hydrologic and hydraulic design of engineering projects has long been recognized. In existing design methods, only the hydrologic uncertainties caused by basic randomness in flood and rainfall frequencies are considered. However, uncertainties could also be contributed from many other sources.

The traditional method of analyzing flood exceedance probabilities has always been controversial in hydrology. This procedure has been to (1) observe historical records of flood events; (2) choose a reasonable generating process or probability density function; (3) estimate the parameters from the historical records; and (4) make inferences about the occurrence of future

flood events. These inferences are normally related to return periods. This procedure ignores uncertainties and introduces others such as those caused by probability density function and those caused by the parameters that describe the density function.

As pointed out by Yevjevich (1977), there is confusion in using the concepts and terms of risks and uncertainties as applied to the design of hydraulic structures. The concept of hydrologic risk caused by the basic stochastic process represented by rainfall events is not new. However, what is new is the concept of an overall or composite risk. The risk involved in hydraulic structure design is actually a result of the interaction of several types of random variables. The procedure of evaluating risk quantitatively for the design of hydraulic structures has been rather elusive even by the most knowledgeable engineers and theoreticians. Because the variables and parameters for the design of hydraulic structures are random variables, the estimation or assessment of the true values of those random variables is usually based on a limited amount of information and data. This results in various uncertainties, many of which can be integrated to define risk and reliability of hydraulic structure designs. A systematic procedure using analysis and synthesis is needed too for the quantification of risks and uncertainties.

In view of the many uncertainties, which will be discussed in later sections, the successfulness of engineering designs is accomplished by adopting a safety factor, possibly in the form of a high return period. Without a scientific basis for this evaluation, the safety factor has been determined

mainly by experience. Consequently, return periods or safety factors for conventional return period design methods are assigned without scientific basis and without accounting for the many uncertainties and economic tradeoffs.

1.2 EXISTENCE OF UNCERTAINTIES

The first item in discussing risk and reliability of hydraulic structure design is to delineate uncertainty and other related terms such as probability and stochasticity because there are various opinions and connotations among engineers and even among theoreticians. Uncertainty could simply be defined as the occurrence of events that are beyond our control. The uncertainty of a water resource system is an indeterministic characteristic and is beyond our rigid controls. In the design of hydraulic structures, decisions must be made under all kinds of uncertainty. In general, uncertainties in water resource engineering projects can be divided into four basic classifications: hydrologic, hydraulic, structural, and economic.

The classification of hydrologic uncertainties for any design problem may be further divided into three types: inherent, parameter, and model uncertainties. Streamflow processes or rainfall events are frequently considered or assumed to be stochastic processes because of the observable natural, or inherent, randomness. Because of the lack of perfect hydrological information about these processes or events, e.g., infinitely long historical records, there exists informational uncertainties about the processes. These uncertainties are referred to as the parameter uncertainty and model

uncertainty. There is seldom enough information available to properly evaluate the parameters of the model, e.g., mean, standard deviation, and skewness coefficient or select the best model with certainty. In the past, stochastic hydrology has focused mainly on the analysis of the natural uncertainties and has generally ignored the informational uncertainties. However, there have been a few recent attempts reported in the literature to explicitly account for the parameter uncertainty through a Bayesian framework.

The classification of hydraulic uncertainties for hydraulic structure design may be divided into several types: model, construction and material, and operational conditions of the flow. The model uncertainty results from the use of a certain hydraulic model to describe flow conditions which is essentially an uncertainty in design discharges. For example, flows through or over hydraulic structures are unsteady and nonuniform, which can only be described in three-dimensional form by the St. Venant equations. However, equations such as Manning's are quite commonly used in practice that cannot adequately describe unsteady and nonuniform flow. This fact results in additional uncertainty that will be referred to as equation errors. The construction and material uncertainty results partly from the structure size, e.g., a sewer diameter or the culvert width and depth. Manufacturers' tolerances or construction tolerances may vary widely resulting in these uncertainties. Another factor is the misalignment of a hydraulic structure as well as settlement resulting in errors such as in the slope. Material variability causes variations in the size and distribution of the surface roughness

resulting in errors of roughness factors. Changes in resistance coefficients and structural size reduction because of deposition could be classified under the operational conditions. Also, factors such as not cleaning the structure to eliminate clogging may result in additional uncertainty.

Structural uncertainty refers to the failure from structural weaknesses. Structural failures can be caused by many things such as: water saturation and loss of soil stability, erosion or hydraulic soil failures, wave action, hydraulic overloading, structural collapse, and many others. A good example is the failure of a levee system either in the levee or the soil near it. The structural failure of a levee may be caused by water saturation and loss of soil stability. A flood wave can cause increased saturation of the levee and an increased pressure gradient through the levee leading to levee failure through slumping. Levees can also fail because of hydraulic soil failures and wave action. As pointed out by Wood (1977), experience has shown that during a flood, most levees fail structurally, rather than by the flood waters overtopping the structure. Methods of analysis rarely include the probability of structural failure in an explicit manner. Results may significantly overestimate the protection offered by a hydraulic structure and underestimate expected damage that may occur.

Economic uncertainties can be the result of uncertainties caused by construction costs, damage costs, operation and maintenance costs, inflation, and inconvenience losses. Construction, damage, and operation and maintenance costs are all subject to uncertainties because of the fluctuation in the rate of increase of construction materials, labor costs, transportation

costs, economic losses, regional differences, and many others. The problem of inflation trends also causes uncertainties and should be accounted for in hydraulic structure design. There are also many other economic and social uncertainties that are referred to as inconvenience losses. An example of this is the failure of a highway culvert resulting in flooding causing traffic related losses (Young, et al., 1974).

1.3 PREVIOUS CONSIDERATIONS OF UNCERTAINTY

As previously mentioned, it is only recently that other uncertainties in addition to the natural or inherent hydrologic uncertainties have been considered explicitly on a scientific basis. Basically there have been works to consider the hydrologic uncertainties (inherent, parameter, and model) and also a few attempts to look at the hydraulic uncertainties. Most of the work reported in the literature that considers the hydrologic uncertainties has been through a Bayesian framework. Some works have considered the natural and parameter uncertainties or the natural and model uncertainties, and some works attempt to consider all three uncertainties [Bernier (1967); Conover (1971); Davis and Dvoranchik (1971); Davis et al. (1972); Vicens et al. (1975); Wood and Rodriguez-Iturbe (1975a); Wood and Rodriguez-Iturbe (1975b); Bodo and Unny (1976); and Wood (1977)]. Most of these works have dealt with improving flood frequency estimates by incorporating parameter or statistical and hydrologic model uncertainties.

A few basic works have been reported to explicitly account for the hydraulic uncertainties of design. Yen and Ang (1971) adopted a scheme to

account for subjective uncertainties and consequently proposed a design method based on risk analysis. Tang and Yen (1972) proposed a model whereby other sources of uncertainties associated with the hydraulic design of storm sewers can be systematically analyzed and combined and incorporated in the evaluation of the overall risk of alternative hydraulic designs. Overall risk refers to the risk caused by several uncertainties, not just the natural or inherent hydrologic uncertainty. In this approach, the natural or inherent hydrologic uncertainty constitutes only a part of the overall risk. Tang, Mays and Yen (1975) have incorporated this risk procedure into a dynamic programming approach for the optimal risk-based design of storm sewer systems. This procedure does not relate expected damages to the volume of flooding; however, it does define a composite or overall risk that includes the inherent hydrologic uncertainty and the hydraulic uncertainties through first-order analysis of uncertainties of the rational formula and Manning's equation. An improved model developed by Tang, Mays and Wenzel(1976) for the optimal design of sewer systems does consider the expected damages as a function of volume of flooding and incorporates various uncertainties. A risk-based procedure incorporating the inherent hydrologic and hydraulic uncertainties was essentially incorporated as a constraint model within a dynamic programming model for selecting the design of pipe crown elevations, slopes, and diameters. Young, Childrey, and Trent (1974) developed an optimal design model for highway drainage culverts that considered economic risks. This model defined economic risks as expected flood losses which were converted to yearly flood risks by using

appropriate probabilities for each flood. This procedure, however, did not consider the existence of the various uncertainties mentioned previously and related these to an overall or composite risk. Watt and Wilson (1978) developed a procedure to allow for risk and uncertainty in an optimal strategy for design of a system of hydraulic structures on a regional economic basis. This procedure did not actually define design uncertainties and risk but did define an optimal return period.

Wood (1977) developed a model for analyzing flood levee reliability. This model considered hydrologic uncertainties for overtopping and structural uncertainties for structural failure of the levee. The hydrologic uncertainty included the inherent and parameter uncertainties through a Bayesian framework. Bogardi, Duckstein, and Castano (1977) studied the effect of stochastic model choice on hydraulic design using as an example the design of a flood levee.

Yen (1978) demonstrated the determination of safety factor on the basis of risk and reliability for hydrologic and hydraulic engineering design. Yen's paper presents six different safety factors and applies a characteristic safety factor to storm sewer design. First-order analysis of uncertainties of the rational formula and Manning's equation is used to define hydrologic and hydraulic uncertainties, respectively. Many other works are reported in the literature that deal with uncertainties in the design and operation of water resources systems; however, these do not attempt to define risk and reliability by integrating the various uncertainties.

1.4 DEFINITION OF RISK AND RELIABILITY

The reliability of a hydraulic component, subsystem, or system is defined as the probability of the strength or resistance, r , exceeding the stress or loading, ℓ , i.e., the probability of survival. The terms stress and strength are more meaningful to structural engineers, while the terms loading and resistance are more descriptive to water resources engineers. The risk of a hydraulic component, subsystem or system is defined as the probability of the loading exceeding the resistance, i.e., the probability of failure. The mathematical representation of the reliability, R , and the risk \bar{R} can be expressed as, respectively,

$$R = P_r(r > \ell) = P_r(r - \ell > 0) \quad (1.1)$$

and

$$\bar{R} = P_r(r \leq \ell) = P_r(r - \ell \leq 0) \quad (1.2)$$

where $P_r()$ refers to probability. The relationship between reliability and risk is

$$R = 1 - \bar{R} \quad (1.3)$$

The resistance of a hydraulic structure is essentially the capacity of the structure and the loading is essentially the magnitude of flows through or over the structure, e.g., from a hydrologic event. Since the loading and resistance are random variables because of the various hydraulic and hydrologic uncertainties, a knowledge of the probability distributions of resistance and loading are required to develop risk and reliability models. The

computation of risk and reliability can be referred to as load-resistance interference as shown in Fig. 1.1. The intersection of the load and resistance curves demonstrates the interaction of two composite stochastic processes.

1.5 SAFETY FACTORS

As previously mentioned the success of engineering designs is accomplished by adopting a safety factor to take into account the ignorances and simplifications in the design processes. Loosely a safety factor can be defined as a measure of the resistance of the project over the loading. The precise definition of the safety factor depends on how the failure is defined and evaluated. Yen (1978) proposed six different safety factors for hydrologic and hydraulic design. They are briefly described as follows:

Pre-assigned safety factor. This is an arbitrarily chosen safety factor that is conventionally used without probabilistic considerations. It is a factor multiplied to a reference design loading (e.g., design discharge) to give the resistance. Usually hydrologic risk is calculated through a frequency analysis and not directly included in choosing the safety factor.

Central safety factor. If the expected value of the random variable r (resistance) and ℓ (loading) are μ_r and μ_ℓ , respectively. The central safety factor is defined as

$$SF_\mu = \mu_r / \mu_\ell \quad (1.4)$$

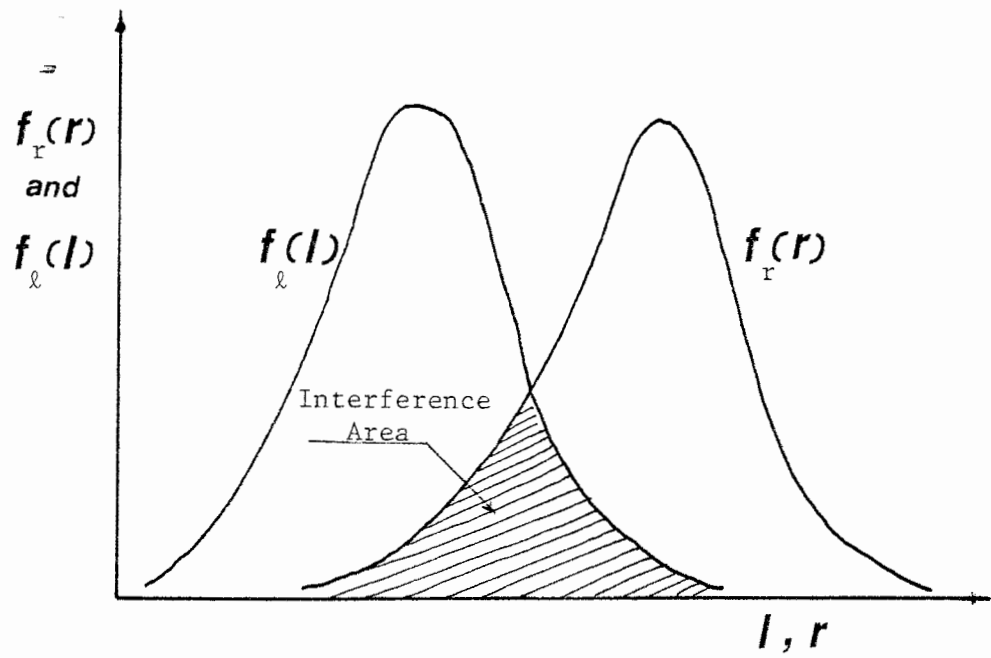


Figure 1.1 Load-Resistance Interference
(Kapur and Lamberson, 1977)

However, the value of μ_r and μ_l cannot be found precisely from the limited data; therefore, the central safety factor, SF_μ , is only of theoretical interest.

Mean safety factor. If the estimates of μ_r and μ_l are \bar{r} and \bar{l} , respectively the mean safety factor is defined as

$$\bar{SF} = \bar{r} / \bar{l} \quad (1.5)$$

Basically, the mean safety factor, \bar{SF} , is an estimate of the central safety factor, SF_μ . Their relationship can be expressed as

$$\bar{SF} = \kappa \cdot SF_\mu \quad (1.6)$$

In practice the value of κ is taken to be unity.

Characteristic safety factor. Often in a project the significant design values for the parameters are not the mean value but rather specified values. For example in culvert or levee design the loading is neither the mean value of all the floods nor the mean value of the selected flood of an annual maximum series. It might just be a specified flood of given magnitude (e.g. a flood with T_r -year return period). Therefore, the characteristic safety factor is defined as

$$SF_c = r_o / l_o \quad (1.7)$$

where r_o and l_o are the specified resistance and loading, respectively. With r_o and l_o assigned without a probabilistic analysis, SF_c in Eq. (1.7) is simply an arbitrarily preassigned safety factor conventionally used and discussed at

the beginning of this section. If the value of r_o and ℓ_o are determined by using the mean of the resistance and the loading, respectively, derived from the sample, SF_c is identical to the mean safety factor defined in Eq. (1.5). In general, r_o and ℓ_o can be determined through a probabilistic analysis of the parameters. Tang and Yen (1972) used the estimated mean value of resistance and specified loading to define a safety factor as

$$SF = \bar{r}/\ell_o \quad (1.8)$$

for storm sewer design.

Partial safety factor. This safety factor is assigned to each of the individual parameters or components in the system. It is particularly useful when the resistance and the loading of the total system are difficult to assess and the design or decision can be made only as long as the resistance exceeds the loading. The component safety factors are not necessarily the same, and each can be determined on a probabilistic basis. However, the safety factor for the total system cannot be given by this method.

Reduced safety factor. In order to evaluate risk or reliability knowledge of the probability density function of the loading as well as the resistance is required. In practice, the probability density function is assessed based on a limited amount of data. Yen and Ang (1971) have shown that for small probability of failure (say, less than 10^{-3}) the result becomes sensitive to the distribution functions, and sensitivity increases with the coefficient of variation. In order to avoid this distribution sensitivity problem, Ang (1970) introduced a judgment factor, which is called reduced

safety factor, v , such that the probability of failure can be divided into two parts, i.e.,

$$P_f = P_r \left(l > \frac{r}{v} \right) \cdot P_r (C > v) \quad (1.9)$$

where C is the correction factor required by virtue of the uncertainties to ensure no failure and is a random variable; and v is a specified value of C .

1.6 PURPOSE OF THE RESEARCH

The design process for many water resources engineering projects can be divided into two general phases: the calculation of design inflows and the determination of the geometry of the structure(s) based on these inflows. Considerable effort has been devoted in the area of hydrology to improving the first phase. However, there is an apparent need for developing procedures used in the second phase. As mentioned previously, the existing conventional hydraulic and hydrologic design methods fail to account explicitly for the cost interaction of the project components and to systematically account for all uncertainties in the design. Only the hydrologic uncertainties such as basic randomness in flood and rainfall frequencies are considered, neglecting the presence of other uncertainties. Present design methods usually consider only a risk associated with the hydrologic uncertainties, or more commonly is either not mentioned or plainly ignored. It would be much more reasonable, realistic, and perhaps easier to justify a recommended design to the public if the costs are associated with the degrees of protection

and risks. Emphasis should be placed on the integrated use of the hydraulics, hydrology, risks, cost-damage-benefit relationships, and optimization for determining optimal designs.

Water resources engineering designs are always under uncertainties that bear important consequences when the best design is being sought. Design procedures need to be developed basing the optimal design on minimum cost by maintaining a proper balance between the cost of the project and potential damages in the event of failure of the project. The purpose of this research is a theoretical development of general procedures for incorporating all the uncertainties and resulting risks into optimal-risk based design of water resources projects. The results will not only be of direct use in planning and design, but also provide a means of evaluating current design methods. Such information should also be of extreme importance to state and Federal agencies, with the ever increasing economic, energy, and environmental considerations.

The overall objective of this research is to develop fundamental techniques for the optimal risk-based design procedures for water resources engineering projects. More specifically, it can be divided as follows:

1. A risk evaluation procedure for water resources projects has been developed such that an overall risk is determined. Previous design risks are based solely on hydrologic risk.
2. A methodology to improve the estimate of the hydrologic parameters as well as hydrologic models has been developed.

3. New methodologies for evaluating expected damages in the event of failure of the project which incorporates the overall risk have been developed.
4. The risk and expected damages have been incorporated into optimization models so that a proper trade-off analysis between potential damages and the cost of the project is performed in determining the design. There are no general procedures of this nature reported in the literature.
5. Finally, the procedures have been developed in a general format such that they are applicable to different water resources engineering projects. For example, the procedures are applicable to the design of storm sewers, open channels, spillways, stilling basins, aqueducts, floodwalls, detention and retention basins, highway drainage culverts, and many others.

1.7 THE SCOPE OF AND LIMITATION OF THE RESEARCH

In this paper the emphasis will be placed on the integrated use of hydrology, hydraulics, risk evaluation, cost-damage-benefit relationships and optimization for determining optimal designs. For the sake of clarity, the scope of the research can be stated as follows:

1. Develop a risk evaluation procedure for systematically analyzing the component uncertainties in the hydraulic and hydrologic designs. The risk contributed from the structural

weakness will not be considered. Risk is defined from the viewpoint of operational condition of the project rather than the structure safety aspect of the project. The method used to analyze the hydraulic uncertainty is first-order analysis. New methods of using weighting procedure to treat hydrologic parameter uncertainty are developed. A composite hydrologic model is developed to take into account the hydrologic model uncertainty. The reliability model for evaluating the "risk" associated with design considers two loading situations, i.e., single loading application referred to as the static case and repeated loading applications referred to as the time-dependent case.

2. Current practices of risk-based water resources engineering projects evaluate the expected flood damage by considering the hydrologic risk only. The procedure will be refined in this report to consider the fact that the resistance of the hydraulic structure is a random variable. In other words, the resulting expected flood damage will be an integrated product considering the hydrologic and hydraulic uncertainties. In order to compute the expected flood damage cost the knowledge of probability distribution function of the loading and the resistance, as well as the flood damage cost function are required. The result of the statistical analysis from the previous step will be used for assessing the

probability density function of the loading and of the resistance. However, to define the flood damage cost function is beyond the scope of the research. A hypothetical damage function or reported one in the literature will be used.

3. This paper considers two types of hydraulic structures, i.e., highway box culvert and flood levee. The optimization technique used for the optimal risk-based levee design is dynamic programming (DP), and discrete differential dynamic programming (DDDP).
4. The area chosen to apply the proposed methodologies is the Southwestern region of the United States. The optimal risk-based flood levee design using DP and DDDP for Victoria, Texas is given as an example in which only three stages, approximately 10,000 feet of total length, are considered. No attempt will be made to compare the resulting optimal levee design with the existing levee system.
5. Conclusions are made and further studies along this line are suggested.

1.8 OVERVIEW OF RESEARCH RESULTS

Both static reliability models, which consider single loading application to hydraulic structures, and time-dependent (dynamic) reliability

models, which consider the random nature of the loading, are developed in Chapter 2. First-order analysis of uncertainties is used to estimate the uncertainty of deterministic hydraulic models such as Manning's Eq. which have uncertain parameters. The first-order analysis of uncertainty enables the estimation of the mean and variance of the capacity of hydraulic structures. An example of developing the risk evaluation procedure by considering the inherent hydrologic uncertainty and hydraulic uncertainties for the culvert design is presented.

Furthermore, a new methodology for treating (minimizing) the hydrologic parameter uncertainty is developed in Chapter 3 that uses generalized parameter (mean, standard deviation, and skewness) values from a weighting between sample and regional hydrologic information. Weights are defined as a function of the variances of the sample parameter estimates and regionalized parameter estimates. The methodology uses either of two non-parametric statistical techniques, the jackknife and the bootstrap, to determine variances of the sample parameter estimates and regression analysis to determine variances of the regionalized parameter estimates. The ability of this methodology is illustrated through a flood frequency analysis study for the Southwestern United States. The result shows that the proposed methods provide more desirable features, such as accuracy as well as stability of the estimates, than currently adopted procedures in which the parameters are estimated. The hydrologic model uncertainty is treated using a weighting procedure by assigning a weight to various probability models considered. The weight is determined by applying Bayes theorem to compute

the posterior probability of the model for a given prior probability of the model. The generalized parameter estimates described above, and the observations of sample data are both used. By doing so, a composite probability model can be developed to define risk and reliability which reduces the uncertainty of adopting the probability model. In Chapter 4 the application is made considering all the hydrologic and the hydraulic uncertainties to define the risk-safety factor relationship for levee design considering both the static case and time-dependent case.

The methods for analyzing the uncertainty of the hydrologic and hydraulic aspects are incorporated in optimization procedures to design the hydraulic structures to minimize total annual expected costs. In Chapter 5 dynamic programming (DP) and discrete differential dynamic programming (DDDP) models are developed to minimize the total annual expected cost for a levee system, taking into account the trade-off between installation cost and expected damage cost. Expected damage functions are developed that consider both hydrologic risk only and also overall risk.

In Chapter 6 the DP and DDDP models for optimal levee design are illustrated using data for the Guadalupe River near Victoria, Texas. This example is given to examine different risk considerations and their resulting economic consequences.

CHAPTER 2

RISK ANALYSIS FOR DESIGN

2.1 INTRODUCTION

The evaluation of reliability and risk using Eqs. (1.1) and (1.2) depends on the state of the resistance and the loading. From the viewpoint of operational conditions of a water resources engineering design the resistance is the capacity of a hydraulic structure and the loading is the magnitude of flows passing through or over a structure. In general, both the resistance and the loading are random variables with certain probability density functions associated. The current practice of risk-based design in water resources engineering considers only loading as a random variable, while the resistance is considered as deterministic.

Many aspects of uncertainty are involved in the design of water resource engineering projects. Uncertainties attributed to both the hydraulic aspects as well as the inherent hydrologic aspect are considered in this chapter. This chapter illustrates how these uncertainties are combined to develop risk and reliability models. Description of first-order, analysis applied to analyze hydraulic uncertainty is given in section 2.2. Loading-resistance inference considering both the loading and the resistance to be random variables for the static case is presented in section 2.3. Static reliability models are good for single loading. Static reliability models with

log-normally distributed resistance and various types of loading distribution commonly used in water resources engineering are presented in Appendix C. Section 2.4 gives examples of developing the risk and safety factor relationship for the design of box culverts considering the static case. Because the number of applications of loading and the time of occurrence of the loading are also random variables, reliability models are extended to time-dependent models that consider the repeated nature of the loading imposed on the structure. Time-dependent reliability models are developed in section 2.5 for random-independent loading and random-fixed resistance. The box culvert design example is also used to develop risk-safety factor relationships considering the time-dependent case.

2.2 ANALYSIS OF HYDRAULIC UNCERTAINTIES

The reliability of an engineering design is a function of several variables and parameters. As mentioned those variables and parameters are often random variables for which the performance of a system is dependent. In general, a function, W , of random variables w_1, w_2, \dots, w_p , whose properties are known, is expressed as

$$W = f(w_1, w_2, \dots, w_p) \quad (2.1)$$

As an example of a hydraulic model Manning's equation can be expressed as a function of several random variables. The problem is to find certain properties of the random variables, w_1, w_2, \dots, w_p , of the function, W , which is also a random variable. The random variables w_1, w_2, \dots, w_p may

be dependent or independent. In practice, it is usually difficult to determine the uncertain feature of the system as a whole. Alternatively, it is easier and more economical to analyze the uncertain feature of the parameters or components and then derive the uncertain properties of the entire system.

Cornell (1972) demonstrated that first-order analysis can be satisfactorily used for uncertainty analysis in hydrologic and water resource systems. First-order analysis is a method of providing an estimate of the uncertainty in a deterministic model involving uncertain variables. The first-order analysis provides an estimate of the mean and the variance (or standard deviation) of W . Through the first-order analysis, the combined effect of uncertainty resulting from use of uncertain variables in a predictive model can be estimated.

The vectors of the expected values and of the standard deviations of w_1, w_2, \dots, w_p , are denoted respectively as $\underline{\mu} = (\mu_1, \mu_2, \dots, \mu_p)$ and $\underline{\sigma} = (\sigma_1, \sigma_2, \dots, \sigma_p)$. The Taylor's expansion of Eq. (2.1) about the expected value for first-order analysis is approximated as [Benjamin and Cornell (1970) and Kapur and Lamberson (1977)].

$$W = f(\underline{\mu}) + \sum_{i=1}^p \left. \frac{\partial f(w)}{\partial w_i} \right|_{w=\underline{\mu}} (w_i - \mu_i) + \frac{1}{2!} \sum_{i=1}^p \sum_{j=1}^p \left. \frac{\partial^2 f(w)}{\partial w_i \partial w_j} \right|_{w=\underline{\mu}} \cdot (w_i - \mu_i)(w_j - \mu_j) + \xi \quad (2.2)$$

where ξ is the remainder.

The expectation of W can be written as

$$E[W] = f(\underline{\mu}) + \frac{1}{2} \sum_{i=1}^p \sum_{j=1}^p \left. \frac{\partial^2 f(\underline{w})}{\partial w_i \partial w_j} \right|_{\underline{w}=\underline{\mu}} \cdot E[(w_i - \mu_i)(w_j - \mu_j)] + E(\xi) \quad (2.3)$$

By assuming w_1, w_2, \dots, w_p are statistically independent and neglecting ξ , Eq. (2.3) then can be approximated as

$$E[W] \approx f(\underline{\mu}) + \frac{1}{2} \sum_{i=1}^p \left. \frac{\partial^2 f(\underline{w})}{\partial w_i^2} \right|_{\underline{w}=\underline{\mu}} \cdot \text{Var}(w_i) \quad (2.4)$$

where $\text{Var}(w_i)$ is the variance of w_i . Eq. (2.4) can then be further simplified if the value of $\text{Var}(w_i)$ is small as compared to $f(\underline{\mu})$, to

$$E[W] \approx f(\underline{\mu}) \quad (2.5)$$

Now, considering the first two terms of Eq. (2.2), the variance of W is

$$\begin{aligned} \text{Var}(W) &\approx \text{Var}[f(\underline{\mu})] + \text{Var} \left[\sum_{i=1}^p \left. \frac{\partial f(\underline{w})}{\partial w_i} \right|_{\underline{w}=\underline{\mu}} \cdot (w_i - \mu_i) \right] \\ &= \sum_{i=1}^p \left(\left. \frac{\partial f(\underline{w})}{\partial w_i} \right|_{\underline{w}=\underline{\mu}} \right)^2 \cdot \text{Var}(w_i) \end{aligned} \quad (2.6)$$

Equation (2.6) can further be expressed as

$$\Omega_W^2 = \frac{1}{E^2(W)} \sum_{i=1}^p \left[\left. \frac{\partial f(\underline{w})}{\partial w_i} \right|_{\underline{w}=\underline{\mu}} \right]^2 \cdot \mu_i^2 \cdot \Omega_{w_i}^2 \quad (2.7)$$

where Ω_W and Ω_{w_i} are the coefficients of variation of W and w_i , respectively. The first-order analysis is to use Eqs. (2.5) and (2.6) or (2.7) to estimate the mean and coefficient of variation of the random variable W .

In water resources engineering, for example, one of the most commonly used mathematical models for computing the capacity of hydraulic conveyance structures is Manning's equation:

$$Q_c = \frac{1.486}{n} A R_h^{2/3} S_f^{1/2} \quad (2.8)$$

in which Q_c is the capacity, n is Manning's roughness factor, A is the cross-sectional area of flow in the conveyance structure, R_h is the hydraulic radius, and S_f is the friction slope. It is realized that Manning's equation is only suitable for describing a uniform flow condition. Since the hydraulic conditions for flow through a conveyance structure is extremely complicated, highly unsteady and nonuniform, a model error term, λ_m , is incorporated,

$$Q_c = \lambda_m \frac{1.486}{n} A R_h^{2/3} S_f^{1/2} \quad (2.9)$$

This equation must be reformulated so that each variable involved in the model can be treated as a statistically independent random variable. The hydraulic radius, $R_h = A/P$, where P is the wetted perimeter, must be introduced,

$$Q_c = \lambda_m \frac{1.486}{n} A^{5/3} P^{-2/3} S_f^{1/2} \quad (2.10)$$

By performing first-order analysis of Eq. (2.10) using Eqs. (2.5) and (2.7), the mean and coefficient of variation of the capacity, Q_c , can be expressed, respectively as:

$$\bar{Q}_c = \bar{\lambda}_m \frac{1.486}{\bar{n}} \bar{A}^{5/3} \bar{P}^{-2/3} \bar{S}_f^{1/2} \quad (2.11)$$

$$\Omega_{Q_c} = \left[\Omega_{\lambda_m}^2 + \Omega_n^2 + 2.78\Omega_A^2 + 0.44\Omega_P^2 + 0.25\Omega_{S_f}^2 \right]^{1/2} \quad (2.12)$$

where (-) indicates the mean and Ω is the coefficient of variation.

2.3 STATIC RISK AND RELIABILITY

The word "static," from the reliability computation viewpoint represents the worst single stress, or load, applied in the unit time span considered. The loading applied to many hydraulic structures is a random variable, and in addition, the number of times of loading is unknown and random. If the distribution of the loading and the resistance is known, the reliability computation is referred to as a load-resistance interference (Fig.

1.1). Following the definitions given in Eqs. (1.1) and (1.2), the reliability and risk of a hydraulic structure can be expressed as, respectively,

$$R = \int_0^{\infty} f_{\ell}(\ell') \cdot \left[\int_{\ell'}^{\infty} f_r(r') \cdot dr' \right] \cdot d\ell' \quad (2.13a)$$

$$= \int_0^{\infty} f_r(r') \cdot \left[\int_{r'}^{\infty} f_{\ell}(\ell') \cdot d\ell' \right] \cdot dr' \quad (2.13b)$$

and

$$\bar{R} = \int_0^{\infty} f_r(r') \cdot \left[\int_{r'}^{\infty} f_{\ell}(\ell') \cdot d\ell' \right] \cdot dr' \quad (2.14a)$$

$$= \int_0^{\infty} f_{\ell}(\ell') \cdot \left[\int_0^{\ell'} f_r(r') \cdot dr' \right] \cdot d\ell' \quad (2.14b)$$

where $f_r(\)$ and $f_{\ell}(\)$ represent the probability density functions of the resistance and the loading, respectively. The reliability computations for a hydraulic structure for the static case require the probability distributions of loading and resistance.

In the reliability analysis of hydraulic structures the probability distribution of the resistance (capacity) and the loading (flood flow) are required. The capacity of hydraulic structures, such as culverts and levees, is a function of several variables, that is illustrated in Manning's Eq. (2.8). The log-normal probability distribution is assumed for the resistance that has the following functional form:

$$f_r(r') = \frac{1}{\sqrt{2\pi} r' \sigma_{\ell nr}} \exp \left[-\frac{1}{2} \left(\frac{\ln r' - \mu_{\ell nr}}{\sigma_{\ell nr}} \right)^2 \right] \quad (2.15)$$

where $\mu_{\ell nr}$ and $\sigma_{\ell nr}$ are the mean and standard deviation of the log-transformed resistance.

Based on Eq. (2.13b) the static reliability model can be written as

$$R = \int_0^{\infty} f_r(r') \cdot F_{\ell}(r') \cdot dr' \quad (2.16)$$

where $F_{\ell}(r')$ is the cumulative distribution function (CDF) of loading,

$$F_{\ell}(r') = \int_0^{r'} f_{\ell}(\ell') \cdot d\ell' \quad (2.17)$$

The probability distributions of loading which are commonly used in hydrology to describe the random mechanism of a flood flow sequence are normal, log-normal, Gumbel, Pearson type III, and log-Pearson type III. The mathematical representation of the static reliability model with log-normal resistance and various types of loading distribution mentioned above are described in Appendix C.

For the case when the loading distribution is the Gumbel and the probability density function has the form

$$f_{\ell}(\ell') = \frac{1}{\alpha_2} \exp\left\{-\left(\frac{\ell' - \alpha_1}{\alpha_2}\right) - \exp\left[-\left(\frac{\ell' - \alpha_1}{\alpha_2}\right)\right]\right\} \quad (2.18)$$

where $\alpha_1 = \mu_{\ell} - \gamma_E \alpha_2$; $\alpha_2 = \sqrt{6} \sigma_{\ell} / \pi$,

and γ_E is Euler's constant (0.5772). The CDF of the Gumbel distribution is

$$\begin{aligned}
 F_{\ell}(\ell) &= \int_0^{\ell} \frac{1}{\alpha_2} \exp\left[-\left(\frac{\ell' - \alpha_1}{\alpha_2}\right)\right] \exp\left[-\left(\frac{\ell' - \alpha_1}{\alpha_2}\right)\right] \cdot d\ell' \\
 &= \exp\left\{-\exp\left[-\left(\frac{\ell - \alpha_1}{\alpha_2}\right)\right]\right\}
 \end{aligned} \tag{2.19}$$

The static reliability model is

$$\begin{aligned}
 R &= \int_0^{\infty} \frac{1}{\sqrt{2\pi}r' \sigma_{\ln r}} \exp\left[-\frac{1}{2}\left(\frac{\ln r' - \mu_{\ln r}}{\sigma_{\ln r}}\right)^2\right] \\
 &\quad \cdot \exp\left\{-\exp\left[-\left(\frac{r' - \alpha_1}{\alpha_2}\right)\right]\right\} \cdot dr'
 \end{aligned} \tag{2.20}$$

2.4 EXAMPLE FOR CULVERT DESIGN (STATIC RELIABILITY MODEL)

The application of the reliability computations for box culvert design is given as an illustration. In this case the reliability of the culvert is defined as the probability of the resistance or culvert capacity exceeding the loading or flood magnitude. Manning's Eq. (2.8) for full flow is used as the hydraulic model to compute the capacity of the culvert. The first step is to perform an uncertainty analysis on the hydraulic model to define the associated hydraulic uncertainties. As previously demonstrated the coefficient of variation of the culvert capacity, Q_c , is expressed as Eq. (2.11). The reason for the existence of the coefficients of variation of the model, Ω_{λ_m} ,

roughness, Ω_n , cross-sectional area, Ω_A , wetted perimeter, Ω_P , and friction slope, Ω_{S_f} , is due to the uncertainties from each of the random variables λ_m , n , A , P , and S_f , that make up the hydraulic uncertainties. The hydraulics of culvert flow are very complicated so the error of this assumption to describe the flow is lumped and accounted for as an uncertainty by the model error, λ_m . The construction and material uncertainty can partially be accounted for through the uncertainties of the area, the wetted perimeter, and slope. Uncertainty of the material variability can be accounted for through Manning's roughness factor, n . Also uncertainties for the operational conditions of flow can be accounted for through n .

The mean and coefficient of variation for the box culvert flow cross-sectional area are computed using

$$\bar{A} = \bar{D} \bar{B} \quad (2.21)$$

$$\Omega_A = (\Omega_D^2 + \Omega_B^2)^{1/2} \quad (2.22)$$

from the first-order analysis of uncertainties where \bar{D} is the mean culvert depth and \bar{B} is the mean culvert width. The mean and coefficient of variation of the wetted perimeter, P , is computed using

$$\bar{P} = 2(\bar{D} + \bar{B}) \quad (2.23)$$

$$\Omega_P = \left[\left(\frac{\bar{D}}{\bar{D} + \bar{B}} \right)^2 \Omega_D^2 + \left(\frac{\bar{B}}{\bar{D} + \bar{B}} \right)^2 \Omega_B^2 \right]^{1/2} \quad (2.24)$$

For the friction slope a full pipe flow is assumed with the depth on the downstream side of the culvert assumed to be D . The surface water elevation on

the upstream side of the culvert, Y_u , is found using the stage-volume relationship.

With these assumptions the energy and momentum equations are used to derive the frictional slope, S_f , and the mean is expressed as

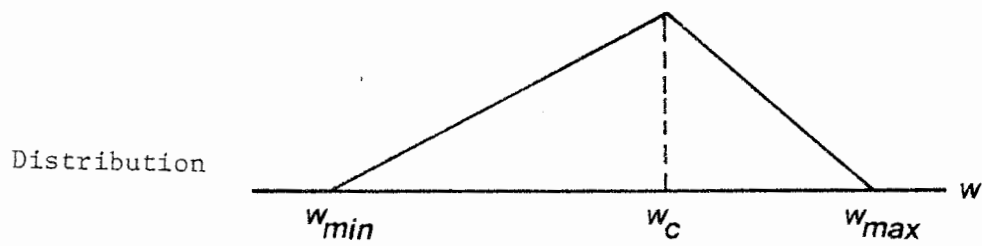
$$\bar{S}_f = \bar{S}_o + \frac{\bar{Y}_u - \bar{D}}{2\bar{L}} \quad (2.25)$$

where \bar{S}_o is the mean slope of the culvert; \bar{Y}_u is the mean depth on the upstream side of the culvert; \bar{D} is the mean culvert depth; and \bar{L} is the mean culvert length. From the first-order analysis, the coefficient of variation of the friction slope, Ω_{S_f} , is

$$\Omega_{S_f} = \left[\frac{4\bar{L}^2\bar{S}_o^2}{\beta^2} \Omega_{S_o}^2 + \frac{\bar{Y}_u^2}{\beta^2} \Omega_{Y_u}^2 + \frac{\bar{D}^2}{\beta^2} \Omega_D^2 + \frac{(\bar{Y}_u - \bar{D})}{\beta^2} \Omega_L^2 \right]^{1/2} \quad (2.26)$$

where $\beta = 2\bar{L}\bar{S}_o + \bar{Y}_u - \bar{D}$.

One technique to evaluate the Ω 's for the random variables λ_m , n , S_o , Y_u , D , B , and L is to use triangular distributions and assumed errors for each variable. In other words by assuming minimum and maximum values of each variable, w_{\min} and w_{\max} it is possible to use a triangular distribution (Fig. 2.1) to compute the coefficient of variation of each variable. This procedure is outlined in detail by Yen et al. (1976) and applied to storm sewers. When the coefficients of variation are as small as those considered here the density



$$\text{Mean } \bar{w} = \frac{1}{3}(w_{min} + w_{max} + w_c)$$

$$\text{Coefficient of variation } \Omega_w = \left[\frac{1}{2} - \frac{1}{6\bar{w}^2}(w_{min}w_{max} + w_{max}w_c + w_cw_{min}) \right]^{1/2}$$

Figure 2.1 Triangular Distribution

functions can also be treated as approximately Gaussian. The form of the distributions could be determined by a Monte Carlo analysis if the analyst so desires.

The probability distribution of the random variable, culvert capacity, is assumed to be log-normal based on the central limit theorem. The mean and coefficient of variation of the culvert capacity can be computed by using Eqs. (2.11) and (2.12), respectively. Knowing these statistical parameters of the culvert capacity, the log-normal probability density function is expressed using Eq. (2.15) as

$$f_{Q_c}(Q'_c) = \frac{1}{\sqrt{2\pi} Q'_c \zeta_{Q_c}} \exp\left[-\frac{1}{2} \left(\frac{\ln Q'_c - \chi_{Q_c}}{\zeta_{Q_c}}\right)^2\right] \quad (2.27)$$

where χ_{Q_c} and ζ_{Q_c} are respectively, the mean and standard deviation of the transformed random variable $\ln Q_c$. The coefficient of variation of the culvert capacity can be used to compute the standard deviation, ζ_{Q_c} , for the distribution, i.e.,

$$\zeta_{Q_c} = [\ln(\Omega_{Q_c}^2 + 1)]^{1/2} \quad (2.28)$$

Clearly the statistical parameters in the resistance or culvert capacity distribution are a function of the design variables, such as culvert

depth, width, bottom slope, length, etc. Therefore, once the geometric variables of the culvert design with associated distribution and tolerance are specified the distribution of culvert capacity can be determined.

The loading to the structure which is a flood magnitude is also a random variable. The distribution of the flood for a particular site can be estimated by performing a flood frequency analysis as mentioned previously. The Type I extremal distribution (Gumbel, 1955) is used as the distribution of annual floods for this example. This probability density function for the loading or flood magnitude is expressed, following Eq. (2.18) as

$$f_{Q_d}(Q'_d) = \frac{1}{\alpha_2} \exp\left\{-\left(\frac{Q'_d - \alpha_1}{\alpha_2}\right) - \exp\left[-\left(\frac{Q'_d - \alpha_1}{\alpha_2}\right)\right]\right\} \quad (2.29)$$

where

$$\alpha_1 = \bar{Q}_d - \gamma_E \cdot \alpha_2 \quad \text{and} \quad \alpha_2 = \frac{\sqrt{6}}{\pi} \sigma_{Q_d}$$

in which γ_E is Euler's constant (0.5772); \bar{Q}_d is the mean; and σ_{Q_d} is the standard deviation of the annual flood magnitudes. The flood magnitude for any return period, T_r , can be approximated using

$$Q_d(T_r) = -\alpha_2 \cdot \ln[-\ln(1 - \frac{1}{T_r})] + \alpha_1 \quad (2.30)$$

knowing \bar{Q}_d and σ_{Q_d} from historical data.

By using Eq. (2.20) the reliability for this example can be expressed as

$$R = \int_0^{\infty} \frac{1}{\sqrt{2\pi} Q'_c \zeta_{Q_c}} \exp\left[-\frac{1}{2}\left(\frac{\ln Q'_c - \chi_{Q_c}}{\zeta_{Q_c}}\right)^2\right] \cdot \exp\left\{-\exp\left[-\left(\frac{Q'_c - \alpha_1}{\alpha_2}\right)\right]\right\} \cdot dQ'_c \quad (2.31)$$

The general practice in water resources engineering is to choose a flood magnitude for a certain return period specified as the design criterion for the structural capacity. The selection of the flood magnitude or return period depends on the importance and consequence of the project. Also, once the design flow for the return period is determined, the capacity can be determined for a specified safety factor. The type of safety factor used is the characteristic safety defined as Eq. (1.8), which can be expressed as

$$SF = \bar{Q}_c / Q_d(T_r) \quad (2.32)$$

The procedure to establish the risk and reliability-safety factor relationships is described as follows:

1. Selection of probability distribution for hydrologic uncertainties and determine the parameters of the distribution.
2. Selection of probability distribution and hydraulic model for hydraulic uncertainties.
3. Selection of design flood, $Q_d(T_r)$.
4. Selection of a structure geometry, and determination of hydraulic variables such as bottom slope, Manning's roughness (determined by material used), etc.
5. Determination of nominal value of geometric variables of structure such as width and depth.
6. Performance of uncertainty analysis on each variable of hydraulic model.

7. Estimation of parameters governing the distribution of capacity such as mean, \bar{Q}_C and standard deviation, σ_{Q_C} .
8. Check whether \bar{Q}_C for a specified dimension and hydraulic condition is greater than $Q_d(T_r)$. If not, then go to 4 or 5 to change hydraulic condition or dimension because in general practice the safety factor is usually selected to be greater than 1. Otherwise, go to next step.
9. Computation of the reliability, R , from Eq. (2.31), risk, \bar{R} , from Eq.(1.3), and corresponding safety factor, SF , from Eq. (2.32).
10. Repeat steps 3 to 9 until whole range of design variation has been examined.

Using the above procedure, an analysis was performed to generate risk-safety factor curves for culvert design using hydrologic data for the Glade near Reston, Virginia (Young, et al., 1974). Tolerances upon which the distribution for S_f , n , Y_u , D , B , and L were 0.0005, 0.0004, 0.1, 0.1, 0.1, and 0.5. For example, if D is 5.0 ft., the interval over which the triangular distribution is defined is from 4.9 to 5.1 ft. A value of $E(\lambda_m)=1$ is used. The mean and standard deviation of flood flow in Gumbel distribution are 536 cfs and 505 cfs, respectively. The results of the analysis are given in Figures 2.2, 2.3, and 2.4. In Fig. 2.2 is the relationship between risk and safety factor for different values of $\sqrt{S_f}/n$ which shows that $\sqrt{S_f}/n$ has little effect on the risk safety factor relationship. In Fig. 2.3 a set of risk-safety factor curves for different return periods is provided. Fig. 2.4 is derived by plotting return

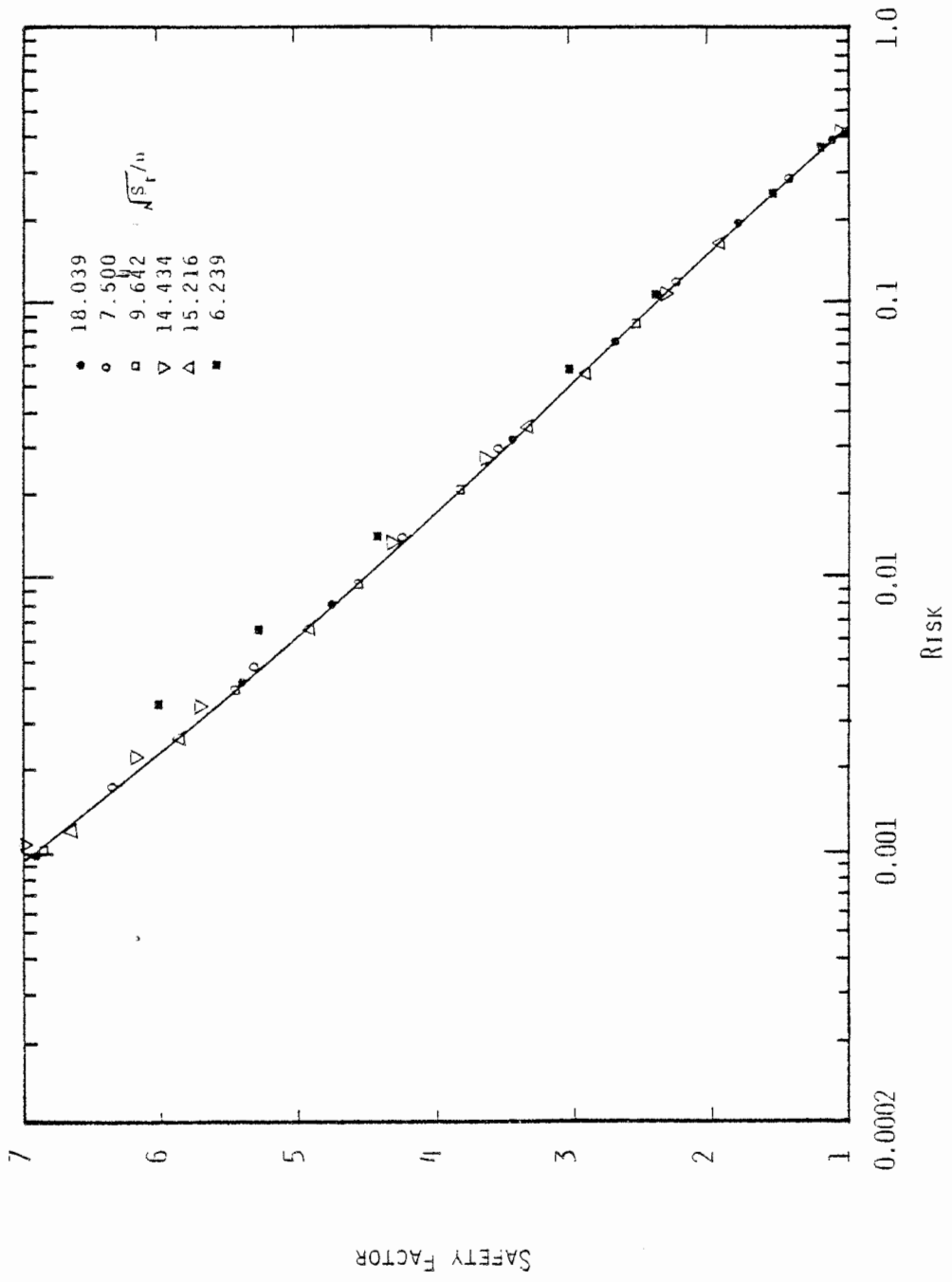


Figure 2.2 Sensitivity of Risk-Safety Factor Relationship with Respect to Different Values of $\sqrt{S_r/n}$

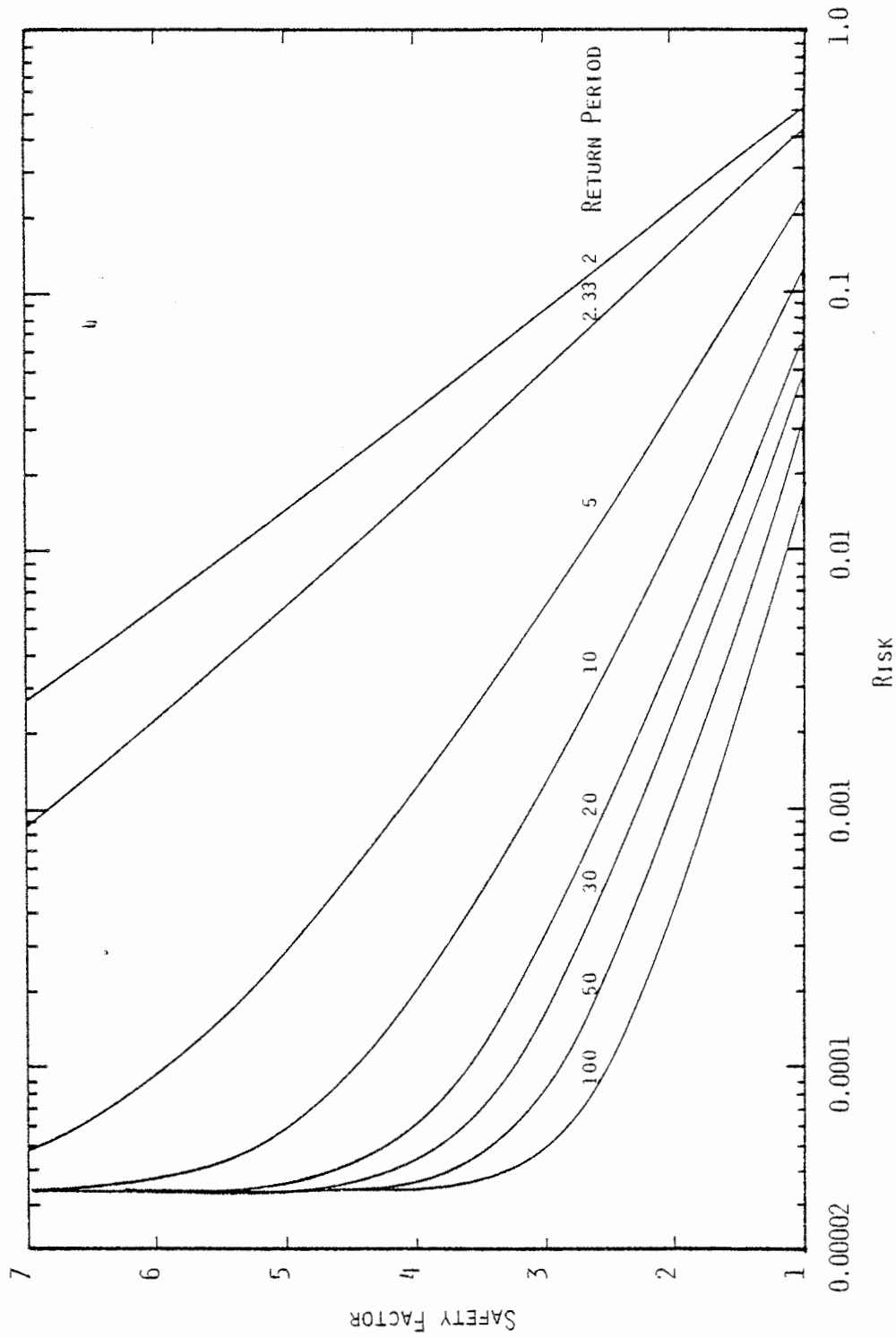


Figure 2.3 Risk-Safety Factor Curves for Culvert Design (Staric Reliability Model)

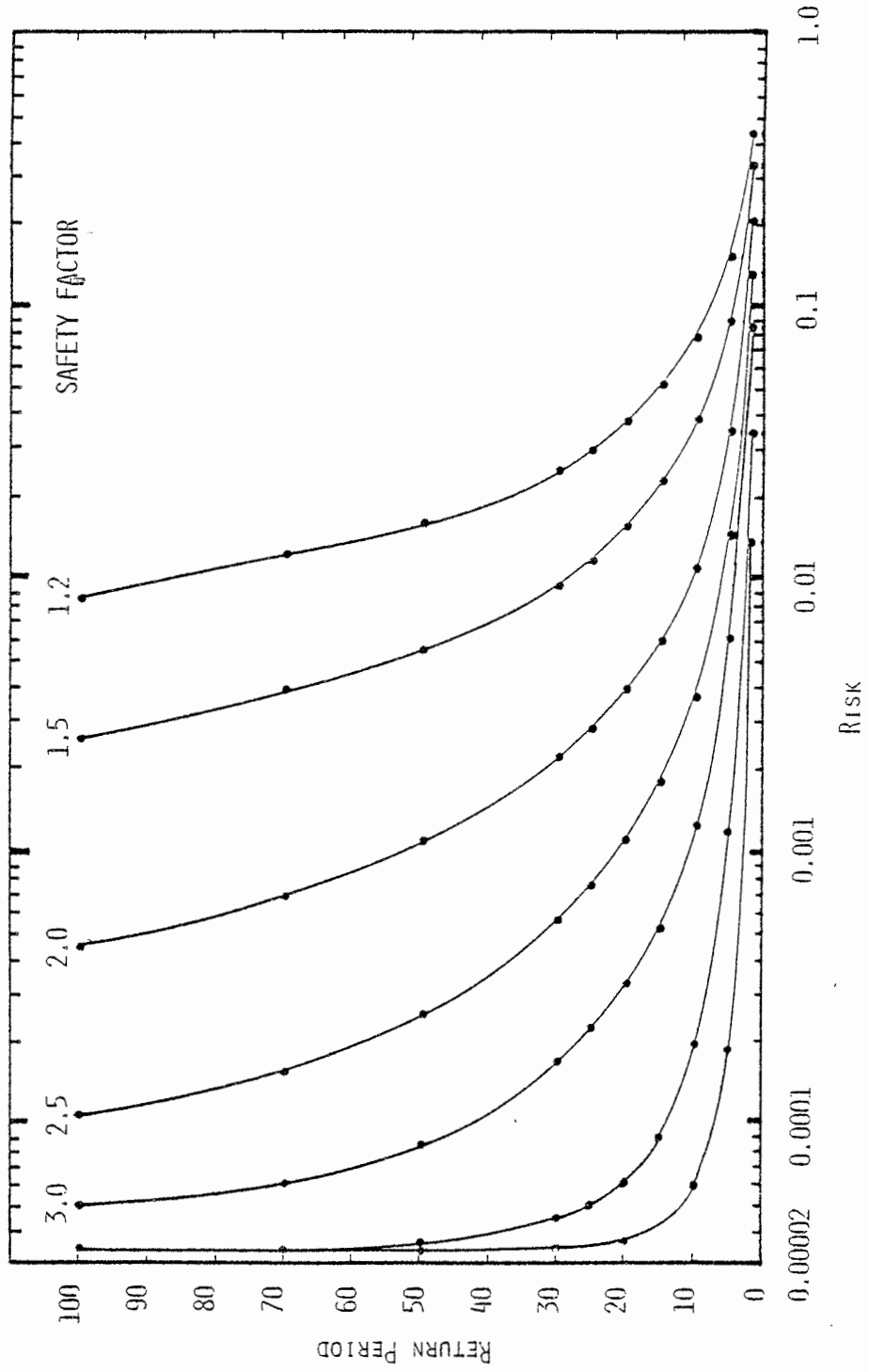


Figure 2.4 Risk vs. Return Period with Different Safety Factor for Culvert Design (Static Reliability Model)

period versus risk for various safety factors. Figs. 2.3 and 2.4 give no provision for various structure dimensions under certain hydraulic conditions. A proposed regression equation to describe the relationship among $AR_h^{2/3}$, $\sqrt{S_f}/n$, and SF for a given T_r is

$$AR_h^{2/3} = a_1 (SF)^{b_1} \left(\frac{\sqrt{S_f}}{n} \right)^{c_1} \quad (2.33)$$

where a_1 , b_1 and c_1 are constants.

The results of the regression analysis for several return periods are listed in Table 2.1

In order to obtain a relationship among T_r , SF, $\sqrt{S_f}/n$, and $AR_h^{2/3}$, the following regression equation for the example was developed.

$$AR_h^{2/3} = 800.5 (\log T_r)^{0.8231} (SF)^{1.0013} \left(\frac{\sqrt{S_f}}{n} \right)^{-0.99768} \quad (2.34)$$

Using Eq. (2.34) in conjunction with Fig. 2.3 or 2.4, the reliability of the structure and dimension parameter, $AR_h^{2/3}$, required can be obtained once the design storm return period, safety factor, and hydraulic variables are determined.

By examining Fig. 2.3, for SF=1, the risk associated with design return periods, T_r , 10, 20, 30, 50, and 100 years are 0.12, 0.064, 0.047, 0.033, and 0.017, respectively. The risk assessed by the conventionally considered inherent hydrologic risks for the above return periods are 0.1, 0.05, 0.033, 0.02, and 0.01, respectively. Comparing these two sets of risk values it is

Table 2.1 Result of Regression Analysis in Culvert Design

T_r	$\log(a_1)$	a_1	b_1	c_1	Correlation Coefficient
2	2.48473	301.302	0.99713	-0.99897	99.99530
2.33	2.53453	342.397	1.00120	-0.98283	99.72772
5	2.78150	604.644	1.00064	-1.00005	99.99975
10	2.90412	801.900	1.00045	-0.99939	99.99970
15	2.94454	880.116	1.00903	-0.98629	99.36715
20	2.99715	993.419	1.00066	-0.99995	99.99963
25	3.07270	1053.659	1.00067	-0.99983	99.99972
30	3.04322	1104.638	0.99973	-0.99999	99.99963
50	3.09361	1240.538	0.99899	-0.99934	99.99950
70	3.12919	1346.449	1.00645	-1.00803	99.84035
100	3.15420	1426.264	0.99969	-0.99983	99.99916

found that the risk is underestimated by 20%, 28%, 42%, 65%, and 70% using the conventional risk evaluation procedure for return periods of 10, 20, 30, 50, and 100 years, respectively. The percentage of underestimation of risk increases as the return period increases. This shows evidence that the risk is underestimated by ignoring the hydraulic uncertainty involved.

2.5 DYNAMIC OR TIME-DEPENDENT RELIABILITY

In the literature on reliability theory, the failure of components under repeated stresses has been investigated primarily with respect to the fatigue behavior of materials (Kapur and Lamberson, 1977). The loading tends to induce failure, and the resistance resists failure with failure occurring when the loading exceeds the resistance. Repeated loadings on a hydraulic structure are characterized by the time each load is applied and by the behavior of time intervals between the application of loads. From reliability theory loads may be classified as applied at known times or at random times. For loads applied at known times the changes may follow a cyclic pattern which is known exactly beforehand. These load occurrences may be constant or may vary from cycle to cycle. For loads applied at random times the cycle times are random and independent rather than known. The randomness of the cycle times may be described by exponential or gamma probability density functions and the loading may be deterministic or stochastic in nature (Kapur and Lamberson, 1977).

From a reliability theory viewpoint, the uncertainty about the loading and resistance variables may be classified into three categories:

deterministic, random-fixed, and random independent (Kapur and Lamberson, 1977). For the deterministic category, the variable assumes values that are exactly known a priori which is not the case for hydraulic structures subjected to hydrologic events. In the random fixed cases the concern is in the behavior of the resistance variable with respect to time or cycles. The resistance is a random variable at any particular time. Fixed refers to the behavior of the random variable with respect to time and/or cycles. This means that the randomness varies in time in a known manner. For example if $f_r(r)$ is the probability density function of the resistance random variable, r_0 , at the initial time, then the resistance $r(t)$ at any instant of time t is given by

$$r(t) = r_0 \cdot \phi(t) \quad (2.35)$$

where $\phi(t)$ is a known function that describes exactly how the resistance changes (decreases) with time. For the random independent case the variable is not only random but the successive values assumed by the variable are statistically independent. Observation of one loading or resistance value gives us no information about the size of the subsequent values. Successive loadings are generally independent. Resistance will vary randomly and will be independent from cycle to cycle only when affected by other environmental factors, which are independent of the process. Resistance depends on the number of load applications, their magnitudes and time durations.

The objective of the reliability computations for the dynamic models is to determine the reliability after n cycles or occurrences of loading, R_n , i.e., the probability of not having a failure on any one of the n cycles or loadings. For hydraulic structures there is uncertainty about the

cycles or loadings. For hydraulic structures there is uncertainty about the loading and the resistance random variables at any instant of time and also about the behavior of the random variables with respect to time and/or loading cycles. The two terms "random fixed" and "random independent" are used to describe these uncertainties. The resistance of the structure is a random variable at any particular instant of time. The behavior of the random variable with respect to time and/or cycles is assumed to be fixed in the sense that the random variable, resistance, changes or varies in time in a known manner. The loading on a hydraulic structure, however, is not only a random variable; but unlike the random fixed case assumed for the resistance, the successive values assumed by the random variable, loading, are statistically independent. The loadings on many hydraulic structures are basically independent hydrologic events. The resistance provided by a hydraulic structure does vary randomly and is somewhat independent from cycle to cycle because of the effect of various environmental factors. However, in this analysis the resistance will be considered as random-fixed.

Reliability computations for dynamic (time-dependent) models can be made for deterministic and for random cycle times. Because the loading on most hydraulic structures is random, the time dependent reliability model for random cycle times is of most importance. However, for simplicity of the discussion, the model for deterministic cycles will be developed that naturally leads into the model for random cycle times. For deterministically known cycle times the reliability at time t , $R(t)$, can be determined from the reliability after n cycles or occurrences of loading, R_n , as

$$R(t) = R_n, \quad t_n < t < t_{n+1} \quad n = 1, 2, \dots \quad (2.36)$$

where t_n is the instant in time at which the n^{th} cycle occurs. Referring to the loading as ℓ and the resistance as r , R_n can be expressed as

$$\begin{aligned} R_n &= P_r [(\ell_1 < r) \cap (\ell_2 < r) \cap \dots \cap (\ell_n < r)] \\ &= P_r [\max (\ell_1, \ell_2, \dots, \ell_n) < r] \end{aligned} \quad (2.37)$$

By letting the maximum loading, $\ell_{\max} = \max (\ell_1, \ell_2, \dots, \ell_n)$, then the distribution function of ℓ_{\max} is

$$F_n(\ell) = [F_\ell(\ell)]^n \quad (2.38)$$

provided the loadings are independent and identically distributed, where $F_\ell(\ell)$ is the cumulative distribution of the loadings or hydrologic events. The reliability for static reliability models of hydraulic structures is expressed as Eq. (2.13). The time-dependent reliability model for deterministic cycles, is expressed as

$$\begin{aligned} R_n &= \int_0^\infty f_r(r) \cdot \left[\int_0^r f_\ell(\ell) \cdot d\ell \right]^n \cdot dr \\ &= \int_0^\infty f_r(r) \cdot [F_\ell(r)]^n \cdot dr \end{aligned} \quad (2.39)$$

As previously mentioned the loadings (hydrologic events) for most hydraulic structures occur at random times. The above reliabilities for random loading times can be expressed in terms of time as

$$R(t) = \sum_{n=0}^{\infty} \pi_n(t) \cdot R_n \quad (2.40)$$

where $\pi_n(t)$ is the probability of n loadings occurring in the time interval $(0, t)$ and R_n is the probability of all n successes. It is now evident that the case of deterministic cycle times is a special case of the above reliability equation for random cycle times.

A Poisson distribution can be used to describe the probability of the number of events occurring in a given time interval. This distribution is given as

$$\pi_n(t) = \frac{e^{-\lambda t} (\lambda t)^n}{n!} \quad (2.41)$$

where λ is the mean rate of occurrence of the loading which may be estimated from historical data. For example, if annual data are being used $\lambda = 1/T_r$ where T_r is the return period and t is considered the expected service life of the hydraulic structure. Other distributions may also be applicable but they lead to more complicated analysis.

For the random-independent loading and random-fixed resistance the time dependent reliability can be expressed as:

$$\begin{aligned} R(t) &= \sum_{n=0}^{\infty} \frac{e^{-\lambda t} (\lambda t)^n}{n!} \int_0^{\infty} f_r(r) \cdot \left[\int_0^r f_l(l) \cdot dl \right]^n \cdot dr \\ &= \int_0^{\infty} f_r(r) e^{-\lambda t} \sum_{n=0}^{\infty} \frac{[\lambda t \int_0^r f_l(l) \cdot dl]^n}{n!} \cdot dr \end{aligned} \quad (2.42)$$

Now using Eq. (2.42) and manipulating the reliability equation becomes

$$R(t) = \int_0^{\infty} f_r(r') \cdot e^{-\lambda t [1 - F_{\ell}(r')]} \cdot dr' \quad (2.43)$$

Based on Eq. (2.43) the time-dependent reliability model for log-normal random-fixed resistance and random-independent loading can be expressed as \rightarrow

$$R(t) = \int_0^{\infty} \frac{1}{\sqrt{2\pi} r' \sigma_{\ln r}} \exp \left[-\frac{1}{2} \left(\frac{\ln r' - \mu_{\ln r}}{\sigma_{\ln r}} \right)^2 \right] \cdot \exp \left\{ -\lambda t [1 - F_{\ell}(r')] \right\} \quad (2.44)$$

where $F_{\ell}(r')$ is the cumulative distribution function of the loading. The CDF $F_{\ell}(r')$ of the loading for normal, lognormal, Gumbel, Pearson type III, and log-Pearson type III are Eq. (C.2), (C.5), (2.19), (C.13), and (C.17), respectively.

2.6 EXAMPLE FOR CULVERT DESIGN (TIME-DEPENDENT MODEL)

As an illustration of time dependent reliability computations, the same example of box culvert design used previously for static reliability models is considered. For this example the reliability of the culvert is defined as the probability of the resistance (culvert capacity) exceeding the loading (flood magnitude). Manning's equation for full flow is used to compute the culvert capacity. The probability distribution for the random

variable, culvert capacity is assumed to be lognormal, Eq. (2.27) and random fixed. The statistical parameters in the resistance distribution are a function of the design variables, culvert depth, width, bottom slope, length, roughness factor, etc. Tolerances upon which the triangular distributions for S_o , n , Y_u , D , B , and L are the same as for the static model. The random variable loading, Q_d , to the structure which is a flood magnitude has a distribution which can be determined from a flood frequency analysis. The Type I extremal distribution, Eq. (2.29) is used as the distribution of annual floods for this example. The reliability model for this random-independent loading and random-fixed resistance example can be expressed using Eq. (2.27), (2.29), and (2.44), as

$$R(t) = \frac{1}{\sqrt{2\pi}\zeta_{Q_c}} \int_0^{\infty} \frac{e^{-\beta}}{Q_c} dQ_c \quad (2.45)$$

where

$$\beta = \frac{1}{2} \left(\frac{\ln Q_c - X_{Q_c}}{\zeta_{Q_c}} \right)^2 + \lambda t \left[1 - \exp \left(- \frac{\alpha_1 + Q_c}{\alpha_2} \right) \right] \quad (2.46)$$

This model was used to generate the risk-safety curves for various service lives, t , and return periods shown in Figs. 2.5 through 2.10. The safety factor used is the characteristic safety factor defined by Eq. (2.32).

2.7 NEED FOR EXPANDED MODEL

In this chapter the static and time-dependent reliability models have been developed. These models evaluate the reliability or risk associated with

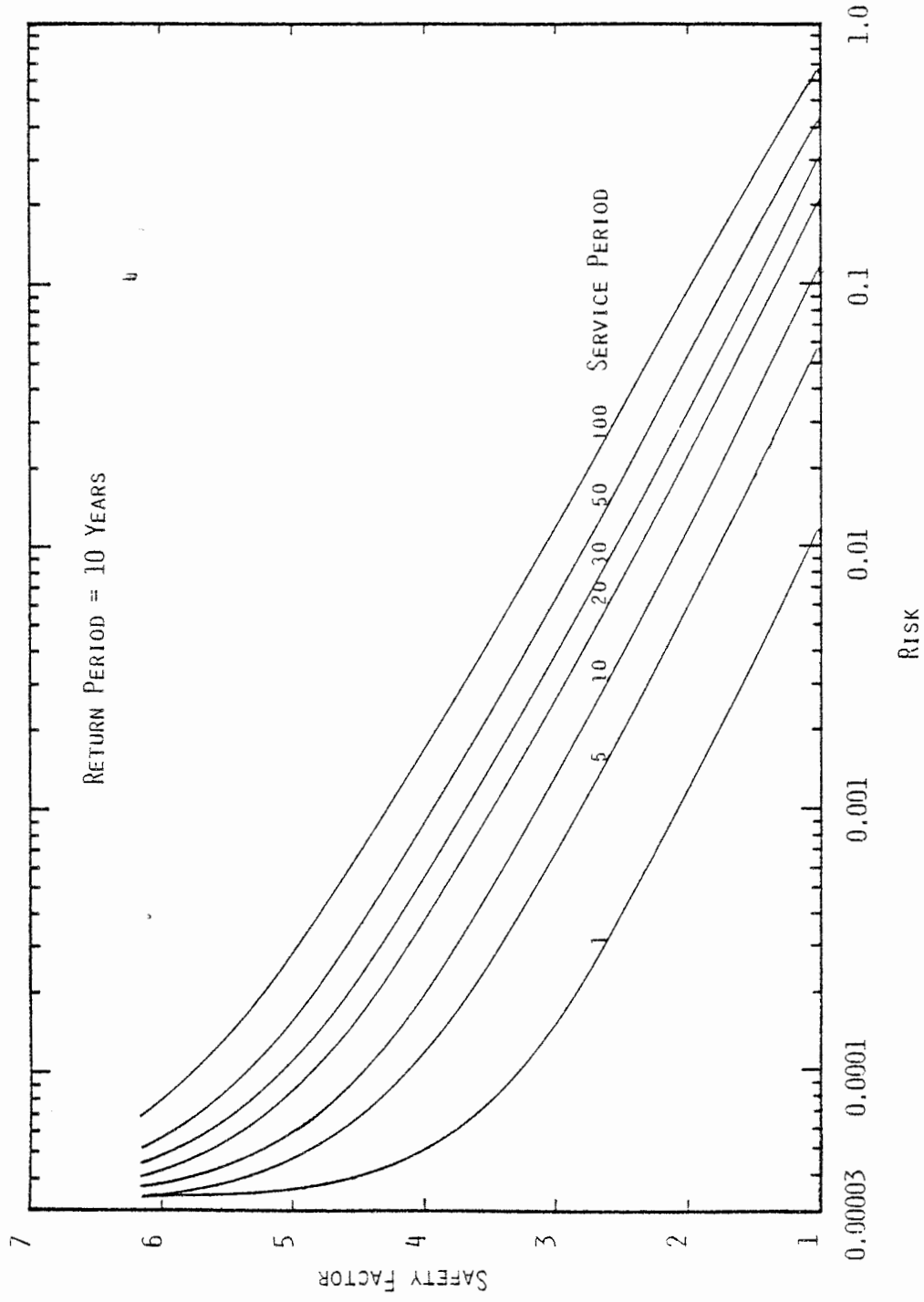


Figure 2.5 Risk-Safety Factor Curves for Culvert Design Based on Return Period 10 Years
(Time-Dependent Reliability Model)

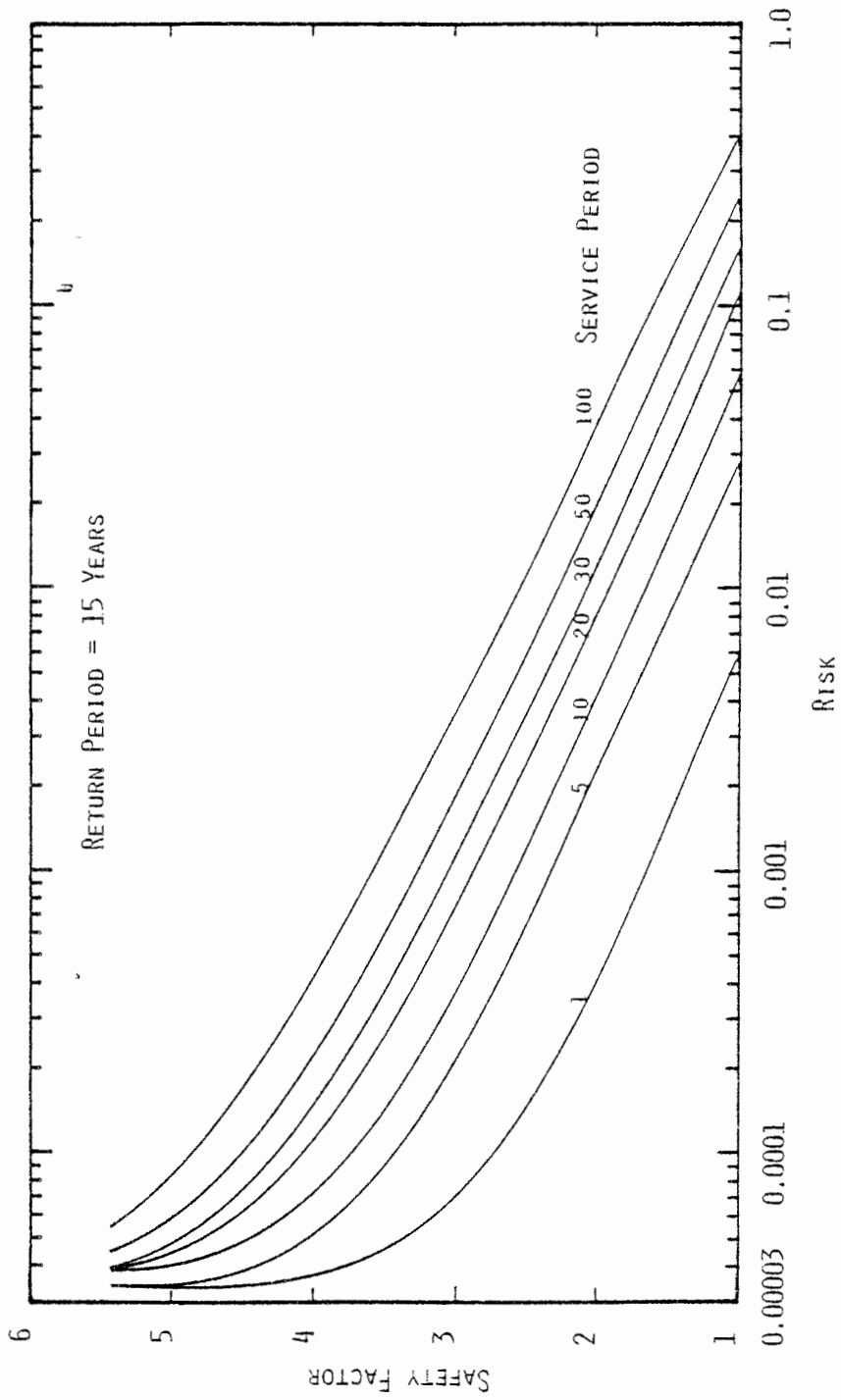


Figure 2.6 Risk-Safety Factor Curves for Culvert Design Based on Return Period 15 Years (Time-Dependent Reliability Model)

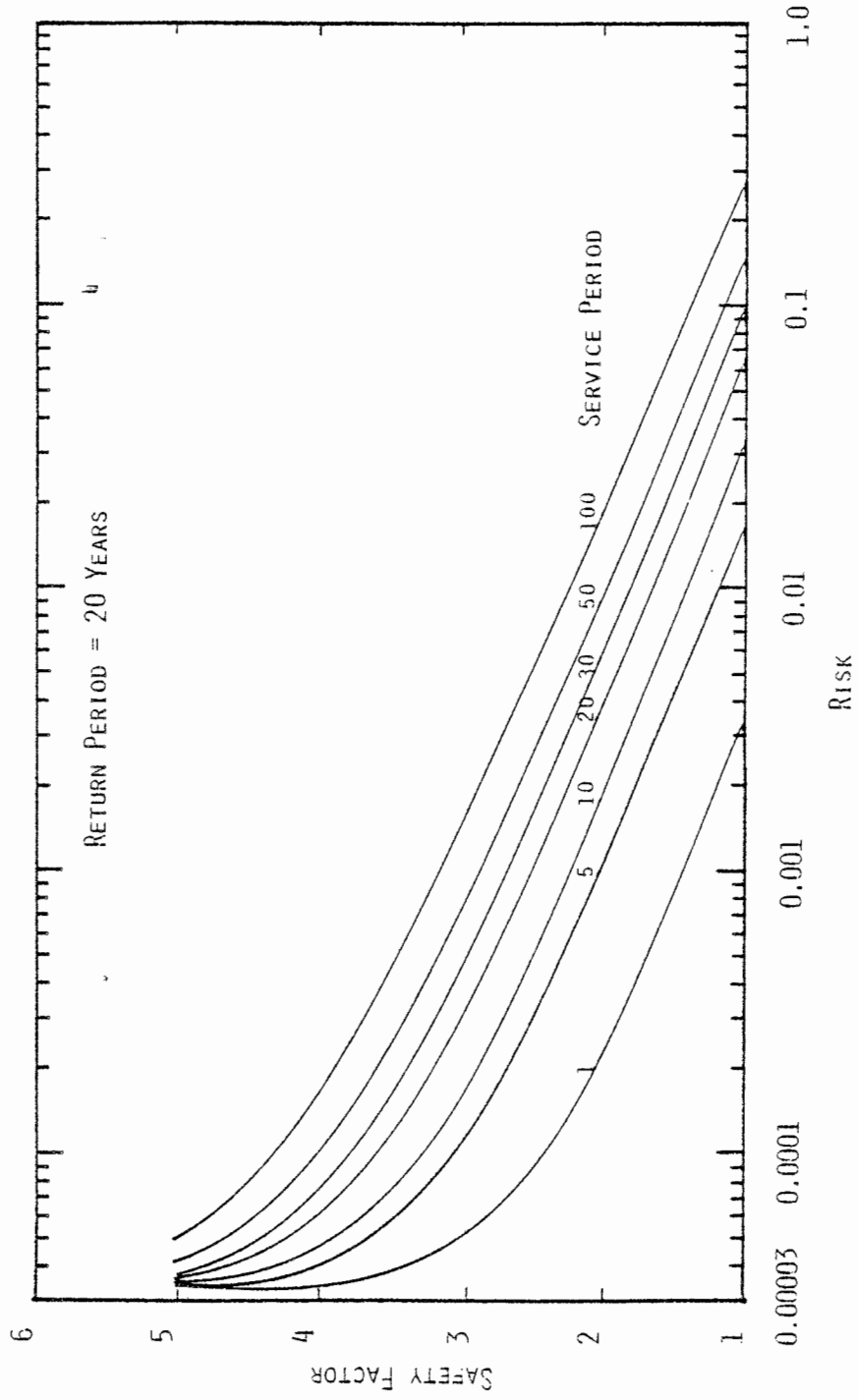


Figure 2.7 Risk-Safety Factor Curves for Culvert Design Based on Return Period 20 Years
(Time-Dependent Reliability Model)

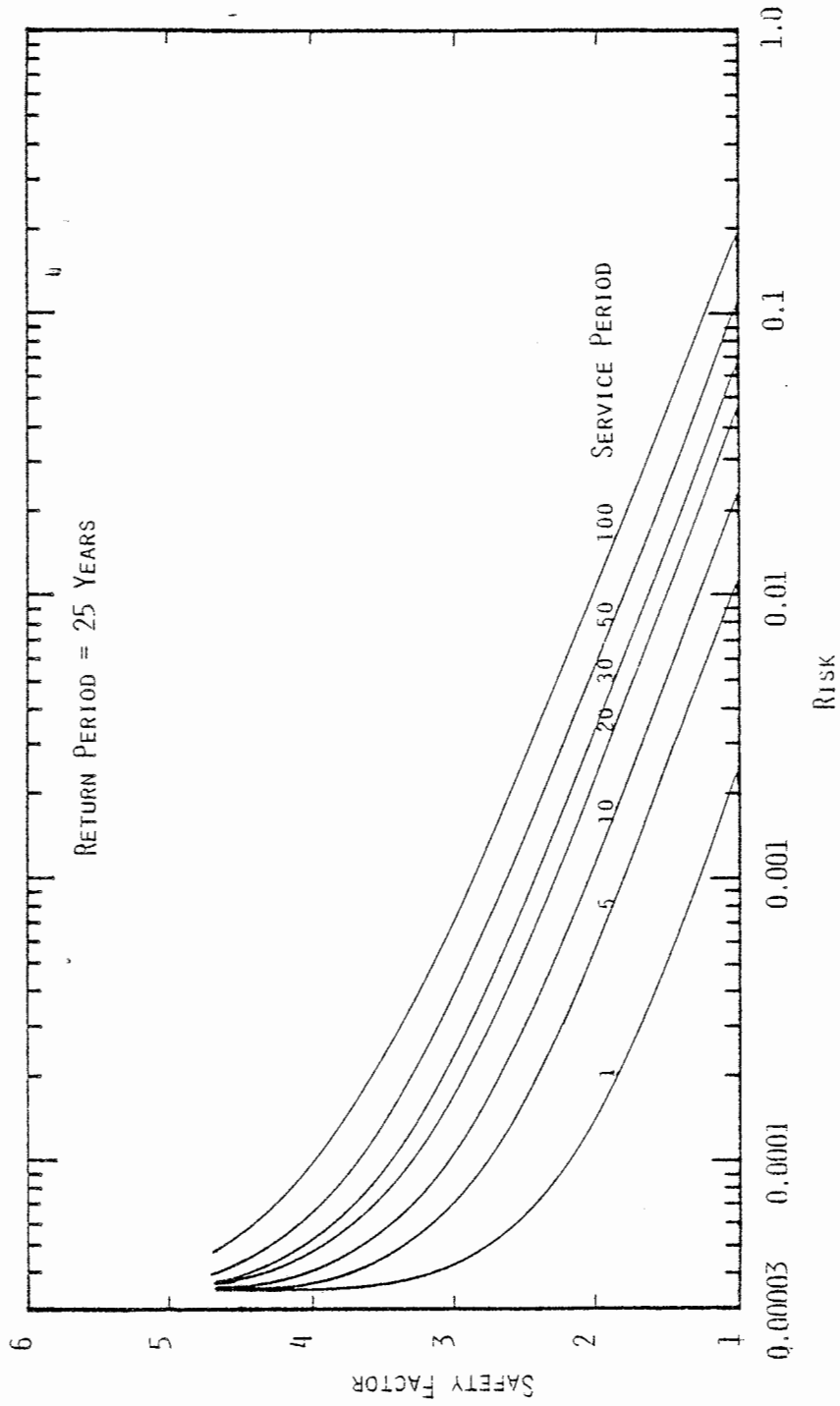


Figure 2.8 Risk-Safety Factor Curves for Culvert Design Based on Return Period 25 Years
(Time-Dependent Reliability Model)

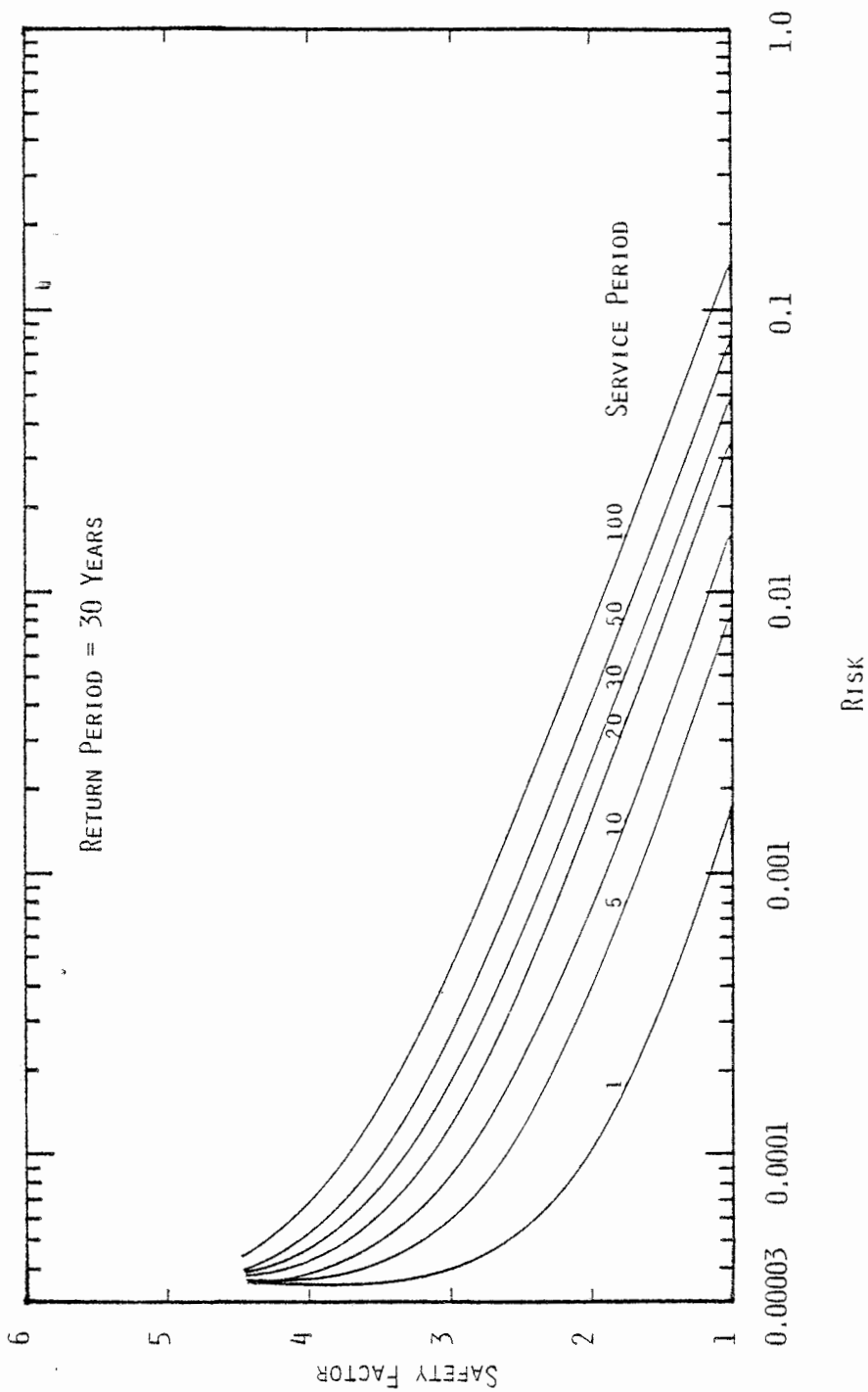


Figure 2.9 Risk-Safety Factor Curves for Culvert Design Based on Return Period 30 Years
(Time-Dependent Reliability Model)

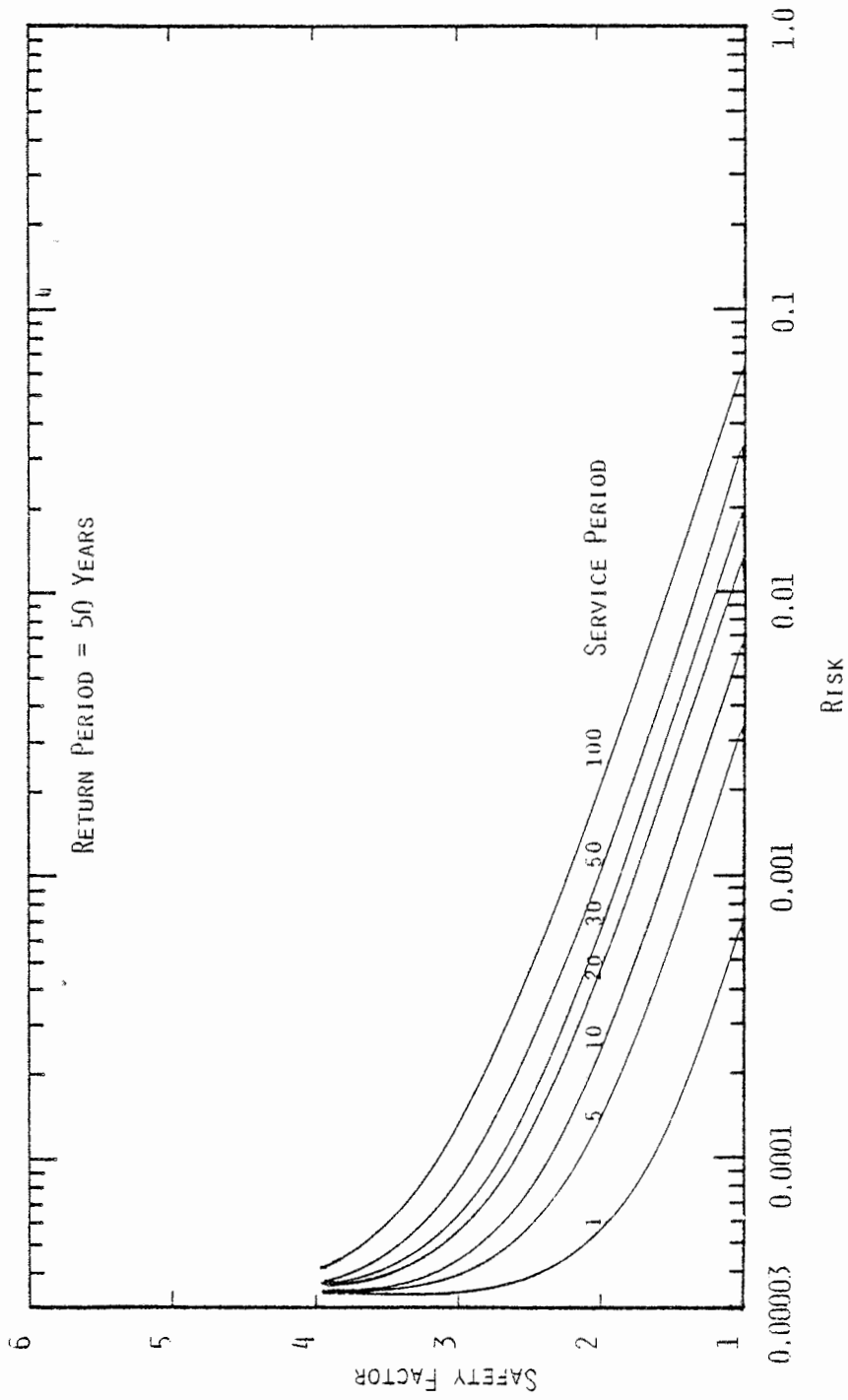


Figure 2.10 Risk-Safety Factor Curves for Culvert Design Based on Return Period 50 Years
(Time-Dependent Reliability Model)

the hydraulic structure taking into account the uncertainties involved in the determination of hydraulic structure capacity as well as the inherent hydrologic loading uncertainty. Examples for applying the static and time-dependent reliability models in determining the risk-safety factor relationship for the culvert design are given. It has been discussed that the risk associated with a design tends to be underestimated by the conventionally considered inherent hydrologic risk only as opposed to including hydraulic uncertainty. As mentioned, in addition to the inherent hydrologic uncertainty, other types of hydrologic uncertainties such as model and parameter uncertainties are involved. The ignorance of the existence model and parameter uncertainties can lead to an inadequate evaluation of the risk. Hence, for a better evaluation of the risk, a procedure is needed that takes into account the uncertainty attributed by the assessment of the hydrologic model and its parameters. In the next chapter procedures for treating the parameter uncertainty as well as model uncertainty are described.

CHAPTER 3

HYDROLOGIC UNCERTAINTIES

3.1 INTRODUCTION

In the risk-reliability analysis of water resources engineering project design, it is always desirable and rather ideal to have procedures for accurate prediction of hydrologic events, e.g. flood magnitudes and rainfall depths. This could be achieved if a large number of hydrologic data are available for the site under investigation. However, hydrologic data commonly extends only over a period of 10 to 30 years, with some locations having longer records and a large number of locations having no records. Stream flow and rainfall processes are assumed to be stochastic processes because of the natural, or inherent, randomness of their occurrence. Because of the lack of better information about these events, e.g. infinitely long historical records, there exists informational uncertainties about the processes which are the parameter and model uncertainties. There is presently much debate among hydrologic researchers concerning these uncertainties and how to consider them. This chapter presents methods for reducing or minimizing the hydrologic parameter and model uncertainties that can be used in the risk and reliability models.

The common practice in hydrologic frequency analysis is to fit observations to theoretical probability distributions. The practical problems

that are encountered are (1) the choice of distribution, and (2) how to estimate the parameters of the distribution. The parameters are commonly derived by the method of moments, but can also be derived by the method of maximum likelihood. Because only a limited number of hydrologic data are usually available, sample sizes are too small to accurately estimate the statistical parameters, the mean, standard deviation and especially high-order moments such as skewness and kurtosis. Consequently these parameters are random variables and subject to sampling errors. A procedure is developed that can be used to modify the hydrologic parameters estimated from a sample to reduce the errors or uncertainty of the estimate.

3.2 HYDROLOGIC PARAMETER UNCERTAINTIES

3.2.1 Hydrologic Parameters for Frequency Analysis

In the hydrologic flood flow frequency analysis the parameters commonly used to characterize the hydrologic frequency distribution are the mean, standard deviation, and skew coefficient which are estimated by the method of moment or the method of maximum likelihood. For a given flood flow sequence of an annual maximum series of record length N years z_1, z_2, \dots, z_N , the mean, standard deviation, and skew coefficient of the series can be estimated respectively, by method of moments using

$$\bar{z}_s = \frac{1}{N} \sum_{i=1}^N z_i \quad (3.1)$$

$$S_{z_s} = \left[\frac{1}{N-1} \sum_{i=1}^N (z_i - \bar{z}_s)^2 \right]^{1/2} \quad (3.2)$$

and

$$G_{Z_s} = \frac{N}{(N-1)(N-2)S_{Z_s}^3} \sum_{i=1}^N (z_i - \bar{z}_s)^3 \quad (3.3)$$

These parameters are required when the flood flow frequency distribution is either a normal, an extremal type I (Gumbel), or a Pearson type III.

The Hydrology Committee of the Water Resources Council (1967) recommended the log-Pearson type III as a base method for flood flow frequency studies. This was an attempt to promote a uniform and consistent approach to flood-flow determination for use in all Federal planning that involves water and related land resources. It was also recommended for use by all state and local governments and private engineers. Further guidelines were set forth by the Water Resources Council (1976) in Bulletin 17. The log-Pearson type III distribution is a three parameter distribution requiring parameters for the log transformed flood flows, i.e., \bar{Y}_s (mean), S_{y_s} (standard deviation), and G_{y_s} (skew coefficient) that are generally used to estimate the population parameters μ_y , σ_y , and γ_y , respectively. These parameters can be estimated using the sample, respectively, by the method of moments, as

$$\bar{Y}_s = \frac{1}{N} \sum_{i=1}^N y_i \quad (3.4)$$

$$S_{y_s} = \left[\frac{1}{N-1} \sum_{i=1}^N (y_i - \bar{Y}_s)^2 \right]^{1/2} \quad (3.5)$$

$$G_{y_s} = \frac{N}{(N-1)(N-2)S_{y_s}^3} \sum_{i=1}^N (y_i - \bar{Y}_s)^3 \quad (3.6)$$

where y_i is the log transformation of the flood magnitude $y_i = \ln(z_i)$; and N

is the number of observations (z_1, z_2, \dots, z_N). For flood flows that follow a log-normal distribution the parameter estimates of the mean and standard deviation are given by Eqs. (3.4) and (3.5) respectively.

The parameter estimates derived from the sample, and also referred to as sample statistics, are functions of random variables. Hence the parameter estimates are random variables with associated sampling distributions. Flood frequency curves generated in a statistical analysis depend on the parameter estimates and therefore are subject to the errors inherent in estimating the population parameters from sample statistics.

3.2.2 Review of Previous Works on Parameter Uncertainty

It is only recently that other uncertainties in addition to the natural or inherent hydrologic uncertainties have been considered explicitly on a scientific basis. Basically, there have been works to consider the hydrologic uncertainties (inherent, parameter, and model) and also a few attempts to look at the hydraulic uncertainties. Some works have considered the natural and parameter uncertainties or the natural and model uncertainties and some works attempt to consider all three uncertainties. Most of these works have dealt with improving flood frequency estimates by incorporating parameter and/or model uncertainties into the hydrologic analysis [Bernier (1967); Bodo and Unny (1976); Conover (1971); Cornell (1972); Davis and Dvoranchik (1971); Davis et al. (1972); Vicens, et al. (1975); Wood (1977); Wood and Rodriguez-Iturbe (1975a); Wood and Rodriguez-Iturbe (1975b)]. Most of these works consider the hydrologic uncertainties through a Bayesian framework.

As previously mentioned, the U.S. Water Resources Council (WRC) recommends the use of the log-Pearson type III distribution as the base method for flood flow frequency studies. This three parameter distribution requires the skew coefficient which has greater variability between samples than the mean and standard deviation. Because the estimate of skewness is biased and subject to large sampling errors, Hardison (1974) developed generalized skew coefficients for use in determining flood frequency curves that follow the log-Pearson type III distribution. These generalized skew coefficients were illustrated by isopleths on a map of the United States. The Hydrology Committee of the Water Resources Council (1976) suggested the use of a generalized or regional value of the skew coefficient as opposed to the skew coefficient from a short record. The generalized skew was provided on maps, Fig. 3.1, to obtain a map (regional) skew coefficient, G_{y_r} , for a specific site. In addition the use of a weighted average of the sample skewness, G_{y_s} , and the map skewness, G_{y_r} , was suggested as

$$\hat{G}_y = W_{G_y} \cdot G_{y_s} + (1 - W_{G_y}) \cdot G_{y_r} \quad (3.7)$$

where G_y is the skewness to be used in flood frequency studies using log-Pearson type III distribution and W_{G_y} is a skew weighting factor ($0 \leq W_{G_y} \leq 1$). The Water Resources Council (1976) further recommends using the sample statistics \bar{Y}_s and S_{y_s} computed by Eqs. (3.4) and (3.5) respectively, along with a weighted skew coefficient defined by Eq. (3.7) to estimate peak flows. The recommended skew weights are defined as

$$W_{G_y, \text{WRC}} = \begin{cases} 0 & N \leq 25 \\ \frac{(N - 25)}{75} & 25 \leq N \leq 100 \\ 1 & N \geq 100 \end{cases} \quad (3.8)$$

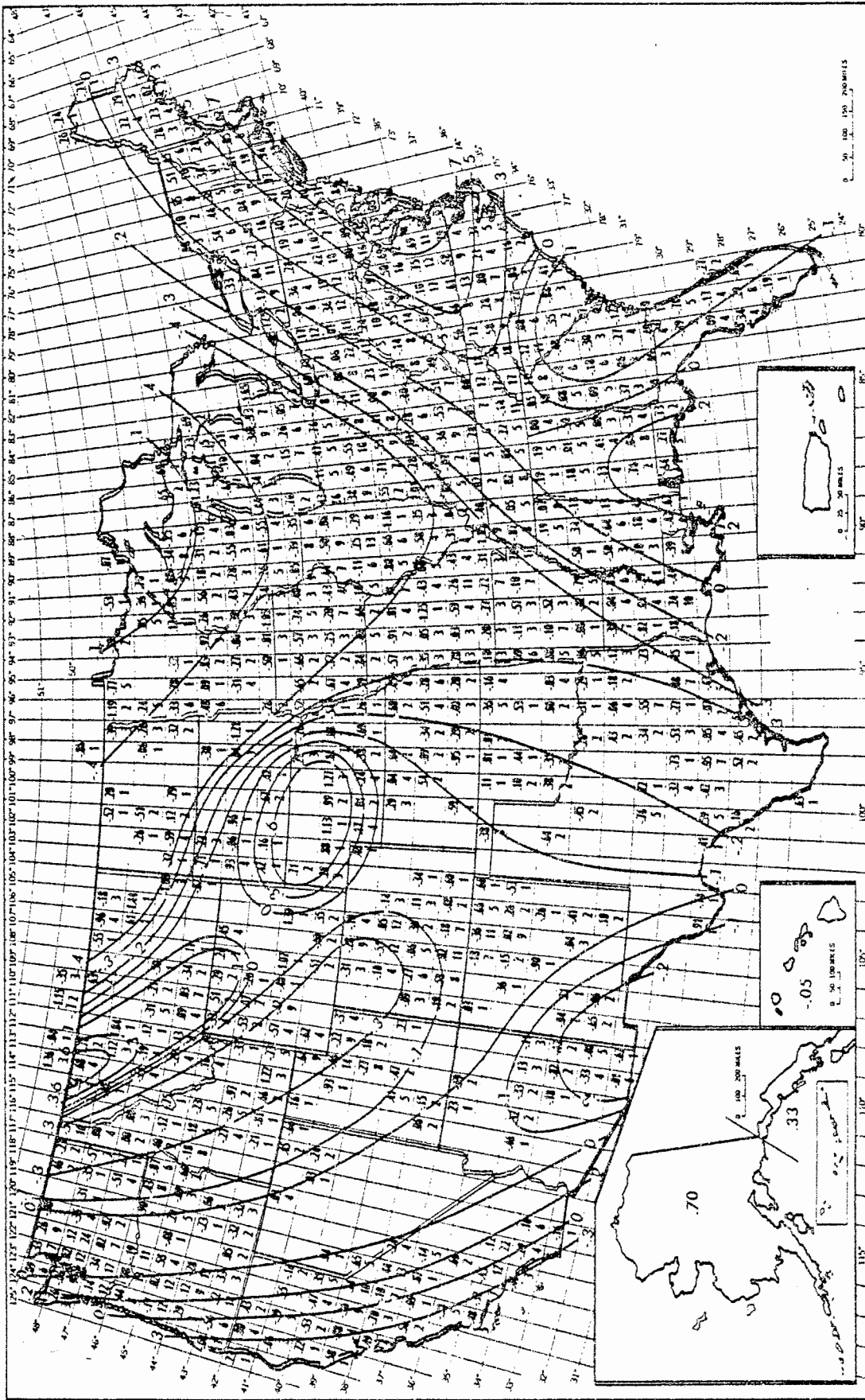


Figure 3.1 Generalized Skew Coefficient Map (W.R.C., 1976)

which are a function of sample size, N , only. This method has no theoretical basis and determines the weight regardless of sample and regional information available. It has the disadvantage of discarding information contained in the sample collection when the size is less than 25 while taking full confidence on the sample skewness when sample size is greater than 100 which neglects the fact that the sample statistic is a random variable with associated variance even though it is derived from a large sample. McCuen (1979) pointed out that the above weighting procedure tends to give excessive weight to the map skewness especially for small sample sizes. For a station with a record length of 25 years, the weighting function, Eq. (3.8) would give a weight of zero to the sample skewness, even though the variance of the map skew, 0.55^2 provided by Bulletin 17 (WRC, 1976) as given by Fig. 3.1, is greater than the variance of the sample skewness.

Wallis, et al. (1974) applied the Monte Carlo method to derive an empirical formula for the standard error of sample statistics which is a function of the population parameters, sample size, and type of distribution from which the sample is taken. Direct application of the derived empirical formulas is not possible because the population parameters and true probability distribution are unknown. Later, Tasker (1978) used the results of Wallis' work and proposed an expression for the weight as

$$W_{G_y, \text{Tasker}} = \frac{N}{N+20} \quad (3.9)$$

which is a function of sample size only, provided that the variance of regional skewness is 0.55^2 , regardless of the value of the population parameters.

The other limitation of Tasker's weighting factor is that the distribution of the annual maximum series is for a log-Pearson type III distribution.

Tasker (1978) examined the sensitivity of estimated peak flows to errors in generalized skew coefficients by Monte Carlo experiments. Using simulated data, 10-, 50-, 100-, and 500-year peak flows were estimated by four methods. Two methods consisted of using the sample mean and variance, with $W_{G_y} = 0$ and then with $W_{G_y} = 1$ in Eq. (3.7). The other two methods were the Water Resources Council Method, Eq. (3.8), and Tasker's Method, Eq. (3.9). Tasker concluded that the use of a generalized skew coefficient can improve the accuracy of estimated peak flows provided its accuracy is evaluated and taken into account in the weighting procedure. It was also concluded that determining a weighted average skew coefficient using the weighting factor recommended by the Water Resources Council (1976) often results in a poorer estimate of the population skew coefficient than using the sample skew coefficient alone.

A methodology is introduced in the next section that can be used in hydrologic frequency analysis to reduce the parameter uncertainty. The methodology consists of developing generalized values of the parameters (mean, standard deviation, and skewness) through the use of a weighting procedure between sample and regionalized parameter estimates. The weights are defined as a function of the variances of the sample parameter estimates and regionalized parameter estimates.

3.2.3 Weighted Parameter Estimates

Weighted parameter estimates (mean, standard deviation, and skewness) are now considered that combine both parameter estimates from sample data and estimates from regional information. Hydrologists have recognized that hydrological information often can be transferred among watersheds or even river basins. The transferring of information has the function of data augmentation which hopefully increases the reliability of the analysis. As a rule of thumb, accuracy increases with the amount of information that is available. For a hydrologist there usually are two sources of information available. One is from local sample data collected and the other is from regional information. A general equation relating parameter estimates, $\hat{\theta}$, based upon the sample data and upon regional information can be expressed as

$$\hat{\theta} = W_{\theta} \cdot \theta_s + (1-W_{\theta}) \cdot \theta_r \quad (3.10)$$

where θ_s and θ_r are hydrological parameter estimates (mean, standard deviation, and skewness) from the sample data and from regional information, respectively and W_{θ} is the weight. The question is how to combine the parameter estimates to yield the "best" result, i.e., to minimize parameter uncertainty. The commonly used expression and measure of uncertainty feature of an estimate is the variance. Assuming that θ_s and θ_r are independent estimates and assuming they have the same mean, the variance of $\hat{\theta}$ can be expressed as

$$\text{Var}(\hat{\theta}) = W_{\theta}^2 \cdot \text{Var}(\theta_s) + (1-W_{\theta})^2 \cdot \text{Var}(\theta_r) \quad (3.11)$$

where $\text{Var}(\theta_s)$ and $\text{Var}(\theta_r)$ are variances of the hydrological parameter estimates derived from the sample data and regional information, respectively. As can be seen from Eq. (3.11) the variance of a weighted parameter estimate, $\hat{\theta}$, is a convex function of W_θ . Hence, the functional form of the weight, W_θ , which minimizes the variance of $\hat{\theta}$ is

$$W_\theta = \frac{\text{Var}(\theta_r)}{\text{Var}(\theta_s) + \text{Var}(\theta_r)} \quad (3.12)$$

which is determined by differentiating Eq. (3.11) with respect to W_θ and solving $d[\text{Var}(\hat{\theta})]/dW_\theta = 0$ for W_θ . This optimal functional form of the weighting factor, Eq. (3.12), takes into account the trade-off between the information contained in the sample estimate and the regional estimate. A measure of information of the estimate is the reciprocal of the variance. A larger value of variance corresponds to less information. In this case, if the value of the variance of the regional parameter estimate is larger than that of the sample estimate, more weight is given to the sample estimate.

The determination of W_θ using Eq. (3.12) requires the values of both $\text{Var}(\theta_s)$ and $\text{Var}(\theta_r)$. The variances of the parameter estimates from the sample data, $\text{Var}(\theta_s)$ can be determined using two non-parametric statistical methods called the bootstrap and the jackknife. While the variance of the regional parameter estimate, $\text{Var}(\theta_r)$ can be derived using regression analysis relating θ_r to physiographic and meteorological characteristics of the watershed or river basin considered. The details and application of the jackknife, bootstrap, and regression analysis are described in later sections.

3.2.4 Variance of Sample Estimators

Two non-parametric statistical methods, namely the jackknife and bootstrap methods which make no assumption about the distribution function are especially useful to determine $\text{Var}(\theta_s)$. These non-parametric methods do pay a computational price for their freedom from normal distribution theory. However, the use of the computer makes these methods very tractable rather than a nightmare for the user.

3.2.4.1 Jackknife Method

The jackknife, introduced in late 1950, is an intriguing attempt to answer an important statistical problem: "Having computed an estimate of some quantity of interest, what accuracy can be attached to the estimate?" Accuracy here refers to the " \pm something" which often accompanies statistical estimates. The usual \pm quantities are based on normal distribution theory, or occasionally on some other parametric theory, while the jackknife is a nonparametric technique which makes no assumption on the distribution. Miller (1974) gave an excellent review of this method. The jackknife method has the function of bias correction which makes this method more favorable. The most commonly used expression for the "accuracy" of an estimate is the standard deviation. The jackknife procedure can be used to compute the standard deviation of parameter estimates as follows:

1. Compute the estimate of interest, θ_s , from the N sample observations.
2. For each observation $i = 1, \dots, N$, compute $\theta_s^{(i)}$ from $N -$

1 observations with the i -th observation deleted from the data set.

3. Compute the accuracy of θ_s using

$$\hat{\sigma}^{(J)} = \left[\frac{N-1}{N} \sum_{i=1}^N (\theta_s^{(i)} - \theta_s)^2 \right]^{1/2} \quad (3.13)$$

where $\hat{\sigma}^{(J)}$ is the jackknifed standard deviation of the estimate θ_s . For the purpose of bias correction, statisticians usually replace θ_s by $1/N \sum_{i=1}^N \theta_s^{(i)}$ in Eq. (3.13); otherwise, with no bias correction, θ_s is made.

Hence, for a given set of observations the jackknifed standard deviation of the estimate, θ_s , can be computed by the procedures described above. The variance of θ_s is expressed as

$$\text{Var}^{(J)}(\theta_s) = [\hat{\sigma}^{(J)}]^2 \quad (3.14)$$

which can be used to calculate the weight using Eq. (3.14). Readers are referred to Efron (1978) and Miller (1974) for the details of the theory of this method.

3.2.4.2 Bootstrap Method

Efron (1977) developed the bootstrap method which can also be used to assess the accuracy of any estimate of interest derived from a sample. From the theoretical point of view, the bootstrap is more widely applicable than the jackknife, and also more dependable (Efron, 1977, 1978). The procedures of this method are outlined as follows (Efron, 1977):

1. Let \hat{F} be an empirical distribution of N observed data points, $\{y_i, i = 1, \dots, N\}$, i.e., $1/N$ is the probability of occurrence assigned to each of the observations.

2. Use a random number generator to draw N new points $\{y_i^*, i=1, \dots, N\}$ independently and with replacement from \hat{F} , so each new point is an independent random selection of one of the N original data points. This set of N new points is called the bootstrap sample which is a subset of the original data points.
3. Compute the estimate θ_s^* for the bootstrap sample $\{y_i^*, i=1, \dots, N\}$.
4. Repeat steps (2) and (3) a large number of times, say $m=1, \dots, M_B$ times each time using an independent set of new random numbers to generate the new bootstrap sample. The resulting sequence of bootstrap statistics are $\theta_s^{*(m)}, m=1, \dots, M_B$.
5. The variance of θ_s can be calculated as

$$\text{var}(\theta_s) = \frac{1}{M_B} \sum_{m=1}^{M_B} \left(\theta_s^{*(m)} - \bar{\theta}_s^* \right)^2 \quad (3.15)$$

in which

$$\bar{\theta}_s^* = \frac{1}{M_B} \sum_{m=1}^{M_B} \theta_s^{*(m)}$$

3.2.5 Applications of Jackknife and Bootstrap

The jackknife and bootstrap methods described above can be used to compute the variance of any number of statistics (e.g. mean, standard deviation, and skew) derived from a sample. Applications of the jackknife and the bootstrap methods of estimating the variance of sample statistics are

made. Two sets of stream flow record are considered; Mill Creek near Los Molinos, California, with a record length of 30 years (Beard, 1962), and Greenbrier River at Alderson, West Virginia, with a record length of 72 years (Zelenhasiz, 1970). Records of annual maximum streamflow for these two locations are listed in Table 3.1. The results of the analysis of accuracy of the sample statistics derived from using Eqs. (3.4), (3.5), and (3.6) for these two sets of records by applying jackknife method and bootstrap method are shown in Tables 3.2 and 3.3. The standard error of the sample statistics, mean, standard deviation and skew are denoted as $\sigma_{\bar{Y}_s}$, $\sigma_{S_{y_s}}$, $\sigma_{G_{y_s}}$, respectively, and M_B is the number of sets of bootstrap samples generated.

The following is a summary of methods used to compute generalized skew coefficients by assuming the flow sequences follow log-Pearson type III distribution.

1. Sample statistics: Uses Eq. (3.6) to determine G_{y_s} then uses $W_{G_y} = 1$ in Eq. (3.7), i.e. $\hat{G}_y = G_{y_s}$.
2. W.R.C. Method: This method uses Eq. (3.6) to compute G_{y_s} and G_{y_r} is obtained from the regional skew map, Fig. 3.1. The weight, $W_{G_{y,WRC}}$ is computed using Eq. (3.8). The generalized skew coefficient, \hat{G}_y , is then computed using Eq. (3.7).
3. Tasker's Method: This method uses Eq. (3.6) to compute G_{y_s} . G_{y_r} is obtained from the regional skew map, Fig. 3.1. The weight, $W_{G_{y,Tasker}}$ is computed using Eq. (3.9). The

Table 3.1a Annual Maximum Series for
Mill Creek near Los Molinos, California

Year	Peak Discharge (cfs)	Year	Peak Discharge (cfs)
1929	1,520	1944	3,220
1930	6,000	1945	3,230
1931	1,500	1946	6,180
1932	5,440	1947	4,070
1933	1,080	1948	7,320
1934	2,630	1949	3,870
1935	4,010	1950	4,430
1936	4,380	1951	3,870
1937	3,310	1952	5,280
1938	23,000	1953	7,710
1939	1,260	1954	4,910
1940	11,400	1955	2,480
1941	12,200	1956	9,180
1942	11,000	1957	6,140
1943	6,970	1958	6,880

Table 3.1b Annual Maximum Series for
Greenbrier River at Alderson, W. Va

Year	Peak Discharge (cfs)	Year	Peak Discharge (cfs)	Year	Peak Discharge (cfs)
1896	28,800	1920	38,000	1944	25,200
1897	54,000	1921	0	1945	19,000
1898	52,500	1922	22,200	1946	43,600
1899	48,900	1923	19,500	1947	24,400
1900	17,100	1924	36,200	1948	40,300
1901	56,800	1925	0	1949	37,100
1902	43,800	1926	20,700	1950	31,500
1903	48,900	1927	40,200	1951	29,300
1904	25,700	1928	18,000	1952	27,600
1905	37,600	1929	32,700	1953	47,100
1906	26,000	1930	36,600	1954	29,700
1907	52,500	1931	0	1955	44,400
1908	52,500	1932	50,100	1956	18,200
1909	20,000	1933	26,400	1957	28,900
1910	45,900	1934	32,300	1958	26,700
1911	43,800	1935	49,600	1959	23,900
1912	35,500	1936	58,600	1960	35,500
1913	47,000	1937	36,600	1961	31,400
1914	0	1938	32,300	1962	35,500
1915	40,000	1939	41,600	1963	47,200
1916	27,200	1940	29,900	1964	39,600
1917	43,000	1941	0	1965	28,400
1918	77,500	1942	35,300	1966	54,500
1919	59,000	1943	36,200		

Table 3.2 Standard Errors of the Sample Statistics for
Mill Creek

	Jackknife Method		Bootstrap Method	
	bias correction	No bias correction	$M_B = 500$	$M_B = 1000$
$\sigma_{\bar{Y}_s}$	0.05533	0.05533	0.05221	0.05144
$\sigma_{S_{Y_s}}$	0.04217	0.04217	0.03578	0.03480
$\sigma_{G_{Y_s}}$	0.45993	0.45945	0.35669	0.35425

Table 3.3 Standard Error of the Sample Statistics for
The Greenbrier River

	Jackknife Method		Bootstrap Method
	with bias correction	with no bias correction	$M_B = 500$
$\sigma_{\bar{Y}_s}$	0.01806	0.01806	0.01884
σ_{S_s}	0.01120	0.01120	0.00559
σ_{G_s}	0.22418	0.22418	0.13491

generalized skew coefficient, G_y , is then computed using Eq. (3.7).

4. Fisher's Method: For the sake of comparison and its popular application in water resource engineering, Fisher's method for computing the standard error of sample skewness is also considered. This method assumes that the sample follows a normal distribution. The variance of the sample skew coefficient is approximated by

$$\text{Var}^{(F)}(G_s) = \frac{6N(N-1)}{(N-2)(N+1)(N+3)} \quad (3.16)$$

using $\text{Var}^{(F)}(G_s)$ from Eq. (3.16) for $\text{Var}(G_{y_s})$ and $\text{Var}(G_{y_r})$ from the W.R.C. skew map, (Fig. 3.1), $W_{G_y, \text{Fisher}}$ can be determined using Eq. (3.12). The generalized skew coefficient, G_y , is then computed using Eq. (3.7). Matalas and Benson (1968) used Eq. (3.16) to analyze standard errors of skew coefficients to assess the values of skew coefficients from any size sample. The most obvious limitation of this procedure is the underlying assumption of normal distribution theory. If the flood sequence investigated follows a distribution other than normal distribution the use of Eq. (3.16) to compute the variance of sample skewness leads to theoretical error.

5. Jackknife Method: This method uses Eq. (3.6) to compute G_{y_s} . G_{y_r} can be obtained from a regional skew map such as

in Fig. 3.1 or from a regression study. $\text{Var}(G_{y_s})$ is computed using Eq. (3.14) and $\text{Var}(G_{y_r}) = 0.55^2$ if from Fig. 3.1 or can be determined from a regression study. Eq. (3.12) is used to compute $W_{G_{y,\text{Jackknife}}}$ and \hat{G}_y is computed using Eq. (3.7)

6. Bootstrap Method: This method is identical to the Jackknife method except here the bootstrap method, Eq. (3.15) is used to compute $\text{Var}(G_{y_s})$.

Table 3.4 shows the skew weighting factors derived using each of the five methods described for these two sets of stream flow records. Variance of regional skewness used is 0.55^2 which is for the skew coefficient map in Fig. 3.1. However, this application gives no indication of which method provides the best answer. An experimental study was performed to compare the validity of these methods. Clearly, Table 3.4 provides evidence supporting McCuen's statement that excessive weight is given to the map skew by WRC method.

An experimental study was performed to compare the various methods described above for determining the generalized skew coefficients including the use of the sample statistic, alone ($W_{G_y} = 1$). As an illustration the log-Pearson type III distribution is adopted in the experimental study. The analytical method of curve fitting used in flood frequency analysis is

$$\log(Z_{T_r}) = \mu_y + K_{T_r} \cdot \sigma_y \quad (3.17)$$

in which Z_{T_r} is the magnitude of a flood of return period T_r , K_{T_r} is the frequency factor which is a function of the skew coefficient and the

Table 3.4 Skew Weights for the Methods

Sample	$W_{G,W.R.C.}$	$W_{G,Fisher}$	$W_{G,Tasker}$	$W_{G,Jackknife}$	$W_{G,Bootstrap}$
Mill Creek N = 30	0.0667	0.60240	0.6000	0.5891	0.7039
Greenbrier River N = 72	0.6267	0.7908	0.7826	0.8575	0.9432

probability of exceedence, $1/T_r$, and μ_y and σ_y are the mean and standard deviation of log-transformed flows which can be estimated using Eqs. (3.5) and (3.6), respectively. The tabulated values of K_{T_r} with respect to $P_r(x \geq X_{T_r})$ and skew coefficient are available in most standard hydrology books. An analytical expression for log-Pearson type III distribution is presented by Kite (1977) as

$$K_{T_r} \approx t + (t^2 - 1) \frac{G}{6} + \frac{1}{3} (t^3 - 6t) \left(\frac{G}{6}\right)^2 - (t^2 - 1) \left(\frac{G}{6}\right)^3 + t \left(\frac{G}{6}\right)^4 + \frac{1}{3} \left(\frac{G}{6}\right)^5 \quad (3.18)$$

where t is the standard normal deviate and G is skew coefficient. Six methods (sample statistics, WRC, Tasker, Fisher, jackknife and bootstrap) are considered to determine the generalized (weighted) skew as discussed above using $G = \hat{G}_y$. Each of these methods provides different weights and different generalized skew coefficient, accordingly. Because the frequency factor, K_{T_r} is dependent on the skew coefficient as shown in Eq. (3.18), different magnitudes of K_{T_r} for the same μ_y and σ_y in Eq. (3.14) are possible.

The skew coefficient and the exceedence probability define the value of the frequency factor in analytical flood flow frequency analysis. In the experimental study, comparison is made of frequency factor values derived by each of the above six methods for determining the skew weighting factor.

The procedure for this experimental study is as follows:

1. For a set of population parameters, a sequence of pseudo random numbers is generated for the log-Pearson type III

distribution. In this study the logarithmic population mean, standard deviation, and skewness used are 3.5, 0.3, and 0.2, respectively, and a return period of 1000 years is used.

2. The generated sequence is divided into I subsets with each subset of size N . The size of subsets examined are $N = 10, 30, 50,$ and $70,$ and the total number of subsets generated for each size is 500.
3. Consider the subsets with size $N = 10$.
4. The sample statistics such as the mean, $\bar{Y}_s,$ standard deviation, $S_{y_s},$ skewness, $G_{y_s},$ using Eq. (3.4) through (3.6) for each subset is computed.
5. The weight, $W_{G_y},$ for each subset is computed for each method.
 - a. Use of sample statistics ($W_{G_y} = 1$).
 - b. WRC method uses Eq. (3.8) to compute $W_{G_y, \text{WRC}}$ for $W_{G_y}.$
 - c. Tasker's method uses Eq. (3.9) to compute $W_{G_y, \text{Tasker}}$ for $W_{G_y}.$
 - d. Fisher's method uses Eq. (3.10) to obtain $\text{Var}^{(F)}(G_{y_s})$ then uses Eq. (3.12) with $\text{Var}(G_{y_r}) = 0.55^2$ to obtain $W_{G_y, \text{Fisher}}$ for $W_{G_y}.$
 - e. Jackknife method uses the jackknifing procedure to obtain $\text{Var}^{(J)}(G_{y_s})$ then uses Eq. (3.12) with $\text{Var}(G_{y_r}) = 0.55^2$ to obtain $W_{G_y, \text{Jackknife}}$ for $W_{G_y}.$
 - f. Bootstrap method uses the bootstrap procedure to obtain

$\text{Var}^{(B)}(G_{y_s})$ then uses Eq. (3.12) with $\text{Var}(G_{y_r}) = 0.55^2$ to

obtain $W_{G_{y, \text{Bootstrap}}}$ for W_{G_y} .

6. Next, the generalized skew coefficient, \hat{G}_y , is determined by each method using Eq. (3.7) for a given value of G_{y_r} ,
7. The frequency factor $\hat{K}_{T_r}^{(i)}$ is determined for each subset i , $i = 1, 2, \dots, 500$, for each method using the respective generalized skew coefficients found in step 6.
8. The root mean square error (rmse) of the frequency factor for each method is now determined. The rmse is defined as

$$\text{rmse} = \left\{ \frac{1}{500} \sum_{i=1}^{500} \left(\hat{K}_{T_r}^{(i)} - K_{T_r} \right)^2 \right\}^{1/2} \quad (3.19)$$
 where K_{T_r} is the frequency factor for a return period of T_r years, computed by Eq. (3.18) using the population skewness defined in step 1.
9. Steps 5 through 8 are repeated to compute the rmse for different values of the regional skewness within the interval of $(G_{y_r} - 0.6, G_{y_r} + 0.6)$. That is, the rmse of each subset of size N for values of $G_{y_r} = 0.80, 0.65, 0.50, 0.35, 0.20, 0.05, -0.10, -0.25,$ and -0.40 are computed.
10. Repeat the above steps 4 through 9 for various sample sizes, N values.

The reason for considering various map skew coefficients is as follows. In practice the true (population) value of skew coefficient is unknown and the map (or regional) skew coefficient is a random variable with an associated variance. It is possible to obtain an interval of specified

confidence level in which the true skewness will lie. For instance, if the true skewness lies between the interval $[G_{y_r} \pm 1.96 \sigma_{G_{y_r}}]$ with 95% confidence provided G_{y_r} is normally distributed with mean G_{y_r} and variance $\sigma_{G_{y_r}}^2$. In the experiment, on the contrary, the true (population) value of skew coefficient is known while the true map skew coefficient is not. Only estimated values are known. The sample skewness and the regional skewness are assumed to be the estimators of the same mean. The regional skewness is assumed to be distributed with mean 0.2 and variance 0.55^2 . More accurate analysis could be performed if the sampling distribution of the map (or regional) skewness is known. Tables 3.5 through 3.8 list the rmse of the frequency factors for each map skew coefficient considered and for each method of determining the skew weight. It is observed that the jackknife method provides the smallest average rmse except when $N = 70$. Based upon the average rmse, use of the sample skew coefficient is the least reliable.

The rmse versus the regional skewness for the WRC and jackknife methods for each sample size are shown in Figs. 3.2 and 3.3, respectively. It is observed that the variation of rmse with respect to regional skewness decreases as the number of observations increase, i.e., the value of rmse becomes less sensitive to the regional skewness as N gets larger. Therefore, as N gets larger, an estimator will have less uncertainty, which is to be expected. Figures 3.4, 3.5, 3.6, and 3.7 illustrate the variation of rmse versus regional skewness for each method for sample sizes of $N = 10, 30, 50,$ and $70,$ respectively. It is interesting to note that the use of sample statistics along ($W_{G_y} = 1$), in general, has the least variation but the highest values of rmse.

Table 3.5 Root-Mean Square Error of Frequency Factor, N = 10

Regional Skewness	Sample	Root-Mean Square Error of Frequency Factor K T				
		W. R. C.	Tasker	Fisher	Jackknife	Bootstrap
.80	0.943	0.908	0.637	0.619	0.599	0.589
.65	0.943	0.678	0.547	0.553	0.519	0.490
.50	0.943	0.450	0.428	0.456	0.398	0.411
.35	0.943	0.223	0.342	0.399	0.308	0.365
.20	0.943	0.000	0.335	0.381	0.299	0.362
.05	0.943	0.220	0.388	0.439	0.347	0.404
-.10	0.943	0.435	0.472	0.500	0.456	0.476
-.25	0.943	0.645	0.567	0.574	0.562	0.567
-.40	0.943	0.849	0.685	0.675	0.664	0.667
Average rmse	0.943	0.490	0.489	0.511	0.461	0.481

Table 3.6 Root-Mean Square Error of Frequency Factor, $N = 30$

Regional Skewness	Sample	Root-Mean Square Error of Frequency Factor K_T				
		W.R.C.	Tasker	Fisher	Jackknife	
.80	0.635	0.846	0.524	0.521	0.512	0.504
.65	0.635	0.630	0.444	0.448	0.443	0.464
.50	0.635	0.418	0.410	0.419	0.389	0.434
.35	0.635	0.209	0.389	0.405	0.379	0.413
.20	0.635	0.043	0.373	0.386	0.370	0.404
.05	0.635	0.213	0.398	0.411	0.373	0.408
-.10	0.635	0.409	0.425	0.435	0.407	0.423
-.25	0.635	0.608	0.461	0.464	0.448	0.449
-.40	0.635	0.798	0.515	0.513	0.504	0.483
Average rmse	0.635	0.464	0.438	0.445	0.424	0.442

Table 3.7 Root-Mean Square Error of Frequency Factor, N = 50

Regional Skewness	Sample	Root-Mean Square Error of Frequency Factor K_T				
		W.R.C.	Tasker	Fisher	Jackknife	
.80	0.508	0.633	0.458	0.457	0.458	0.453
.65	0.508	0.467	0.392	0.394	0.398	0.424
.50	0.508	0.325	0.387	0.394	0.363	0.399
.35	0.508	0.221	0.362	0.373	0.349	0.381
.20	0.508	0.181	0.344	0.358	0.312	0.366
.05	0.508	0.216	0.367	0.367	0.359	0.369
-.10	0.508	0.333	0.389	0.394	0.372	0.370
-.25	0.508	0.475	0.413	0.415	0.395	0.380
-.40	0.508	0.602	0.423	0.421	0.412	0.398
Average rmse	0.508	0.384	0.393	0.396	0.380	0.393

Table 3.8 Root-Mean Square Error of Frequency Factor, N = 70

Regional Skewness	Sample	Root-Mean Square Error of Frequency Factor K_T				
		W.R.C.	Tasker	Fisher	Jackknife	Bootstrap
.80	0.420	0.413	0.384	0.385	0.384	0.373
.65	0.420	0.380	0.365	0.365	0.378	0.356
.50	0.420	0.295	0.355	0.358	0.340	0.342
.35	0.420	0.287	0.328	0.331	0.330	0.334
.20	0.420	0.240	0.311	0.314	0.300	0.331
.05	0.420	0.269	0.318	0.320	0.307	0.338
-.10	0.420	0.294	0.332	0.336	0.313	0.347
-.25	0.420	0.361	0.349	0.350	0.337	0.362
-.40	0.420	0.455	0.403	0.402	0.391	0.380
Average rmse	0.420	0.333	0.349	0.351	0.342	0.352

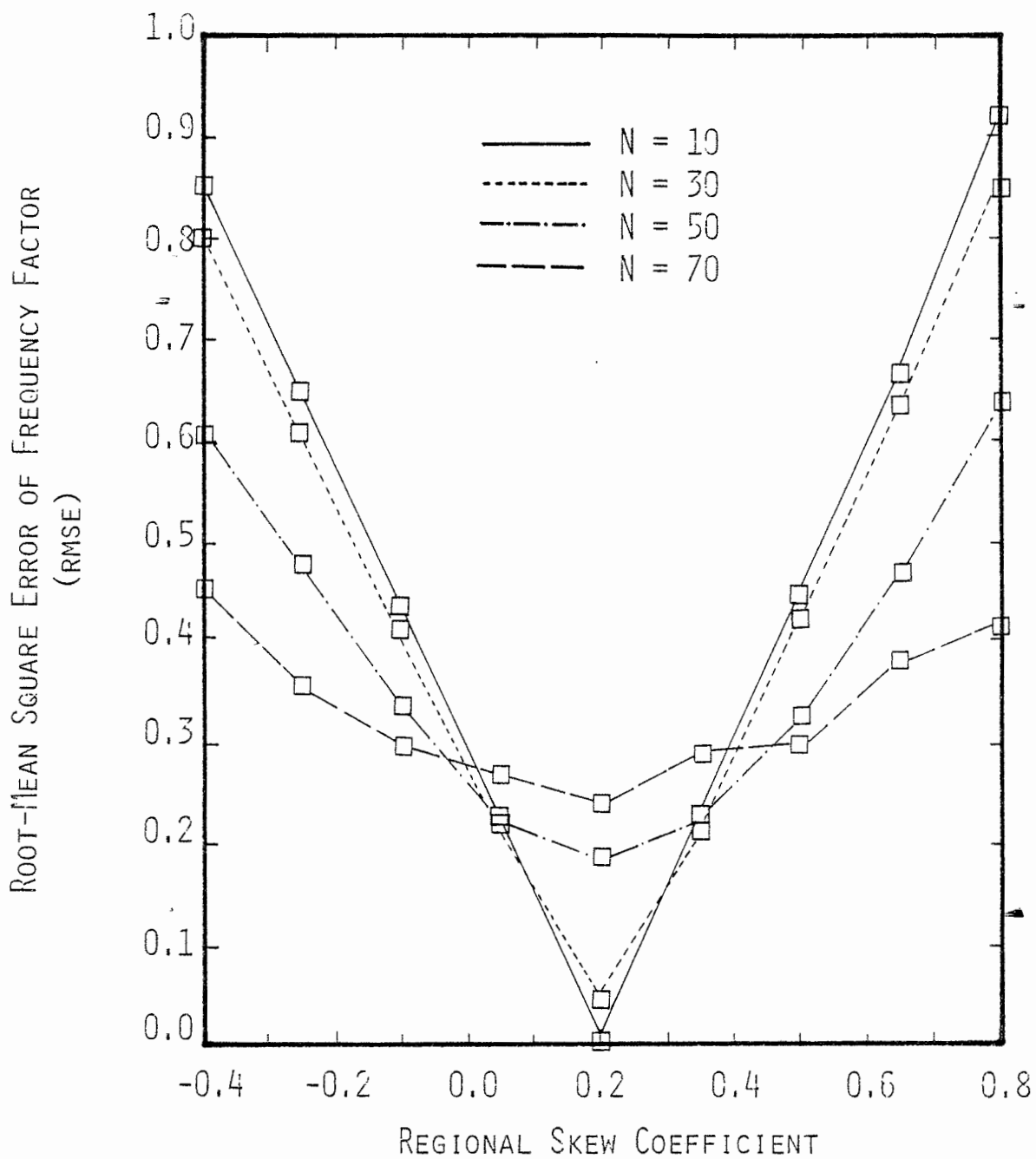


Figure 3.2 Comparison of Root-Mean Square Errors of K_T Using the W.R.C. Method for Different Sample Size

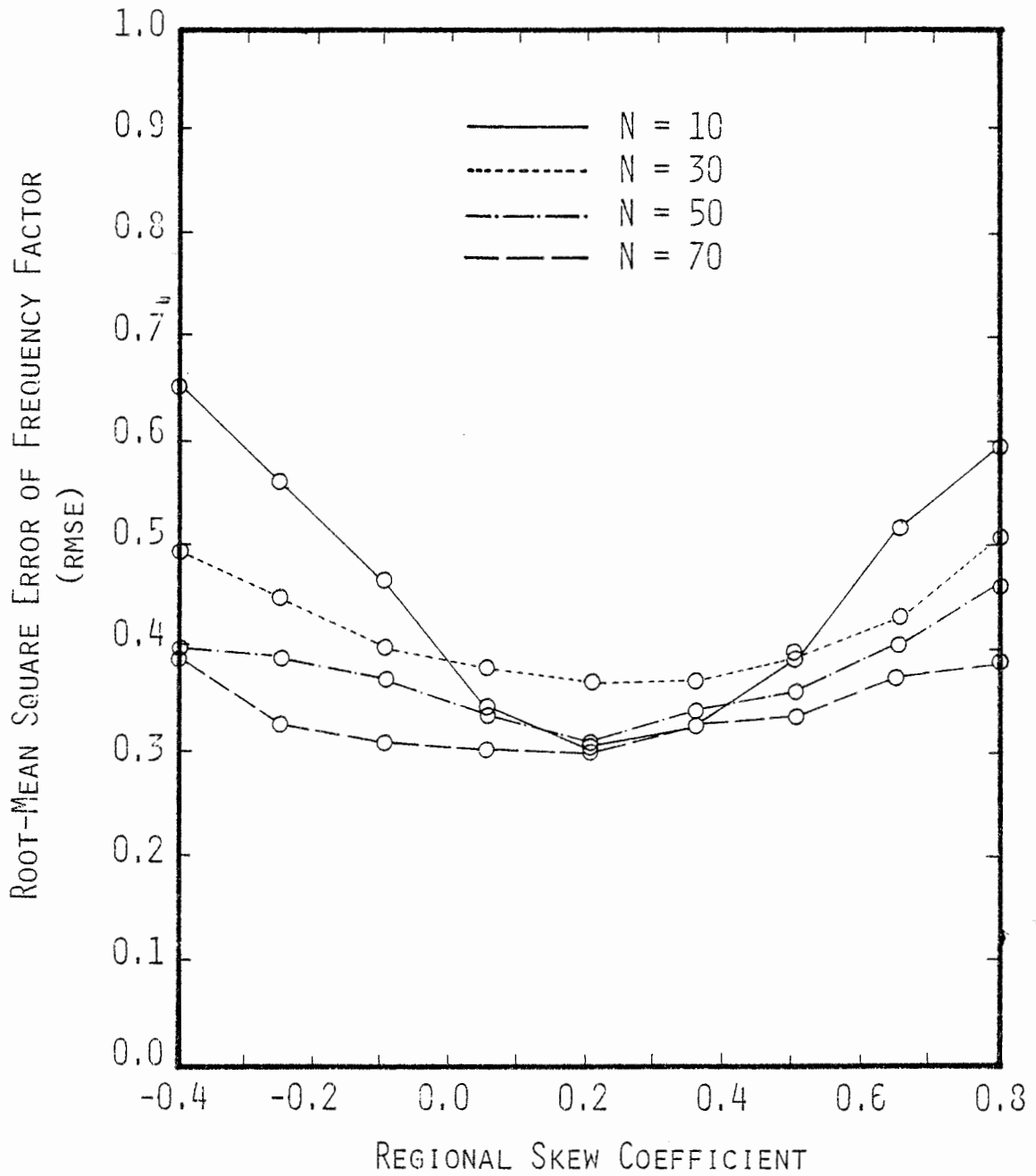


Figure 3.3 Comparison of Root-Mean Square Errors of K_T Using the Jackknife Method for Different Sample Size

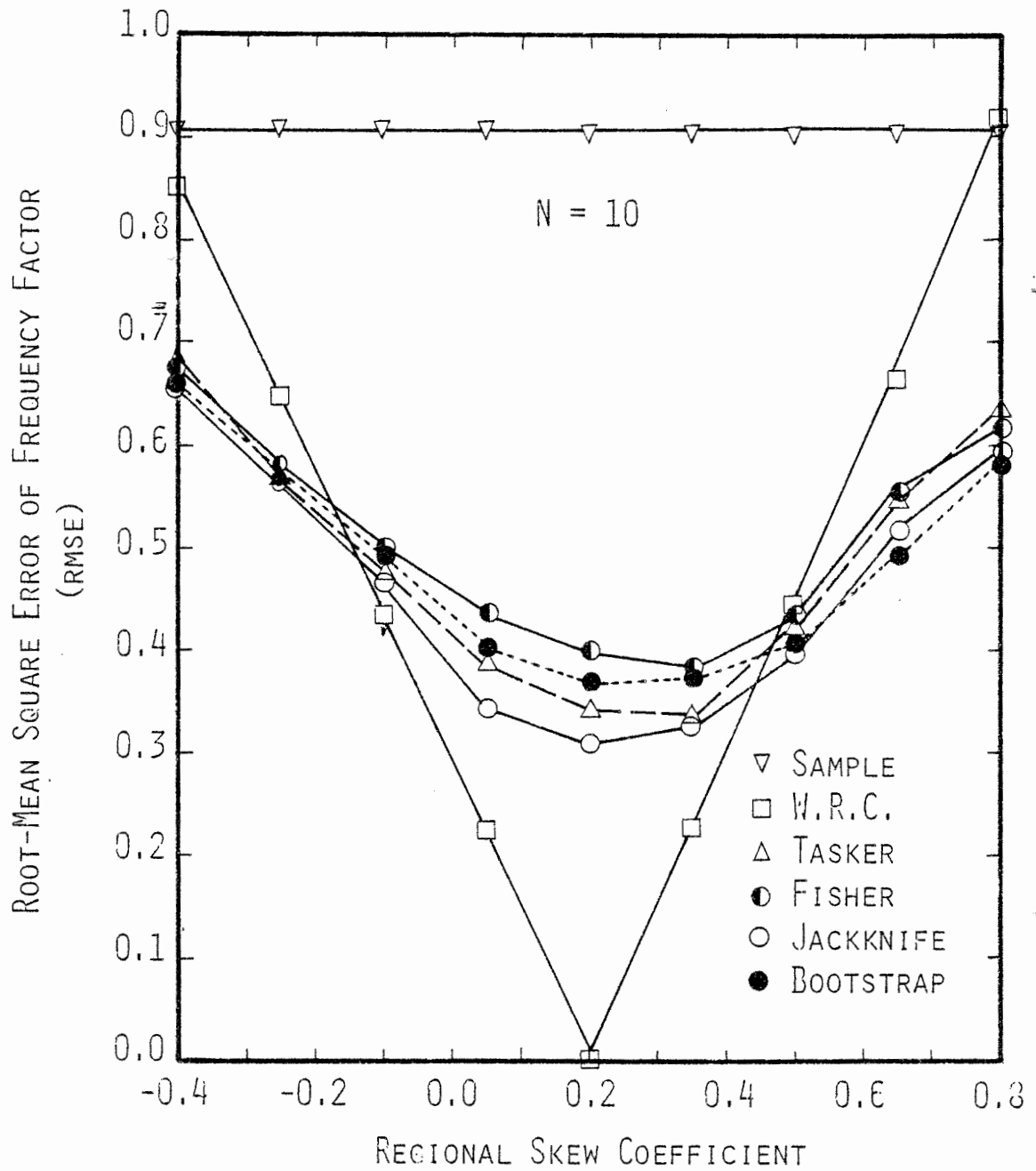


Figure 3.4 Root-Mean Square Errors of K_T Using Different Methods for Sample Size $N = 10$

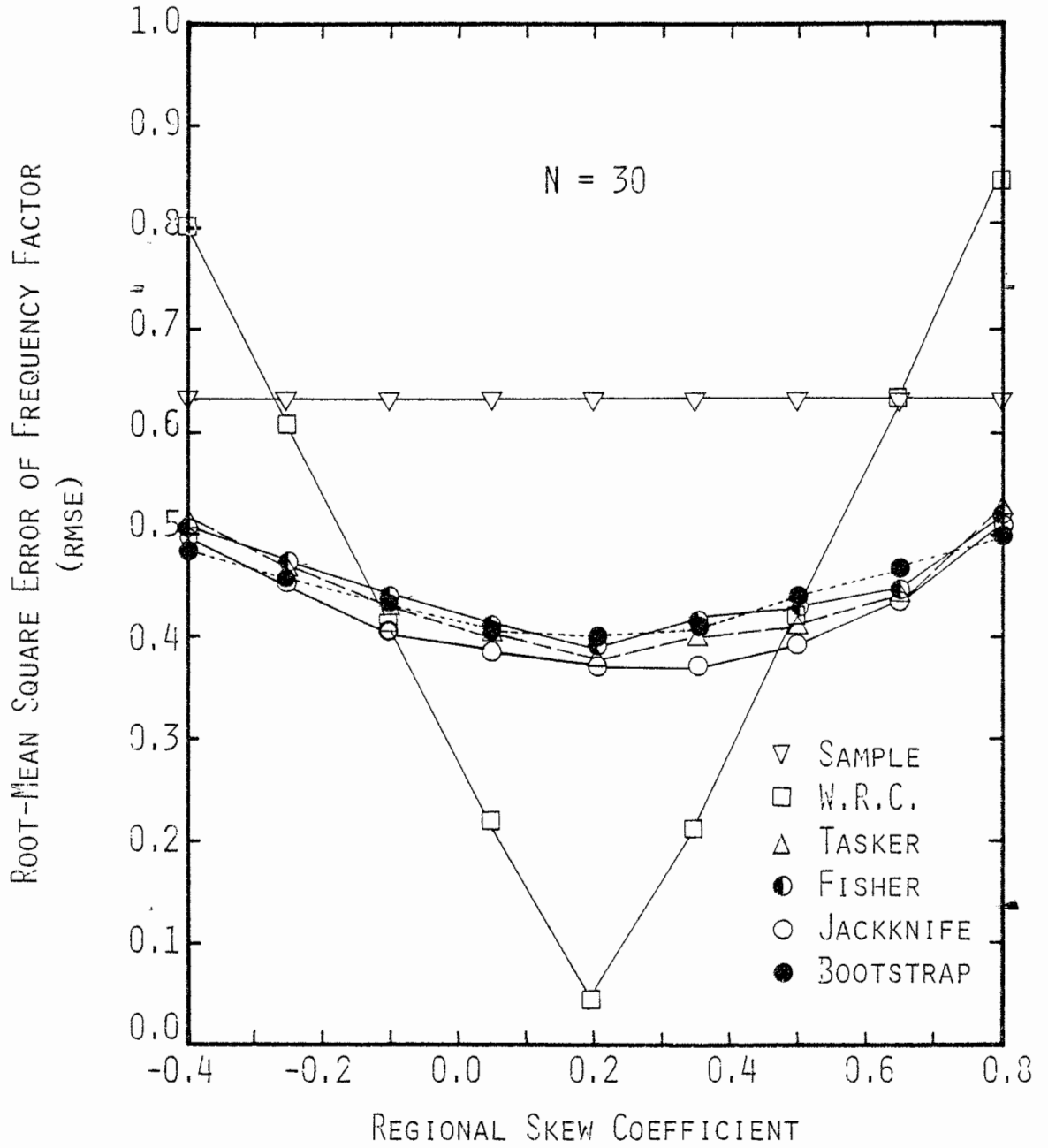


Figure 3.5 Root-Mean Square Errors of K_T Using Different Methods for Sample Size $N = 30$

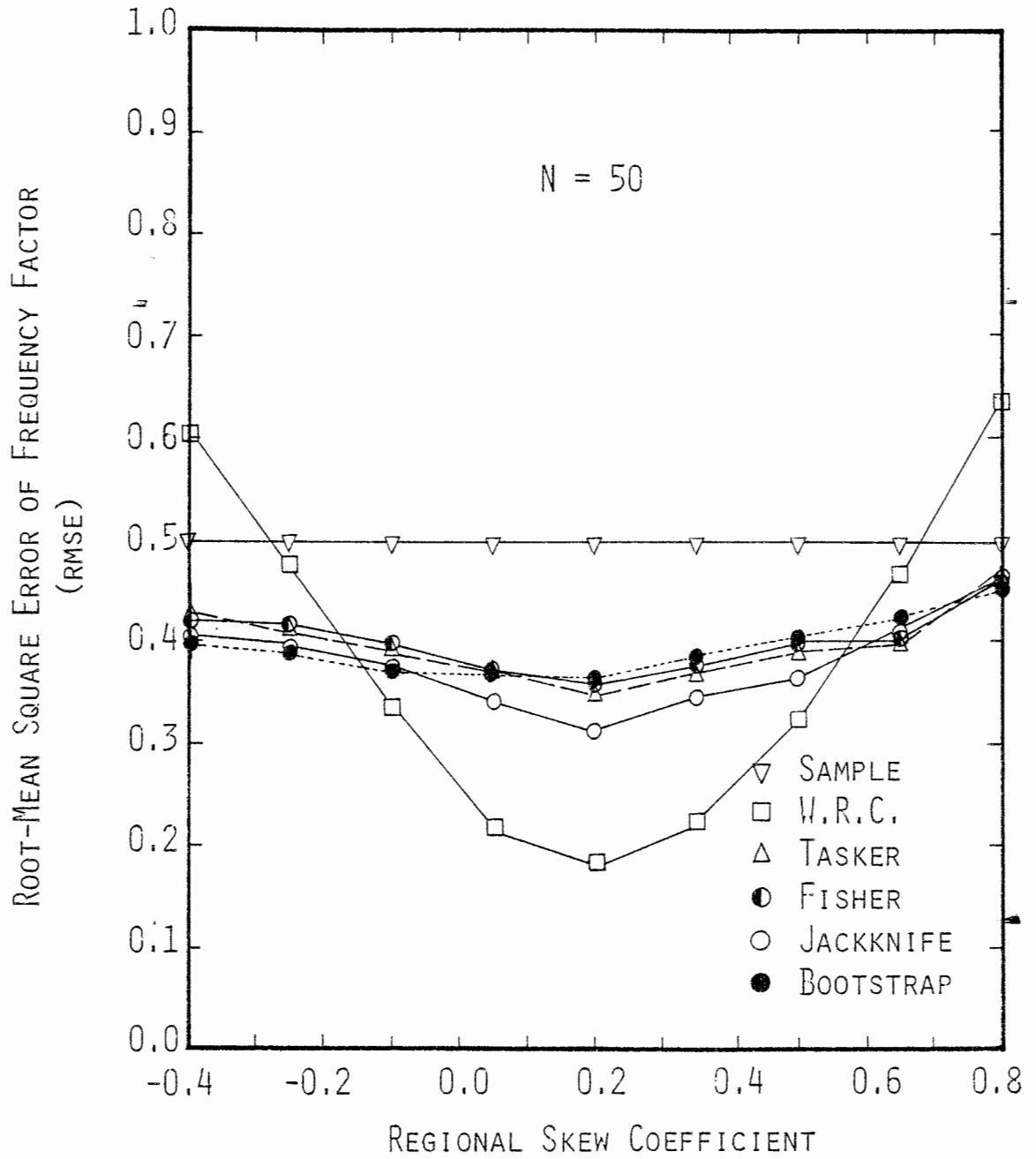


Figure 3.6 Root-Mean Square Errors of K_T Using Different Methods for Sample Size $N = 50$

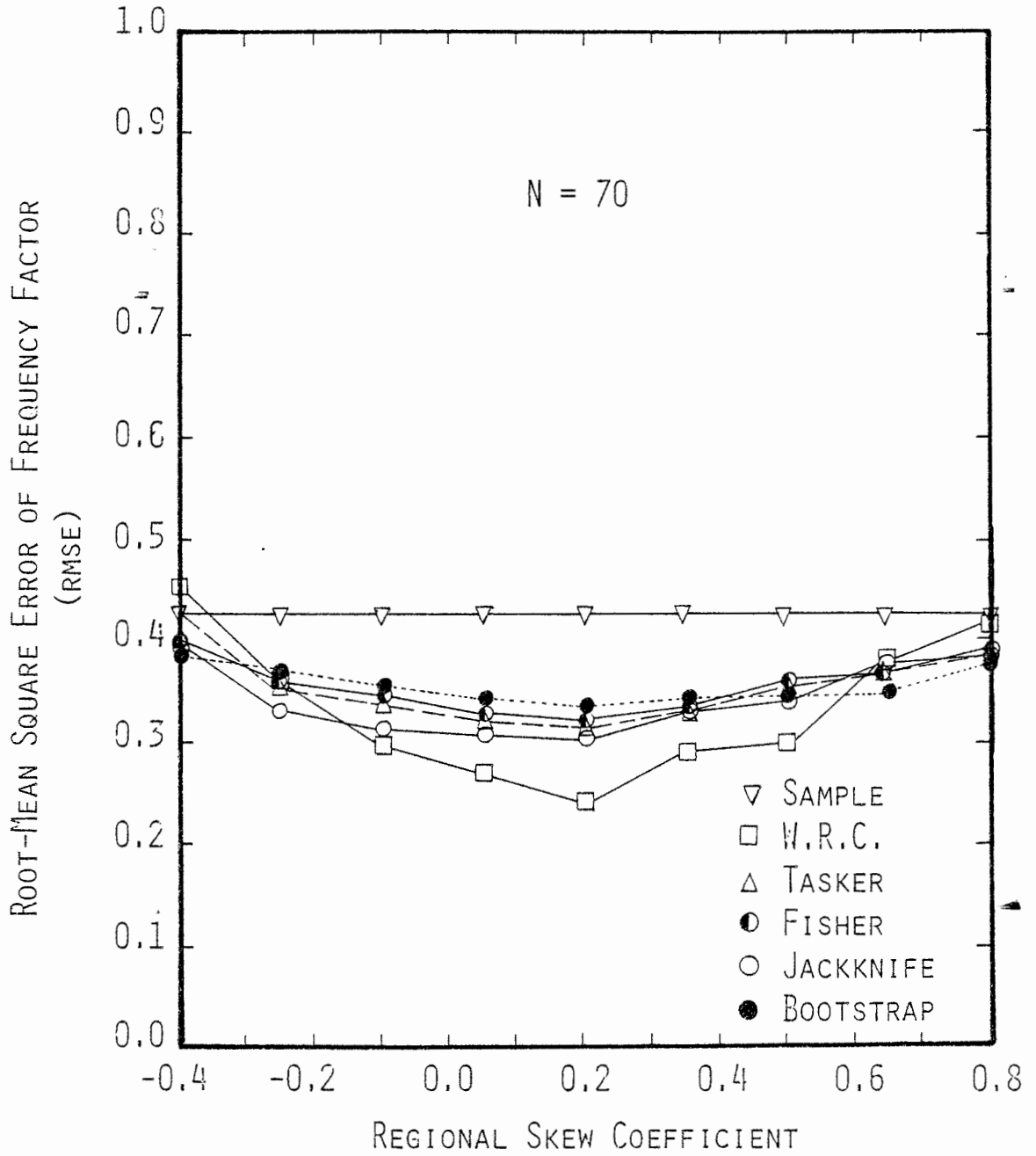


Figure 3.7 Root-Mean Square Errors of K_T Using Different Methods for Sample Size $N = 70$

The WRC method provides the largest variation among the six methods implying that the accuracy of the generalized skewness, \hat{G}_y , and the flood magnitude depend heavily on the accuracy of the regional skewness. Therefore, the use of the WRC method possesses high uncertainty especially when the sample size is small.

The use of sample statistics and the WRC method appear to be the least reliable of the six methods and in some cases the WRC method provided worse results than the sample statistics alone within the range of regional skewness considered. It is worthwhile to point out that even the bootstrap method does not present the smallest value of average rmse in this experiment but it does show that it has the second smallest variation among these six methods and the value of rmse is considerably close to the jackknife and Tasker's methods.

It commonly assumes that the sampling distribution of a statistic, in this case \hat{K}_{T_r} , is normally distributed once the standard error is computed. In Table 3.9 comparisons are made of the rmse of the frequency factor, \hat{K}_{T_r} , for different regional skewness derived by assuming normality and no assumption for the \hat{K}_{T_r} of bootstrap sample generated. Sample sizes of $N = 10, 30, 50,$ and 70 are considered. It is also noted from Table 3.9 that the rmse's of the frequency factor derived with and without the normality assumption on \hat{K}_{T_r} are almost exactly the same for sample sizes of $N = 50,$ and $70,$ but not for sample sizes of $N = 10,$ and $30.$ From these findings it appears that for larger sample sizes the sampling distribution of the estimator, \hat{K}_{T_r} , can be approximated as normal; however, without further testing this statement may be generalized a little too much.

Table 3.9
 Comparison of Root-Mean Square Error of Frequency Factor K_T for Bootstrap
 Method With and Without Normality Assumption on the Bootstrap Samples

Regional Skewness	N = 10		N = 30		N = 50		N = 70	
	A	B	A	B	A	B	A	B
.80	0.580	0.589	0.508	0.504	0.453	0.450	0.373	0.373
.65	0.490	0.490	0.469	0.464	0.423	0.424	0.355	0.356
.50	0.419	0.411	0.440	0.434	0.398	0.399	0.342	0.342
.35	0.380	0.365	0.420	0.413	0.380	0.381	0.335	0.334
.20	0.380	0.362	0.411	0.404	0.364	0.366	0.333	0.331
.05	0.419	0.404	0.415	0.408	0.368	0.369	0.337	0.338
-.10	0.485	0.476	0.429	0.423	0.369	0.370	0.347	0.347
-.25	0.569	0.567	0.454	0.449	0.380	0.380	0.361	0.362
-.40	0.663	0.667	0.483	0.483	0.399	0.398	0.380	0.380
Average rmse	0.487	0.481	0.448	0.442	0.393	0.393	0.352	0.352

A - With Normality Assumption

B - Without Normality Assumption

Among these six methods, the jackknife and bootstrap provide satisfactorily robust estimation of parameters. Of the six methods considered, the jackknife method, in general, results in the smallest rmse over the range of sample sizes and regional skewness considered for the experiment. The Fisher, Tasker, bootstrap, and jackknife, from a practical viewpoint, provide fairly consistent results.

The jackknife and bootstrap methods described above can be used to compute the variance of any number of statistics (e.g., mean, standard deviation, skewness, etc.) derived from the sample. The other information required for computing the weight is the variance of the parameter derived from the regional basis. As previously mentioned, the variance of regional parameters, θ_r , can be computed from the regional regression study. A brief review on the regression analysis and its application to derive the regional parameter estimates are given in following sections.

3.2.6 Variance of Regional Estimators

3.2.6.1 Regression Analysis

The variance of regional estimators $\text{Var}(\theta_r)$ can be obtained by regression analysis which relates the regional estimators θ_r to physiographic and/or meteorological variables. θ_r represents the mean, standard deviation, and skewness of streamflows based upon the regional information. The applications of regression analysis are very fruitful and extensive by hydrologists. However, there has not been an equivalent amount of effort in understanding all the effect of assumptions that the regression theory has on the regression models by the hydrologists. Among regression models the

linear model is the most popular one used which has the general form

$$Y_j = \beta_0 + \beta_1 X_{1j} + \cdots + \beta_k X_{kj} + \varepsilon_j, \quad j=1, \dots, n \quad (3.20)$$

or in the matrix notation:

$$\underline{Y} = \underline{X} \underline{\beta} + \underline{\varepsilon} \quad (3.21)$$

where \underline{Y} is an $(n \times 1)$ vector of dependent variables (or responses); \underline{X} is an $(n \times k)$ matrix with k independent variables; $\underline{\beta}$ is a $(k \times 1)$ vector of unknown regression parameters; and $\underline{\varepsilon}$ is a $(n \times 1)$ vector of random errors.

The method often employed for equation fitting is the least squares having the following assumptions:

- A.1 The form of model is correct, i.e., if the wrong model is used the values given by that model will be biased..
- A.2 The responses \underline{Y} are statistically independent.
- A.3 The conditional mean of the random response vector \underline{Y} for a given \underline{X} is $E(\underline{Y} | \underline{X}) = \underline{X} \underline{\beta}$, where $E(\underline{Y} | \underline{X})$ is the expected value.
- A.4 Homoscedasticity, i.e. $\text{Var}(\underline{Y} | \underline{X}) = \sigma^2 \underline{I}$, where \underline{I} is an $n \times n$ identity matrix.
- A.5 The distribution of \underline{Y} is multi-normal with mean $\underline{X} \underline{\beta}$ and covariance matrix $\sigma^2 \underline{I}$.

Assumption A.4 is not necessary in the least squares method. If A.4 does not hold, a weighted least squares (WLS) or a transformation of dependent variables, which stabilizes the variance, can be applied. In most

hydrologic applications this assumption is implicitly taken and the ordinary least squares method (OLS) is applied. Assumption A.5 is required which validates the statistical inference of the regression parameters estimated. The variance of \underline{Y} given \underline{X} in the OLS method, $\hat{\sigma}^2$, can be estimated by

$$\hat{\sigma}^2 = \frac{\underline{e}^T \underline{e}}{(n - k)} \quad (3.22)$$

where $\underline{e} = \underline{Y} - \underline{X}\hat{\underline{\beta}}$, \underline{e}^T is the transpose of \underline{e} , and $\hat{\underline{\beta}} = (\underline{X}^T \underline{X})^{-1} \underline{X}^T \underline{Y}$ which is the OLS estimator of the regression parameters, $\underline{\beta}$, in the model.

It is always necessary to examine the validity of the above assumptions after the regression analysis is made, which can be done by the analysis of residuals. The most commonly used method is to analyze the scatter plots. Excellent discussions of analysis of residuals are given by Anscombe and Tukey (1963). Draper and Smith (1966) and Daniel and Wood (1971) provide good illustrations on this topic. In general, the analysis of residuals helps the analyst to test the validity of his model and to provide the necessary information for modifying the model. It always pays to identify the influential observations, which affect the results of analysis a great deal. Cook (1977) developed a statistic, D_i , named Cook's distance, which measures the overall impact of any single data point on the least squares solution, as

$$D_i = \frac{(\hat{\underline{\beta}}_{(i)} - \hat{\underline{\beta}})^T \underline{X}^T \underline{X} (\hat{\underline{\beta}}_{(i)} - \hat{\underline{\beta}})}{k \hat{\sigma}^2}, \quad i = 1, \dots, n \quad (3.23)$$

where D_i is a measure of the distance between $\hat{\underline{\beta}}$ and $\hat{\underline{\beta}}_{(i)}$, where $\hat{\underline{\beta}}_{(i)}$ is the OLS estimator of $\underline{\beta}$ with the i -th observation deleted.

Furthermore, D_i can be expressed as

$$D_i = \frac{1}{k} \left[\frac{Y_i - \underline{x}_i^T \hat{\underline{\beta}}}{\hat{\sigma} \sqrt{1 - v_i}} \right]^2 \left[\frac{v_i}{1 - v_i} \right], \quad i = 1, \dots, n \quad (3.24)$$

where \underline{x}_i is the vector of the i -th independent variables, and $v_i = \underline{x}_i^T (\underline{X}^T \underline{X})^{-1} \underline{x}_i$. The first term on the right of Eq. (3.24) is the square of the studentized residual while the second term is the moment arm. It has been shown by Cook (1977) that D_i is derived from an F-statistic with k and $n-k$ degrees of freedom. Standard hypothesis test can then be applied to assess the influence of data points on the regression estimation.

Maximum values of the coefficient of determination (r^2) was not the only criterion used to select the best subset of independent variables in the regression model as the value of r^2 can always be increased by adding more terms to the model. An adjusted square of the multiple correlation coefficient can be used as

$$\bar{r}^2 = r^2 - \frac{k - 1}{n - 1} (1 - r^2) \quad (3.25)$$

The \bar{r}^2 will increase only when the t-statistic of added regression coefficients are larger than unity. Other criteria such as the residual standard error, $\hat{\sigma}$, and Mallows' C_p statistic (Mallows, 1964), which measures the sum of squared bias plus the squared random error in Y at all data points are used. Another purpose of employing Mallows' C_p statistic is to examine the biasness of the regression model provided so that the validity of assumptions about

the regional parameter estimate in deriving the weighting factor for the generalized parameter estimate in 3.2.3 are justified. Mallows C_p statistic is defined as

$$C_p = \frac{RSS_p}{\hat{\sigma}^2} - (n-2p) \quad (3.26)$$

in which RSS_p = sum of square of residual of regression model with p unknown coefficients to be estimated. The Mallows C_p statistic provides a measure of the mean square error of the predicted value, i.e., the discrepancy between Y and $E(Y)$, for a p -parameter regression model. Then, the best subset of independent variables in the regression model are selected with the smallest value of C_p associated. In addition to finding the regression equation with the smallest C_p , Mallows (1964) suggested plotting C_p against p for each regression model. The C_p 's for those with small bias will tend to cluster around the line $C_p = p$, and C_p 's for those models with substantial bias lie above the line as point B shown in Fig. 3.8. It is suggested that the regression equation associated with point B is chosen, because it has smaller C_p value than point A, even though B has substantial bias compared to that of A. In other words, it pays accepting some biasness in order to have lower total average squared error. In the computation an unbiased estimate of σ^2 is needed to calculate C_p . Often the residual mean square from the complete equation serves this purpose by assuming that the complete equation has been carefully chosen to have negligible bias. This is an ad hoc procedure which is described in Appendix A.

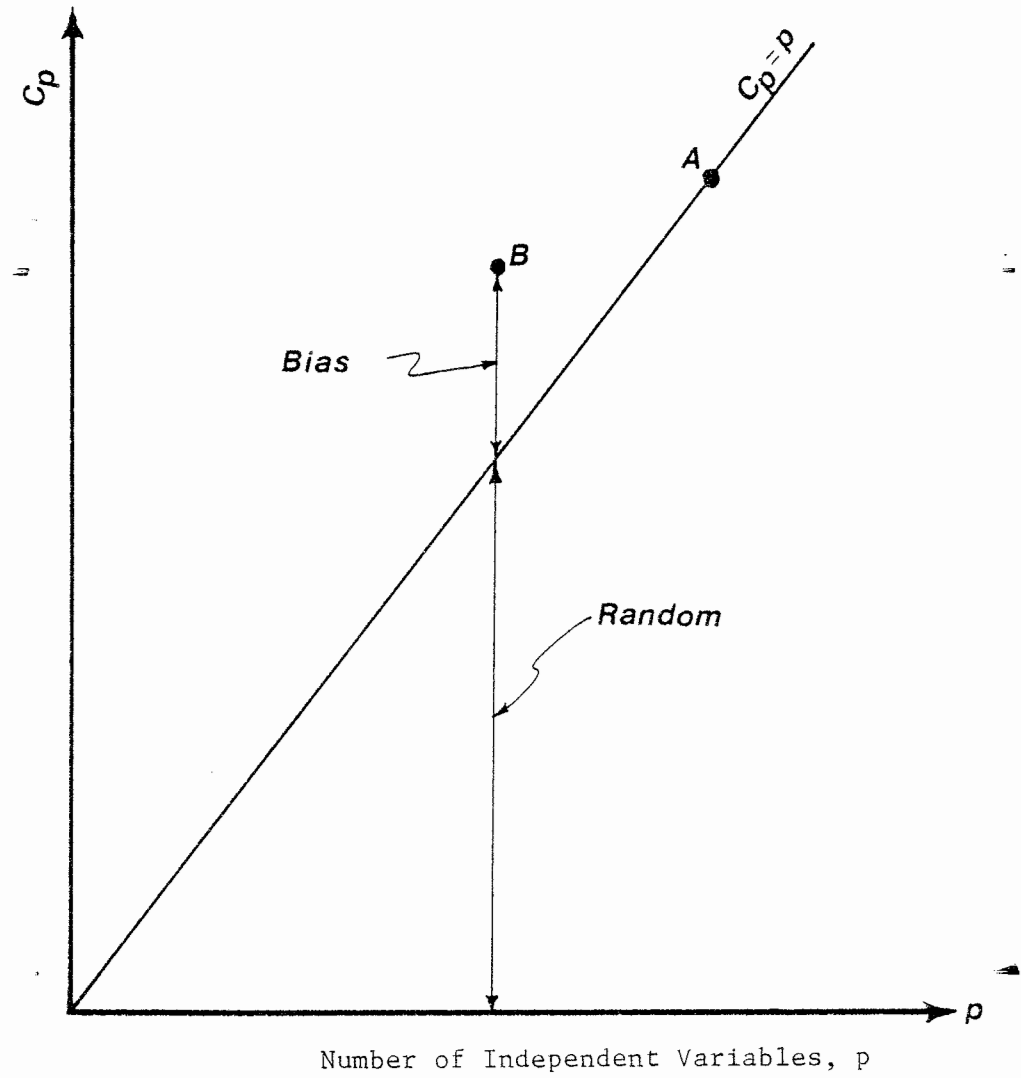


Figure 3.8 Mallows' C_p Statistic vs. Number of Independent Variables in Regression Model

3.2.6.2 Regression Analysis Study for a Southwest Region

To reduce parameter uncertainty by using the weighting procedure mentioned in Section 3.2.5 requires the knowledge of information contained in both sources, i.e., region and local sample data which is expressed as the variance of the estimate. The variance of these parameter estimates derived from the sample can be determined by the method of jackknife and bootstrap.

The values of the parameters and their respective variances for the region are determined by regression analysis. Benson (1964) applied regression analysis to the Southwestern region of the United States relating the flood magnitudes of specified return periods to meteorological and physiographical characteristics of the river basins. He divided the region into two subregions based on the mechanism as to how the floods are generated, i.e., floods produced by snowmelt and local thunderstorms or widespread tropical storms. The data used herein involved the subregion where floods are produced by thunderstorms which includes the central and eastern part of Texas and a small part of western Louisiana.

The ordinary least squares method is applied to determine regression equations for the regional parameters, mean (\bar{Z}_r), standard deviation, (S_{Z_r}), and skewness (G_{Z_r}), of the annual maximum series and also regression equations for the mean (\bar{Y}_r), standard deviation (S_{Y_r}), and skewness (G_{Y_r}), of the log-transformed flows of the annual maximum series. The independent variables of the regression equations consider the following physiographical and meteorological characteristics:

1. the contributing drainage area (A_d) in square miles,
2. the main channel slope (S_ℓ) (85 to 10 percent points in feet per mile),
3. the percentage of surface storage (S_t),
4. the total main channel length (L) in miles,
5. the 10-year, 24-hour rainfall intensity (I) in inches,
6. the mean annual number of thunderstorm days (N_t), and
7. the ratio of runoff to precipitation during the month when the annual maximum peak discharge occurred (R_t).

A total of 95 gaging stations with the length of record at least 30 years are analyzed in this region using Benson's data. For each gaging station selected in this study the station number, value of parameter estimates described above, and the corresponding physiographic and meteorologic characteristics are listed in Appendix A. The locations of those gaging stations in Texas used are shown in Fig. 3.9. The procedure for examining the validity of assumptions in the OLS method consisted of an analysis of the residuals and of Cook's distance. Detailed descriptions of the procedures in deriving the regression equations of the regional parameters are given in Appendix A. The resulting regression equations for the regional parameters are as follows:

for the mean

$$\begin{aligned} \ln(\bar{Z}_r) = & 6.442 + 0.63\ln(A_d) + 0.064S_\ell - 0.730\ln(S_t) \\ & - 0.259\ln(L) + 0.400\ln(R_t) \end{aligned} \quad (3.27)$$

for the standard deviation

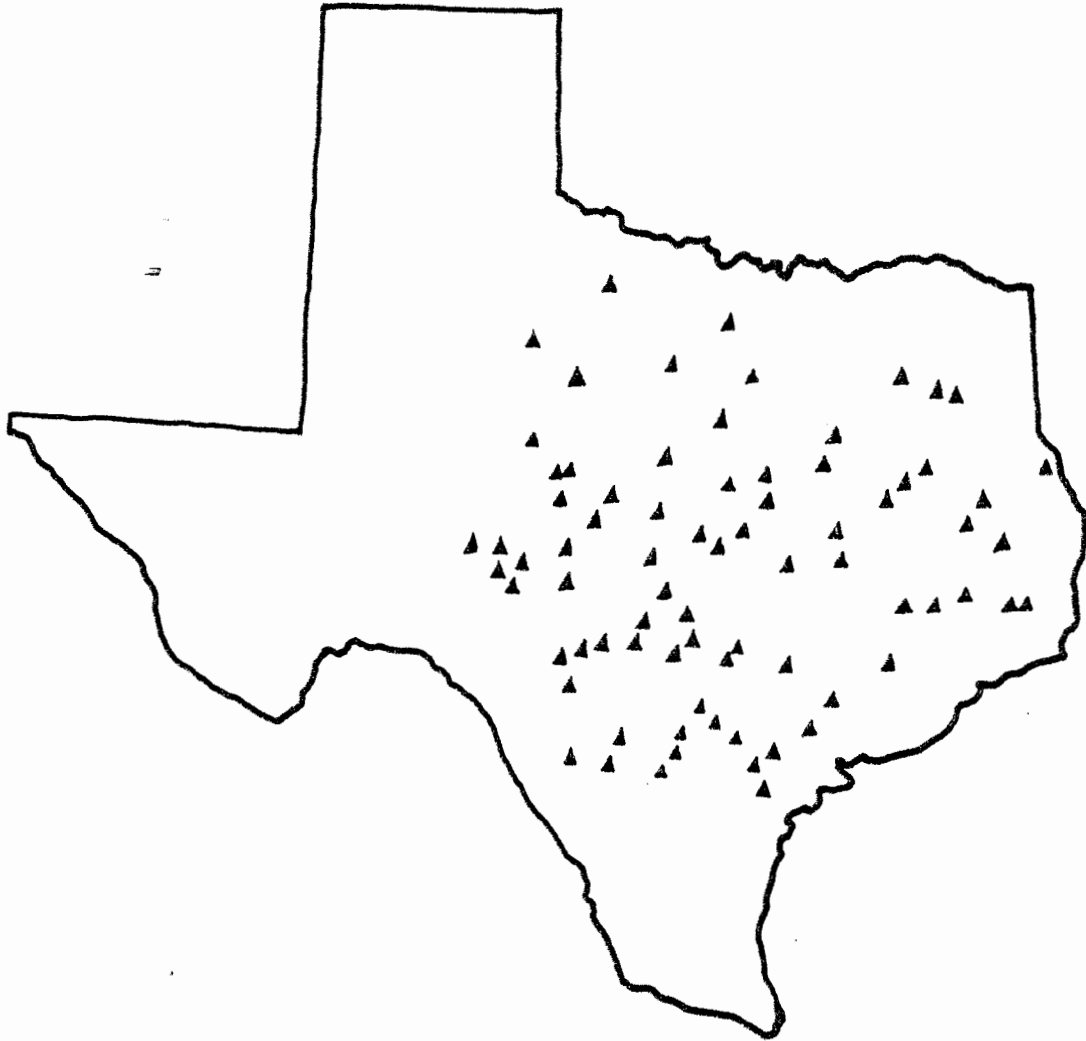


Figure 3.9 Location of Streamflow Gaging Stations
Selected in Texas for Regression Study

$$\frac{1}{S_{Z_r} + 2500} = 2.16 \times 10^{-4} - 4.16 \times 10^{-5} \ln(A_d) - 3.90 \times 10^{-6} S_\ell + 5.99 \times 10^{-5} \ln(S_t) + 3.24 \times 10^{-5} \ln(L) - 1.14 \times 10^{-5} \ln(R_t) \quad (3.28)$$

for the skew coefficient

$$\ln(G_{Z_r}) = 0.197 \ln(A_d) + 0.158 \ln(S_\ell) - 0.254 \ln(L) + 0.905 \ln(I) - 0.358 \ln(N_t) \quad (3.29)$$

for the mean of the log transformed flows

$$\ln(Y_r) = 1.424 + 0.064 \ln(A_d) + 0.0083 S_\ell - 0.064 \ln(S_t) + 0.091 \ln(N_t) + 0.057 \ln(R_t) \quad (3.30)$$

for the standard deviation of the log transformed flows

$$\ln(S_{y_r}) = 3.24 + 0.178 \ln(A_d) - 0.264 \ln(S_t) - 0.41 \ln(L) + 0.41 \ln(I) - 0.894 \ln(N_t) - 0.065 \ln(R_t) \quad (3.31)$$

for the skew coefficient of the log-transformed flows

$$G_{y_r} = -3.601 + 0.102 \ln(A_d) - 2.564 \ln(S_t) + 4.201 (\ln(S_t))^2 + 0.724 \ln(N_t) \quad (3.32)$$

The statistics of the regression equations (3.27-3.32) are listed in Table 3.10, (i.e., coefficient of determination r^2 , adjusted coefficient of determination \bar{r}^2 , Mallow's C_p statistic, and standard error of residual).

In order to apply the weighting procedure for reducing parameter uncertainty the value of sample parameter estimates and their respective variance as well as those for the regional parameter estimates are required. Examining all the regression equations developed for the regional parameter

Table 3.10 Statistics of Regression Equations
for Regional Parameter Estimates

Regional Parameter	Equation	Coefficient of Determination	Adjusted Coefficient of Determination	Mallows Cp Statistic	Standard Error of Residual
\bar{Z}_R	3.24	0.6318	0.6122	4.3	0.4074
SZ_R	3.25	0.6065	0.5855	4.5	0.0000228
GZ_R	3.26	0.1674	0.1317	2.8	0.4766
\bar{Y}_R	3.27	0.6667	0.6488	4.7	0.04817
Sy_R	3.28	0.6244	0.6002	6.2	0.2131
Gy_R	3.29	0.1637	0.1281	1.3	0.5080

estimates, Eq. (3.27-3.32), the square of standard error of estimate provided by the regression equation cannot be used as the variance of the regional parameter estimate, except for the skewness of log-transformed flow, Eq. (3.32). By an analysis of residuals for the rest of the regression equations the normality assumption holds, which enables the retransformation of the variables back to their original scale and then the computation of the corresponding mean and variance. For example, by analysis of residuals for Eq. (3.24) the normality assumptions hold; therefore, \bar{Y}_r is log-normally distributed so that the variance of \bar{Y}_r for a given \underline{x}^* can be computed using

$$\text{Var}(\bar{Y}_r | \underline{x}^*) = U_1^2 \left\{ e^{\text{Var}[\ln(\bar{Y}_r | \underline{x}^*)]} - 1 \right\} \quad (3.33)$$

where

$$U_1 = \exp \left\{ E[\ln(\bar{Y}_r | \underline{x}^*)] + \frac{\text{Var}[\ln(\bar{Y}_r | \underline{x}^*)]}{2} \right\} \quad (3.34)$$

3.2.7 Illustration of Procedure for Minimizing Hydrologic Parameter Uncertainty

In previous sections a comparison was presented concerning the use of the jackknife and bootstrap methods to derive the variance of sample skewness which was used in the weighting procedure to derive a generalized skewness. An experimental study (Monte Carlo simulation) was performed to compare the frequency factor derived by the six methods (i.e., sample statistics, WRC, Taskers, Fisher, jackknife and bootstrap). The experimental study considered a population skewness, then varied the skewness above and

below the population value, to determine frequency factors by the six methods. The jackknife and bootstrap provided consistent results, whereas the WRC method provided the largest variation in error among the methods tested.

It can be observed that the parameters with uncertainty featured in Eq. (3.17) in addition to the skewness, are the mean and standard deviation. In this section the application of the parameter uncertainty reducing procedure is extended to consider the mean and standard deviation and the comparison of its capability in flood prediction are made considering different weighting procedures. The methodology can be applied to any probability distribution for frequency analysis; however, for the sake of illustration only flood flow frequency analysis using the log-Pearson type III distribution is considered. The ability of this methodology is illustrated using flood flow frequency data for the Southwestern United States. Five drainage basins in the region are considered. The U.S. Geological Survey gaging station number, length of record, and values of their physiographical and meteorological characteristics are tabulated in Table 3.11.

Six different procedures considered in this comparison study are now briefly described as follows:

1. Sample statistics: Use Eqs. (3.4), (3.5), and (3.6) to compute parameters, i.e., the mean, standard deviation, and skewness, respectively.
2. WRC Method: This method uses Eqs. (3.4) and (3.5) to compute the mean and standard deviation, Eq. (3.7) to

Table 3.11 Basin Characteristics for Streamflow
Gaging Stations Tested

Station	N	A _d	S _ℓ	S _t	L	I	N _t	R _t
8022500	64	4839	1.25	1.27	235	6.33	49	.62
8030500	66	9329	0.96	1.18	427	6.78	57	.63
8033500	75	3637	1.29	1.13	253	6.61	52	.63
8057000	73	6106	3.67	1.72	188	5.68	47	.40
8096500	79	20007	2.77	1.23	706	5.14	43	.38

- compute a generalized skewness in which G_{y_s} is from Eq. (3.6), G_{y_r} is a map skew from Fig. 3.1, and the weight $W_{G_{y,WRC}}$ is from Eq. (3.8).
3. Tasker's Method: This method uses Eq. (3.4) and (3.5) to compute the mean and standard deviation, Eq. (3.7) to compute a generalized skewness in which G_{y_s} is from Eq. (3.6), G_{y_r} is a map skew from Fig. 3.1, and the weight, $W_{G_{y,Tasker}}$ is from Eq. (3.9).
 4. Fisher's Method: This method uses Eqs. (3.4) and (3.5) to compute the mean and standard deviation, Eq. (3.7) to compute a generalized skew in which G_{y_s} is from Eq. (3.6), G_{y_r} is a map skew from Fig. 3.1, and the weight is computed using Eq. (3.12) where $\theta = G_y$. The $\text{Var}(G_{y_r}) = 0.55^2$ from WRC Bulletin 17 (1976) and $\text{Var}^{(F)}(G_{y_s})$ is found using Eq. (3.16).
 5. Tung and Mays Method J: Computes a generalized mean, $\hat{\bar{Y}}_r$, using Eq. (3.10), i.e.

$$\hat{\bar{Y}} = W_{\bar{Y}} \cdot \bar{Y}_s + (1-W_{\bar{Y}}) \cdot \bar{Y}_r \quad (3.35)$$

where \bar{Y}_s is computed using Eq. (3.4), \bar{Y}_r is computed using Eq. (3.30), and $W_{\bar{Y}}$ is computed using Eq. (3.12) or

$$W_{\bar{Y}} = \frac{\text{Var}(\bar{Y}_r)}{\text{Var}(\bar{Y}_s) + \text{Var}(\bar{Y}_r)} \quad (3.36)$$

The $\text{Var}(\bar{Y}_r)$ is computed using Eqs. (3.33) and (3.34) and $\text{Var}^{(J)}(\bar{Y}_s)$ is

computed using the jackknife method Eqs. (3.13) and (3.14). A generalized standard deviation \hat{S}_y is computed using Eq. (3.10), i.e.

$$\hat{S}_y = W_{S_{y, \text{Jackknife}}} \cdot S_{y_s} + (1 - W_{S_{y, \text{Jackknife}}}) \cdot S_{y_r} \quad (3.37)$$

where S_{y_s} is computed using Eq. (3.5), S_{y_r} is computed using Eq. (3.31), and $W_{S_{y, \text{Jackknife}}}$ is computed using Eq. (3.12) or

$$W_{S_{y, \text{Jackknife}}} = \frac{\text{Var}(S_{y_r})}{\text{Var}^{(J)}(S_{y_s}) + \text{Var}(S_{y_r})} \quad (3.38)$$

The $\text{Var}(S_{y_r})$ is computed in the same manner as $\text{Var}(\bar{Y}_r)$ and $\text{Var}^{(J)}(S_{y_s})$ is computed using the jackknife method, Eqs. (3.13) and (3.14).

A generalized skew \hat{G}_y is computed using Eq. (3.10). The form of which is Eq. (3.7) where G_{y_s} is computed using Eq. (3.6), G_{y_r} is computed using Eq. (3.32), and $W_{G_{y, \text{Jackknife}}}$ is computed using Eq. (3.12) or

$$W_{G_{y, \text{Jackknife}}} = \frac{\text{Var}(G_{y_r})}{\text{Var}^{(J)}(G_{y_s}) + \text{Var}(G_{y_r})} \quad (3.39)$$

The $\text{Var}(G_{y_r})$ is 0.508^2 associated with Eq. (3.32) as stated in Table 3.10 and $\text{Var}^{(J)}(G_{y_s})$ is computed using the jackknife method, Eqs. (3.13) and (3.14).

6. Tung and Mays Method B: This method is identical to the Tung and Mays Method J except here the $\text{Var}^{(B)}(\bar{Y}_s)$, $\text{Var}^{(B)}(S_{y_s})$, and the $\text{Var}^{(B)}(G_{y_s})$ are computed using the bootstrap, Eq. (3.15).

The test procedure is:

1. Use the first chronological $N_p = 10$, observations of the total N

observations to perform the flood frequency analysis by using the six different methods discussed above for parameter estimation. The analytical method of curve fitting computes (estimates) flood magnitudes, \hat{Z}_{T_r} , for various return periods, T_r , for the methods of using sample statistics, WRC, Tasker and Fisher, using

$$\ln(\hat{Z}_{T_r}) = \bar{Y}_s + K_{T_r} \cdot S_{y_s} \quad (3.40)$$

where \bar{Y}_s is the mean of the log-transformed N_p observations, S_{y_s} is the standard deviation of the log-transformed N_p observations and K_{T_r} is the frequency factor which is a function of the skewness and the probability of exceedance, $1/T_r$. For the TMJ and TMB methods the frequency equation is

$$\ln(\hat{Z}_{T_r}) = \hat{\bar{Y}} + K_{T_r} \cdot \hat{S}_y \quad (3.41)$$

where K_{T_r} is a function of the return period and generalized skewness.

2. Calculate ERR_1 for each method,

$$ERR_1 = \left\{ \frac{1}{N} \left[\sum_{t=1}^N \frac{\hat{Z}_{T_r}(t) - Z_{T_r}(t)}{\hat{Z}_{T_r}(t)} \right]^2 \right\}^{1/2} \quad (3.42)$$

where N is total number of observations at the gaging station tested, $Z_{T_r}(t)$ is the N observed flood magnitudes with return period of $T_r(t) = (N + 1)/t$, and $\hat{Z}_{T_r}(t)$ is the estimate of the flood magnitude with the same return period determined from the frequency Eq. (3.40) or (3.41) based upon the N_p observations and method used. The reason for choosing such a criterion as

Eq. (3.42) is that it reveals the average value of the ratio to which the actual observations deviate from the predicted values.

3. Calculate ERR_2 for each method

$$ERR_2 = \left\{ \frac{1}{N} \left[\sum_{t=1}^N \hat{z}_{T_r}(t) - z_{T_r}(t) \right]^2 \right\}^{1/2} \quad (3.43)$$

4. Repeat steps 1 and 2 using $N_p = 20$, then $N_p = 40$.

The above testing procedure is performed for each of the five gaging stations tabulated and the values of the error criterion, ERR_1 and ERR_2 , are determined for each method and different sample sizes. The number of bootstrap samples generated for the TMB method is 500 for all analyses in this study. The values of ERR_1 from Eq. (3.42) and ERR_2 from Eq. (3.43) for each gaging station using different sample sizes are listed in Tables 3.12 to 3.16. This analysis considered the first N_p data points of the sample. Considering generalized parameter estimates for all three parameters resulted in decreasing values of ERR_1 . This is true for all the cases, except for station 8030500 with $N_p = 40$ by TMB method. The reduction in parameter uncertainty (smaller values of ERR_1) was the most significant for small sample sizes.

Based upon the results (values of ERR_1 and ERR_2) listed in Table 3.12 or 3.16, the TMJ and TMB methods gave consistently better results than the other methods tested. This illustrates the importance of reducing the parameter uncertainty through methods such as the TMJ and TMB presented

Method \ N_p	10		20		40	
	ERR ₁	ERR ₂	ERR ₁	ERR ₂	ERR ₁	ERR ₂
Sample	0.454	9290	0.172	4740	0.138	4580
W.R.C.	0.445	10500	0.177	4490	0.139	4600
Tasker	0.441	10100	0.171	4420	0.138	4590
Fisher	0.441	9970	0.171	4390	0.138	4590
Tung & Mays Method J	0.239	6930	0.130	3200	0.123	3830
Tung & Mays Method B	0.305	7200	0.126	3110	0.124	3900

Table 3.12 ERR₁ and ERR₂ for Station 8022500

Method \ N_p	10		20		40	
	ERR ₁	ERR ₂	ERR ₁	ERR ₂	ERR ₁	ERR ₂
Sample	0.327	9130	0.156	6130	0.0767	3260
W.R.C.	0.342	7410	0.165	7410	0.0820	3620
Tasker	0.330	7150	0.158	6630	0.0738	3400
Fisher	0.322	7200	0.157	6590	0.0787	3390
Tung & Mays Method J	0.278	6190	0.156	5070	0.0758	3130
Tung & Mays Method B	0.279	6640	0.154	5010	0.0750	3150

Table 3.13 ERR₁ and ERR₂ for Station 8030500

Method \ N_p	10		20		40	
	ERR ₁	ERR ₂	ERR ₁	ERR ₂	ERR ₁	ERR ₂
Sample	0.188	4000	0.0325	797	0.0041	2130
W.R.C.	0.104	2300	0.0408	992	0.0087	2270
Tasker	0.126	2800	0.0365	892	0.0060	2220
Fisher	0.131	2930	0.0362	885	0.0059	2210
Tung & Mays Method J	0.0876	2040	0.0351	857	0.0063	2010
Tung & Mays Method B	0.0958	2210	0.0389	948	0.0065	2230

Table 3.14 ERR₁ and ERR₂ for Station 8033500

Method \ N_p	10		20		40	
	ERR ₁	ERR ₂	ERR ₁	ERR ₂	ERR ₁	ERR ₂
Sample	0.983	36400	0.207	13700	0.0940	5800
W.R.C.	0.911	13300	0.237	5390	0.1200	5470
Tasker	0.324	10700	0.233	7000	0.0226	4510
Fisher	0.323	15000	0.229	4670	0.0107	4200
Tung & Mays Method J	0.521	15300	0.156	4670	0.0907	4290
Tung & Mays Method B	0.560	13600	0.160	5260	0.0915	4390

Table 3.15 ERR₁ and ERR₂ for Station 8057000

Method \ N_p	10		20		40	
	ERR ₁	ERR ₂	ERR ₁	ERR ₂	ERR ₁	ERR ₂
Sample	0.176	14400	0.0847	15400	0.177	13000
W.R.C.	0.171	15300	0.0937	6790	0.102	11300
Tasker	0.172	14900	0.0823	9690	0.179	11900
Fisher	0.172	14900	0.0818	10000	0.179	12000
Tung & Mays Method J	0.119	7950	0.0600	6300	0.166	10600
Tung & Mays Method B	0.120	3160	0.0606	7050	0.166	11000

Table 3.16 ERR₁ and ERR₂ for Station 8096500

herein which considers uncertainties in the mean, standard deviation and skewness, and weigh the importance between sample and regional information.

In the total of fifteen cases, i.e., five gaging stations and three different samples used for each gaging station, the percentage of cases for one method is better than the other based on the error criteria, ERR_1 , Eq. (3.42), and ERR_2 , Eq. (3.43), are presented in Tables 3.17 and 3.18, respectively. For example, when ERR_1 is used, in only 38% of the cases the result obtained by method of WRC has better performance over that of using only sample statistics. Based on this study using five gaging stations in Texas, the methods of TMJ and TMB have "superiority" over the other methods as far as the accuracy of estimation is concerned. Method of TMJ presents more desirable results than method of TMB in this study, which is the same finding as is in the previous experimental study of skew coefficient.

It is interesting to note that, for stations 8033500 and 8096500, the value of ERR_1 for $N_p = 40$ is larger than for $N_p = 20$ and about the same as for $N_p = 10$. This can be explained by examining the streamflow sequence of these two stations keeping in mind that the observations are drawn chronologically from the record. The annual maximum streamflow values observed between the first twenty years and the first forty years are more or less on the high flow region of the frequency curve determined by the total record. Then after the first forty records, the flows observed are mostly on the low flow region. This leads to the frequency curve having a better fit on the high flow part for $N_p = 40$ than for $N_p = 20$ and the reverse situation on the

Table 3.17 Percentage of Cases in Flood Flow Frequency
Analysis for One Method Is Better Than the Other
Based on the Error Criteria ERR1

ERR1	Sample	W.R.C.	Tasker	Fisher	TMJ	TMB
Sample		62	41	41	12	13
W.R.C.	38		25	25	0	0
Tasker	59	75		56	12	7
Fisher	59	75	44		12	7
TMJ	88	100	88	88		69
TMB	87	100	93	93	31	

Table 3.18 Percentage of Cases in Flood Flow Frequency
Analysis for One Method Is Better Than the Other
Based on the Error Criteria ERR2

ERR2	Sample	W.R.C.	Tasker	Fisher	TMJ	TMB
Sample		43	41	43	7	7
W.R.C.	57		53	40	13	20
Tasker	57	47		45	7	7
Fisher	57	60	55		7	7
TMJ	93	87	93	93		73
TMB	93	80	93	93	27	

intermediate and low flow parts. In other words, because of the criterion for comparison used and the realization of high/low flow in the flow sequence, the peculiar results happen for stations 8033500 and 8096500. However, the main purpose of this study is to compare the capability of the different methods in their flow prediction based on the same situation, for instance, same amount of data available for analysis.

Tables 3.19 through 3.23 lists the variances of the sample statistics and the variances of the regional estimates from the regression equations. The variances of the sample statistics derived by the jackknife and bootstrap methods are listed. The weights for each parameter estimates, $W_{\bar{Y}}$, W_{S_y} and W_{G_y} are also listed for both the jackknife and bootstrap methods. As would be expected, the variances of the sample statistics decreased with an increasing number of data, resulting in larger weights for larger sample sizes. In other words, more weight is given to the sample statistics for larger sample sizes. The $\text{Var}(\bar{Y}_s)$ and $\text{Var}(S_{y_s})$ show little variation between using the jackknife and bootstrap methods. However, the $\text{Var}(G_{y_s})$ computed by these two methods does show significant differences, resulting in W_{G_y} varying significantly between the two methods.

In all cases examined, the variance of regional mean, $\text{Var}(\bar{Y}_r)$, was much larger than the variance of the sample mean, $\text{Var}(\bar{Y}_s)$. For example, considering station 8030500 $\text{Var}(\bar{Y}_r)$ is 0.2577 whereas the $\text{Var}(\bar{Y}_s) = .0418$ was computed using the jackknife with $N_p = 10$. For the same station with $N_p = 40$, the $\text{Var}(\bar{Y}_s) = .0066$ was computed using the jackknife. The

Table 3.19 Variance of Sample and Regional Parameter Estimates
and Weight for Station 8022500

	Regional Variance	N					
		10		20		40	
		J ¹	B ²	J	B	J	B
Var(\bar{Y})	.2397	.0404	.0354	.0260	.0289	.0119	.0112
$W_{\bar{Y}}$.8558	.8711	.9022	.8924	.9527	.9552
Var(S)	.0328	.0110	.0087	.0047	.0049	.0039	.0033
W_S		.7497	.7899	.8739	.8699	.8948	.9078
Var(G)	.2581	.3490	.2276	.1445	.0842	.0992	.0341
W_G		.4251	.5314	.6410	.7540	.7225	.8833

¹Jackknife to compute $\text{Var}(\theta_S)$

²Bootstrap to compute $\text{Var}(\theta_S)$

u
 Table 3.20 Variance of Sample and Regional Parameter Estimates
 and Weight for Station 8030500

	Regional Variance	N _p					
		10		20		40	
		J	B	J	B	J	B
Var(\bar{Y})	.02577	.0418	.0393	.0140	.0139	.0066	.0064
$W_{\bar{Y}}$.8604	.8678	.9484	.9490	.9750	.9757
Var(S)	.0183	.0356	.0226	.0092	.0079	.0028	.0025
W_S		.3393	.4475	.6642	.6985	.8672	.8784
Var(G)	.2581	1.1961	.2271	.5132	.1212	.1075	.0453
W_G		.1775	.4822	.3346	.6804	.7060	.8507

Table 3.21 Variance of Sample and Regional Parameter Estimates
and Weight for Station 8033500

	Regional Variance	N _p								
		10			20			40		
		J	B		J	B		J	B	
Var(\bar{Y})	.2248	.0659	.0635		.0378	.0383		.0157	.0170	
$W_{\bar{Y}}$.7732	.7824		.8561	.8544		.9349	.9296	
Var(S)	.0241	.0394	.0256		.0178	.0136		.0074	.0073	
W_S		.3800	.4853		.5752	.6387		.7654	.7675	
Var(G)	.2581	.6122	.2465		.1351	.0634		.0615	.0168	
W_G		.7965	.5115		.6565	.8027		.8076	.9390	

Table 3.22 Variance of Sample and Regional Parameter Estimates
and Weight for Station 8057000

	Regional Variance	N p								
		10			20			40		
		J	B		J	B		J	B	
$\text{Var}(\bar{Y})$.2267	.1102	.0929		.0499	.0511		.0189	.0190	
$W_{\bar{Y}}$.6729	.7094		.8195	.8160		.9233	.9227	
$\text{Var}(S)$.0276	.2769	.1339		.0184	.0156		.0072	.0066	
W_S		.0906	.1708		.5996	.6395		.7929	.8067	
$\text{Var}(G)$.2581	1.1941	.4812		.2481	.1270		.0974	.0566	
W_G		.1777	.3491		.5098	.6701		.7259	.8201	

Table 3.23 Variance of Sample and Regional Parameter Estimates
and Weight for Station 8096500

	Regional Variance	N p								
		10			20			40		
		J	B	J	J	B	J	J	B	
$\text{Var}(\bar{Y})$.2573	.0647	.0580	.0323	.0328	.0128	.0120	.0120	.0120	
W_Y		.7991	.8160	.8884	.8871	.9528	.9555	.9555	.9555	
$\text{Var}(S)$.0217	.0188	.0146	.0084	.0084	.0042	.0036	.0036	.0036	
W_S		.5358	.5985	.7207	.7220	.8375	.8590	.8590	.8590	
$\text{Var}(G)$.2581	.3644	.1868	.1686	.1020	.0808	.0348	.0348	.0348	
W_G		.4146	.5801	.6048	.7168	.7615	.8813	.8813	.8813	

weights $W_{\bar{y}}$ for this station ranged from 0.8604 to 0.9757. The variances of the standard deviation showed somewhat differing results. Considering the same station, $\text{Var}(\bar{Y}_r) = 0.0183$ whereas the $\text{Var}(\bar{Y}_s) = 0.0356, 0.0092,$ and 0.0028 for $N_p = 10, 20,$ and $40,$ respectively, were computed using the jackknife. The regional variance, $\text{Var}(S_{y_r})$, is smaller than the $\text{Var}(S_{y_s})$ for $N_p=10$ by a factor of approximately 2, whereas for $N_p=20$, it is larger by a factor of 2. These results illustrate that the standard deviation is quite sensitive to the sample size and the uncertainty involved in the standard deviation is significant, especially for small sample sizes. This shows the evidence that the estimate of standard deviation derived from regional regression study is more reliable than that derived from the sample for small sample size. Note that the WRC method does not consider uncertainties caused by the mean and standard deviation derived from the sample.

The variances of the skewness derived from sample data, $\text{Var}(G_s)$, varied significantly between those computed by the jackknife and bootstrap methods, resulting in significant differences between the weights, W_{G_y} . This is illustrated further in Tables 3.19 through 3.23. The differences are smaller for larger sample sizes, as can be seen by examining Table 3.20. For $N_p = 10,$ $W_{G_y} = 0.1775$ computed by the jackknife as compared to $W_{G_y} = 0.4822$ computed by the bootstrap. For $N_p = 40,$ $W_{G_y} = 0.7060$ computed by the jackknife as compared to $W_{G_y} = 0.8507$ computed by the bootstrap. Using the WRC method $W_{G_y} = 0$ for $N_p = 10$ and $N_p = 20,$ giving no weight to the skewness computed with the sample statistics. For $N_p = 40,$ the weight, W_{G_y} using the WRC method, Eq. (3.8) would be 0.2. The 0.2 is considerably too

low as compared to the results provided in Tables 3.19 through 3.23 where the weights would range from approximately 0.7 to 0.94 depending upon the variance of the sample skewness.

The above procedures to derive a generalized parameter estimate that minimizes the parameter uncertainty can be applied to various types of hydrologic frequency studies. It is obvious that the procedure of reducing hydrological parameter uncertainty can also be integrated into the risk or reliability analysis of hydraulic structure such that the parameter estimates in the loading distribution can be accurately defined so that the error in defining the risk and reliability is minimized.

3.3 HYDROLOGIC MODEL UNCERTAINTY

The hydrologic model uncertainty results from the assessment of a representative model to describe the random mechanism of the hydrologic process based upon a limited amount of data. In other words, the uncertainty is associated with the choice of model based on an insufficient amount of data. In order to perform the reliability computation the probability distribution of the loading has to be determined. In reality, the probability distribution of the loading is not known so that the engineer has to resort to some statistical inferences based on the data collected. The determination of the loading distribution of floods based on annual maximum series, for example, is of this type.

3.3.1 Review of Model Selection Techniques

This section reviews the statistical methods that are commonly applied in determining the "best" probability model that describes a random

process.

Non-parametric goodness-of-fit techniques use a statistical hypothesis test that is based on a statistic T for measuring the fit of an unknown discrete or continuous distribution function to an empirical distribution function. The hypothesis test for these methods can be stated as

$$H_0 : f(z)=f^*(z) \text{ or } F(z)=F^*(z) \quad (3.44a)$$

$$H_1 : H_0 \text{ is not true} \quad (3.44b)$$

where f and F represent a probability density function and a cumulative distribution function, respectively, and f^* and F^* are a specific probability density function and cumulative distribution function under investigation, respectively. Because of limited data, a measuring statistics, T , is required to facilitate the hypothesis test. The hypothesis that the data are from a specified distribution, f^* , is rejected if

$$T > T_{1-\alpha}^C \quad (3.45)$$

where $T_{1-\alpha}^C$ is the critical value for a significance level $(1-\alpha)$ of the type I error.

Chi-Square Goodness-of-Fit--This method is often applied to fit a set of data to a specified theoretical probability distribution. This test makes a comparison between the actual number of observations and the expected number of observations (expected according to the distribution under test) that fall in the class intervals. The expected number of observations is calculated by multiplying the expected relative frequency by the total number of observations. The test statistic is defined as

$$T_{\chi^2} = \sum_{i=1}^k \frac{[N_i - E(N_i)]^2}{E(N_i)} \quad (3.46a)$$

$$= \sum_{i=1}^k \frac{(N_i - N \cdot P_i^*)^2}{N \cdot P_i^*} \quad (3.46b)$$

where k is the number of class intervals, N_i is the actual number of observations in interval i , N is the total number of observations, i.e., $N = \sum_{i=1}^k N_i$, P_i^* is the relative frequency of interval i for probability density function of f^* and $E(N_i)$ is the expected number of observations in interval i . The distribution of T_{χ^2} is a χ^2 distribution with $k-p-1$ degrees of freedom where p is the number of parameters estimated from the data. The hypothesis that the data follow a specified distribution f^* is rejected if

$$T_{\chi^2} \geq \chi_{1-\alpha, k-p-1}^2 \quad (3.47)$$

Whenever the value of each expectation NP_i^* ($i=1, \dots, k$) is not too small the χ^2 distribution is a good approximation to the actual distribution of T_{χ^2} . Specifically, the approximation will be very good if $NP_i^* \geq 5$ for $i=1, \dots, k$, and the approximation should still be satisfactory if $NP_i^* \geq 1.5$ for $i=1, \dots, k$ (DeGroot, 1975). The improvement of using χ^2 test can be made by using unequal length of class interval to satisfy the above criteria.

The following non-parametric statistical goodness-of-fit techniques use the criteria which are measures of the discrepancy, which is termed distance function, between $F^*(z)$, the estimator of the distribution $F(z)$ under H_0 and the empirical distribution function, $F_n(z)$ which estimates the distribution under H_0 or H_1 .

The Kolmogorov-Smirnov Test--Strictly speaking, the statistics that are functions of the vertical distance between $F_n(z)$ and $F^*(z)$ are considered to be Kolmogorov-type statistics. Statistics which are functions of the vertical distance between two empirical distribution functions are the Smirnov-type (Conover, 1971). In this method the procedure of grouping of data as χ^2 as Eq. (3.46) is not necessary. A statistic (distance function) is defined as

$$T_{KS} = \max | F_n(z) - F^*(z) | \quad (3.48)$$

In other words, T_{KS} is the maximum difference between the empirical distribution function $F_n(z)$ and the hypothesized distribution $F^*(z)$. The critical values for the Kolmogorov-Smirnov test statistic, Eq. (3.48) of various sample size and significance level are tabulated in most statistical books. Therefore, for the chosen significance level, the hypothesis is rejected for the observed value of T_{KS} is greater than or equal to the critical tabulated value of the Kolmogorov-Smirnov statistic.

For the Kolmogorov-Smirnov test, $F^*(z)$ is a completely specified cumulative distribution function. That is no parameters for the distribution must be estimated from the data. Lilliefors (1967) and Crutcher (1975) point out that when a parameter must be estimated to specify $F^*(z)$, the Kolmogorov-Smirnov test is conservative with respect to Type I error. That is if the critical value is exceeded by the test statistic obtained from the observed values, the hypothesis is rejected with considerable confidence. In this situation other tables must be used in order to obtain a valid conclusion. Lilliefors (1967, 1969, 1973) has applied Monte-Carlo techniques to define the

critical values of Kolmogorov-Smirnov test statistics for the normal, the exponential, and the gamma and extreme value distributions when parameters of these distributions must be estimated.

The Cramer-von Mises Goodness-of-Fit Test--This method is only good for simple hypothesis testing. Unlike Kolmogorov-Smirnov test, the Cramer-von Mises test not only considers the largest difference, but also considers N differences between the two curves. The Cramer-von Mises test statistic is

$$T_{\text{CvM}} = \frac{1}{12N} + \sum_{i=1}^N \left[F^*(z_i) - \frac{i - 0.5}{N} \right]^2 \quad (3.49)$$

where N is total number of observations. Intuitively the Cramer-von Mises test statistic makes more complete use of the data and therefore should be more effective than the Kolmogorov-Smirnov test statistic; however, this cannot be proven (Conover, 1971).

The choice of model using the above non-parametric goodness-of-fit techniques can be made by comparing the test statistic that derived using different candidate models. For example, if χ^2 goodness-of-fit method is used, the test statistic, T_{χ^2} is computed based on sample data and various probability distribution models, f^* or F^* , investigated. Then, the model choice is made by selecting the model for which the likelihood of the observed value of T_{χ^2} is largest.

Beside the non-parametric statistical goodness-of-fit techniques, another intuitive approach is to select the model based on the value of likelihood of the observed sample data under each model investigated. For a

sample of size N the sample likelihood given $f^*(z)$ is

$$\begin{aligned}
 L(\underline{z}) &= f^*(z_1) \cdot f^*(z_2) \cdot \dots \cdot f^*(z_N) \\
 &= \prod_{i=1}^N f^*(z_i) \qquad (3.50)
 \end{aligned}$$

provided that z_1, z_2, \dots, z_N are independent and identically distributed. For a set of candidate probability distribution models for which the parameters have to be estimated, the model chosen by using this criterion would be the model with the maximum value of sample likelihood among all the models considered. The model chosen has the maximum posterior probability of being the true model when the prior distribution for the true model is uniform.

3.3.2 Philosophy of Proposed Method

In regard to model choice, Wood et al. (1974) raise an important point: "Most hydrologic processes are so complex that no model yet devised may be the true model or that no hydrologic events follow one particular model. Consequently, it could be reasonably expected that a combination of models would better 'explain' the hydrologic process than does a single model." Many hydrologists discourage the use of the previously described nonparametric goodness-of-fit techniques for testing hydrologic frequency distributions because of the importance of the tails of the hydrologic frequency distributions and the insensitivity of these statistical tests on the tails of the distributions. Furthermore, the power of these nonparametric

tests, i.e. the probability of rejecting the false hypothesis, is not high. This is true especially for small sample which is the case for most hydrologic data.

In the previous sections generalized parameter estimates are defined that reduce parameter uncertainty by weighting the regional and sample parameter estimates based on their respective variances of the estimates. These generalized parameter estimates are then utilized to compute the value of likelihood based on the sample collected which is used as the basis for model selection or define to a composite model.

The Bayesian technique enables the computation of the posterior probability of the distribution models investigated for a given prior probability of the model, the data observations, and the model parameters to develop a composite model. Here, the generalized parameter estimates are used without considering their corresponding variance and the posterior probability of a model can be computed by using Bayes' theorem as

$$P''(m_i) = \frac{L(\underline{z}|\hat{\underline{\theta}}, m_i) \cdot P'(m_i)}{\sum_{m_i \in M} L(\underline{z}|\hat{\underline{\theta}}, m_i) \cdot P'(m_i)} \quad (3.51)$$

in which $P''(m_i)$ is the posterior probability for model m_i , $P'(m_i)$ is the prior probability for model m_i , $L(\underline{z}|\hat{\underline{\theta}}, m_i)$ is the likelihood function for model m_i with parameters $\hat{\underline{\theta}}$ and observations \underline{z} , and M is the set of candidate models (normal, log-normal, Gumbel, Pearson III, log-Pearson III, etc.) investigated. The use of the Bayesian theorem enables the incorporation of prior knowledge

about the probability distribution, which may be based on experiences or other physical evidences, then updated with the data collected.

The value of the posterior probability is a measure of the likelihood for a model being the "true" one among all the models considered based on the data collected and prior knowledge. This approach enables the derivation of a composite probability distribution for the loading from different models considered and weighted by their associated posterior probability as

$$f_{\ell, m_c}(\ell) = \sum_{m_i \in M} P''(m_i) \cdot f_{\ell, m_i}(\ell) \quad (3.52)$$

where $f_{\ell, m_c}(\ell)$ is the composite probability distribution of the loading, $f_{\ell, m_i}(\ell)$ is the probability distribution of the loading for model m_i . Therefore, if a composite probability distribution of loading is used in the reliability models, such as Eq. (2.13) for the static case and Eq. (2.43) for dynamic case, a composite reliability model for the static case can be expressed as

$$\begin{aligned} R_c &= \int_0^\infty f_r(r') \left[\int_0^{r'} f_{\ell, m_c}(\ell') d\ell' \right] dr' \\ &= \sum_{m_i \in M} P''(m_i) \int_0^\infty f_r(r') \left[\int_0^{r'} f_{\ell, m_i}(\ell') d\ell' \right] dr' \end{aligned} \quad (3.53)$$

and a composite reliability model for the time-dependent case can be expressed as

$$\begin{aligned} R_c(t) &= \int_0^{\infty} f_r(r') e^{-\lambda t [1 - F_{\lambda, m_c}(r')]} dr' \\ &= \sum_{m_i \in M} P''(m_i) \int_0^{\infty} f_r(r') e^{-\lambda t [1 - F_{\lambda, m_i}(r')]} dr' \quad (3.54) \end{aligned}$$

The use of the composite hydrologic model in the static and time-dependent reliability models reduces hydrologic model uncertainty.

CHAPTER 4

RISK AND RELIABILITY MODELS FOR FLOOD LEVEE DESIGN

4.1 INTRODUCTION

In the design of flood levee systems many design variables must be considered. One of the most important variables is the height of the levee which is used as the principal measure of flood protection against overtopping. Also involved are soil properties which are important in preventing structural failure. The protection offered by a levee system is extremely important from an economical viewpoint in that if the protection cannot be evaluated properly, the expected damage that may occur could be underestimated. In other words, certain economic tradeoffs exist between the objectives of the levee system reliability and economic benefits. Because of the many design variables and their associated uncertainties, the risk of failure is difficult to analyze. This chapter presents a procedure to define the risk and reliability of overtopping for a flood levee system and systematically accounts for the hydrologic and hydraulic uncertainties.

The failure of levee systems can be divided into four common modes (Bogardi and Zoltan, 1968): (1) overtopping due to elevation of flood waters exceeding that of the levee, (2) structural failure of the levee resulting from water saturation and loss of soil stability, (3) structural failure resulting

from boils and hydraulic soil failure, and (4) wave action causing scour which reduces the levee strength. These failure modes can be considered as two major groups: (1) overtopping and (2) structural failure. Because the probabilities of structural failure of levees have not been defined to the extent of those related to hydrologic failure it is rather meaningless to attempt to define risk and reliability models that would consider both overtopping and structural failure. Wood (1977) has attempted to develop flood levee reliability models that can consider both structural failure and overtopping; however, there are many shortcomings of this work. These include: (1) the form of probability functions to model flood events which considered an exponential exceedance model, (2) no considerations given to hydrologic parameter and model uncertainties, (3) hydraulic uncertainties which are encountered in defining flood water elevations and conveyance capacities ignored, and (4) simplified probability of structural failure models (uniform and quadratic distributions) considered without any justification, etc.

Because of the lack of information available to define probabilities of structural failure of levees, the work presented in this chapter deals entirely with levee failure due to overtopping. The evaluation of risk and reliability of water resource projects such as flood levee systems using conventional approaches fails to provide adequate scientific and explicit means to define the uncertainties and associated risks involved. Conventional procedures consider only the hydrologic randomness of loading (i.e., flood flows) imposed on the structure and treats the capacity of the structure

as deterministic.

In Chapter 2 static and time-dependent risk and reliability models are developed for culvert design. The models are extended to include the hydrologic parameter and model uncertainties in Chapter 3. This chapter applies the methodologies described in previous chapters to treat various types of uncertainties for flood levee systems to define overall risks of overtopping. The static and time-dependent risk and reliability models for a levee system are determined using data for an area in southeastern Texas near Victoria, on the Guadalupe River. A U.S. Geological Survey gaging station is located on the Guadalupe River near Victoria for which seventy-five years of data are available. The annual maximum flood series for this gaging station are tabulated in Table 4.1

4.2 ANALYSIS OF HYDRAULIC UNCERTAINTIES

The main concern to a water resource engineer is the capacity of the structure that can sustain a certain level of design load, or flood. In the determination of the capacity of the structure several design variables are involved which can be considered as random variables with some associated variation. These design variables could be statistically dependent or independent of each other. First-order analysis which has been described in Chapter 2 is a method of providing an estimate of the uncertainty in a deterministic model involving variables with uncertainty.. Through a first-order analysis the mean and variance of the capacity of a flood levee system can be derived, provided that the statistical properties of the underlying

Table 4.1 Annual Maximum Series for Guadalupe River near Victoria, Tex.

Year	Peak Discharge (cfs)	Year	Peak Discharge (cfs)	Year	Peak Discharge (cfs)
1903	11,000	1928	79,000	1953	3,560
1904	10,560	1929	4,980	1954	4,950
1905	4,140	1930	4,920	1955	1,730
1906	10,560	1931	13,700	1956	25,300
1907	12,440	1932	5,790	1957	58,300
1908	4,040	1933	11,460	1958	10,100
1909	7,010	1934	38,500	1959	23,700
1910	3,300	1935	179,000	1960	55,300
1911	7,880	1936	17,200	1961	10,800
1912	10,350	1937	25,400	1962	4,100
1913	25,400	1938	4,940	1963	5,720
1914	14,690	1939	55,900	1964	15,000
1915	6,320	1940	58,000	1965	9,790
1916	3,300	1941	56,000	1966	70,000
1917	6,660	1942	7,710	1967	44,300
1918	13,900	1943	12,300	1968	15,200
1919	15,990	1944	22,000	1969	9,190
1920	8,530	1945	17,900	1970	9,740
1921	13,510	1946	46,000	1971	58,500
1922	7,200	1947	6,970	1972	33,100
1923	12,270	1948	20,600	1973	25,200
1924	1,050	1949	13,300	1974	30,200
1925	17,160	1950	12,300	1975	14,100
1926	1,490	1951	28,400	1976	54,500
1927	5,040	1952	11,600	1977	12,700

design variables involved are known. The specification of the uncertain feature of the variables can be expressed in terms of the mean, or mode, tolerance, and a distribution.

The cross-sectional configuration of streams and rivers, in general, are highly irregular as shown in Fig. 4.1. For computational purposes, the cross section is simplified as shown in Fig. 4.2. The simplified cross section in which the levee of a given size is constructed has idealized assumptions about the geometry for the purposes of model development, i.e. (1) the height of embankment on both sides of channel is the same, as well as along the reach considered; (2) the channel cross sectional geometry and location of the levee are symmetrical to the center line of the channel; (3) the traverse slope of the flood plain is small, i.e., $\cos\tau \approx \tau$, and (4) the width of encroachment of the levee, W_e , along the channel reach is constant. In addition to the geometry, assumptions are made about the hydraulic characteristics of the channel reach (e.g. roughness and slope are made), i.e. the surface roughness of both sides of flood plain has the same characteristics. With those assumptions and idealizations for the sake of simplicity the total levee capacity can be expressed using Manning's equation (Chow, 1959) as

$$Q_c = 1.49\lambda_m \left[\frac{1}{N_c} A_c^{5/3} P_c^{-2/3} + \frac{2}{N_b} A_{bh}^{5/3} P_{bh}^{-2/3} \right] S_f^{1/2} \quad (4.1)$$

where λ_m is used to take into account the error of using Manning's equation to describe the unsteady, non-uniform flow; N_c and N_b are surface roughness for the channel, and flood plain, respectively; S_f is the friction slope which is

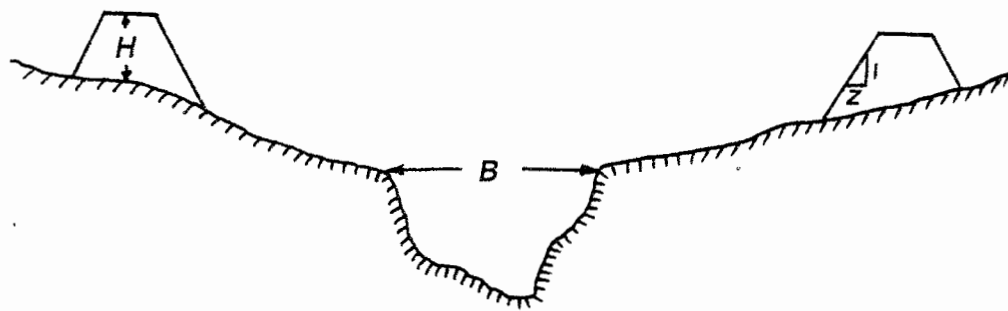
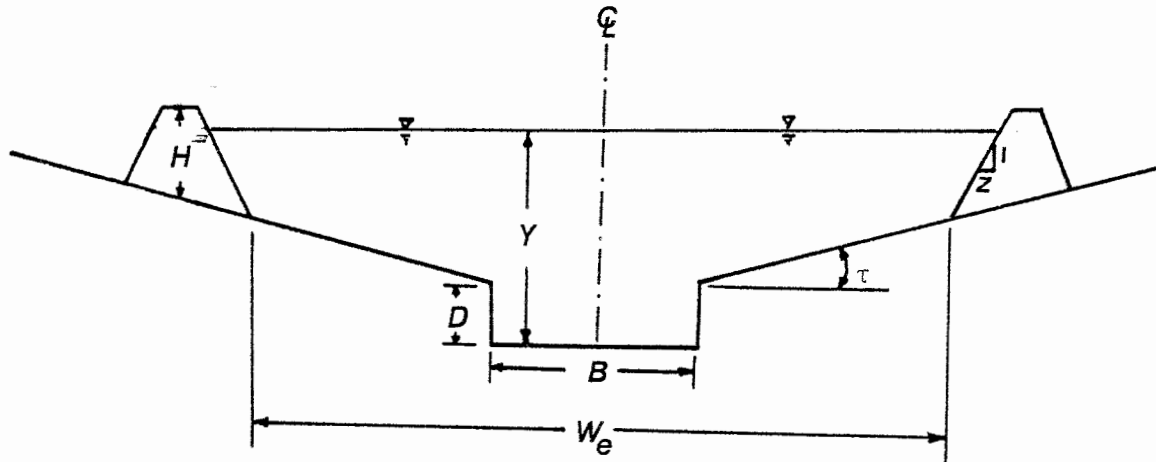


Figure 4.1 Cross-sectional Configuration of Rivers



$$A_c = B \cdot Y$$

$$P_c = B + 2D$$

$$A_{bh} = \frac{1}{2}zH^2 + \frac{1}{4}(Y-D+H)(W_e-B)$$

$$P_{bh} = H\sqrt{1+z^2} + \frac{W_e - B}{2\sqrt{1-\tau^2}}$$

$$S_f = S_0 + S_b$$

$$D = A_{fb}/B$$

Figure 4.2 Idealization of River Cross-section

equal to the sum of the channel bottom slope S_o and flood plain slope along the channel S_b under the idealizations of the levee layout mentioned, and A_c , P_c , A_{bh} , P_{bh} are defined in Figure 4.2. The simplifications are not necessary to the model development but are done here for explanation purposes.

In the analysis of uncertainty for the levee capacity, the height of the levee and the width of encroachment, which are design parameters, are considered to have insignificant uncertainties so that their uncertainty can be ignored as compared to the rest of the variables involved in Eq. (4.1). In order to define risk and reliability the probability density function must be evaluated which requires the parameters, mean and standard deviation of the resistance. A first order analysis of uncertainties of Eq. (4.1) is used to estimate the mean and coefficient of variation for Q_c .

The mean of the levee capacity can be expressed as

$$\bar{Q}_c = \bar{\lambda}_m \left[\frac{1.49}{\bar{N}_c} \bar{A}_c^{5/3} \bar{P}_c^{2/3} + \frac{2.98}{\bar{N}_b} \bar{A}_{bh}^{5/3} \bar{P}_{bh}^{-2/3} \right] \bar{S}_f^{1/2} \quad (4.2)$$

The coefficient of variation of the levee capacity is

$$\begin{aligned} \Omega_{Q_c}^2 = & \Omega_{\lambda_m}^2 + \frac{1}{4} \Omega_{S_f}^2 + \frac{1}{\psi^2} \left[\Omega_{N_c}^2 + \frac{25}{9} \Omega_{A_c}^2 + \frac{4}{9} \Omega_{P_c}^2 \right] \\ & + \frac{4}{\phi^2} \left[\Omega_{N_b}^2 + \frac{25}{9} \Omega_{A_{bh}}^2 + \frac{4}{9} \Omega_{P_{bh}}^2 \right] \end{aligned} \quad (4.3)$$

where

$$\Psi = 1 + 2 \left(\frac{\bar{N}_c}{\bar{N}_b} \right) \left(\frac{\bar{A}_{bh}}{\bar{A}_c} \right)^{5/3} \left(\frac{\bar{P}_c}{\bar{P}_{bh}} \right)^{2/3} \quad (4.4)$$

and

$$\phi = \frac{2 \Psi}{\Psi - 1} \quad (4.5)$$

The parameters A_c , P_c , A_b , P_b , and S_f , are related to channel top width B ; width of encroachment of levee W_e ; traverse slope on the flood plain; slope of flood plain along the channel S_b and channel bottom slope, S_o . Each of these is considered as a random variable with the exception of the width of encroachment, W_e , and levee height, H . Their uncertainty is considered small enough that it can be ignored as compared to the other variables using an idealized cross section. The functional relationships for A_c , P_c , A_b , P_b , and S_f , are expressed in Fig. 4.2.

The random nature of A_{fb} , B , τ , S_o , and S_b , requires use of the first order analysis to determine the mean and coefficient of variation of A_c , P_c , A_{bh} , P_{bh} , and S_f . The mean and coefficient of variation of these variables are expressed as:

for A_c ,

$$\bar{A}_c = \bar{B} \bar{Y} \quad (4.6)$$

$$\Omega_{A_c}^2 = \Omega_B^2 + \Omega_Y^2 \quad (4.7)$$

for P_c ,

$$\bar{P}_c = 2\bar{D} + \bar{B} \quad (4.8)$$

$$\Omega_{P_c}^2 = (4\bar{D}^2\Omega_D^2 + \bar{B}^2\Omega_B^2) / \bar{P}_c^2 \quad (4.9)$$

for A_{bh} ,

$$\bar{A}_{bh} = \frac{(zH^2)}{2} + \frac{(\bar{Y} - \bar{D} + H)}{2} \left(\frac{W_{e-\bar{B}}}{2} \right) \quad (4.10)$$

$$\Omega_{A_{bh}}^2 = \left[\bar{Y}^2 \left(\frac{W_{e-\bar{B}}}{2} \right)^2 \Omega_Y^2 + \bar{D}^2 \left(\frac{W_{e-\bar{B}}}{2} \right)^2 \Omega_D^2 + \bar{B}^2 \left(\frac{\bar{Y} - \bar{D} + H}{2} \right)^2 \Omega_B^2 \right] / 4\bar{A}_{bh}^2 \quad (4.11)$$

for P_{bh} ,

$$\bar{P}_{bh} = H\sqrt{1+z^2} + \frac{(W_{e-\bar{B}})}{2\sqrt{1-\bar{\tau}^2}} \quad (4.12)$$

$$\Omega_{P_{bh}}^2 = \left[\left(\frac{\bar{B}}{2\sqrt{1-\bar{\tau}^2}} \right)^2 \Omega_B^2 + \frac{\bar{\tau}^4}{(1-\bar{\tau})^3} \left(\frac{W_{e-\bar{B}}}{2} \right)^2 \Omega_\tau^2 \right] / \bar{P}_{bh}^2 \quad (4.13)$$

and for S_f ,

$$\bar{S}_f = \bar{S}_o + \bar{S}_b \quad (4.14)$$

$$\Omega_{S_f}^2 = (\bar{S}_o^2\Omega_o^2 + \bar{S}_b^2\Omega_b^2) / \bar{S}_f^2 \quad (4.15)$$

in which

$$\bar{Y} = H + \frac{\bar{\tau}}{2}(W_e - \bar{B}) + \bar{D} \quad (4.16)$$

$$\Omega^2_{\bar{Y}} = \left[\left(\frac{\bar{\tau}\bar{B}}{2} \Omega_B \right)^2 + \left(\frac{W_e - \bar{B}}{2} \right)^2 (\bar{\tau} \Omega_{\tau})^2 + (\bar{D} \Omega_D)^2 \right] / \bar{Y}^2 \quad (4.17)$$

$$\bar{D} = \bar{A}_{fb} / \bar{B} \quad (4.18)$$

$$\Omega^2_D = \Omega^2_{A_{fb}} + \Omega^2_B \quad (4.19)$$

The probability distribution of the random variable, levee capacity, is assumed to be log-normal. The underlying random variables on which the mean and coefficient of variation of levee capacity are based are channel cross sectional area with full bank flow A_{fb} and top width of channel B , S_o , S_b , and τ . Simple distributions (uniform and triangular) are used to describe the nature of variation of the variables, (Fig. 4.3). By considering minimum and maximum values of each variable, w_l and w_u , it is possible to use these distributions (Fig. 4.3) to compute the coefficient of variation of each

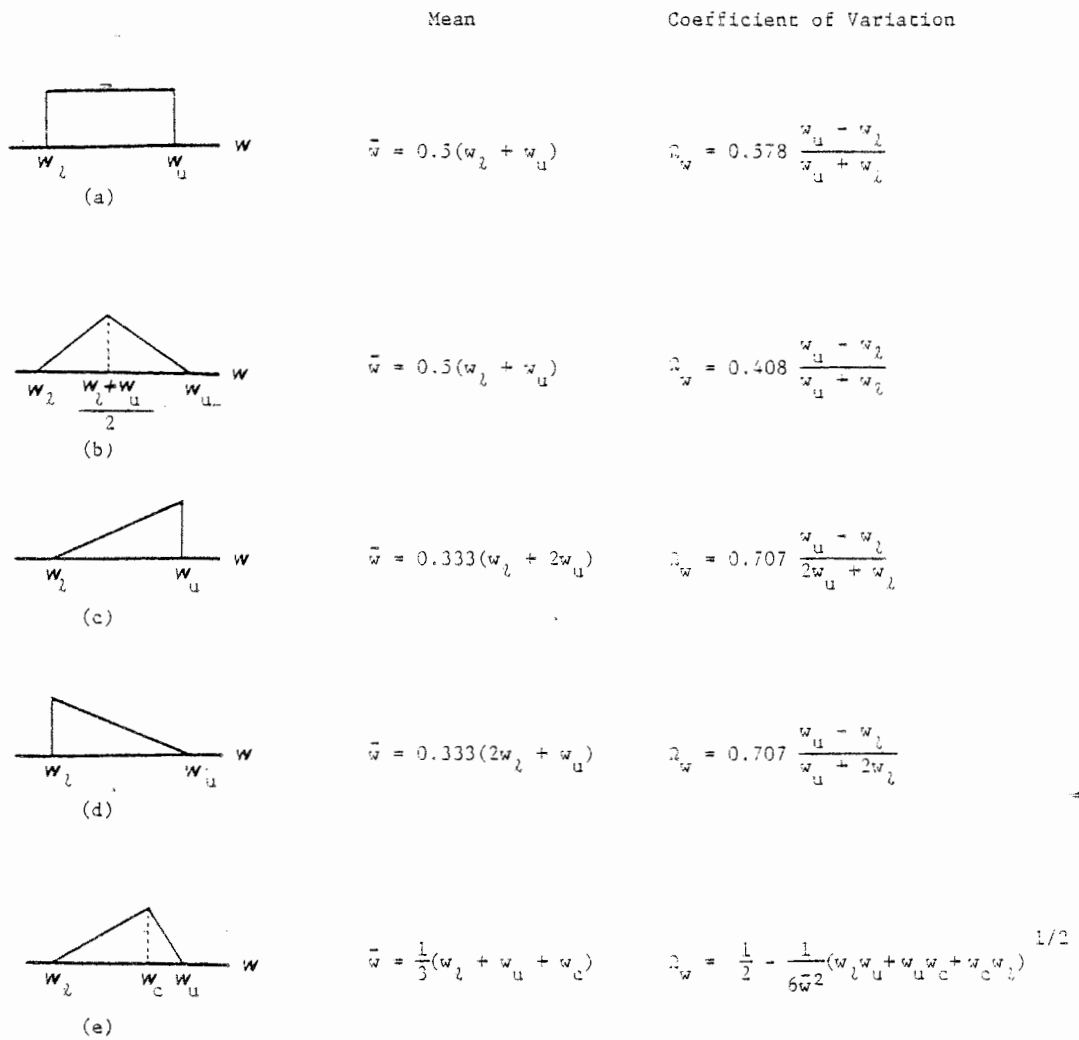


Figure 4.3 Statistics of Five Simple Distributions

variable. The lower and upper bounds of tolerance used for each variable and their associated mean and coefficient of variation are tabulated in Table 4.2. For a given width of encroachment and levee height the mean and coefficient of variation of the variables D , A_c , P_c , A_{bh} , and S_f in Eq. (4.1), and corresponding levee capacity Q_c are tabulated in Table 4.3. Since the resistance is assumed to be log-normally distributed Eq., (2.44), and the mean Eq. (4.2) and the coefficient of variation Eq. (4.3) of the resistance characterize the shape of the distribution.

4.3 ANALYSIS OF HYDROLOGIC UNCERTAINTIES

Hydrologic uncertainties as described can be classified into three types: (1) the inherent uncertainty, (2) the model uncertainty, and (3) the parameter uncertainty. In traditional practice the parameter and model uncertainties are ignored. In this chapter the procedure used to determine the generalized values of the parameters (mean, standard deviation, and skewness of the loading distribution described in Chapter 3 is applied. The weights are defined as a function of the variance of both the sample parameter estimates and the regionalized parameter estimates, Eq. (3.12), such that the variance of the generalized parameter is minimized.

For the study area the values of the physiographic and meteorologic characteristics for the regression equations are tabulated in Table 4.4. The regional parameter estimates, i.e. the mean (Z_r), standard deviation (S_{Z_r}), and skewness (G_{Z_r}), of the annual maximum series and also the mean (Y_r),

Table 4.2 Means, Tolerances, and Distribution of Hydraulic Variables in the Levee Design

Random Variable	Distribution Figure (4.3)	w_l	w_u	w_c	Mean	Coefficient of Variation
A	d	3200	4400		3600	0.079
B	c	195	245		228	0.052
S_o	a	0.0005	0.0011		0.0008	0.217
S_b	b	0.0006	0.0014		0.0010	0.163
τ	b	0.0020	0.0028		0.0024	0.068
λ_m	b	0.90	1.10		1.00	0.041
N_c	c	0.043	0.063	0.050	0.052	0.080
N_b	e	0.060	0.100	0.070	0.077	0.128

Table 4.3
Sample Hydraulic Data for a Levee Height and Encroachment Width

Variable	W	H	A _c	P _c	A _{bh}	P _{bh}	S _f	Q _c
Mean	3428.3	2.50	5047.6	259.9	7075.6	1067.9	0.0018	75541
Coefficient of Variation			0.085	0.047	0.2383	0.004	0.1523	0.211

Table 4.4 Physiographic and Meteorologic Characteristics
for Guadalupe River near Victoria, Tx.

Contributing drainage area (A_d)	= 5198 sq. miles
Main channel slope (S_λ)	= 5.23 feet per mile
Percentage of surface storage (S_t)	= 1.03
Total main channel length (L)	= 351 miles
10-yr, 24-hr rainfall intensity (I)	= 6.14 inches
Mean annual number of thunderstorm days (N_t)	= 41
Ratio of runoff to precipitation during the month when the annual maximum peak discharge occurred (R_t)	= 0.32

standard deviation (S_{Y_r}), and skewness (G_{Y_r}), of the log-transformed values of the annual maximum series, derived by using Eq. (3.27), (3.28), (3.29), (3.30), (3.31), and (3.32), respectively are tabulated for the study area in Table 4.5. The above mentioned parameters estimated from the sample data using Eqs. (3.1)-(3.6) are also given in Table 4.5. The variances of the regional parameter estimates and the variances of the sample parameter estimates derived from using the jackknife method as well as the bootstrap method are presented in Table 4.5. Once the sample and regional parameter estimates and their variances are computed, the weighting factor and the generalized parameter estimate can be derived using Eqs. (3.12) and (3.10), respectively. Table 4.5 lists the generalized parameter estimates for the streamflows and also for the log-transformed streamflows. In reality, the probability model describing the random mechanism of the hydrologic flood flow sequence is not known. Using the generalized parameter estimates the procedure of selecting a composite model described in Chapter 3.3 can be applied. The probability models considered for the loading include the normal, log-normal, Gumbel, Pearson type III, and log-Pearson type III. Table 4.6 lists the posterior probability of the five loading probability distributions in which the parameter estimates derived from different method, using Eq. (3.51), with equal prior probability, i.e., 0.2, for each model considered. No attempt is made to examine what effect different prior probabilities have on the resulting posterior probability of the model.

Table 4.5
Parameter Estimates, Variances and Weights for Victoria Data

θ 's	\bar{Z}	SZ	GZ	\bar{Y}	Sy	Gy
$\hat{\theta}_s$	21495	25792	3.586	9.524	0.938	0.142
$\hat{\theta}_r$	29338	20597	2.420	9.848	0.861	-0.115
Var ($\hat{\theta}_r$)	1.55×10^8	2.91×10^8	1.493	0.225	0.0344	0.2581
Var ($\hat{\theta}_s$)	1.55×10^5	5.7×10^7	5.755	0.001	0.0066	0.2676
W_θ	1.00	0.836	0.206	1.000	0.840	0.491
$\hat{\theta}$	21786	24931	2.647	9.653	0.933	-0.194
Var ($\hat{\theta}_s$)	9.36×10^6	4.04×10^7	1.113	0.013	0.007	0.091
W_θ	0.943	0.878	0.573	0.944	0.833	0.740
$\hat{\theta}$	21944	25157	3.087	9.542	0.925	0.0750

*Bias corrected sample statistics by jackknife method are used for $\hat{\theta}_s$.

Table 4.6 Posterior Probability of the Loading
Distribution Models

Model	Normal	Log-normal	Gumbel	Pearson III	Log-Pearson III
$P'(m_i)$	0.2	0.2	0.2	0.2	0.2
$P''(m_i \hat{\theta}_{TMJ})$	0.000	0.498	0.000	0.000	0.502
$P''(m_i \hat{\theta}_{TMB})$	0.000	0.611	0.000	0.000	0.389

4.4 DEVELOPMENT OF STATIC AND TIME-DEPENDENT RISK-SAFETY FACTOR CURVES

Once the probability distributions for the loading and resistance are described and the parameters for each are estimated the static and time-dependent risk-safety factor curves for levees are developed. The probability models considered for the loading include the normal, log-normal, Gumbel, Pearson III, and log-Pearson III. The procedure to establish the risk-safety factor relationships for the levee system are as follows:

1. Select the design flood, $Q_d(T_r)$ depending on the loading distribution model adopted. If the generalized mean, standard deviation and skewness are computed by the TMJ method and the loading is normally or Pearson type III distributed, then the frequency equation is

$$Q_d(T_r) = 21786 + 24931 K_{T_r} \quad (4.20)$$

where K_{T_r} is frequency factor. If the loading is log-normal or log-Pearson type III distributed, then the frequency equation is

$$\ln(Q_d(T_r)) = 9.653 + 0.933 K_{T_r} \quad (4.21)$$

If the loading is a Gumbel distribution, the frequency equation is

$$Q_d(T_r) = -19439 \ln[-\ln-(1 - \frac{1}{T_r})] + 10566 \quad (4.22)$$

2. Vary the width of encroachment of the levee, W_e .
3. Vary the height of the levee, H .
4. Compute the mean, \bar{Q}_c , and coefficient of variation, Ω_{Q_c} , of the levee capacity using Eqs. (4.2) and (4.3), respectively.

5. Check whether \bar{Q}_C for a specified encroachment width and levee height is greater than $Q_d(T_r)$. If not, then go to step (2) or (3) to change the dimension of the levee structure and layout. Otherwise, go to the next step.

6. Compute the reliability or risk associated with a given dimension of the levee. For static case the reliability is computed using Eq. (2.13) for the time-dependent case use Eq. (2.61). Also compute the characteristic safety factor, \bar{u} using Eq. (2.49).

7. Repeat steps (2) through (6) until the entire range of variables has been examined.

Figures 4.4 through 4.8 are the static risk-safety factor curves using the Victoria data for the different loading distributions. Figures 4.9 through 4.13 present the risk-safety factor curves for the time-dependent risk model for different loading distributions with a design return period of 100 years. The jackknife method was used to compute the variance of the sample statistics. Figures 4.14 through 4.18 and 4.19 through 4.23 are risk-safety factor curves developed with design return periods of 200 years and 500 years, respectively, for different service lives for each loading distribution of the time-dependent model. The shape of the risk-safety factor curves vary significantly, depending upon the loading probability model used.

Because the model describing the true random mechanism of the flood event is not known, the choice of one particular probability model can give a significantly different answer from that of another. Hence, a composite risk-safety factor curve can be developed which results from weighting each of the different loading distributions considered by the model

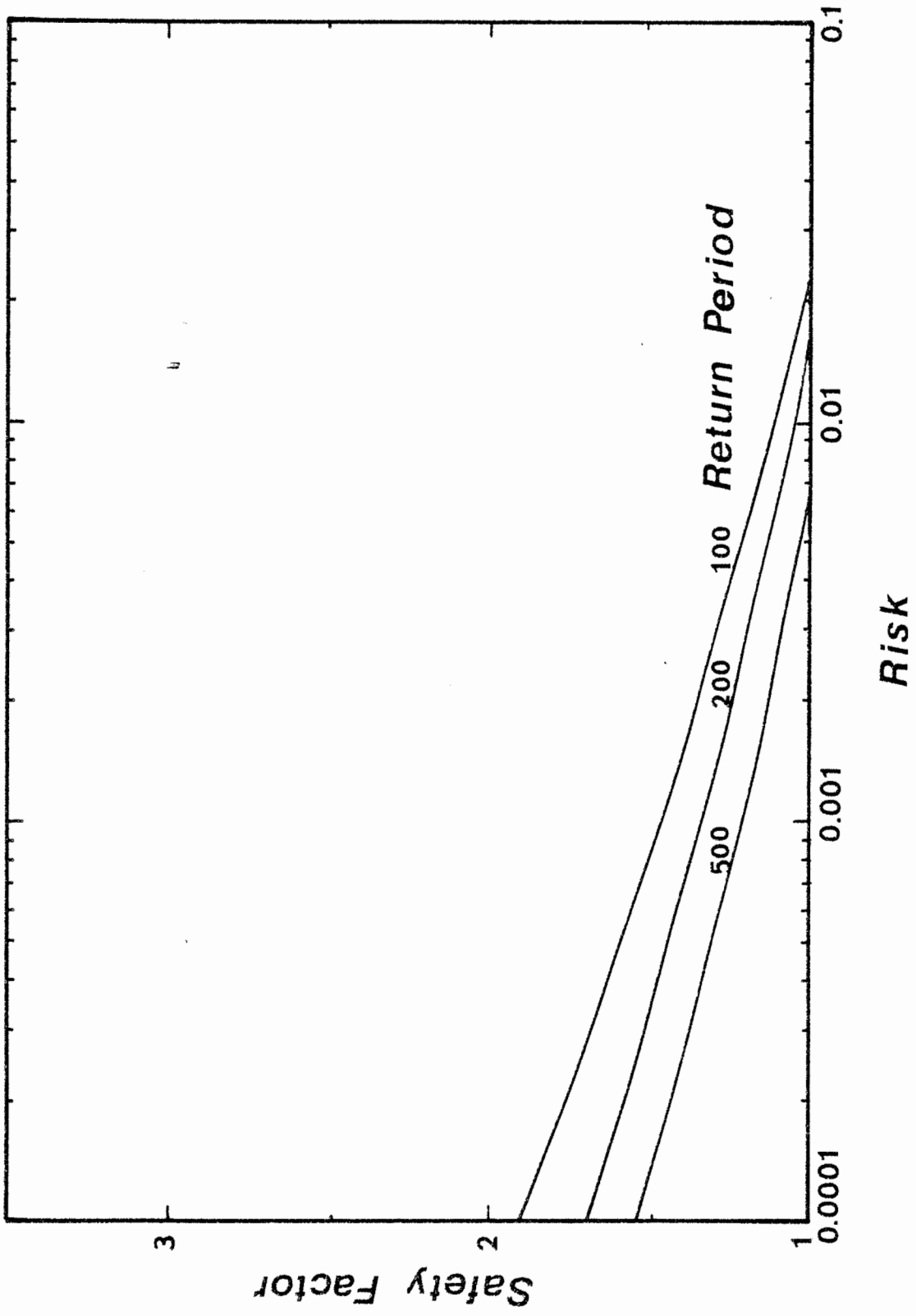


Figure 4.4 Static Risk-Safety Factor Curves for Levee Design Using Normal Loading Distribution

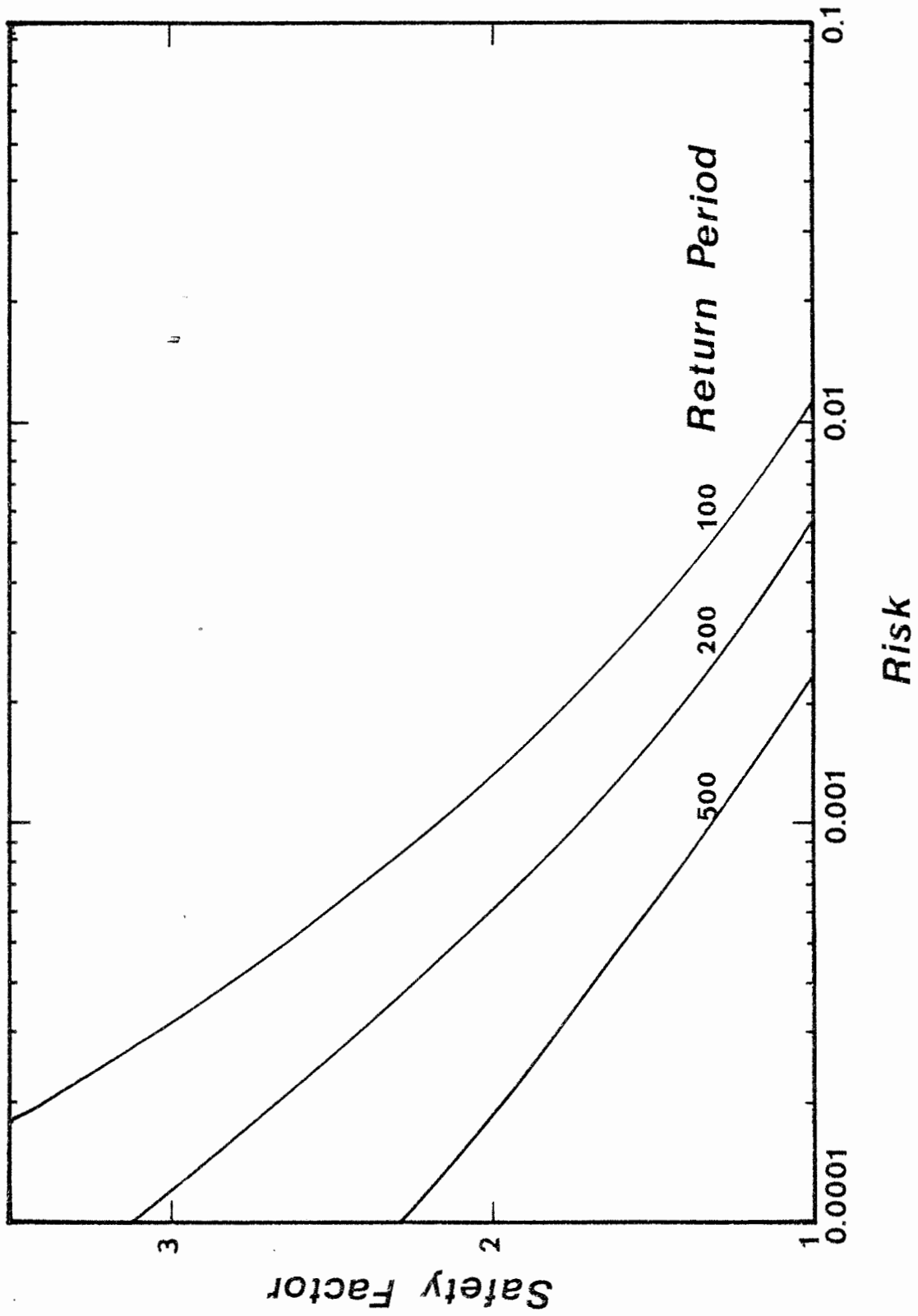


Figure 4.5 Static Risk-Safety Curves for Levee Design
Using Lognormal Loading Distribution

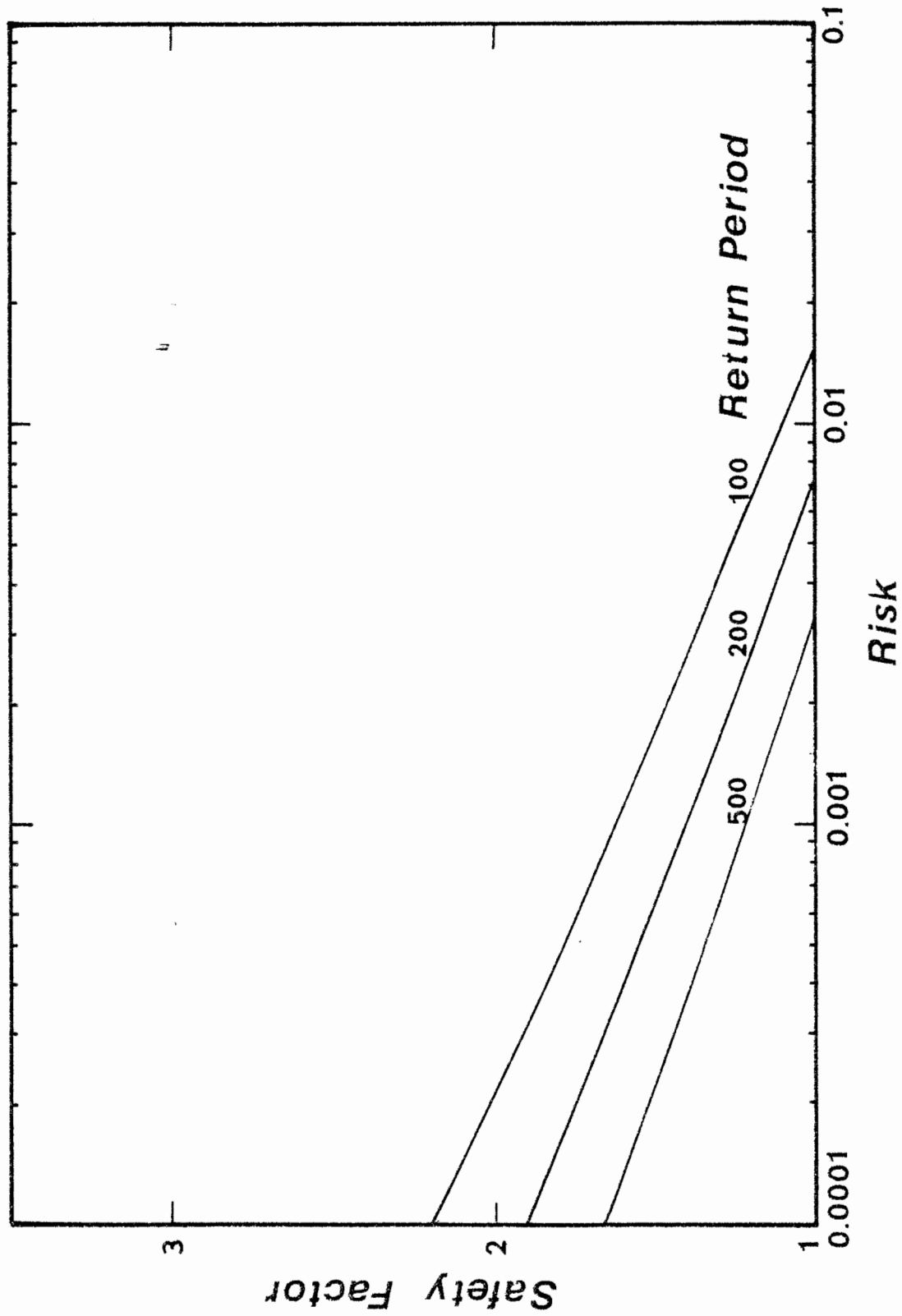


Figure 4.6 Static Risk-Safety Factor Curves for Levee Design Using Gumbel Loading Distribution

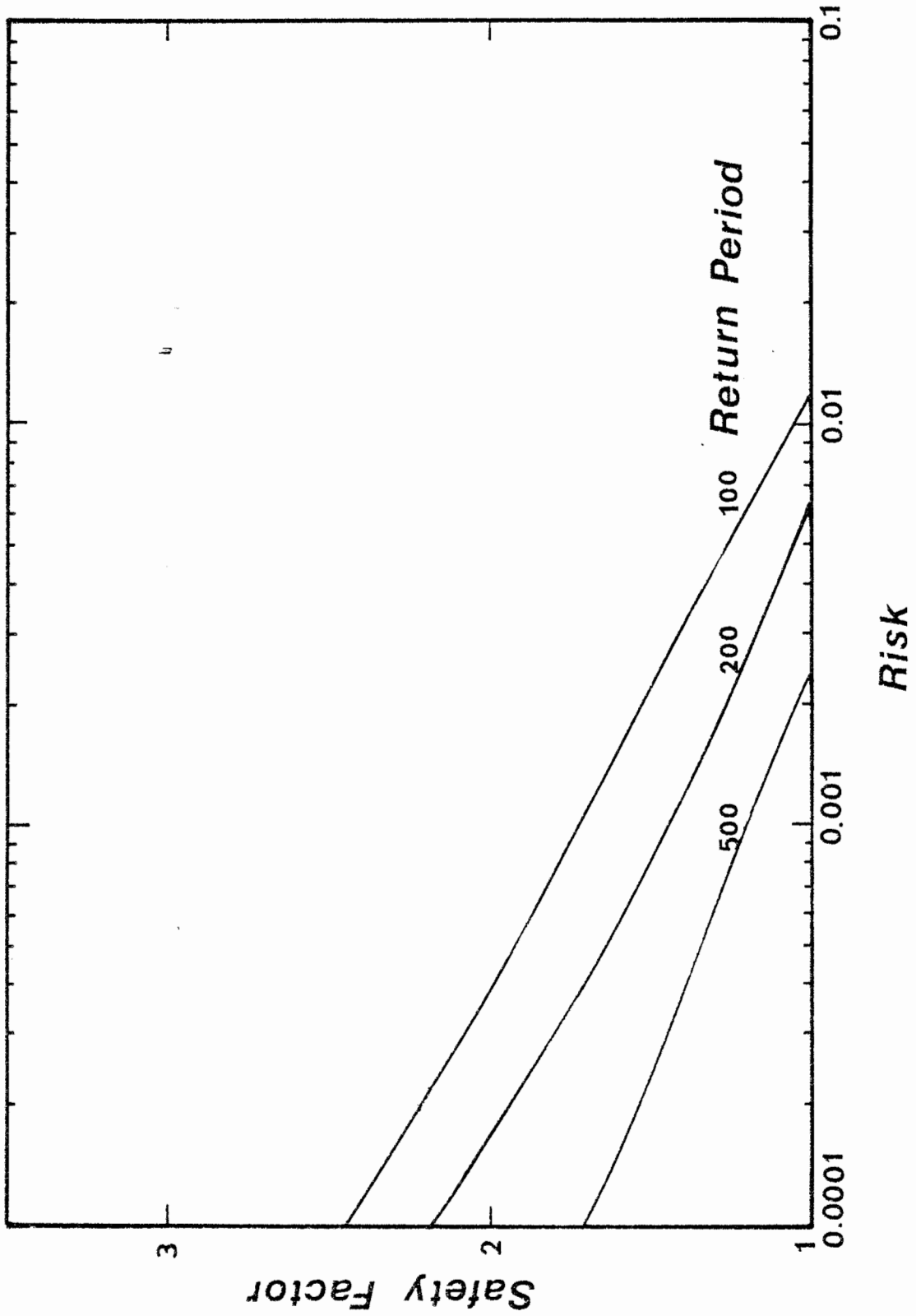


Figure 4.7 Static Risk-Safety Factor Curves for Levee Design Using Pearson III Loading Distribution

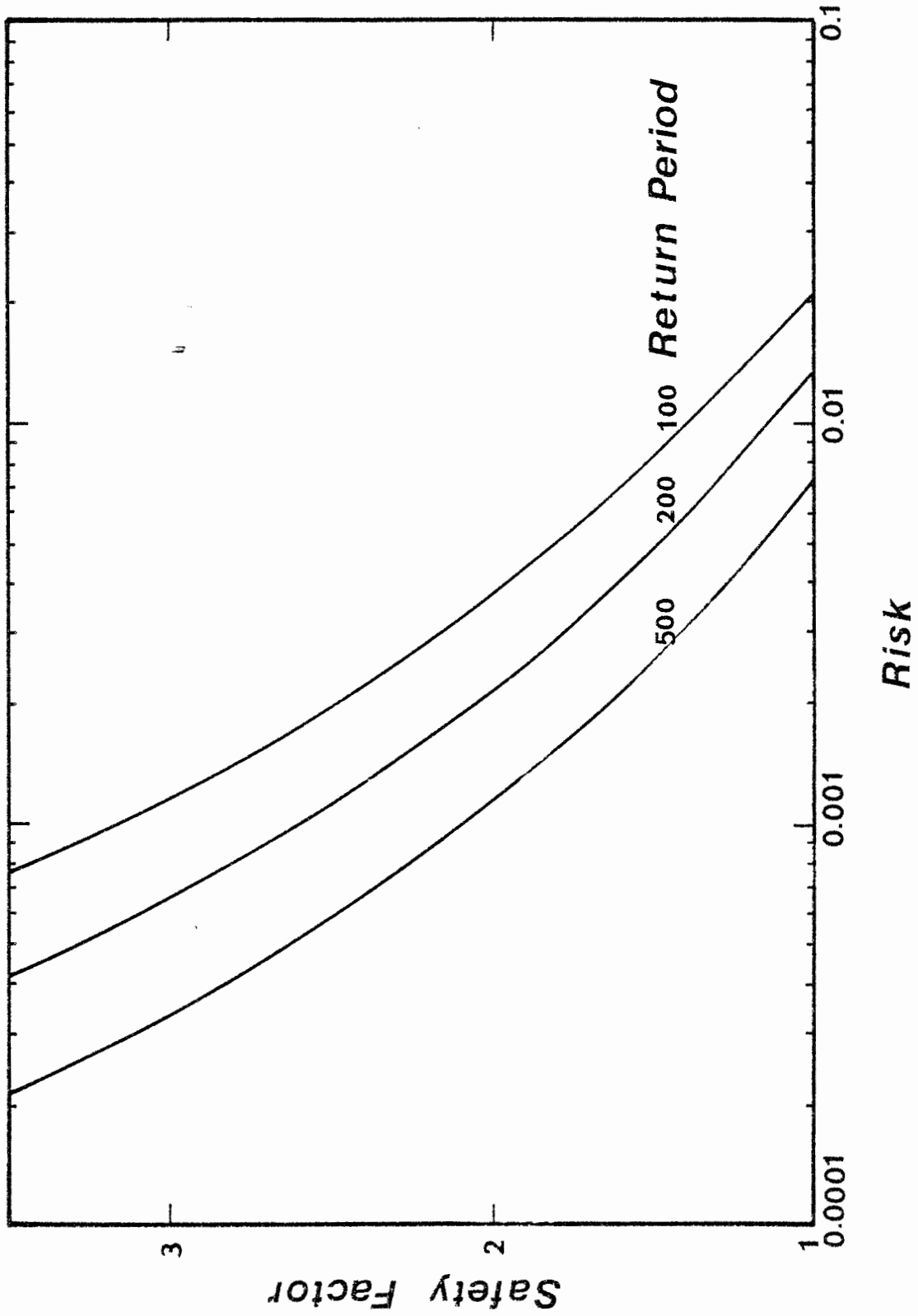


Figure 4.8 Static Risk-Safety Factor Curves for Levee Design Using Log-Pearson III Loading Distribution

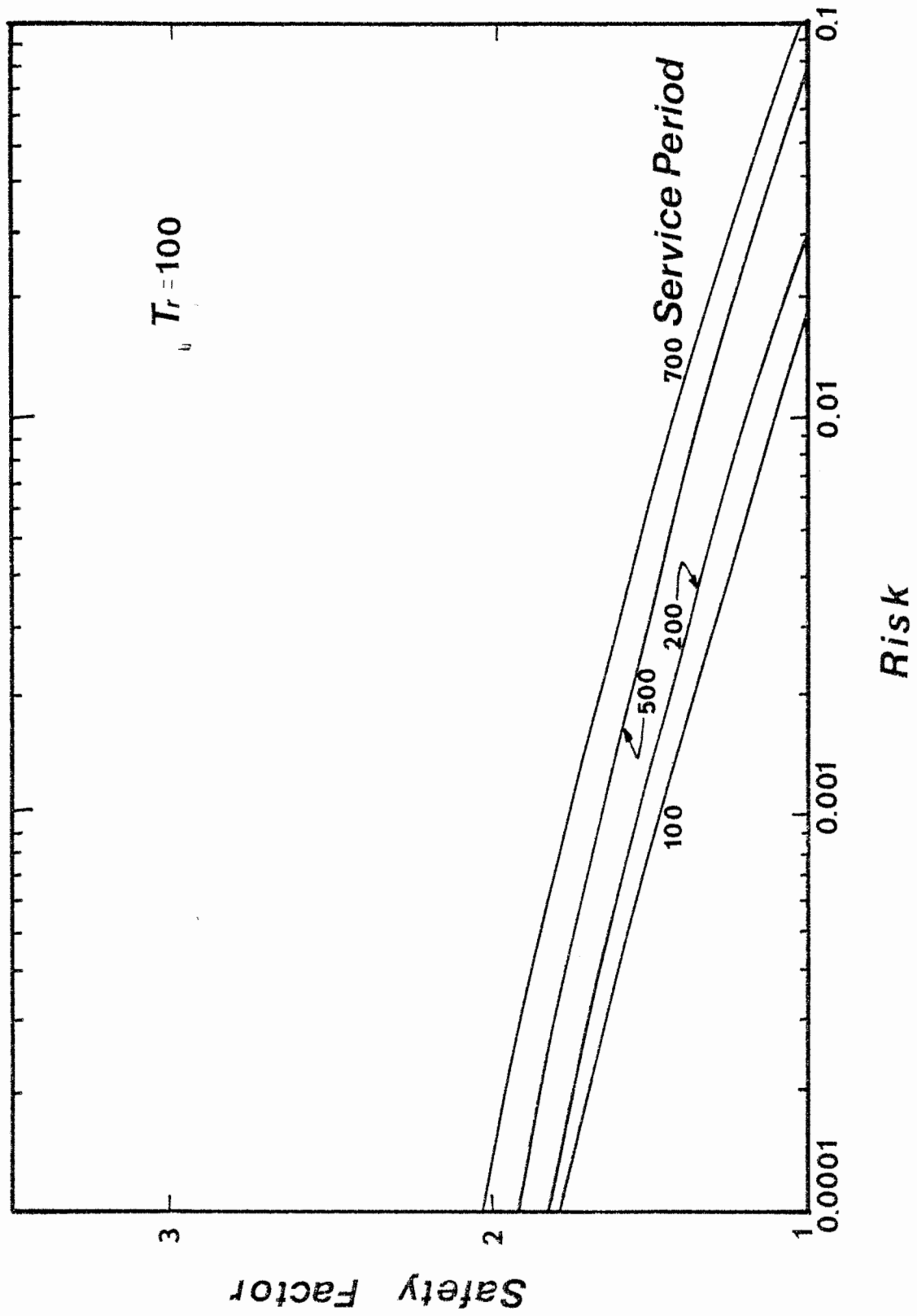


Figure 4.9 Time-Dependent Risk-Safety Factor Curves for Levee Design Using Normal Loading Distribution Based on $T_r = 100$ Years

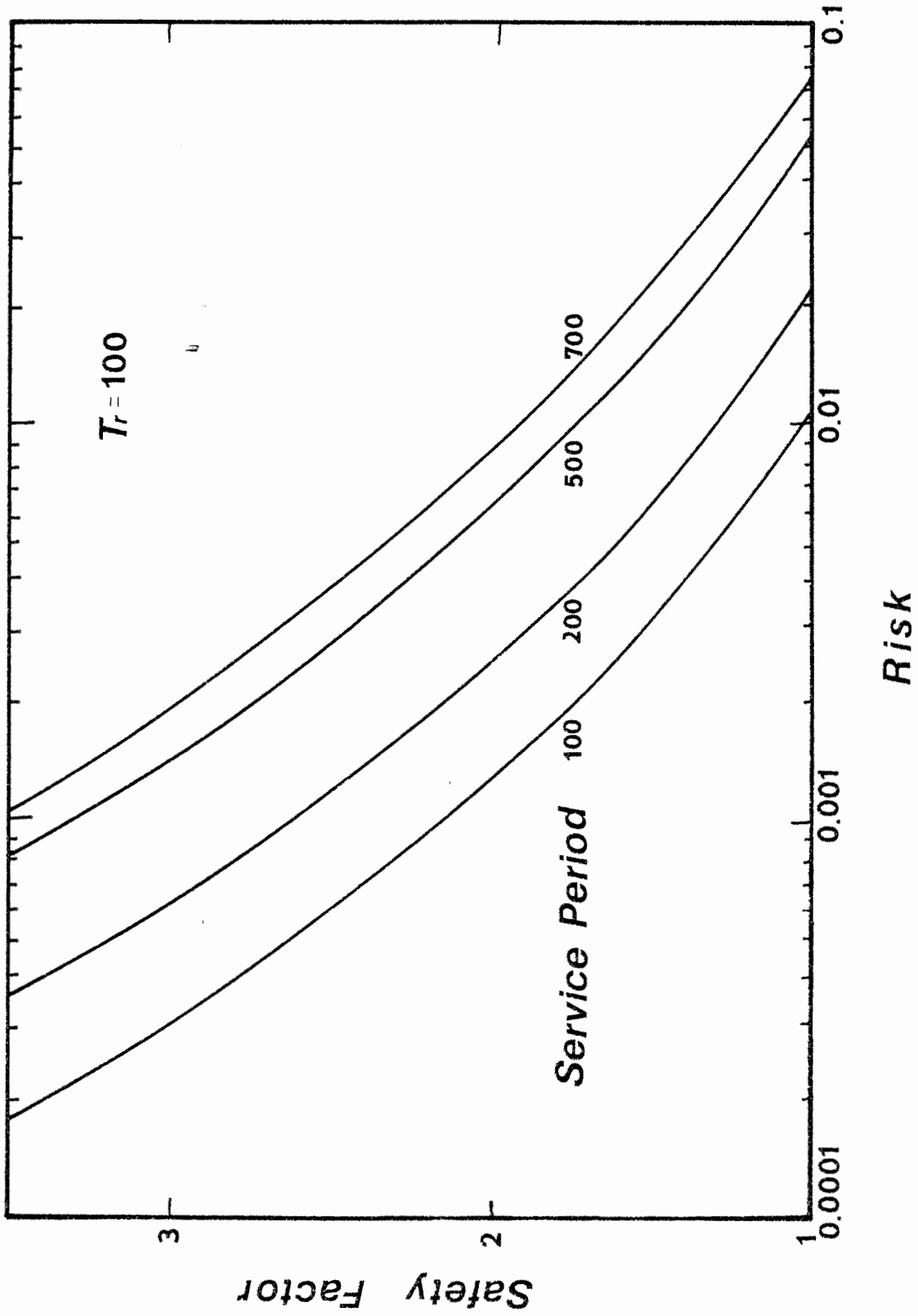


Figure 4.10 Time-Dependent Risk-Safety Factor Curves for Levee Design Using Lognormal Loading Distribution Based on $T_r = 100$ Years

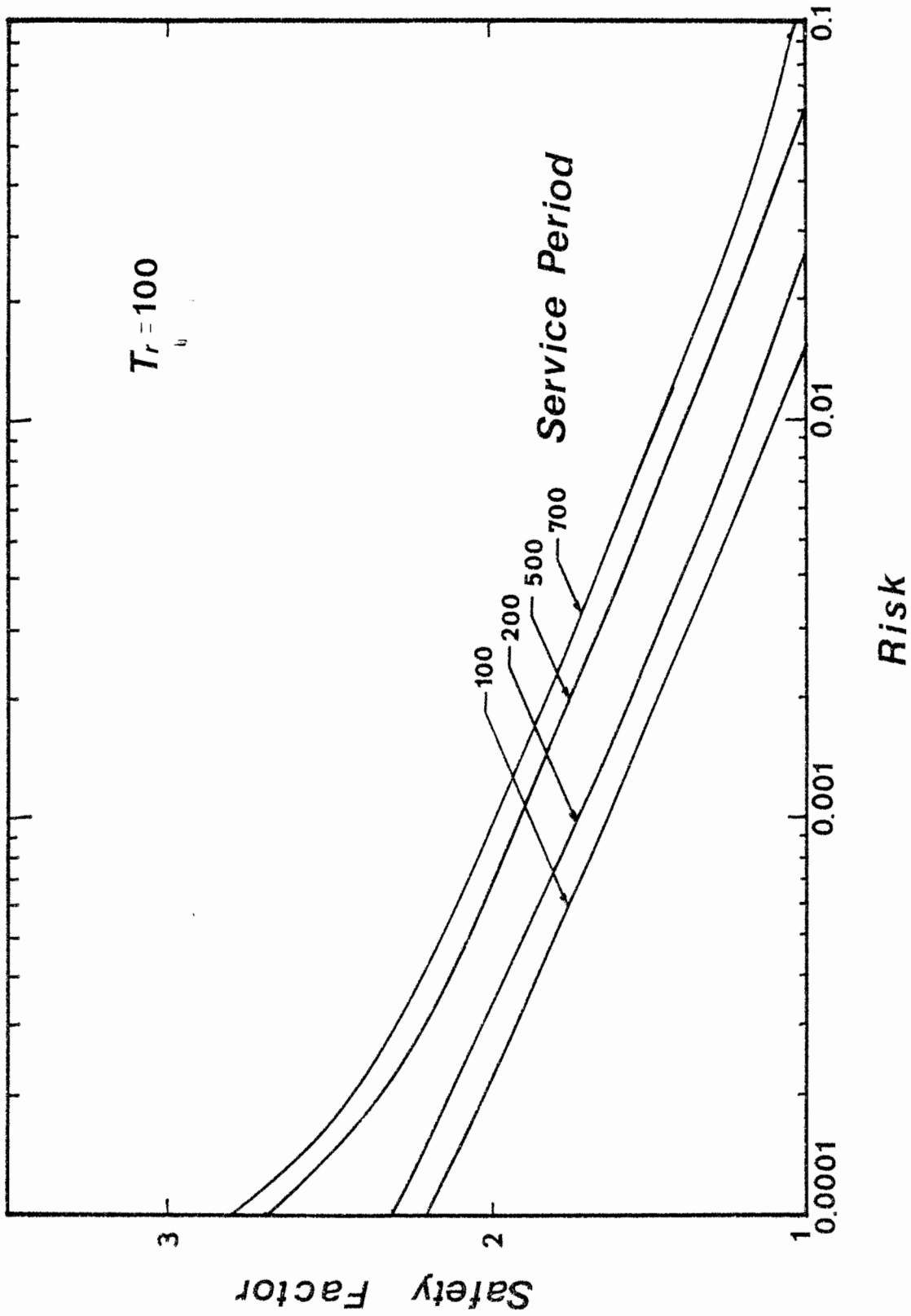


Figure 4.1.1 Time-Dependent Risk-Safety Factor Curves for Levee Design Using Gumbel Loading Distribution Based on $T_r = 100$ Years

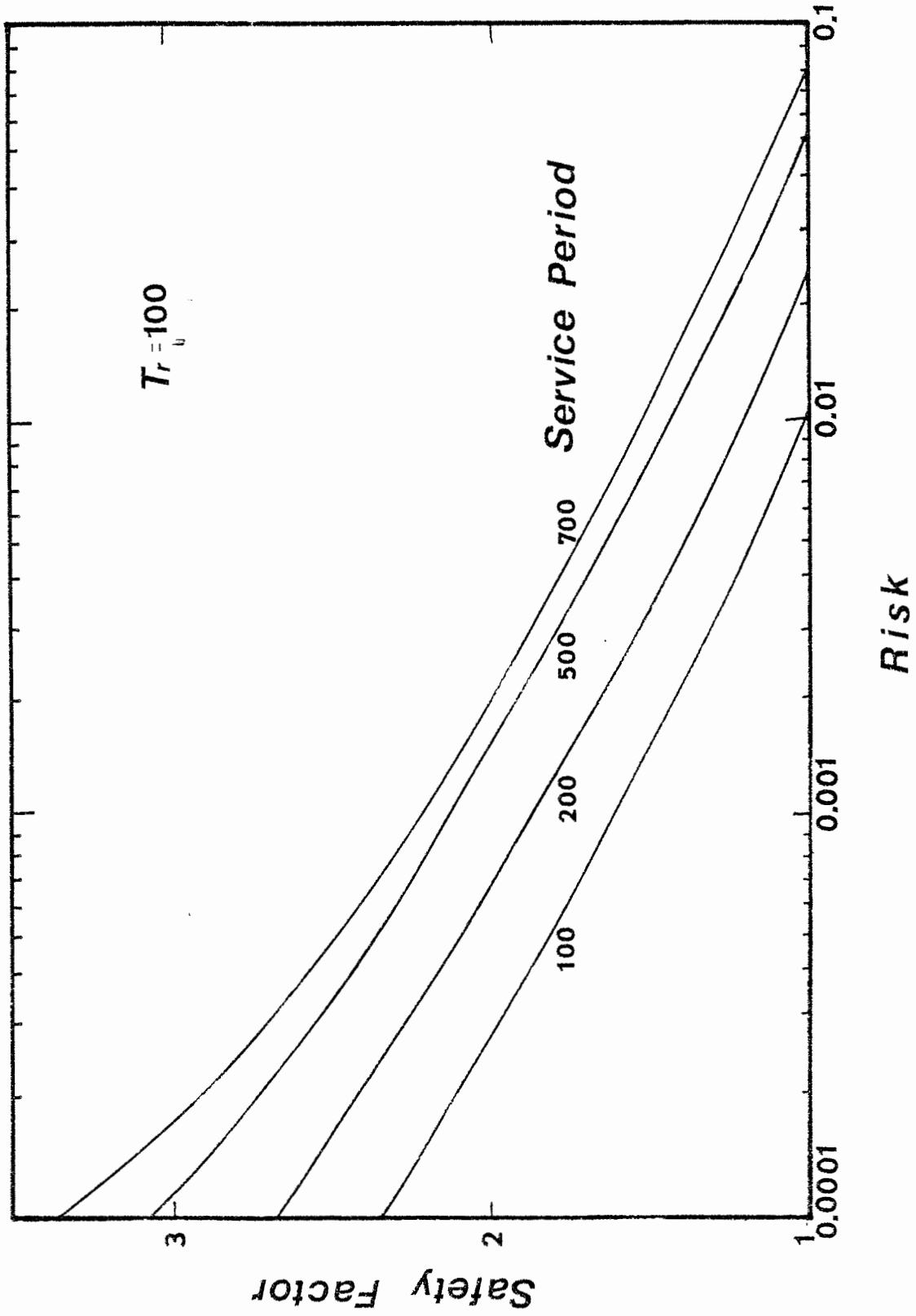


Figure 4.12 Time-Dependent Risk-Safety Factor Curves for Levee Design Using Pearson III Loading Distribution Based on $T_r = 100$ Years

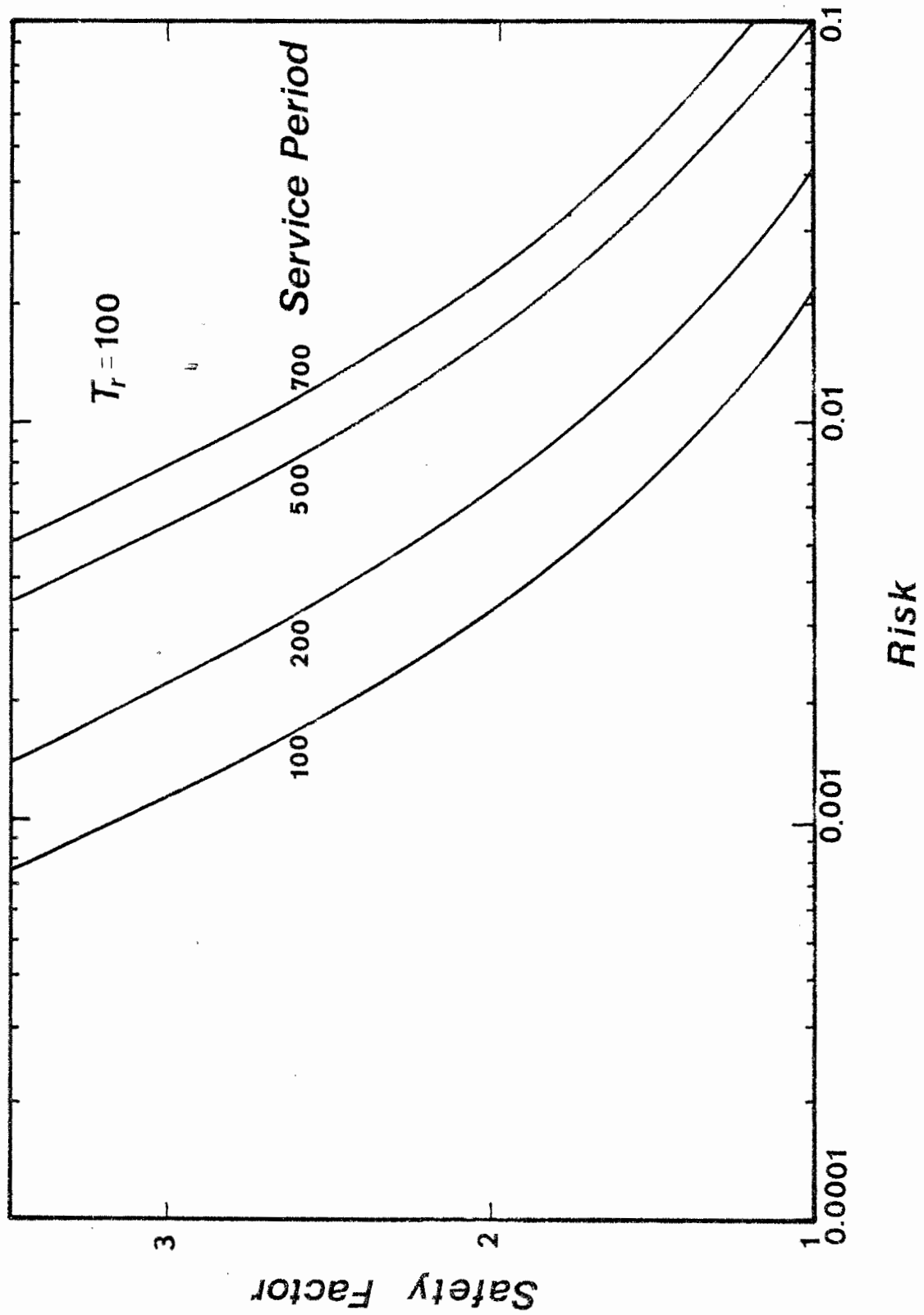


Figure 4.13 Time-Dependent Risk-Safety Factor Curves for Levee Design Using Log-Pearson III Loading Distribution Based on $T_r = 100$ Years

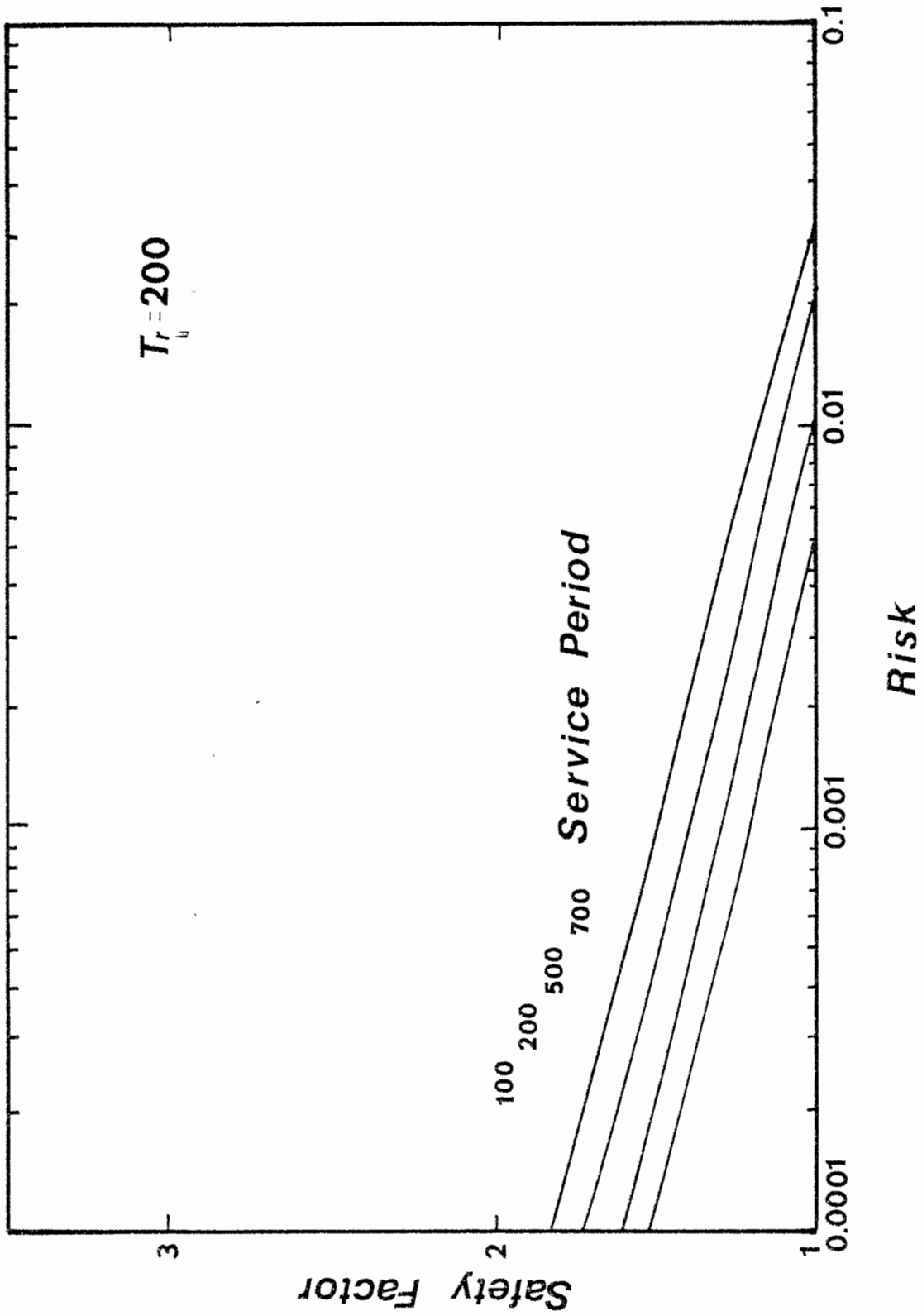


Figure 4.14 Time-Dependent Risk-Safety Factor Curves for Levee Design Using Normal Loading Distribution Based on $T_r = 200$ Years

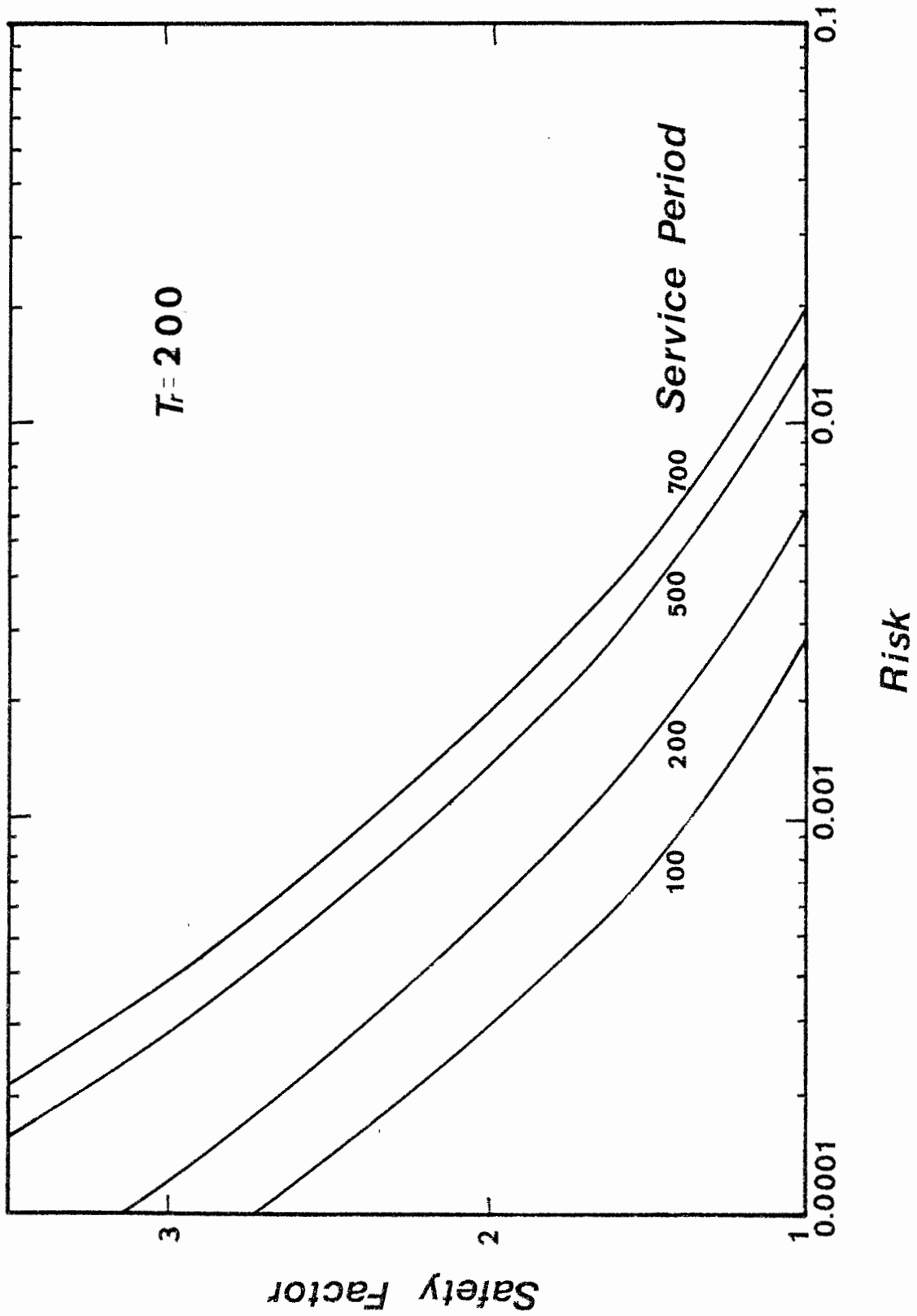


Figure 4.15 Time-Dependent Risk-Safety Factor Curves for Levee Design Using Lognormal Loading Distribution Based on $T_r = 200$ Years

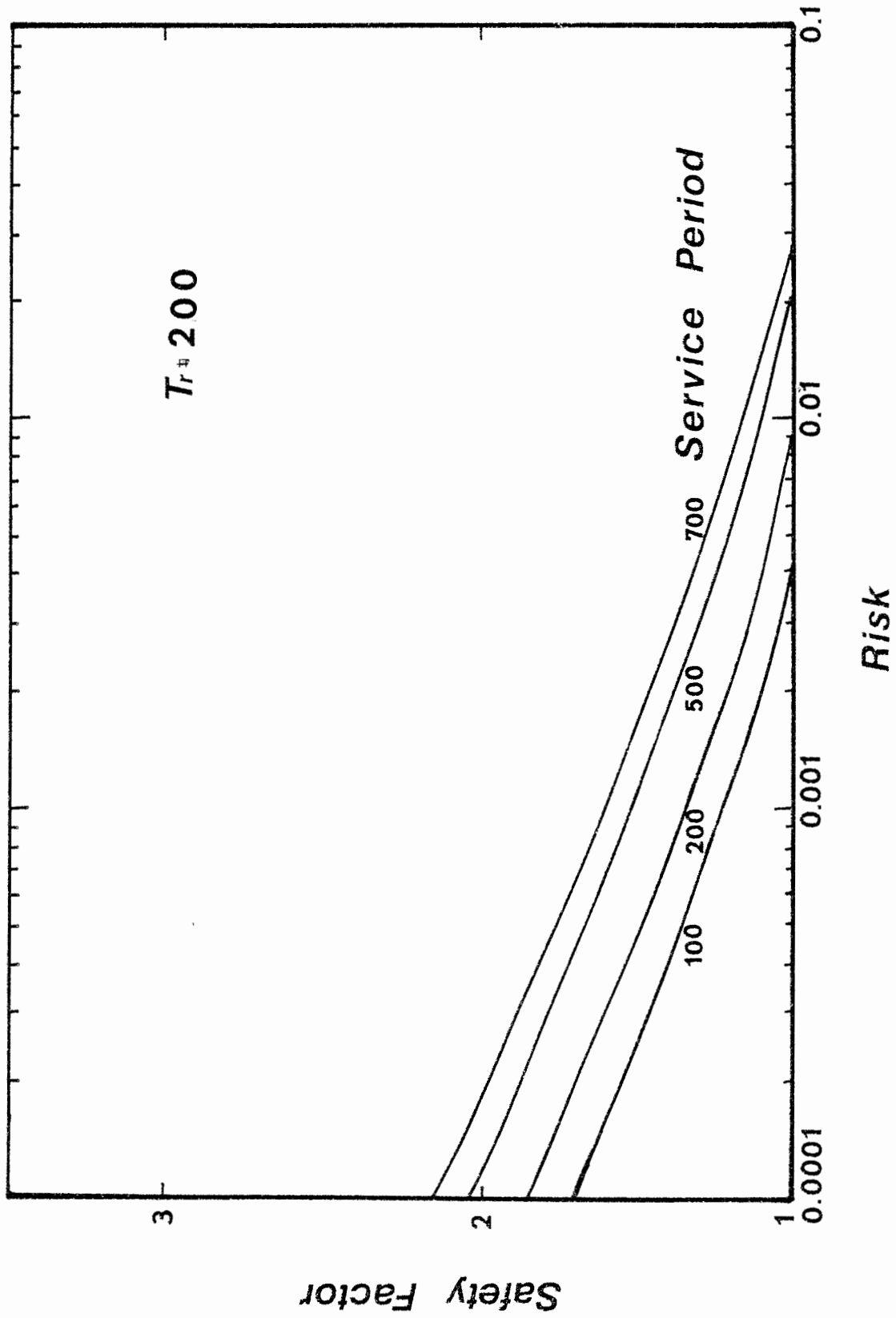


Figure 4.16 Time-Dependent Risk-Safety Factor Curves for Levee Design Using Gumbel Loading Distribution Based on $T_r = 200$ Years

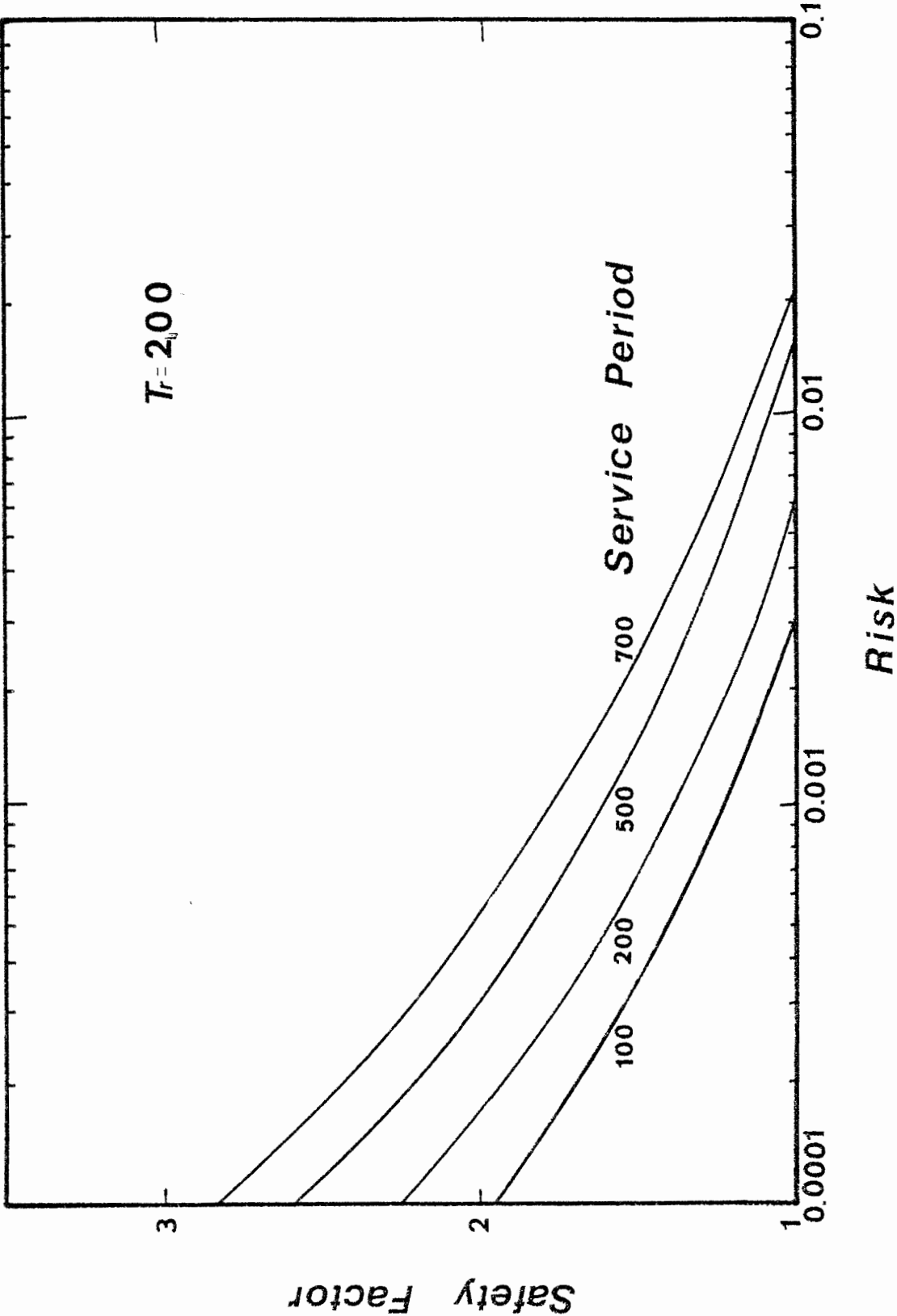


Figure 4.17 Time-Dependent Risk-Safety Factor Curves for Levee Design Using Pearson III Loading Distribution Based on $T_r = 200$ Years

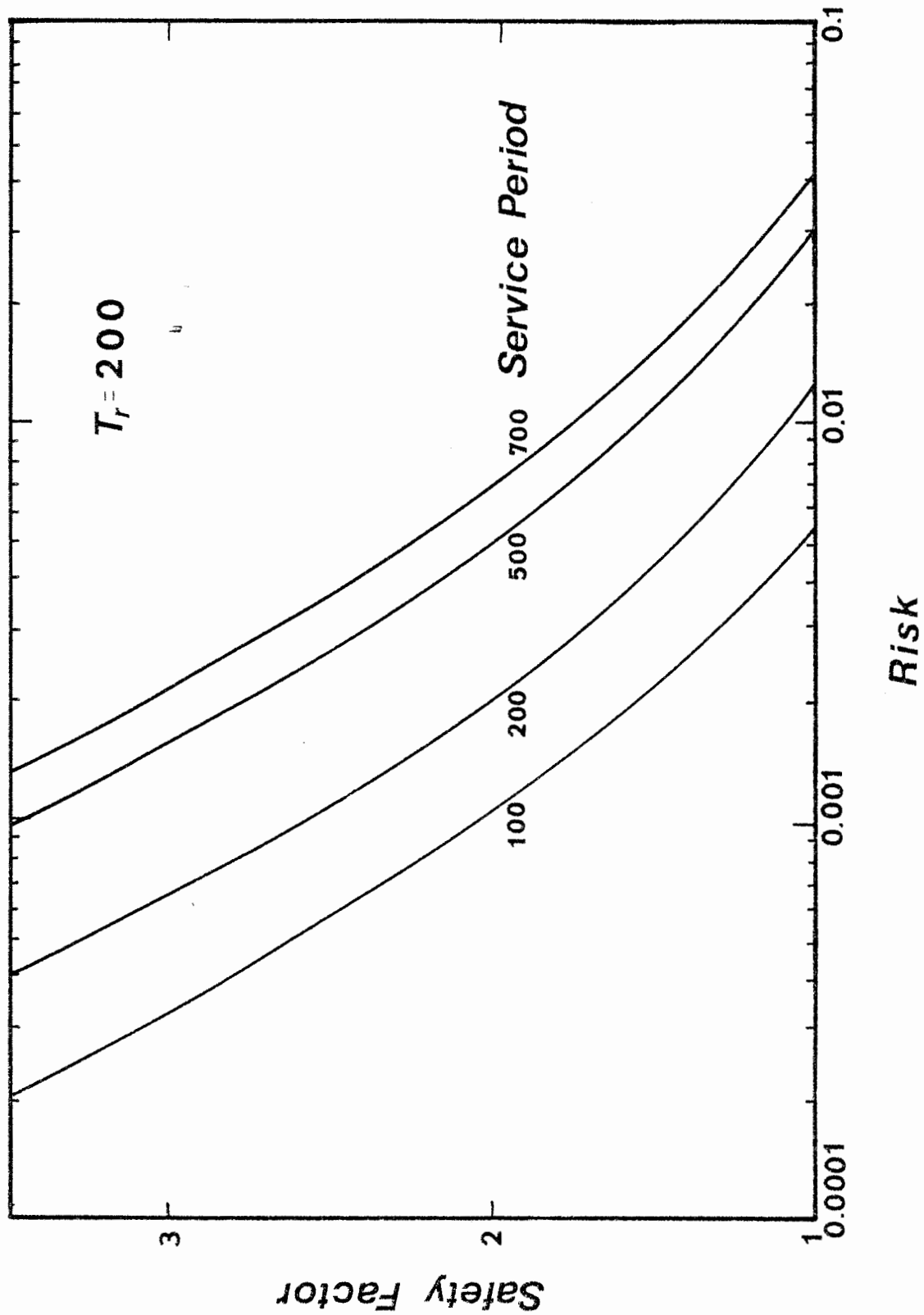


Figure 4.18 Time-Dependent Risk-Safety Factor Curves for Levee Design Using Log-Pearson III Loading Distribution Based on $T_r = 200$ Years

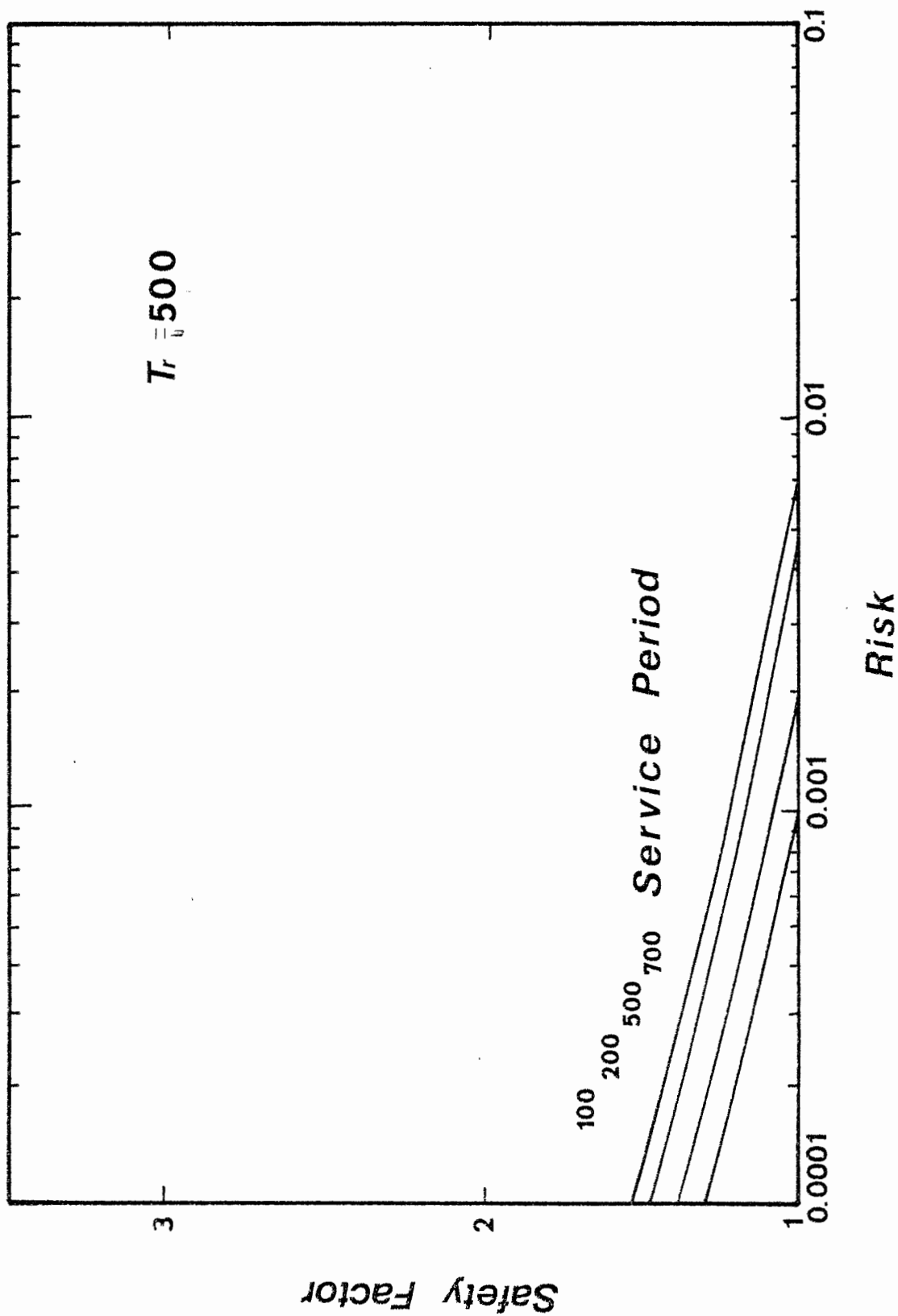


Figure 4.19 Time-Dependent Risk-Safety Factor Curves for Levee Design Using Normal Loading Distribution Based on $T_r = 500$ Years

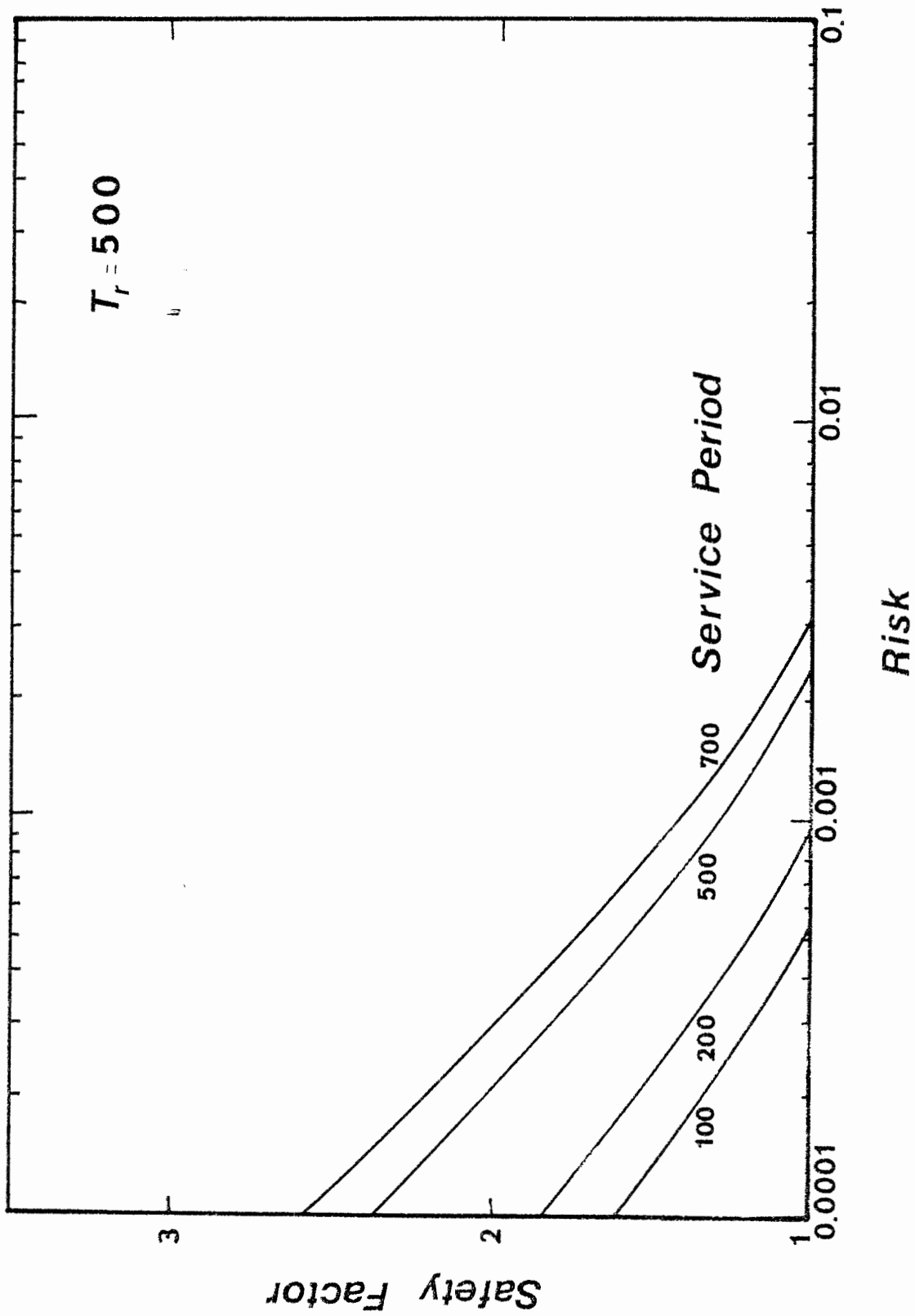


Figure 4.20 Time-Dependent Risk-Safety Factor Curves for Levee Design Using Lognormal Loading Distribution Based on $T_r = 500$ Years

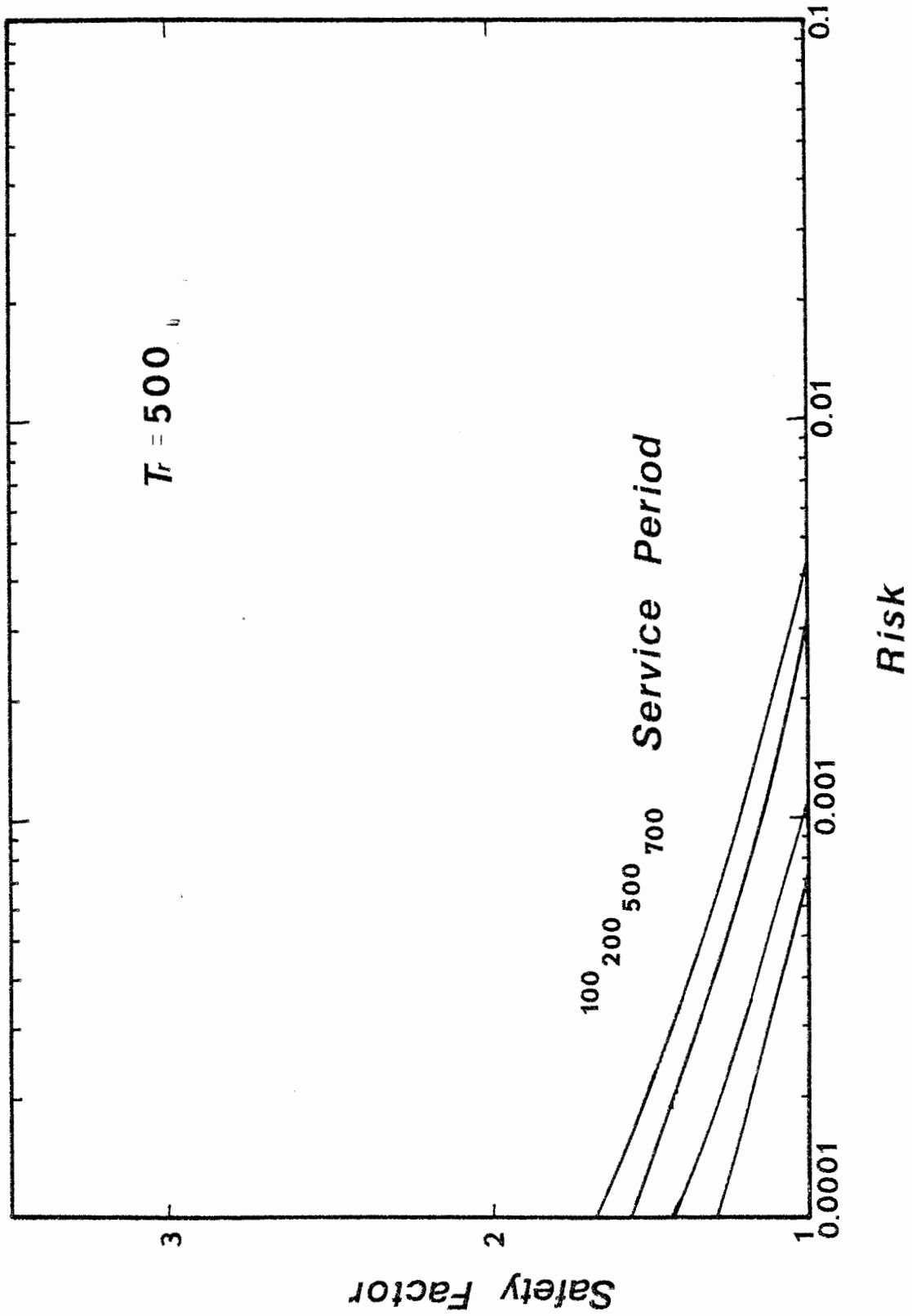


Figure 4.21 Time-Dependent Risk-Safety Factor Curves for Levee Design Using Gumbel Loading Distribution Based on $T_r = 500$ Years

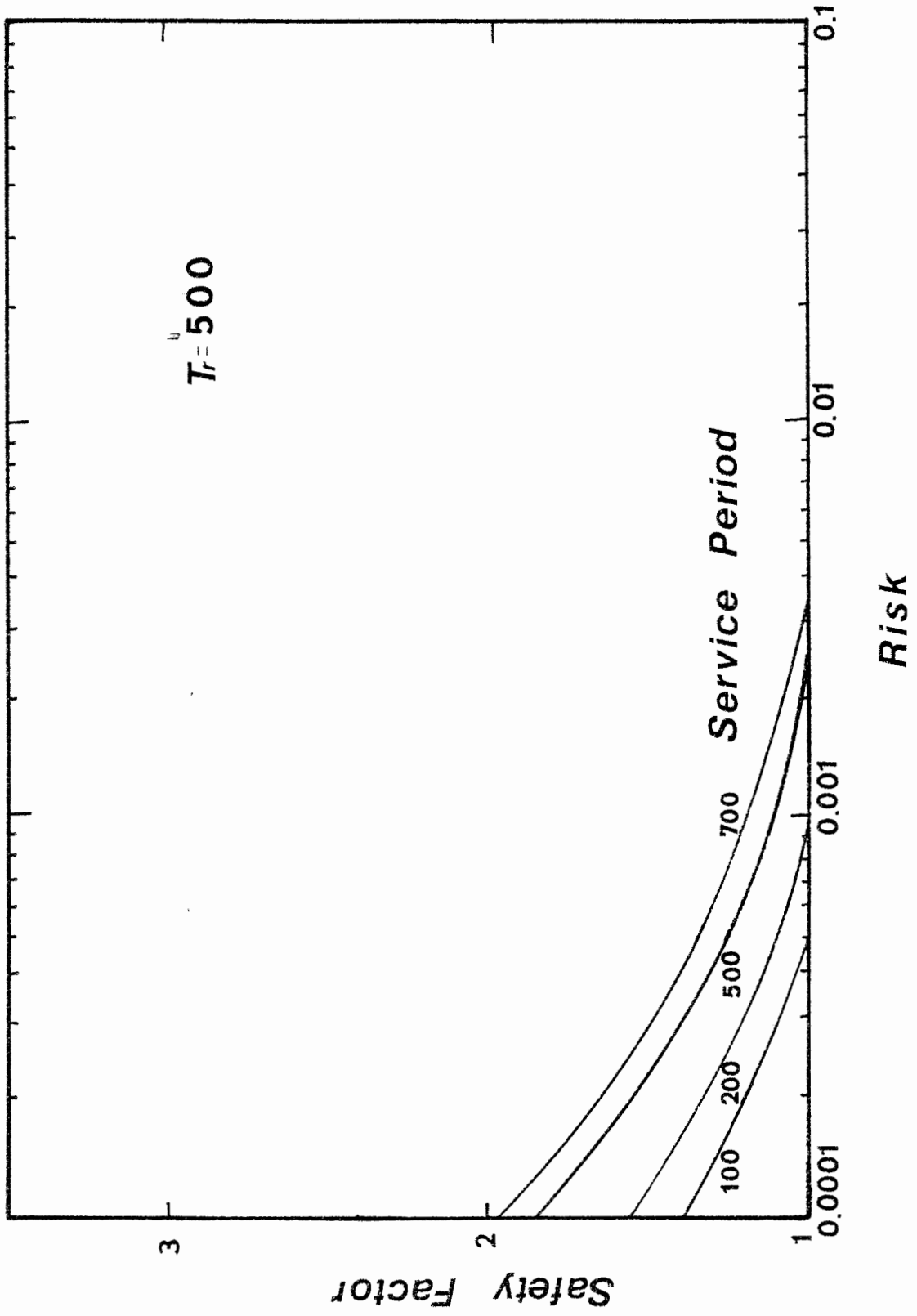


Figure 4.22 Time-Dependent Risk-Safety Factor Curves for Levee Design Using Pearson III Loading Distribution Based on $T_r = 500$ Years

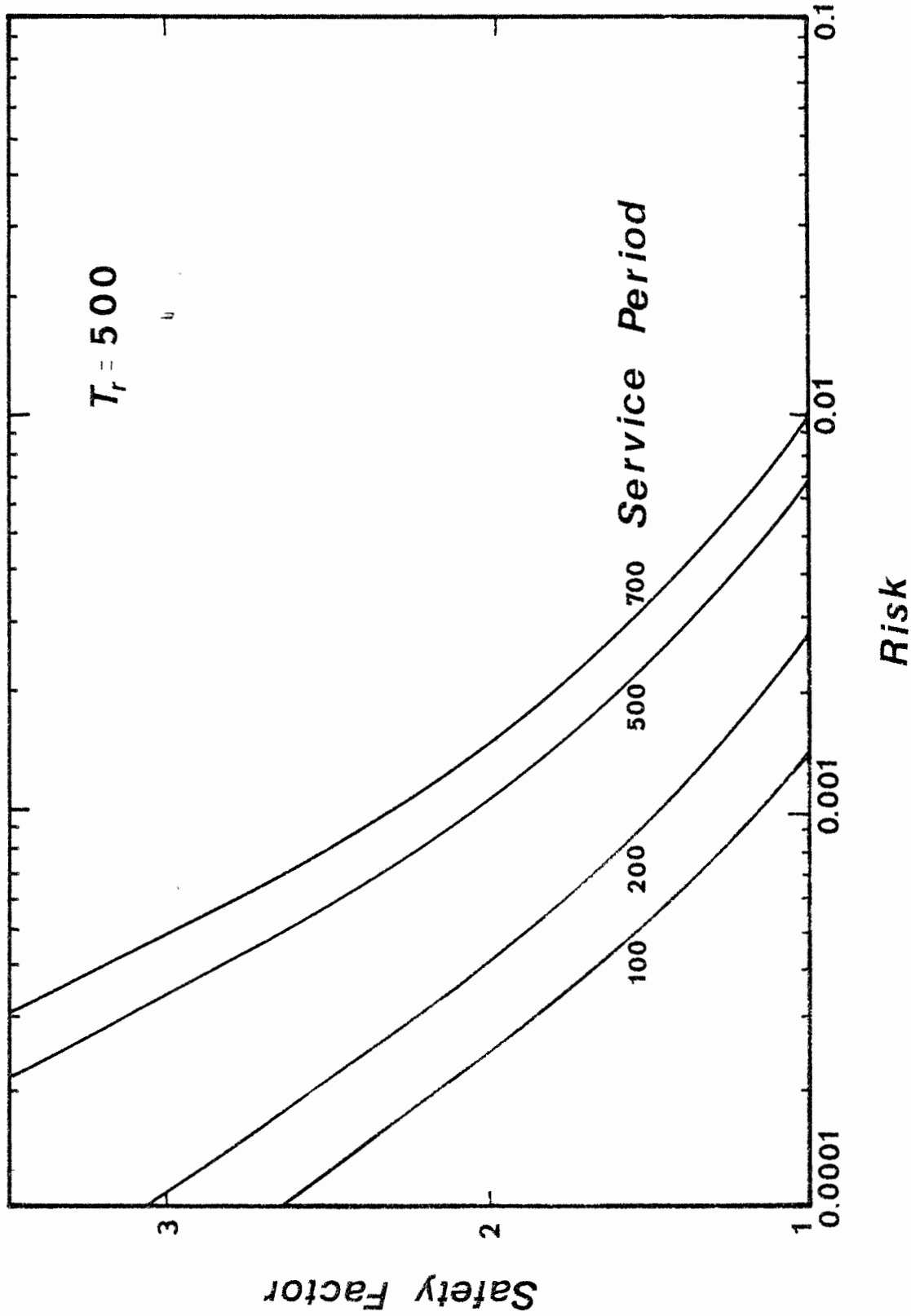


Figure 4.23 Time-Dependent Risk-Safety Factor Curves for Levee Design Using Log-Pearson III Loading Distribution Based on $T_r = 500$ Years

posterior probability provided by Eq. (3.51). The weight for the model where the parameters are estimated by TMJ method has been shown in Table 4.6. In this case, the composite reliability model for the static case, Eq. (3.53), can be expressed as

$$R_c = 0.498 \int_0^{\infty} f_{Q_c, LN}(r) \left[\int_0^r f_{Q_d, LN}(\ell) d\ell \right] dr \\ + 0.502 \int_0^{\infty} f_{Q_c, LN}(r) \left[\int_0^r f_{Q_d, LP}(\ell) d\ell \right] dr \quad (4.23)$$

The composite reliability model for the time-dependent case, Eq. (3.54), can be expressed as

$$R_c(t) = 0.498 \int_0^{\infty} f_{Q_c, LN}(r) \cdot \exp \left\{ -\lambda t [1 - F_{Q_d, LN}(r)] \right\} dr \\ + 0.502 \int_0^{\infty} f_{Q_c, LN}(r) \cdot \exp \left\{ -\lambda t [1 - F_{Q_d, LP}(r)] \right\} dr \quad (4.24)$$

Eqs. (4.23) and (4.24) can be used in step (6) to generate the composite risk-safety factor curves for static and time-dependent models, respectively. Figures 4.24, 4.25, 4.26, and 4.27 are the composite risk-safety factor curves for static and time-dependent cases with design return periods of 100, 200, and 500 years, respectively.

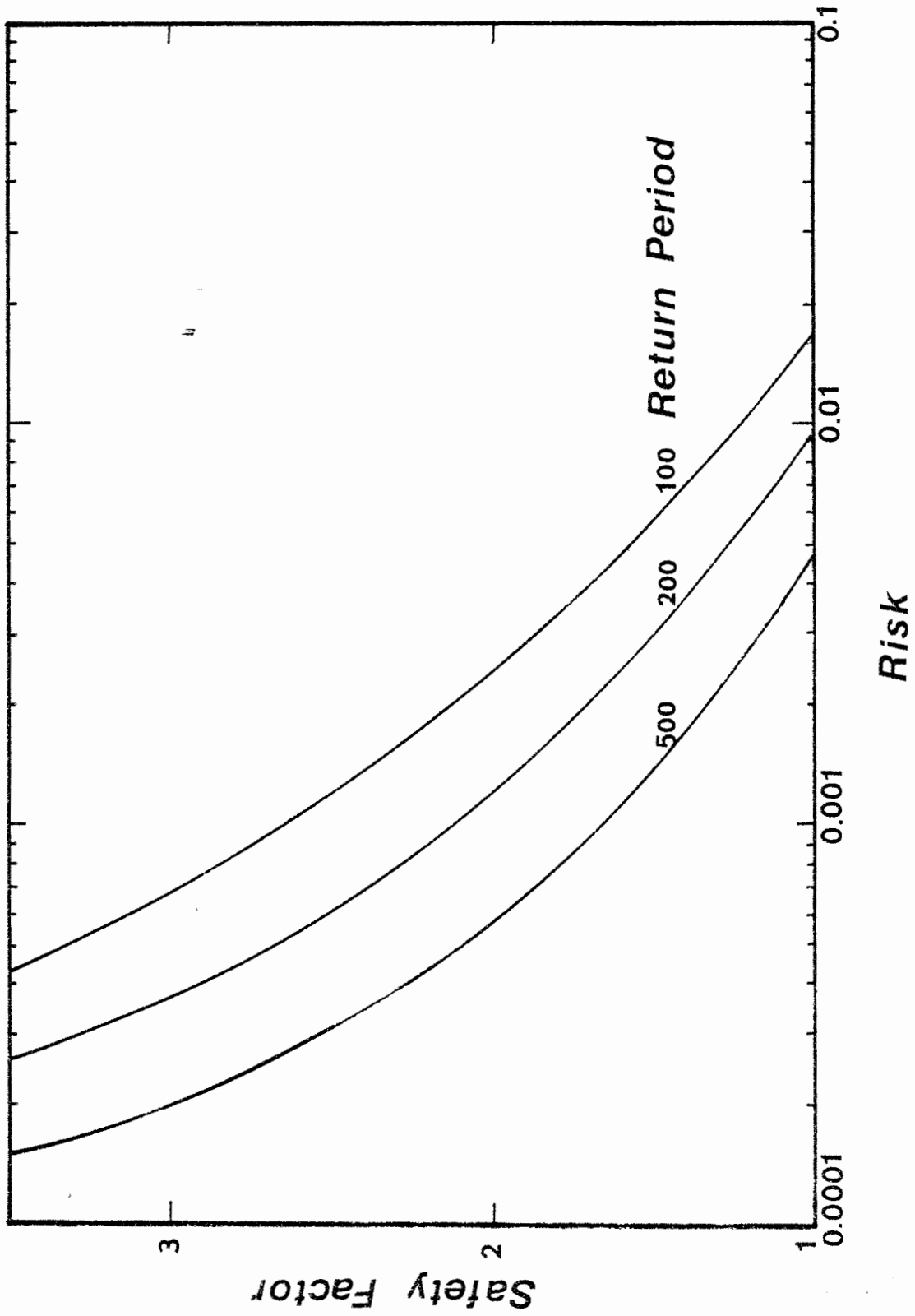


Figure 4.24 Static Risk-Safety Factor Curves for Levee Design Using a Composite Probability Model for Loading

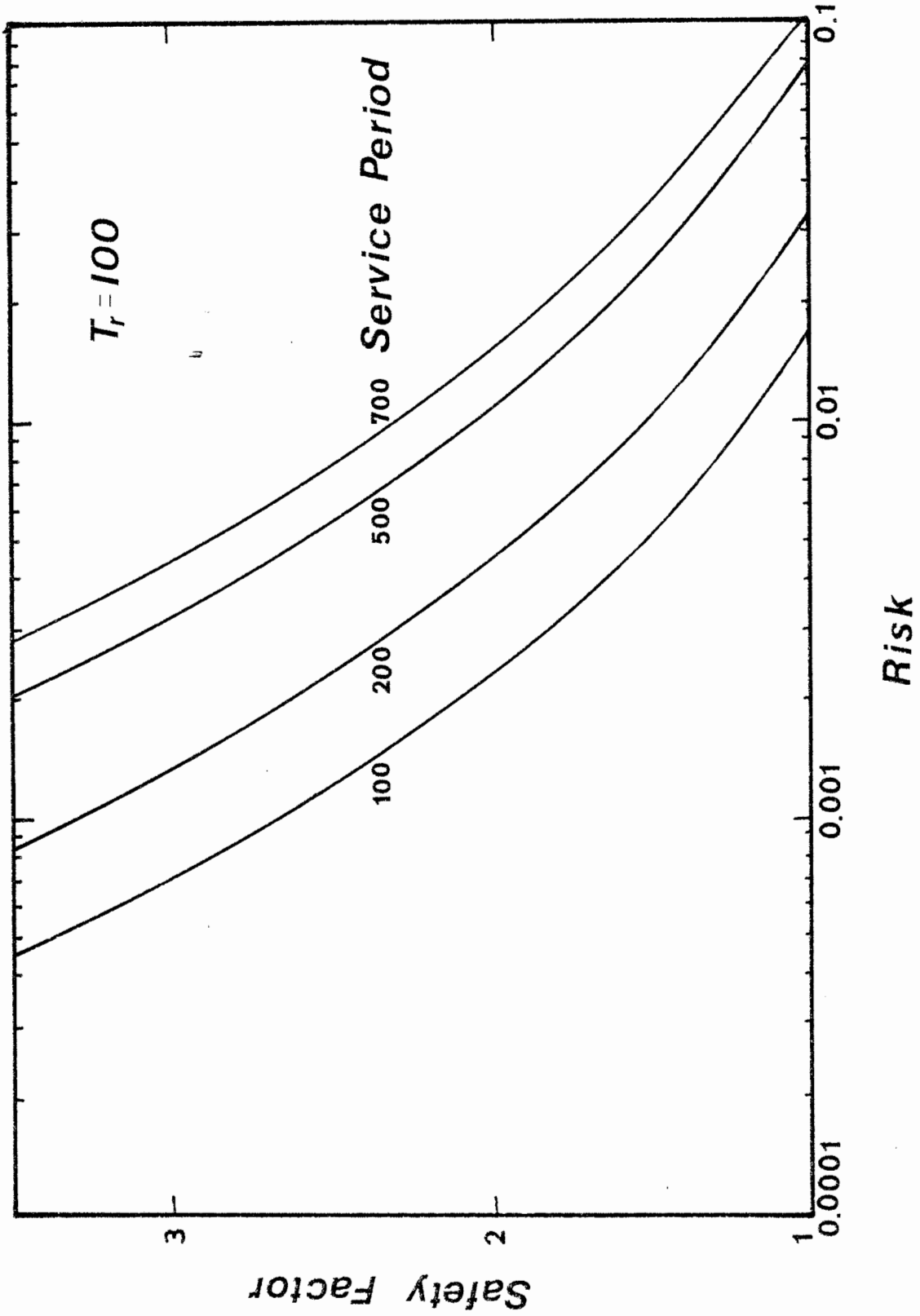


Figure 4.25 Time-Dependent Risk-Safety Factor Curves for Levee Design Using a Composite Probability Model for Loading Based on $T_r = 100$ Years

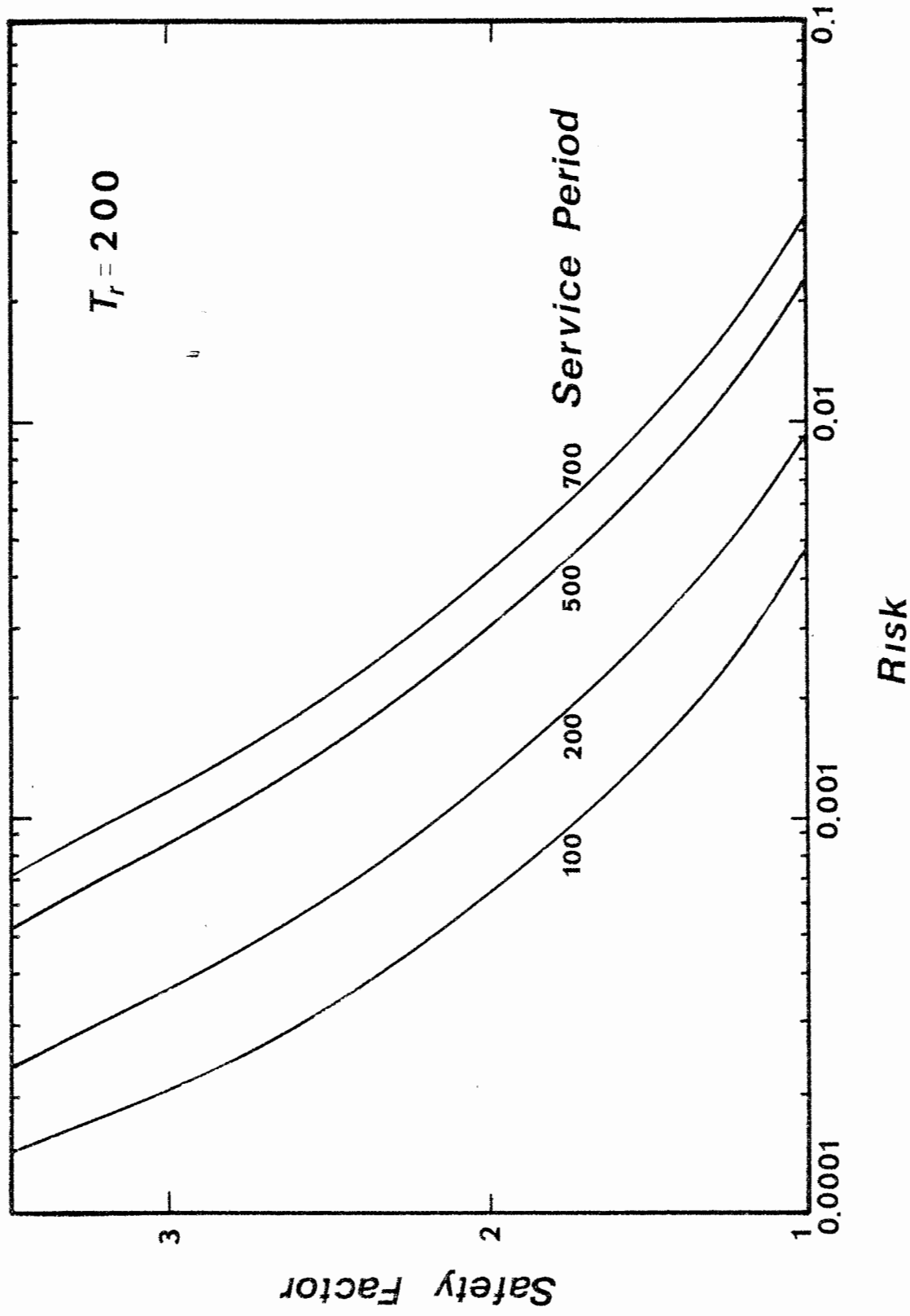


Figure 4.26 Time-Dependent Risk-Safety Factor Curves for Levee Design Using a Composite Probability Model for Loading Based on $T_r = 200$ Years

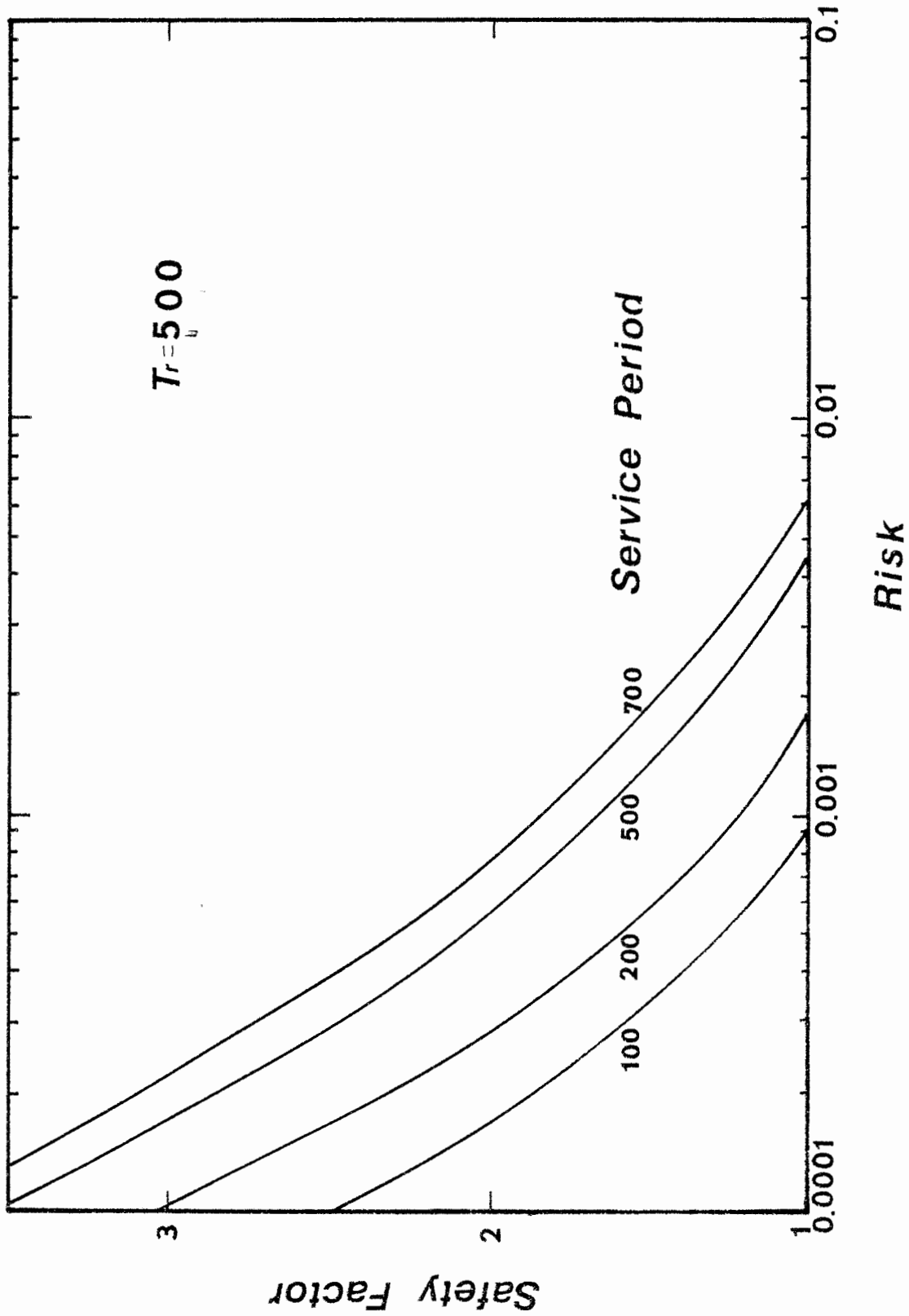


Figure 4.27 Time-Dependent Risk-Safety Factor Curves for Levee Design Using a Composite Probability Model for Loading Based on $T_r = 500$ Years

4.5 DISCUSSION

Considering only the inherent hydrologic uncertainty the annual probability of failure, i.e., the annual risk of overtopping is equal to the reciprocal of the return period upon which the design capacity is based, that is, provided that the safety factor is unity. For example, the return periods considered in the levee problem are 100, 200, and 500 years and the corresponding annual inherent hydrologic risks of overtopping ($1/T_r$) are 0.01, 0.005, and 0.002, respectively. For a levee capacity using a design flow for a return period of 100 years and safety factor on one ($\bar{Q}_C = Q_{T_r}$), the overall static risk of overtopping from Figs. 4.4 to 4.8, ranges from 0.0110 for the log-normal loading model to 0.0215 for the normal model. As compared with the inherent hydrologic risk of $1/T_r = 0.01$ it is shown that the risk of overtopping can be underestimated from 10% to 50%, depending upon the loading distribution model used by ignoring other uncertainties and not reducing (minimizing) parameter uncertainty. The ratio of annual overall risk of overtopping of the levee to the annual inherent hydrologic risk (for $SF = 1$, i.e., $\bar{Q}_C = Q_{T_r}$) for different design return periods and various loading probability models are tabulated in Table 4.7. The shape of risk-safety factor curves is very sensitive to the probability model of loading used. The choice of probability model of loading should be carefully made and a composite model considered.

Considering only the inherent hydrologic uncertainty underestimates the risk of overtopping as compared to considering the overall risk. Consequently, the corresponding economic losses could be significantly under

Table 4.7
Comparison of Overall Risk and Inherent Hydrologic Risk

	$\bar{R}/(1/Tr)$		
	100 yr	200 yr	500 yr
Normal	2.15	3.00	3.15
Log-Normal	1.10	1.16	1.10
Gumbel	1.50	1.40	1.60
Pearson III	1.15	1.24	1.15
Log-Pearson III	2.00	2.60	3.50

estimated by not considering an overall uncertainty. If the issue of reliability of a project is of paramount importance, such as the case that the levee project is to protect an urban area, the concept of analyzing overall uncertainty should be adopted in the design process because any ignorance of existing uncertainty may lead to serious disaster in the region.

Furthermore, in the example given the resulting risk-safety factor curves by using a particular loading probability differ significantly from that of using the others. This shows the evidence that the result of risk-reliability analysis is extremely sensitive to the loading probability model used. The effect of choosing a loading probability model on the project decision making and its associated economic impacts and consequences are understandable. An example of illustrating the effect of model selection on the levee design decision making based on its economic consequence was given by Bogardi et al. (1977). Under this situation, a composite loading probability model, as developed in Section 3.3.2, is suggested as a good alternative because it takes into account model uncertainty. In case of analyzing the risk-safety factor relationship for the levee capacity in Guadalupe River the resulting curves using composite model lie within the range of those curves obtained with the component models.

Chapter 6 presents an example illustrating the effect of risk issue considered and the significance of the choice of model on the optimal levee design.

CHAPTER 5

OPTIMAL RISK-BASED DESIGN OF LEVEE SYSTEM

5.1 PROBLEM STATEMENT

The problem under consideration is the determination of an optimal design (minimum cost) flood levee system. The main purpose for construction of a levee system is to protect land from being flooded. The capacity of a levee system is an important measure of degree of protection. Usually the capacity is expressed in terms of a design flood with an associated return period. The basic information for designing a levee system requires both hydrologic as well as hydraulic studies. The hydrologic aspect involves the studying of rainfall-runoff processes and flood flow frequency analysis which provides the magnitude of the design flood flow used as the basis for designing the levee capacity. The hydraulic study involves the investigations of the hydraulic properties, such as surface roughness, slope, geometry, etc., of the channel and the flood plain. These hydraulic properties are input parameters to the hydraulic model for determining the levee capacity. The design parameter include the levee height and the width of encroachment. The optimization model to solve the problem must select the levee layout (widths of encroachment) and the levee height simultaneously because of their interrelation in determining the capacity.

The principal task in this phase of the study is to incorporate the methodologies of analyzing the uncertainties involved in both the hydrologic

aspect and the hydraulic aspect into the framework of an optimization model. Prior to discussing the optimization models a brief description of the levee configuration is given.

Levees are earthen embankments placed at varying distances from a river bank to serve as artificial banks during floods when water spills over the nature banks. The main function of the levees is to protect the major flood plain, in which human activities such as agriculture, industry, and business, etc., are most likely to take place. The use of levees for flood control is extensive throughout the world and is one of the oldest engineering applications in history. As early as 4,000 years ago, Kun, Father of Yu, the legendary leader of the Hsia Dynasty in China, used levees to confine the flood water of the Yellow River. His efforts failed due to the tremendous amount of sediment content in the Yellow River and lead to his death by the Emperor.

The standard section suggested by the United Nations for use in Asia and the Far East have side slopes of 2(H):1(V) to 4(H): 1(V) on the river side and 3(H): 1(V) to 5(H): 1(V) on the land side. The standard section recommended by the Mississippi River commission has side slopes of 3(H): 1(V) on each side and the standard section of the Upper Yazoo District uses slopes of 3(H):1(V) on the riverside and 4(H): 1(V) on the land side, respectively.

In the process of developing an optimization model several assumptions and constraints that are either the inputs or are built into the model are made and discussed in the next section.

5.2 ASSUMPTIONS AND CONSTRAINTS

Several assumptions for the geometry and layout of the levee based on the foregoing descriptions and hydraulic variables of flow are made. These assumptions are as follows:

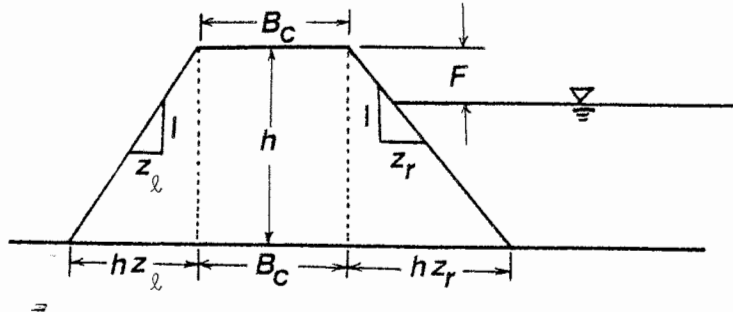
1. With the predetermined side slopes and crown width of the levees, Figure 5.1, the volumetric content of levees is a function of the height only. Consequently, the construction cost of levees is assumed to be a function of the height. The cost for construction of other accessories such as interior ditches, gates, pumping facilities, etc., will not be considered in developing the cost function for the levee construction. The unit construction cost per length of levees varies with location; however, it is assumed that the spatial variation of unit construction cost within an economic district is small.

2. In addition to the levee construction cost, the unit land purchasing cost is assumed to be constant within the subreach considered.

3. Within a subreach in which the levee is to be constructed the river is assumed to be straight without meandering.

4. For the sake of simplicity only, the levees are assumed to be located symmetrical to the center line of the straightened channel, based on the assumption (3), with equal height at any point in a specific reach investigated.

5. Hydraulic variables such as the roughness, surface slope of the flood plain along the channel on both sides of the river have the same characteristics.



$$A_{LV} = \frac{h}{18} [2B_c + h(z_l + z_r)]$$

$$V_{LV} = 97.78A_{LV}$$

where

B_c = crown width, in feet

h = levee height, in feet

z_l = side slope on the land face

z_r = side slope on the river face

F = free board, in feet

A_{LV} = levee cross sectional area, in sq. yard

V_{LV} = volume of embankment per mile, in cu.yd./mile

Figure 5.1 Configuration of Levee Section

6. The magnitude of flood used as the basis for designing the levee capacity is obtained from a hydrologic study. No hydraulic routing techniques will be applied to route the flood hydrograph through the levee system. An idealized triangular hydrograph with predetermined time base will be used. The flow condition during flood is taken to be subcritical. No backwater effect will be considered.

7. The capacity of the levee system within the reach considered is computed using Manning's equation. The levee capacity of a specific cross section with known levee layout and hydraulic variables, Manning's equation, expressed as Eq. (4.1), can be applied. It is understood, theoretically, that the energy slope, S_f , is equal to the slope of the longitudinal water surface profile and to the slope of the channel bottom. If the variation of velocity in a natural stream is not significant the application of Manning's equation is valid. On the other hand, if the variation of velocity along the channel is appreciable from one end of the reach to the other, due to the irregularity of the channel section, the energy slope will be taken as the difference of total head at the two ends of the reach divided by the length of the reach. Since the total head includes the velocity head, which is unknown, a solution by successive iteration is necessary for determining the capacity of the levee with different heights and width of encroachment at both ends of the reach. The area-slope method (Chow, 1959) is adopted as the means to compute the levee capacity within the reach considered. Detailed descriptions of the method and derivations of the mean and coefficient of variation of the levee capacity for a given reach, using first-order analysis of uncertainties are

illustrated in Appendix C. The energy coefficient applied to the velocity head at both ends of the reach is assumed to be unity.

Several constraints commonly used in the design of levees are incorporated in the optimization model. These constraints are either the design criteria adopted in practice or some physical constraints on the layout of the levee system at particular locations. The constraints considered are:

1. Maximum width of the flood plain which can be used for the levee project, is a physical constraint that defines the feasible state space within which the optimization model investigates.

2. The capacity of the levee must satisfy certain design criteria. The criteria provide the guidelines to select the design flood such that the levee capacity must equal or exceed that value. The criteria used depends on the object which needs to be protected by the levees. Design-flood criteria for the levees are usually incorporated considering local flood control facilities such as reservoirs system, if there is any, to determine the return period of floods. The selection of design flood of specific return period for the rural areas varies with location. For instance, Missouri River agricultural levees were designed based on the 100 year flood; levees in Portland, Oregon, have grades height to protect against the 50 year flood; and a system of 40 levee units on the Wabash River in Illinois and Indiana authorized in 1946 would protect the rural areas and substantial developments against 15 year floods. (Davis and Sorensen, 1969).

Design-flood criteria for urban-protection projects involving high levees require high performance standards, in view of the potential hazards

to life and severe property damages associated with levee overtopping. The standard project flood is sometimes used in order to assure project safety during extraordinary floods. Basically, under this context, the mathematical expression for the constraint is

$$Q_c \geq Q_{\text{design}} \quad (5.1)$$

where Q_c is the levee capacity determined by the area-slope method using Manning's equation, and Q_{design} is the magnitude of the design flood based on hydrologic studies. The capacity of the levee, Q_c , is the function of the width of encroachment, height of levee and other hydraulic variables involved. For an idealized cross section, Fig. 4.2, the functional relationships between Q_c using Manning's equation and design variables at given section are given in Eq. (4.1).

Other constraints such as the foundation condition which might have the limitation on the maximum height of the levees or embankments will not be considered in the optimization model.

3. In the practice of designing a levee system, an extra height, called the freeboard, is added to the design height. The purpose of the freeboard is to provide as a safety measure to prevent the embankment being overtopped due to the effect of surface water waves produced by the wind.

5.3 OPTIMIZATION TECHNIQUES

This section briefly reviews the optimization techniques commonly applied in water resource engineering.

5.3.1 Linear Programming

Linear programming has been applied quite extensively as an optimization model in water resources engineering. The general linear programming (LP) model is stated in the form of a linear objective function to be optimized (maximized or minimized) subject to certain restrictions. The restrictions or constraints are expressed as a set of linear equations. Linear programming provides a method of comparing all possible solutions that satisfy the constraints and obtaining the solution(s) that optimize the objective function. All linear programming problems can be expressed in standard form as

$$\text{Min } \underline{C} \underline{X} \quad (5.2)$$

subject to a set of linear constraints

$$\underline{A} \underline{X} = \underline{B} \quad (5.3)$$

and

$$\underline{X} \geq 0 \quad (5.4)$$

in which \underline{C} is a K-dimensional row vector; \underline{A} is a J x K matrix; \underline{X} is a K-dimensional column vector; and \underline{B} is a J-dimensional column vector.

5.3.2 Dynamic Programming

Dynamic programming is a powerful tool for optimizing many types

of water resource systems, especially those involving staging and scheduling. It is a mathematical technique which is useful for solving sequential decision problems for which a sequence of interrelated decisions, called a policy, must be made. Although there exists no standard mathematical formulation for dynamic programming, it is an approach-oriented technique, with the actual equations developed to fit the particular application. Many examples of its application to water resource problems are contained in Yeh and Asfur (1971) and Chow and Meredith (1969).

The basic components that characterize water resource systems which have counterparts in the dynamic programming application are:

1. The problem must be divisible into what are called stages. A stage represents a point in time (operational) or space (allocation) depending on the physical system.
2. Each stage of the problem must have a finite number of state variables, where the state variable describes the condition of the system at that stage. The state variable is discretized into several states which define the possible conditions.
3. The effect of a decision at each stage of the problem is to transform the current state of the system into a state associated with the next stage. Associated with the decisions are benefits or costs referred to as returns which define the effectiveness of that set of decisions.
4. For a given stage and state of the system, the optimal sequence of decisions must be independent of the decisions made in the previous stages.

Dynamic programming is characterized by a recursive equation. The recursive equation is a partial objective function which expresses the benefit or cost for each combination of states for a given stage in terms of the possible decisions that can be made during that stage and the given states of the system in the next stage that result from making these decisions. The partial objective for stage n , $f_n(S_{n,i})$ where $i = 1, \dots, I$ is defined as follows in the backward algorithm case:

$$f_n(S_{n,i}) = \begin{matrix} \min \\ \text{or} \\ \max \end{matrix} \left\{ r_n(d_{n,i}, S_{n,i}) \circ f_{n-1}(S_{n-1,i}) \right\}_{i=1,2, \dots, I, n = 1, 2, \dots, N_s} \\ d_{n,i}$$

(5.5)

where $f_{n-1}(S_{n-1,i})$ is known, and $r_n(d_{n,i}, S_{n,i})$ is the return function depending on the current state and decision made. The interpretation of the operator "o" specifies how r_n and f_{n-1} are combined to obtain f_n . For most water resource problems this operator is normally a summation; however, it can be a product or a max-min problem. By applying the recursive equation at each stage in sequence, beginning with stage 1 and terminating at stage N_s , the overall objective may be found by solving a sequence of related problems starting at the last stage and processing backwards in time to the initial stage.

5.3.3 Nonlinear Programming

Geometric programming (GP) (Beightler and Phillips, 1977) is a relatively new technique, developed for solving algebraic nonlinear programming problems subject to linear and/or nonlinear constraints. The technique applies arithmetic-geometric mean inequality relationship to transform a mathematic programming problem having nonlinear inequality constraints into an equivalent problem formulation with only linear inequalities. Two basic types of problem formulation are posynomial GP and signomial GP. The generalized geometric programming formulation can be expressed as follows.

Define $M+1$ generalized polynomials f_0, f_1, \dots, f_M by

$$f_m(\underline{x}) = \sum_{t=1}^{T_m} \sigma_{mt} C_{mt} \prod_{k=1}^K x_k^{a_{mtk}}, \quad m=0, 1, 2, \dots, M \quad (5.6)$$

$$C_{mt} > 0, \quad m=0, 1, \dots, M; \quad t=1, \dots, T_m \quad (5.7)$$

$$x_k \geq 0, \quad k=1, \dots, K \quad (5.8)$$

where $\sigma_{mt} = \pm 1$ and is called a signum function. The primal program is

$$\text{Min } f_0(\underline{x}) \quad (5.9)$$

subject to

$$f_m(\underline{x}) \leq \sigma_m, \quad m=1, \dots, M \quad (5.10)$$

and

$$x_k > 0, \quad k=1, \dots, K \quad (5.11)$$

where $\sigma_m = \pm 1$. A geometric programming is called posynomial if the values of σ_{m_i} 's and σ_m 's are all +1, otherwise the problem is called signomial. Generally, instead of solving the primal program, a dual program, in which the constraints are transformed to be linear inequalities rather than nonlinear, is solved.

Other constrained nonlinear programming methods using gradient search techniques such as the reduced gradient method, etc., are useful tools for solving nonlinear problems.

5.3.4 Selection of Optimization Technique

Most optimization problem formulations in water resource engineering are highly nonlinear. The representation of nonlinearity of the problem formulation used in the constraints, e.g. Eq. (5.1), limit the application of most constrained nonlinear optimization methods except DP. Hence, the basic optimization technique adopted in this study to formulate the model for simultaneous determination of the optimal levee system layout and design is dynamic programming (DP). The flexibility of DP to handle various forms of cost functions, design constraints, etc. is of extreme importance. In addition the model described here must have the flexibility of DP in order to incorporate risk models.

5.4 DYNAMIC PROGRAMMING TECHNIQUE

As a prelude to the following discussion on the dynamic programming technique applied to levee systems, it is desirable to define the terms:

objective function, stage, state, decision, and transition function and to indicate their analogous counterparts in the levee system.

5.4.1 Objective Function

The objective of employing the DP optimization model for the levee design is to obtain the optimal system design which minimizes the total cost. The components involved in the term "total cost" depend on the risk issue considered in the design procedure. Basically, the cost component is attributed to the installation cost which consists of the levee construction cost and the land purchasing cost. The construction cost of levees can be expressed as

$$Z_{1,n} = C_{LV} \cdot V_{LV,n} \cdot L_n \quad (5.12)$$

where $Z_{1,n}$ is the construction cost in dollars of levee reach n , C_{LV} is unit cost of levee construction in dollars per cubic yard, $V_{LV,n}$ is the volume of embankment per mile for reach n defined in Fig. 5.1, and L_n is the length of reach n in miles considered. If the heights of levee at two ends of the reach n are different, an average value is used to compute the volume of embankment, $V_{LV,n}$ and its associated construction cost for the reach.

The cost of land purchasing based on the assumption (3) is expressed as

$$Z_{2,n} = C_{LND,n} \cdot A_{LND,n} \quad (5.13)$$

where $Z_{2,n}$ is the land purchasing cost for reach n , $C_{LND,n}$ is the unit cost of land in dollars per acre, and $A_{LND,n}$ is the area of land encroached by the levee in acres. For a simplified channel cross section as shown in Fig. 4.2 and described by assumption (4) the functional form for $A_{LND,n}$ can be expressed as

$$A_{LND,n} = \{(w_n - B_n) + 2[B_c + h_n(z_\ell + z_r)]\} \cdot L_n \quad (5.14)$$

where w_n and h_n are the average width of encroachment and the average levee height, respectively, \bar{B}_n is the average top width of the channel, for reach n , B_c , z_ℓ , and z_r are defined in Fig. 5.1.

Hence the total installation cost for the levee in reach n , r'_n is

$$r'_n = Z_{1,n} + Z_{2,n} \quad (5.15)$$

If the project does not consider any risk issue the objective function for this case will be

$$\min \text{TIC} = \sum_{n=1}^{N_s} r'_n \quad (5.16a)$$

where TIC is the total installation cost, and N_s is the total number of reaches considered, or

$$\min \text{ATIC} = \sum_{n=1}^{N_s} r'_n \cdot \text{CRF} \quad (5.16b)$$

where ATIC is the annual total installation cost, and CRF is the capital recovery factor which brings the present worth of the installation cost to an annual basis.

Recently, the risk-based design has been drawing more and more attention in the field of water resource engineering. The risk-based design incorporates the risk and associated expected damages into the design procedure. Current practice of risk-based water resource engineering design considers only the hydrologic risk due to the randomness of the hydrologic process. In addition to the installation cost described above, the annual expected damage is taken into account in the objective function. The mathematical representation of the annual expected damage cost considering only the hydrologic risk can be expressed as

$$E(D) = \int_{Q_c^*}^{\infty} D(Q_d, Q_c^*) \cdot f_l(Q_d) \cdot dQ_d \quad (5.17)$$

where $E(D)$ is the annual expected damage cost associated with the specified corresponding structure capacity, Q_c^* , damage-discharge relationship, $D(Q_d, Q_c^*)$, and the governing probability distribution of the loading (flood) $f_l(Q_d)$. The schematic diagram for computing the annual expected damage cost is shown in Fig. 5.2. The objective function, considering the hydrologic risk only, is to minimize the annual expected total damage cost which can be written as

$$\min \text{ATEC} = \sum_{n=1}^{N_s} [r'_n \cdot \text{CRF} + E(D)_n] \quad (5.18)$$

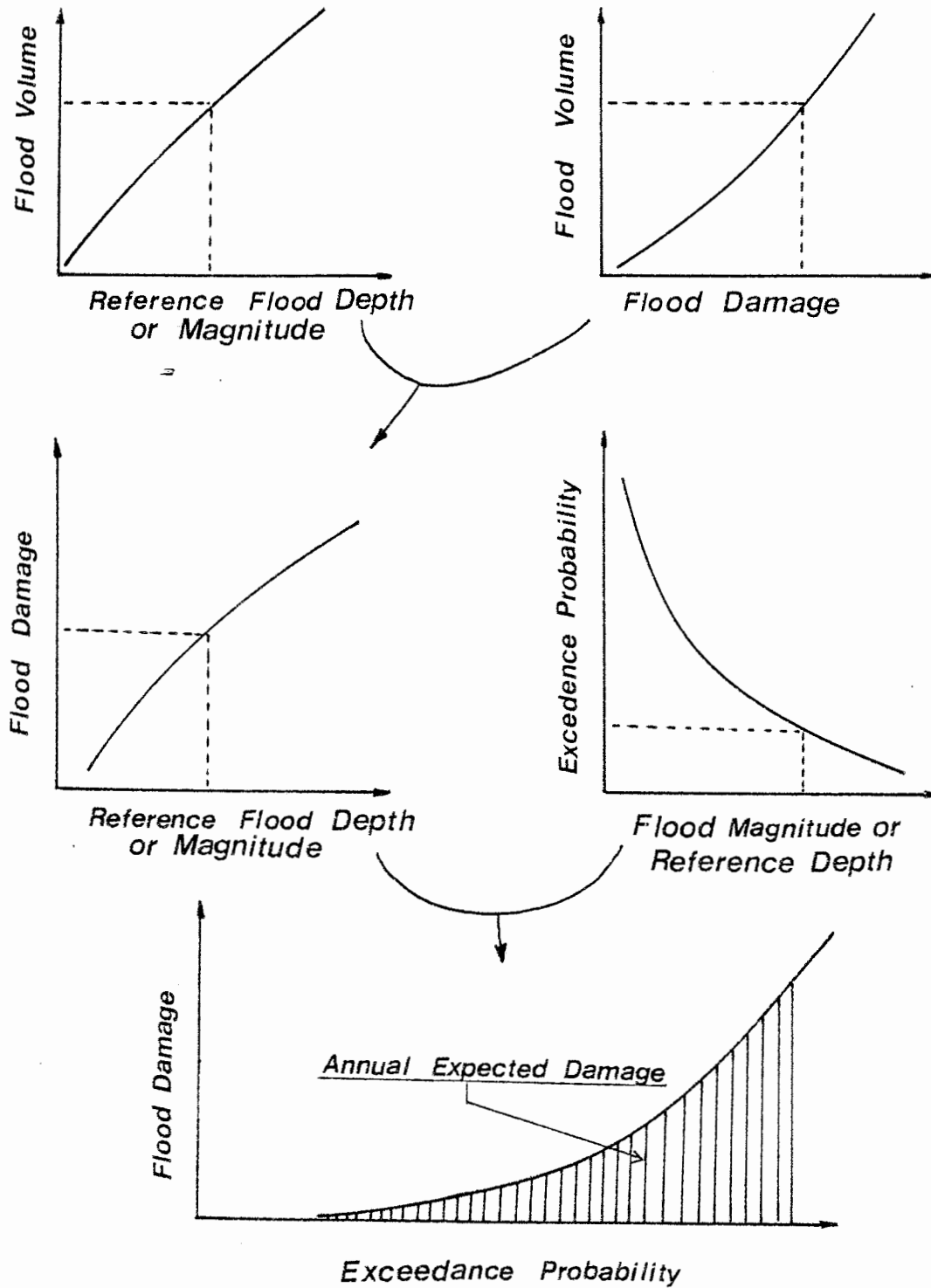


Figure 5.2 Schematic Diagram for Calculating the Annual Expected Damage Cost

where ATEC is annual total expected cost which is the sum of the total annual installation costs and annual expected damage cost. The incorporation of annual expected damage cost into the objective function enables the evaluation of trade-off between installation cost and damage cost.

The evaluation of annual expected damage cost considering only hydrologic risk does not take into account the uncertainty feature of the capacity of the levee. The capacity of the levee in such circumstances is taken to be deterministic without error. Very often the negligence of hydraulic uncertainty might lead to an underestimate of the risk and, consequently, the annual expected damage. Consideration of incorporating both the hydrologic and hydraulic uncertainty to evaluate the annual expected damage cost is considered. By going through an analysis of uncertainty for the levee capacity, such as first order analysis, the statistical properties of the levee capacity can be derived. Using the probability density function for the levee capacity, $f_r(Q_c)$, the annual expected damage cost is expressed as

$$E(D) = \int_0^{\infty} \left[\int_0^{Q_d} D(Q_c, Q_d) \cdot f_r(Q_c) \cdot dQ_c \right] \cdot f_l(Q_d) \cdot dQ_d \quad (5.19)$$

where the damage function $D(Q_c, Q_d)$, is a function of the levee capacity as

well as the loading. The annual expected damage cost, Eq. (5.19) can be used in the Eq. (5.18) which considers the overall risk.

5.4.2 System Components

In addition to the objective function discussed in the previous section other system components in the dynamic programming technique applied for the levee design are described in the following subsections.

5.4.2.1 Stages

Due to the significant meandering of many rivers, variation in land values, variation in topography and maximum land on the flood plain available for levee projects, etc., the total levee system is divided into reaches or stages. If the land cost in one reach is more expensive than the other, it is more likely to use a levee with narrower encroachment and higher embankment in the reach (stage) with high land cost as opposed to use wider encroachment and lower embankment in the other reach that all meet certain design criteria with less cost associated. Within each reach or stage the variation of the factors involved in the planning or optimization model are considered to be small. Also, the division of an entire levee system into stages within which the river is considered to be straight so that the validity of applying the uniform-flow equation is more justified. The total number of in which the system is divided is the total number of stages considered for the DP optimization .

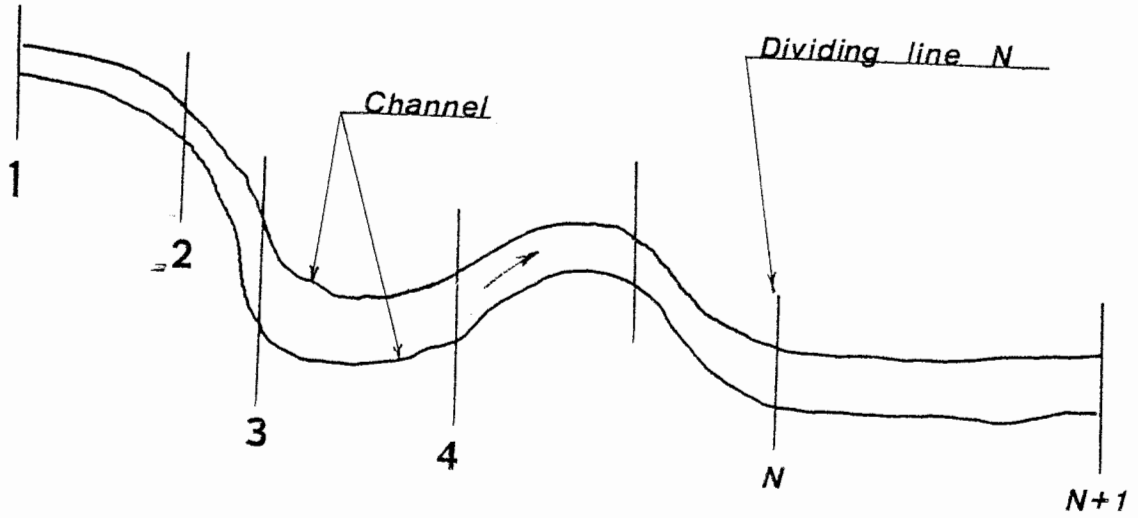
To illustrate this concept a schematic diagram of river reach is shown in Fig. 5.3. The channel in which the levee project is considered is subdivided into N_s reaches, or stages as shown in Fig. 5.3a and the simplification is shown in Fig. 5.3b. The two most upstream dividing lines (1 and 2) represent stage 1. The succeeding stages proceed downstream (toward the direction of flow), each defined by adjacent upstream and downstream dividing lines, n and $n+1$, for $n=1, 2, \dots, N_s$, where N_s is the total number of reaches, i.e. stages, in the system. A stage n is analogous to the levees that connect the upstream dividing line n and the downstream dividing line $n+1$.

5.4.2.2 States

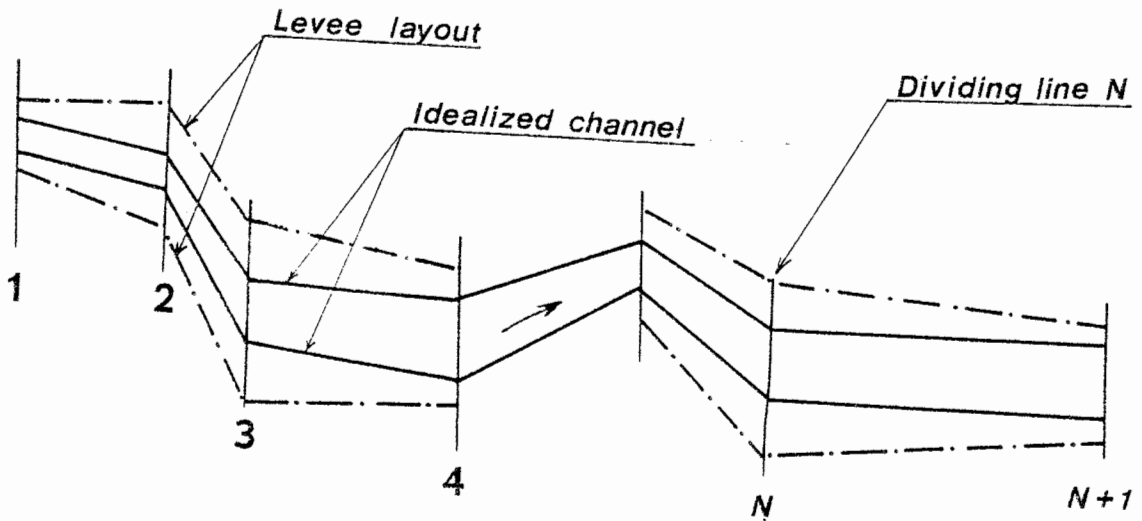
The state space in the levee problem is two dimensional. One state variable is the width of encroachment and the other is the height of the levee. The input state matrix at each stage $n+1$ of the system is represented by a set encroachment widths and a set of levee heights at the downstream side of stage n . The notation for the input state matrix at dividing line n is \underline{S}_n . For each possible levee layout and design considered at stage n , the input states are defined as the set encroachment widths $\{w_{n,i}\}_{i=1,2,\dots,N_{W,n}}$, and levee heights $\{h_{n,j}\}_{j=1,2,\dots,N_{H,n}}$, where $N_{W,n}$ is the number of possible widths of encroachment at stage n and $N_{H,n}$ is the number of possible levee heights considered in the state space at upstream end of stage n . In matrix form the state space in any stage n can be represented as

$$\underline{S}_n = \{(w_{n,i}, h_{n,j})\}_{N_{W,n} \times N_{H,n}} \quad (5.20)$$

The output states are the set of encorachment widths and levee



(a) Real Situation



(b) Idealization

Figure 5.3 Channel Reach Configuration and Levee Layout

heights at the downstream end of each possible levee layout of an arbitrary stage n , i.e., on the dividing line $n+1$. The notation for the output state matrix is \tilde{S}_n which has the similar form of matrix representation to the input states as

$$\tilde{S}_n = \{(w_{n,m}, h_{n,n'})\}_{N_{W,n+1} \times N_{H,n+1}} \quad (5.21)$$

where $m=1, 2, \dots, N_{W,n+1}$, $n'=1, 2, \dots, N_{H,n+1}$. The output state space of each stage depends on the input state space, the decision made in the decision space, and their functional relationship is called the transition or transformation function. The schematic diagram of two dimensional state space is shown as Fig. 5.4.

5.4.2.3 Decisions

The independent decision variables at each stage are the changes in encroachment width and the levee height from the upstream end to the downstream end of the stage for possible connection of levee design. The increment, herein, may be positive or negative. The decision space at stage n , \underline{D}_n , consists of the two decision variables which can be expressed as

$$\underline{D}_n = \{(d_{n,k}^W, d_{n,l}^H)\}_{K \times L} \quad \begin{array}{l} \text{for } n=1, 2, \dots, N_s \\ k=1, 2, \dots, K \\ l=1, 2, \dots, L \end{array} \quad (5.22)$$

where K and L are respectively the number of possible increments for the

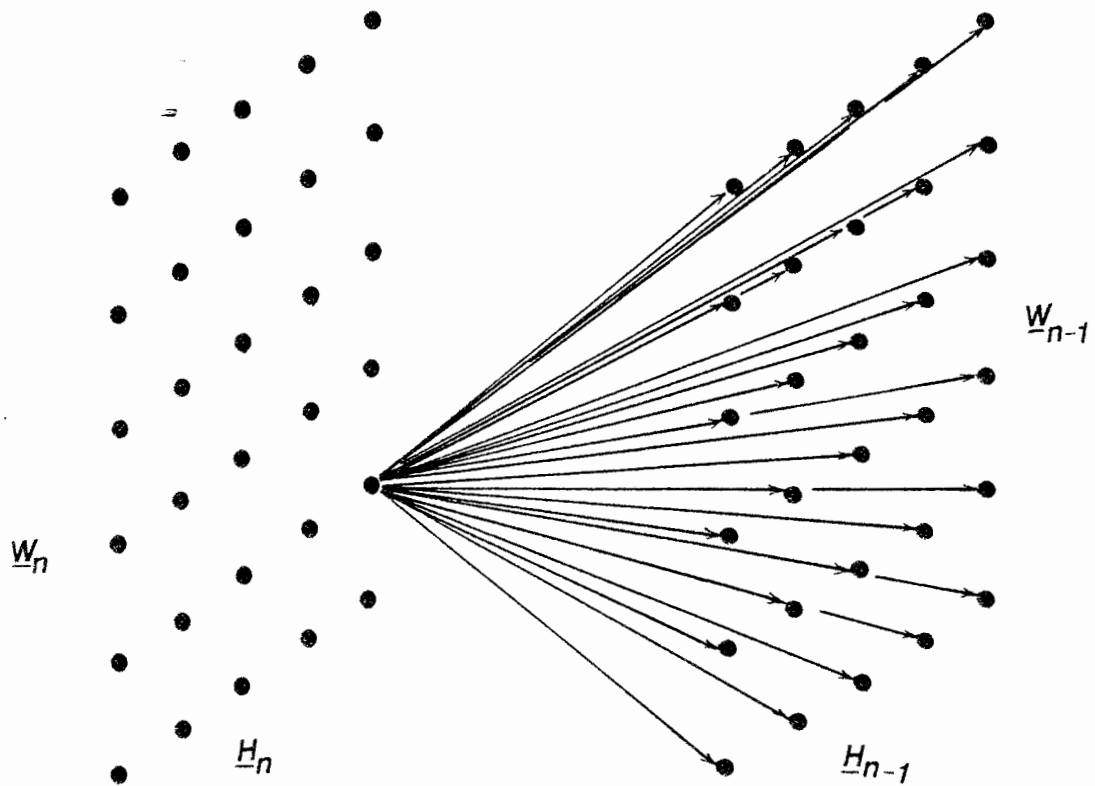


Figure 5.4 State Space for a Two Dimensional Problem

encroachment width and of the levee height considered, respectively. The increment of encroachment width is defined as the difference of the upstream levee encroachment width (input state) and the downstream levee encroachment width (output state). The increment of levee height can be defined in the same manner.

5.4.2.4 Transition Function

The transition function transforms the input states at a given stage with specified decision variables to the output states. For an arbitrary stage n the transition function can be expressed as

$$\tilde{S}_n = S_n \circ D_n, \quad n=1,2, \dots, N_s \quad (5.23)$$

in which "o" is an operator. For the levee problem the transition function can be written as

$$\begin{aligned} \tilde{S}_n &= \{(\tilde{w}_{n,m}, \tilde{h}_{n,n'})\} \\ &= \{(w_{n,i}, h_{n,j}) + (d_{n,k}^W, d_{n,l}^H)\} \end{aligned} \quad (5.24)$$

in which $i=1, 2, \dots, N_{W,n}$, $j = 1,2, \dots, N_{H,n}$, $k = 1,2, \dots, K$, $l = 1,2, \dots, L$, $m=1, 2, \dots, N_{W,n+1}$, and $n' = 1,2, \dots, N_{H,n+1}$.

The relationship between input state, output state, and decision variable for the encroachment width of levees is illustrated in Fig. 5.5 showing the possible connection between upstream (input) and downstream (output) states. Each dash line corresponds to an element decision in the decision space. By utilizing the transition function the state variables, i.e.,

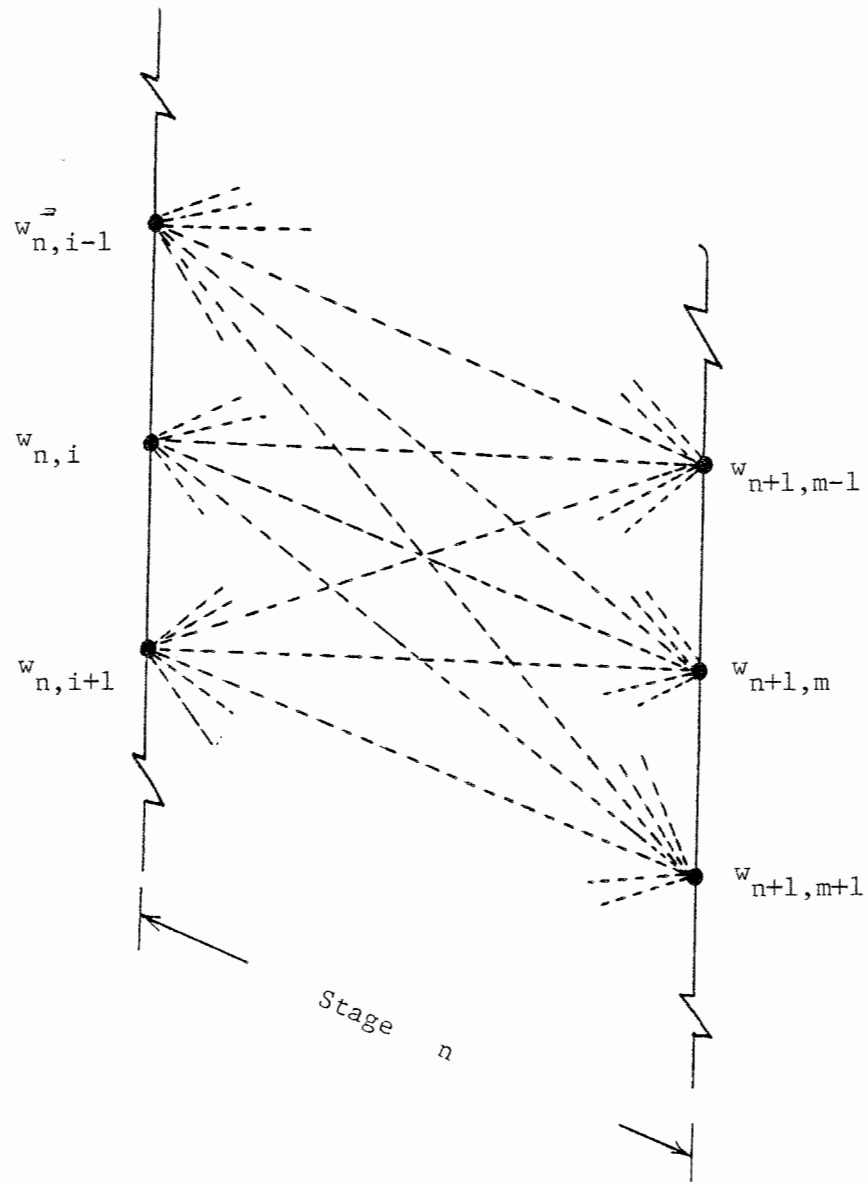


Figure 5.5 Transition Relationship Between Input State, Output State, and Decision Variable for Encroachment Width of Levees

the width of encroachment and levee height on both ends of the stage can be derived which enable the computation of the capacity of the levee by the area-slope method using the uniform-flow equation, Manning's formula. Therefore, the transition function and problem constraints, such as capacity of the levee system must be greater than a certain design flood, can be used jointly to define the feasible state space at each stage of the problem.

5.4.3 DP Optimization Procedure

The nature of the problem results in a highly nonlinear objective function and constraints such that a dynamic programming approach is adopted. Basically, two types of system layout, i.e. serial and non-serial (branching) types, are especially suitable for applying dynamic programming procedures. Mays and Yen (1975) developed an optimization model for a branched storm sewer system using dynamic programming and discrete differential dynamic programming. For the type of problem considered herein the levee design is a serial dynamic programming optimization; however, the technique for nonserial or branching levees where two streams meet can be applied.

A serial levee system consists of segments of levees connected in series as shown in Fig. 5.3. The manner in which the stages are linked is given by the incidence identity, which is the relationship that the output from each stage forms the input to the next succeeding stage. The downstream encroachment width and level height of stage $n+1$ are expressed in vector form as

$$\underline{S}_{n+1} = \tilde{S}_n \quad (5.25)$$

or more explicitly

$$\{(w_{n+1,i}, h_{n+1,j})\}_{N_{W,n+1} \times N_{H,n+1}} = \{(\tilde{w}_{n,m}, \tilde{h}_{n,n'})\}_{N_{W,n+1} \times N_{H,n+1}} \quad (5.26)$$

For the general stage n of an N_s -stage system the stage transition function is given by Eq. (5.23), and the return at stage n for the decisions \underline{D}_n , the increments of encroachment width and the levee height from an initial state \underline{S}_n is $r_n = (S_n, D_n)$. The explicit functional representations of r_n can be written as

$$r_n = r'_n \cdot \text{CRF} \quad (5.27a)$$

in which no risk consideration is given, or

$$r_n = r'_n \cdot \text{CRF} + E(D)_n \quad (5.27b)$$

in which the annual expected damage, $E(D)_n$, is brought into consideration.

The evaluation of $E(D)$ depends on the issue of risk considered, i.e., hydrologic risk only or overall risk (both hydrologic and hydraulic risk). From Eqs (5.23) and (5.24) the upstream or input states at stage $n + 1$ are a function of the input states and decision variables at stage n , and the return at stage n is a function of the state and decision variables at stage n . The system cost, or return, is the sum of the individual stage costs (return), i.e.,

$$R_N = \sum_{n=1}^{N_s} r_n.$$

In the dynamic programming optimization procedure the most important concept is Bellman's "principle of optimality," i.e., an optimal policy has the property that whatever the initial state and decision are, the remaining decisions must constitute an optimal policy with regard to the state resulting from the first decision (Nemhauser, 1966). The mathematical

functional form of the principle of optimality is the recursive equation that represent the stage-by-stage optimization of dynamic programming which can be expressed as

$$f_n(S_n) = \min_{D_n} \left\{ r_n(S_n, D_n) + f_{n-1}(S_{n-1}) \right\} \quad n=1, \dots, N_s \quad (5.28)$$

where $f_n(S_n)$ represents the minimum cost of the system through stage n and $f_0(S_0) = 0$.

The dynamic programming computations start from the most upstream end (stage 1) of the levee system and proceed downstream stage by stage. The maximum and minimum allowable encroachment widths and allowable levee heights on the upstream end and their increments of changes for each input state are required. The feasible output state space for the stage can be generated using the transition function and physical constraints in the stage. The incidence identity states that the feasible output state space of stage 1 is the feasible input state space for stage 2. By doing this recursively through all the stages the feasible state space for each stage in the system can be defined. Once the feasible state space for each stage is defined the optimization procedure starts from stage 1 and proceeds successively in the downstream direction through stage N_s . For a particular downstream (output) state, $(\tilde{w}_{n,m}^0, \tilde{h}_{n,n'}^0) \in \tilde{S}_n$ of stage n in the system the capacity of the levee is computed for each possible upstream (input) state $(w_{n,i}, h_{n,j}) \in S_n$ with which it is connected. The cost (return) associated for stage n , r_n , is computed for the capacity of possible connections of the current downstream state considered, $(\tilde{w}_{n,m}^0, \tilde{h}_{n,n'}^0)$ to all the upstream states which satisfy the design flow criteria, Eq (5.1). This stage cost $r_n(S_n,$

\underline{D}_n) associated with the downstream state, $(w_{n,m}^o, h_{n,n'}^o)$, is added to the minimum cost $f_{n-1}(S_{n-1})$ associated with the upstream state with which it is connected. This total cost $r_n(S_n, \underline{D}_n) + f_{n-1}(S_{n-1})$ is compared to determine whether it is less than the previously computed minimum cost of getting to state $(w_{n,m}^o, h_{n,n'}^o)$ at stage n . If it is, this total cost will replace the previous minimum cost for state $(w_{n,m}^o, h_{n,n'}^o)$ as a basis for further comparison. This procedure is repeated until all the possible input states are evaluated for the output state. After the minimum total cost for each output state in stage n is computed, the computation is then continued downstream to stage $n+1$ in the same manner and repeated until the last stage N_s is evaluated.

When the computational procedures are completed for the last stage of the system the total cost associated with each output state in the last stage is the minimum total cost of the system for that particular final state. A search for the optimal layout and design of the levee system is performed among the final output states. Then, a trace back through the stored encroachment widths and levee heights, and levee capacity for each of the upstream stages. A flow chart showing the steps in DP approach is given in Fig. 5.6.

5.4.4 Limitations of DP Approach

The dynamic programming approach as described can be adaptable for analyzing multi-stage multi-branch processes such as levee system. However, when DP is applied in a discrete fashion to a state space that is continuous, there exist difficulties in determining the optimal solution

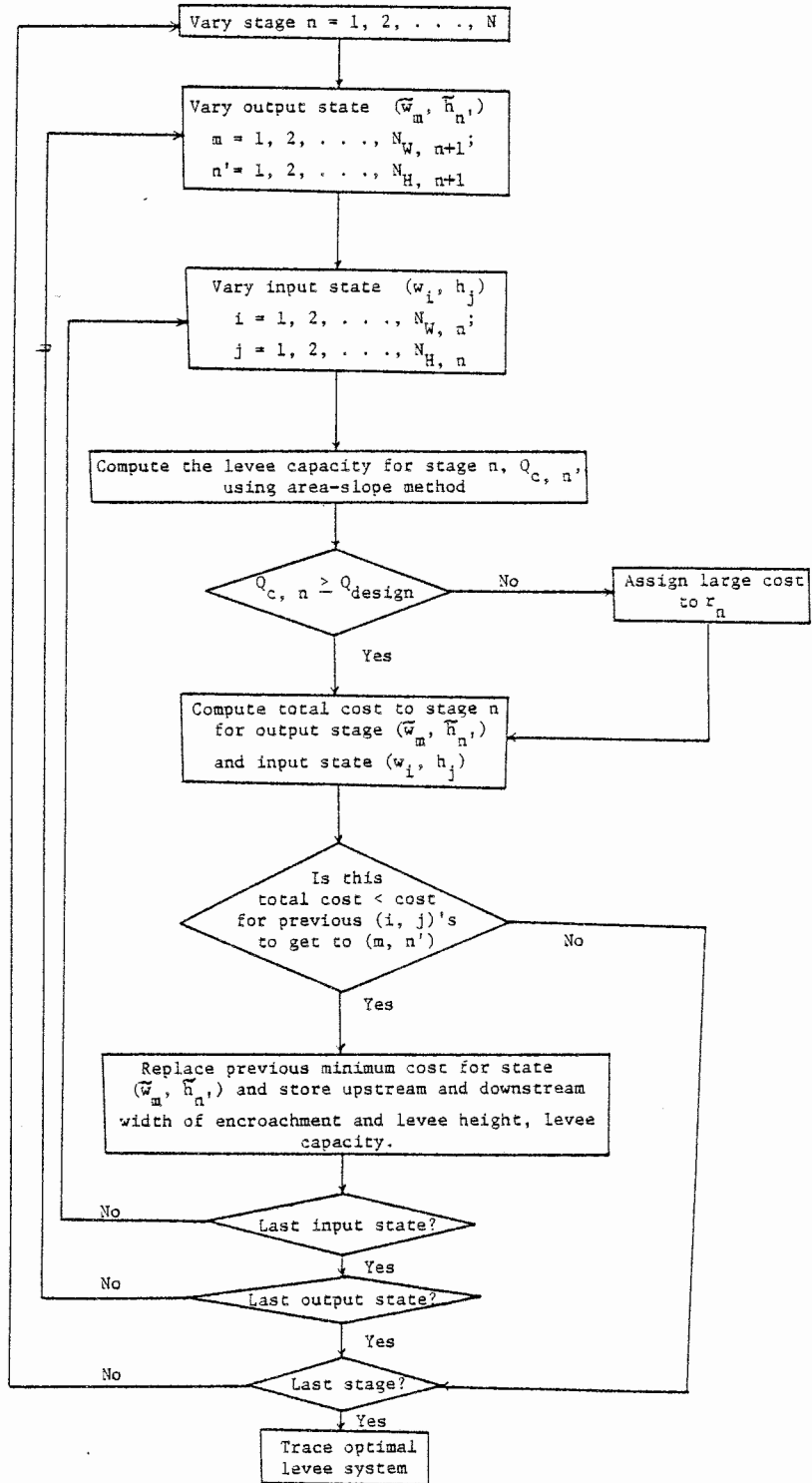


Figure 5.6 Flow Chart of DP Approach for Serial Levee Systems

without a considerable increase in discretization of the state space, i.e., increase in the number of states of each state variable.

When DP is applied to large systems (numerous stages and states) there are difficulties in obtaining an accurate optimal solution without a considerable increase in computer time due to the number of possible values (states) of the state variable. The savings realized by DP as compared with direct enumeration increase exponentially as the number of stages increases. However, the comparison of the efficiency of DP with direct enumeration does not give a complete picture. The optimization by DP can indeed be computational, time consuming and expensive, especially with the evaluation of damage functions.

Consequently, one tempts to investigate other techniques that could possibly reduce the computer time. Several techniques based upon DP have been developed including successive approximation, state increment dynamic programming, and discrete differential dynamic programming (DDDP). The DDDP technique has been successful in analyzing water resources systems, substantially reducing the high-speed computer time and storage requirements (Heidari et al., 1971) and is adopted in this study for the design of levee systems. The procedure of DDDP is applied as an alternative and described in the following section.

5.5 DISCRETE DIFFERENTIAL DYNAMIC PROGRAMMING (DDDP) APPROACH

The discrete differential dynamic programming approach has proven

to be a very effective method in the analysis of various types of water resources systems (Chow et al., 1975). This method is able to overcome the chief limitations of dynamic programming (DP) which include the number of state variables and/or the level of discretization of the state space. In the study of branched storm sewer system design using DP and DDDP, it was shown that the use of DDDP to obtain an optimal solution is very effective in decreasing computation time over that of DP for about the same level of accuracy of the optimal results (Mays and Yen, 1975). This is mostly because of the level of discretization of the state space required in DP to obtain equivalent results using DDDP.

DDDP is defined by Heidari (1970) and Heidari et al. (1971) as an "iterative technique in which the recursive equation of dynamic programming is used to search for an improved trajectory among the discrete states in the neighborhood of a trial trajectory." This optimization procedure is solved through iterations of trial states and decision to find the optimal return (minimum cost) for a system subject to the constraints such that trial states and decisions should be within the respective admissible domain of the state and decision spaces governed by the physical constraints of the problem.

In DDDP the first step is to assume a trial sequence of admissible decisions \underline{D}_n called the trial policy, and the state space of each stage is computed accordingly. This sequence of states within the admissible state space for different stages is called the trial trajectory and can be designated

as T_n for $n=1,2, \dots, N_s$. An alternative procedure which initially determines a sequence of states within the admissible state space for each stage to form an initial trial trajectory and the trial policy (decision) for this trajectory can be computed accordingly. In the levee system design, for example, at any stage n the initial trial trajectory connecting the upstream state (the width of encroachment and height of levee) on the dividing line n , $(w_{n,i}, h_{n,j}) \in S_n$, and output state on the dividing line $n+1$, $(\tilde{w}_{n,m}, \tilde{h}_{n,n'}) \in \tilde{S}_n = S_{n+1}$, the trial policy, $(d_{n,k}^W, d_{n,l}^H) \in D_n$, for this trial trajectory can be derived by using the transition function Eq. (5.24). Note that the capacity of the levee associated with the initial trial trajectory does not necessarily satisfy the design flow criteria because this initial trial trajectory is only used as a basis to define the initial state space.

Several different encroachment widths and levee heights in the neighborhood of a trial trajectory can be introduced to form a two-dimensional band called a "corridor" around the trial trajectory. A configuration of corridor and trial trajectory is given in Fig. 5.7. The traditional dynamic programming approach is applied to the states within the system of corridors using the recursive relationship of dynamic programming to search for the optimal (least cost) trajectory to define the levee system which satisfies the constraints, i.e. design criteria. The least cost trajectory is then adopted as the improved trajectory to form a new corridor. A corridor indicates the range of possible connection between input states and output

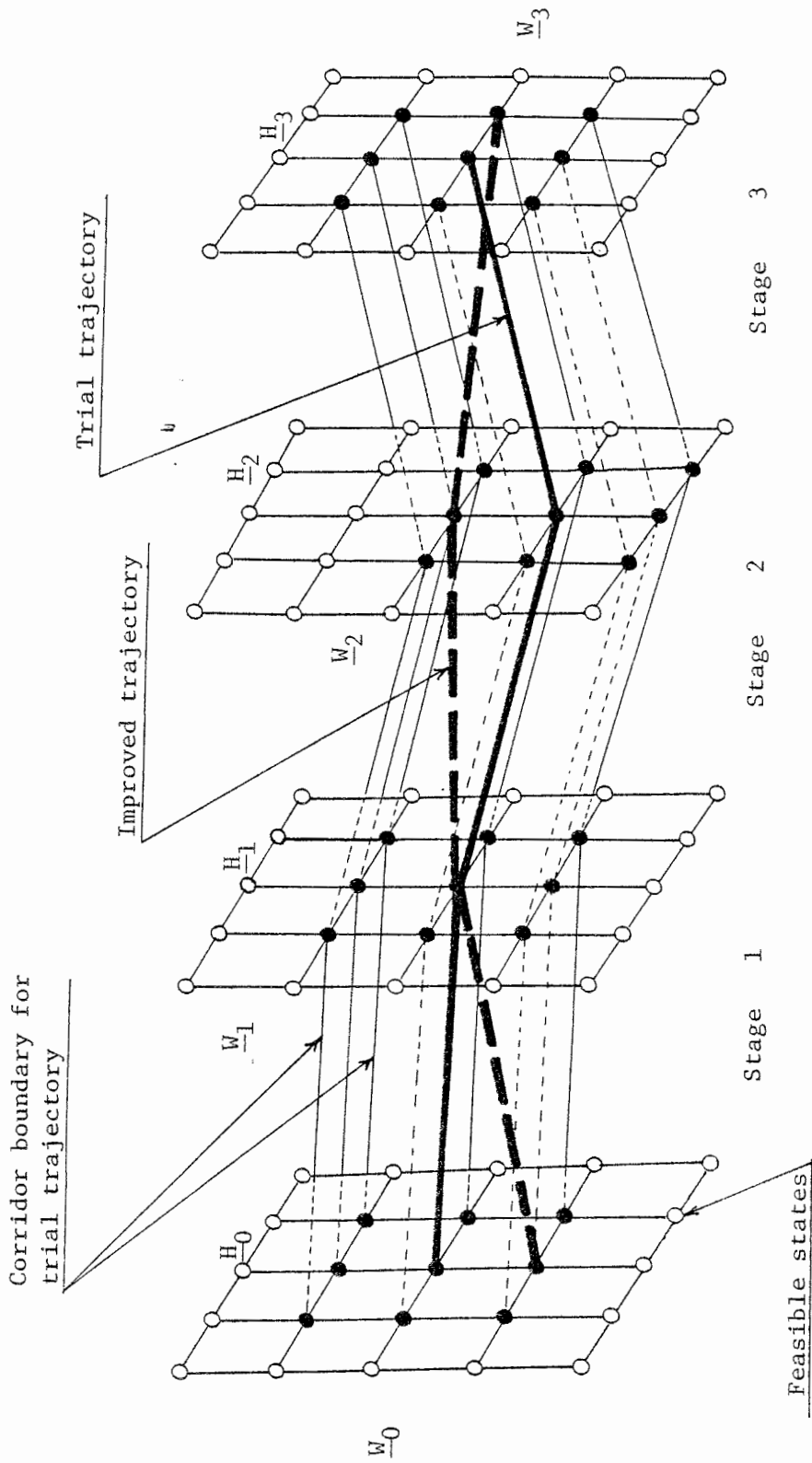


Figure 5.7 Schematic Diagram for Corridor and Trial Trajectory in DDDP Applied to Serial Levee System

states at a stage. This process of corridor formation, optimization with respect to the states in the corridor and trace back to obtain an improved trial trajectory for the entire system is called an "iteration of DDDP."

The corridor at stage n defined by the upstream states on the dividing line n and the downstream states on the dividing line $n+1$ is determined using the trial trajectory at stage n . An increment, Δ , of distance between neighboring (adjacent) encroachment widths, Δ_W , and levee heights, Δ_H , at both ends of a stage can be used to form a corridor for the stage. For example, if a set of five encroachment widths or states (also referred to as lattice points) and three levee heights are used for the upstream end of stage n , the trial state space would be

$$S_n = \begin{bmatrix} (w_{n,i-2\Delta_W}, h_{n,j-\Delta_H}) & (w_{n,i-2\Delta_W}, h_{n,j}) & (w_{n,i-2\Delta_W}, h_{n,j+\Delta_H}) \\ (w_{n,i-\Delta_W}, h_{n,j-\Delta_H}) & (w_{n,i-\Delta_W}, h_{n,j}) & (w_{n,i-\Delta_W}, h_{n,j+\Delta_H}) \\ (w_{n,i}, h_{n,j-\Delta_H}) & (w_{n,i}, h_{n,j}) & (w_{n,i}, h_{n,j+\Delta_H}) \\ (w_{n,i+\Delta_W}, h_{n,j-\Delta_H}) & (w_{n,i+\Delta_W}, h_{n,j}) & (w_{n,i+\Delta_W}, h_{n,j+\Delta_H}) \\ (w_{n,i+2\Delta_W}, h_{n,j-\Delta_H}) & (w_{n,i+2\Delta_W}, h_{n,j}) & (w_{n,i+2\Delta_W}, h_{n,j+\Delta_H}) \end{bmatrix} \quad (5.29)$$

where $(w_{n,i}, h_{n,j})$ is the upstream state associated with trial trajectory T_n at

stage n.

It is apparent that the corridor must fall within the admissible domain of the state space. The upper bound for the encroachment width is the maximum width of land available, and the lower bound is the channel width. The least cost trajectory, defining the system through optimization of the trial corridor, is subsequently adopted as the new trajectory to establish the improved corridor for the next iteration. This procedure is repeated to some iteration i until there is very little or no improvement of the objective function and cost associated with the optimal system is f_i . If there is no improvement using the corridor size then the corridor size can be reduced. The increments of the state variables Δ_W and Δ_H are reduced by same fraction and then used to set up a new corridor in which the lattice points in the state space are closer together. This smaller corridor is formed around the least cost trajectory obtained from the last iteration. The iterations continue reducing Δ_W and Δ_H throughout the system accordingly until a specified minimum increment or corridor size is reached.

The criterion used to determine when the magnitude of Δ_W and Δ_H should be reduced is based on the relative change of the minimum cost of the last (i -th) iteration, i.e.,

$$\left| \frac{f_i - f_{i-1}}{f_{i-1}} \right| \leq \epsilon_r \quad (5.30)$$

When the ratio is equal to or smaller than a specified value ϵ_r the state space increments Δ_W and Δ_H are reduced to one-half or any other desired

fraction of their previous value and then the iterations are resumed. A flow chart of DDDP approach for serial levee systems is illustrated in Fig. 5.8.

The factors governing the performance of the DDDP technique are the initial trial trajectory, the number of lattice points used in the corridor, the size of the state space increments of each state variable, the rate of reduction of the state space, and the criterion, ϵ_r , for reducing Δ_W and Δ_H . Two of the main issues concerned in the optimization technique are the accuracy of the results and the efficiency of the algorithm. Apparently, the choice of the initial trial trajectory close to the optimal trajectory will naturally reduce the number of iterations and computer time required to arrive at or near the optimal. Although, in reality, choosing the initial final trajectory close to the optimal trajectory may be impossible; therefore, knowledge of the problem background and engineering judgment can often be helpful. If the number of lattice points in the corridor is large the reduction in number of lattice points is expected to provide improvement in computer time and memory requirements. However, this improvement diminishes as the number of lattice points is reduced beyond a certain amount.

The choice of increment size for each iteration is an important factor in the rate of convergence of the solution. The choice of initial trial trajectory and increment size are somewhat interrelated. The rate of reduction of increment size also has effect on the rate of convergence of the solution. A fast reduction rate of Δ_W or Δ_H provides a fast convergence into the near optimal region, but the convergence becomes very slow within the

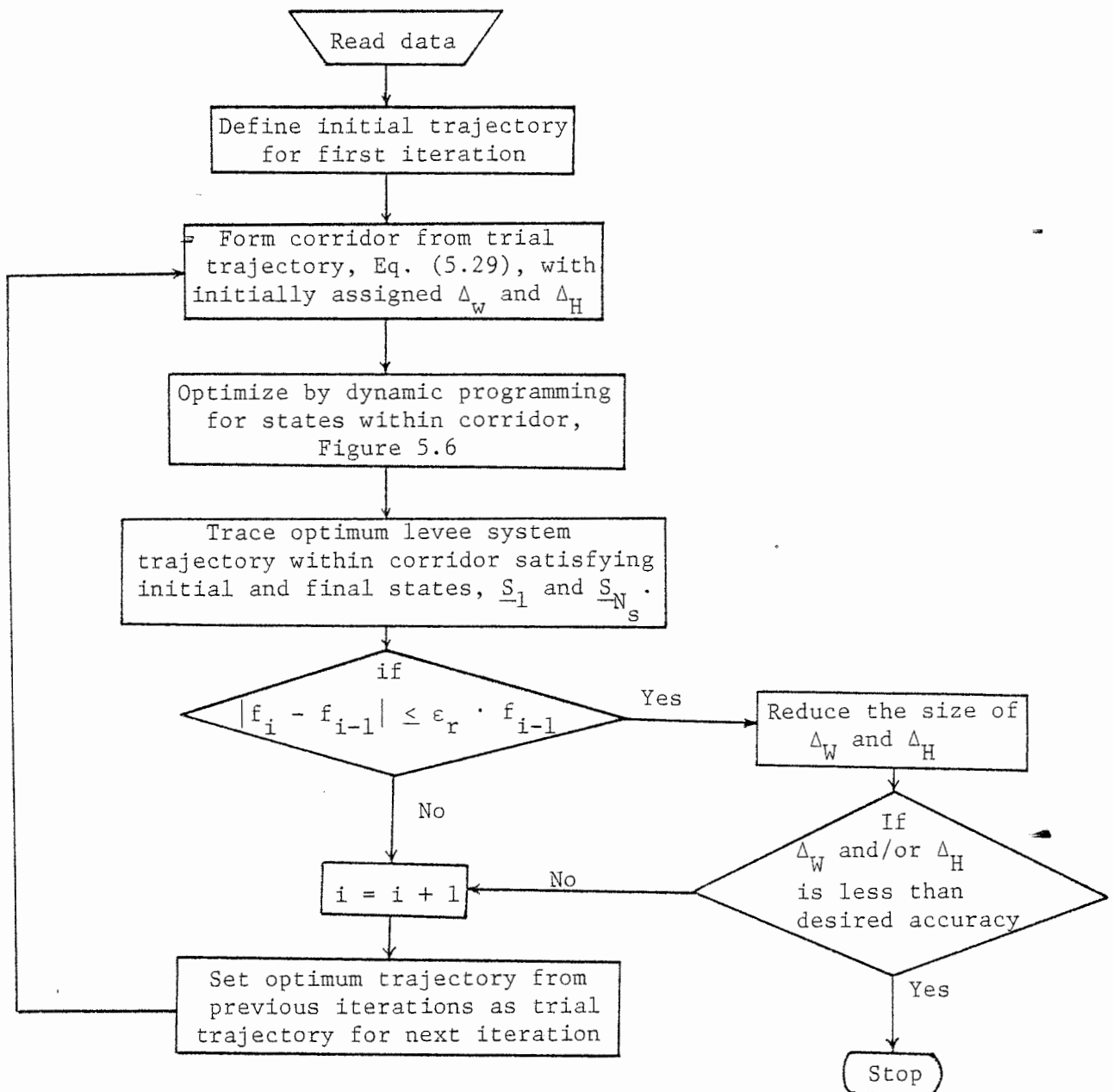


Figure 5.8 Flow Chart of DDDP Approach for Serial Levee Systems

region. Moreover, too rapid a reduction rate of the increment size may miss the optimal region. The effect of ε_r on the solution procedure is two-fold, i.e., accuracy and computer time. The smaller the value of ε_r provides a more accurate solution but the number of iterations required tends to increase. The value of ε_r for a problem usually depends on the level of accuracy desired. Nevertheless, it should be noted here that the problem is highly nonlinear in nature, the DDDP solution may converge to a local minimum rather than a global minimum. However, in view of the uncertainties involved in the input data, from engineering viewpoint a local optimum often is nearly as useful in practice as the global optimal (Mays and Yen, 1975).

No attempt is made in this chapter to study the sensitivity of above governing factors on the DDDP procedure in levee design. An excellent presentation of this aspect on the storm sewer system design is given by Mays and Yen (1975).

CHAPTER 6

RISK CONSIDERATIONS AND ECONOMIC IMPLICATIONS

6.1 INTRODUCTION

The DP and DDDP models for optimal levee design are illustrated using data for the Guadalupe River near Victoria, Texas. This example is given more specifically for the purpose of examining different design philosophies (risk considerations), their associated optimal (least cost) designs, and the resulting economic consequences. The different design philosophies examined include:

1. Design without considering any risk with objective function Eq. (5.16)
2. Considering inherent hydrologic risk only with objective function Eq. (5.18) and the annual expected damage cost, $E(D)$, computed using Eq. (5.17), and
3. Considering overall risk with objective function Eq. (5.18) and the annual expected damage cost, $E(D)$, computed using Eq. (5.19).

As illustrated in the Chapter 4, the choice of probability model for the loading has a significant effect on the value of the resulting risk associated with a particular design. The effects of the least cost levee design and economic consequences resulting from different loading probability models

are also examined. The parameters in the loading probability model in this chapter are estimated by the weighting procedure presented in section 3.2, which uses the jackknife method to compute the variances of the sample parameter estimates and regression analysis to compute the variances of the regional parameter.

6.2 EXAMPLE

The portion of river considered for the levee project in this example is divided into three reaches, i.e., there are a total of three stages, $N_s = 3$, involved in the DP and DDDP optimization models. The maximum width of land available for the project in each reach is 3000 feet on each side of the flood plain. No maximum height of levee is considered in the optimization model. The levee for each reach must be built such that the levee capacity satisfies the design criterion of a 100-year flow. Three feet of freeboard for the levee is required.

In this study, the shape of the levees have a slope of 3(hor.):1(vert.) on the river side and a 4(hor.):1(vert.) on the land side. The crown width of all levees is 6 feet. Hence, the volumetric content of levees is a function of levee height only and can be expressed in cubic yards per mile as

$$V_{LV} = 1173.3 h_n + 684.4 h_n^2 \quad (6.1)$$

where $h_n = (h_{u,n} + h_{d,n})/2$, $h_{u,n}$ is the levee height at the upstream end of stage n , and $h_{d,n}$ is the levee height at the downstream end. The cost of levee construction is largely due to the cost of soil compaction. For simplification the cost of installing other accessories is not considered. The

unit cost of soil compaction for common road construction is \$0.86 per cubic yard at 1973 prices (Basco and Rahman, 1973) and is used in the optimization model to compute the cost of levee construction of given height, h_n , in a reach n of length L_n (in miles)

$$Z_{1,n} = 2(0.1009 h_n + 588.6 h_n^2) \cdot L_n \quad (6.2)$$

The length of levee on one side of the channel, L_n , (in miles) and the unit cost of land $C_{LND,n}$ (\$/acre) for each reach n is tabulated in Table 6.1. With the above information the cost of levee construction Eq. (6.2), and the land purchasing cost Eqs. (5.13) and (5.14) can be easily computed for each reach n . The total installation cost is converted to an annual basis for a 100-year period, using an interest rate of 8%. A hypothetical relationship between the volume of water, the flood stage, and the associated flood damage costs are tabulated in Table 6.2. Based on the historical flood records for the study area the time base for flood hydrographs is assumed to be 500 hours. For simplification, a triangular flood hydrograph with a time base of 500 hours is used in the computations of flood damage associated with the volume of water that exceeds the levee capacity.

This optimization model considers no flood routing procedure for the levee system. Thus for an assumed triangular flood hydrograph of known peak discharge with certain probability of exceedance and time base, the volume of water that spills over the levee of specified capacity can be easily determined as shown in Fig. 6.1. Using either Eq. (5.17) or Eq. (5.19), this information can be integrated to evaluate the annual expected damage cost that is associated with levee capacity design.

Table 6.1
 Uncertain Characteristics of Hydraulic Variables, Length, and Unit Land
 Cost of Each Channel Reach in Levee Design

Channel Reach	Variable	Nominal value	Tolerance	Distribution Fig. (4.3)	Mode
1	λ_m	1.0000	.2000	a	0.0000
	B(ft)	230.0000	15.0000	b	0.0000
	S_c	.0005	.0002	c	0.0000
	N_c	.0500	.0100	e	.0520
	A(sq.ft)	3800.0000	700.0000	d	0.0000
	τ	.0017	.0010	b	0.0000
	S_b	.0015	.0003	a	0.0000
	N_b	.0750	.0150	e	.0700
	L(mile) C_{LND} (\$/ac)	.7580 3000.0			
2	λ_m	1.0000	.3000	a	0.0000
	B(ft)	235.0000	20.0000	b	0.0000
	S_c	.0005	.0001	c	0.0000
	N_c	.0500	.0100	e	.0520
	A(sq.ft)	3400.0000	300.0000	d	0.0000
	τ	.0015	.0008	b	0.0000
	S_b	.0004	.0001	a	0.0000
	N_b	.0800	.0200	e	.0750
	L(mile) C_{LND} (\$/ac)	.6630 2000.0000			
3	λ_m	1.0000	.1000	a	0.0000
	B(ft)	225.0000	25.0000	b	0.0000
	S_c	.0025	.0005	b	0.0000
	N_c	.0500	.0100	d	0.0000
	A(sq. ft)	3800.0000	100.0000	d	0.0000
	τ	.0040	.0010	b	0.0000
	S_b	.0008	.0002	a	0.0000
	N_b	.0800	.0200	e	0.0750
	L(mile) C_{LND} (\$/ac)	0.568 1500.0000			

Table 6.2

Hypothetical Relationship Between the Volume of Water,
the Flood Stage, and the Flood Damage Cost

Volume (AF)	Damage (\$)	Flood Stage (ft)
0.000	0.000	43.000
290.000	5000.000	45.000
1250.000	20000.000	46.000
2360.000	100000.000	47.000
12390.000	400000.000	48.000
19860.000	600000.000	49.000
23500.000	1000000.000	50.000

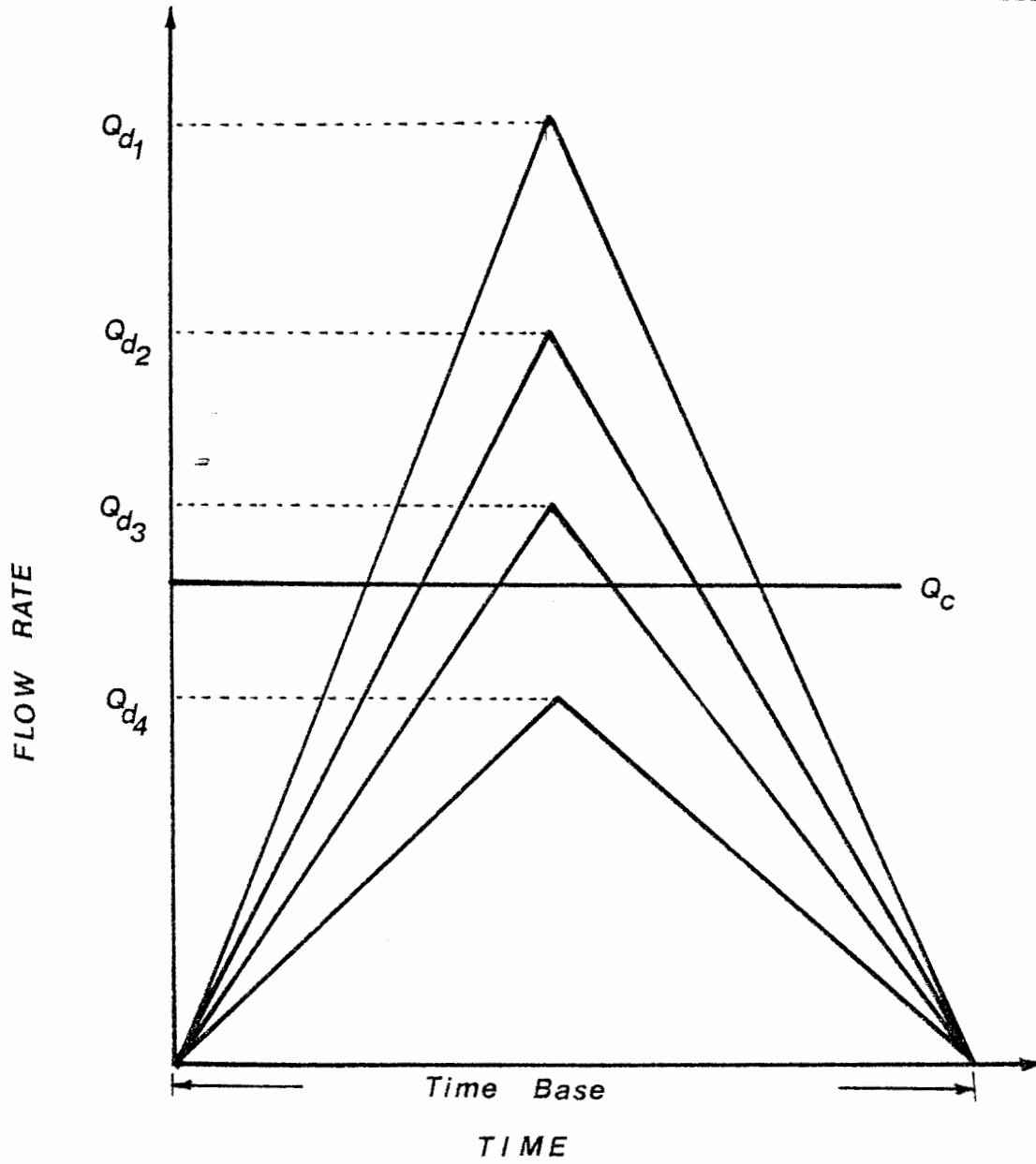


Figure 6.1 Hypothesized Triangular Inflow Hydrograph

In order to evaluate the overall risk associated with a particular levee capacity for reach n , an analysis of hydraulic uncertainty is required. The basic variables with uncertainty involved in the hydraulic calculation of levee capacity mentioned in the previous chapter and their corresponding nominal values, tolerance, and types of distribution (Fig. 4.3) are listed in Table 6.1. The derivations of the mean and coefficient of variation of levee capacity with specified encroachment widths and levee heights at both ends of the reach are given in Appendix B. The levee capacity is determined using the area-slope method (Chow, 1959).

6.3 EFFECT OF DESIGN PHILOSOPHY

Three design philosophies, i.e., no risk, IRISK = 0; hydrologic risk only, IRISK = 1; and overall risk, IRISK = 2, are considered. The size of the state space used in the DP are $3(W) \times 3(H)$, 5×5 , and 10×10 and the corresponding state space increments are 2000 ft. in width and 7 ft. in height; 1000 ft. and 4 ft.; and 400 ft. and 2 ft., respectively. For example, considering the first reach, the states for a state space of size $3(W) \times 3(H)$ in the DP are

$$\{(w_{1,i}, h_{1,j})\}_{3 \times 3} = \begin{bmatrix} (2230,7) & (2230,14) & (2230,21) \\ (4230,7) & (4230,14) & (4230,21) \\ (6230,7) & (6230,14) & (6230,21) \end{bmatrix} \quad (6.3)$$

In the DDDP approach the state space used is $3(W) \times 3(H)$ with initial states the same as that in the DP approach, shown as Eq. (6.3). The reduction rate of state increments for encroachment width as well as levee height is 0.5. The criterion in Eq. (5.30) used to determine when the increment of state

should be reduced, ϵ_r is 0.01. The maximum number of times the corridor size is to be reduced is 5.

Table 6.3 tabulates the computer time in seconds required for executing the 3-stage DP problem in this application using different sizes of the state space and various risk considerations in the design for the case when the flood loading distribution is log-Pearson type III. The computer system used is a CDC Dual Cyber 170/750 system at The University of Texas at Austin. The computer time required to solve the problem is not linear with respect to the size of the state space. This is further illustrated by plotting the computer time required versus the state space (Fig. 6.2) for different design philosophies. This shows that the required computer time increases approximately exponentially with respect to the increase in the number of states. A state space of 10×10 for IRISK = 2 was not considered because of the large suspected computer time requirement. The results in Table 6.3 illustrate that the DDDP procedure results in a tremendous savings in computer time. On the other hand the computer time required to solve the

Table 6.3 Computer Time (in Seconds) Required to Execute the 3-Stage DP Problem with Different Sizes of State Space and Various Risk Considerations Using Log-Pearson III Loading Distribution

Method Time IRISK	DP 3x3	DP 5x5	DP 10x10	DDDP 3x3
0	0.614	2.442	33.876	2.858
1	1.017	5.227	70.985	8.103
2	6.882	45.586		81.953

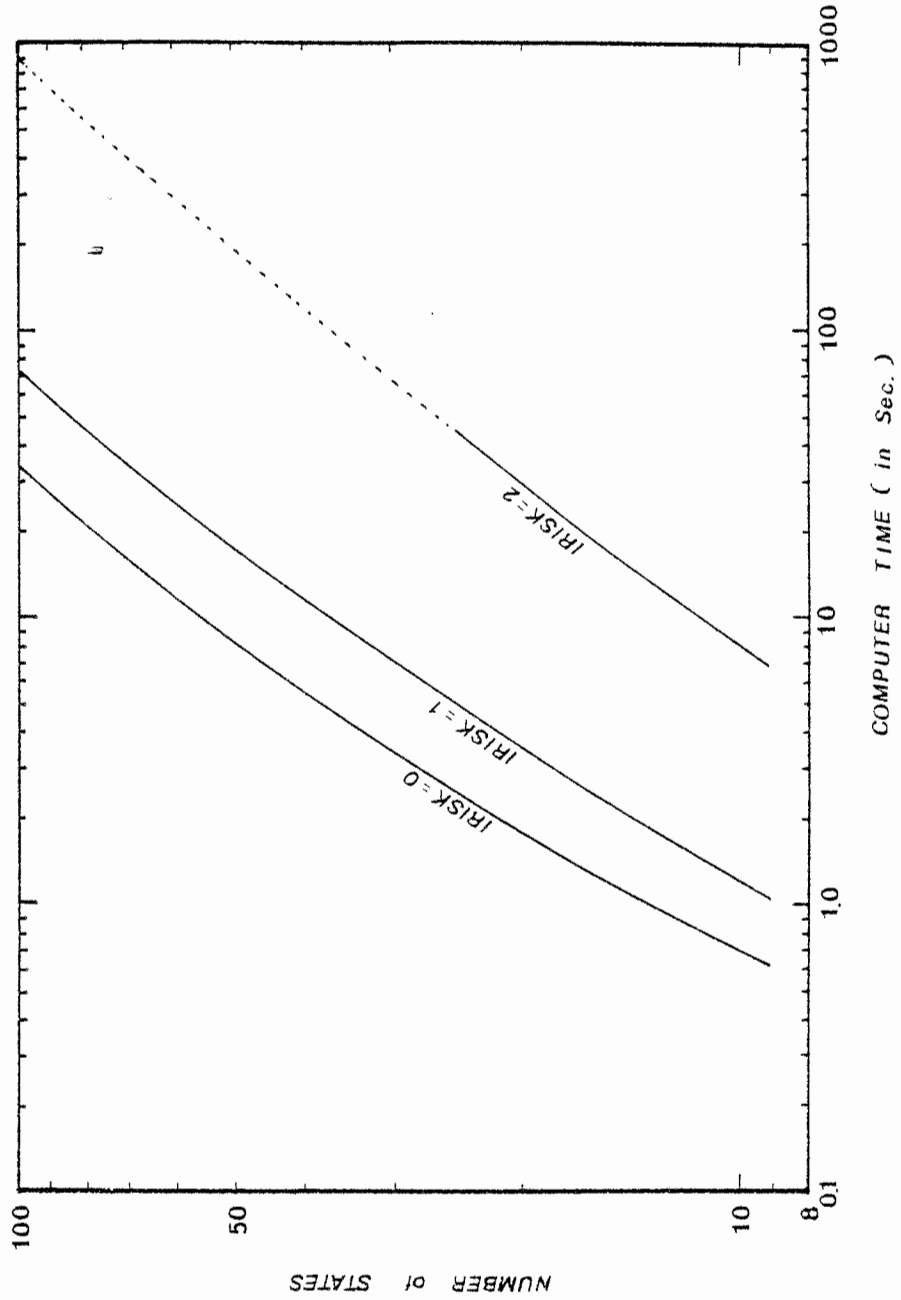


Figure 6.2 Computer Time vs. Number of States in DP Approach for Levee Problem

problem increases with complexity of the damage function. For example using the DDDP the computation times were 2.856 sec. for IRISK = 0; 8.103 sec. for IRISK = 1; and 81.453 sec. for IRISK = 2. This is because of the difference in damage functions integrated.

The minimum total annual expected cost and its components, annual installation cost and annual expected damage cost, for various risk considerations are listed in Table 6.4 and the corresponding optimal layout and design are listed in Table 6.5. By examining Table 6.4 the total annual expected cost associated with the optimal design derived by the DDDP (\$128,230) is less than that derived by the DP (\$132,247) with 10 x 10 states. From Table 6.3 the DDDP required only 8.103 seconds of computation time as compared to 70.985 seconds for the DP. Furthermore, the final optimal result of levee design is more accurately computed by the DDDP approach. These evidences show the desirability of the DDDP approach over the DP is not only the computer time saving but also the accuracy and the improvement in the results. For no risk consideration in the optimization (IRISK = 0), the trade-off between the installation cost and the flood damage cost is not considered. The optimal levee system in this case is expected to have a capacity that just satisfies the design criterion. For instance, when the flood loading is log-Pearson type III distributed, the flow magnitude for a return period of 100 years is 119,398 cfs in which the parameters in the loading model are estimated using jackknife method jointly with regression analysis. The safety factors for the optimal levee design using DDDP for the reaches are 1.008,

Table 6.4
 The Minimum Total Annual Cost and Its Component Costs
 for Various Risk Considerations Using Log-Pearson III Loading Distribution

IRISK	DP (3x3)	DP (5x5)	DP (10x10)	DDDP (3x3)	
0	Annual Installation Cost	128,392	100,352	87,199	82,970
	Annual Installation Cost	166,918	134,611	131,124	125,210
1	Annual Expected Damage Cost	34	2,074	1,123	3,020
	Annual Total Expected Cost	166,952	136,685	132,247	128,230
2	Annual Installation Cost	170,402	161,667		137,203
	Annual Expected Damage Cost	3,522	17,795		7,332
	Annual Total Expected Cost	173,924	179,462		144,535

Table 6.5 Optimal Levee Layout and Design for Various Risk Considerations
Using Log-Pearson Type III Loading Distribution

RISK	Reach	DP 3x3			DP 5x5			DP 10x10			DDDP 3x3		
		1	2	3	1	2	3	1	2	3	1	2	3
		0	U/S	2230	2235	2225	1230	1235	1235	630	635	1925	230
	D/S	2235	2225	2225	1235	1225	2225	635	1825	1025	235	19125	15375
	U/S	10.0	17.0	10.0	15.0	19.0	11.0	17.0	17.0	13.0	20.5	18.1	11.5
	D/S	17.0	10.0	10.0	19.0	11.0	7.0	17.0	13.0	9.0	18.1	11.5	6.7
1	U/S	2230	2235	4225	1230	1235	3275	630	1435	2225	230	1298	1975
	D/S	2235	4225	4225	1235	3225	2225	1435	2225	3425	1298	1975	2975
	U/S	17.0	17.0	10.0	19.0	19.0	15.0	21.0	21.0	13.0	22.0	21.2	14.4
	D/S	17.0	10.0	10.0	19.0	15.0	7.0	21.0	13.0	7.0	21.2	14.4	7.8
2	U/S	2230	2235	2225	1230	1235	3225				230	1485	2287
	D/S	2235	2225	2225	1235	3225	4225				1485	2287	3350
	U/S	17.0	24.0	17.0	23.0	23.0	15.0				23.1	21.6	14.6
	D/S	24.0	17.0	10.0	23.0	15.0	7.0				21.6	14.6	8.0

W - Encroachment width (in feet) ; U - Levee height (in feet)
U/S - Upstream end of the reach ; D/S - Downstream end of the reach

1.003, and 1.005. If damage costs are included, the optimal design changes considerably.

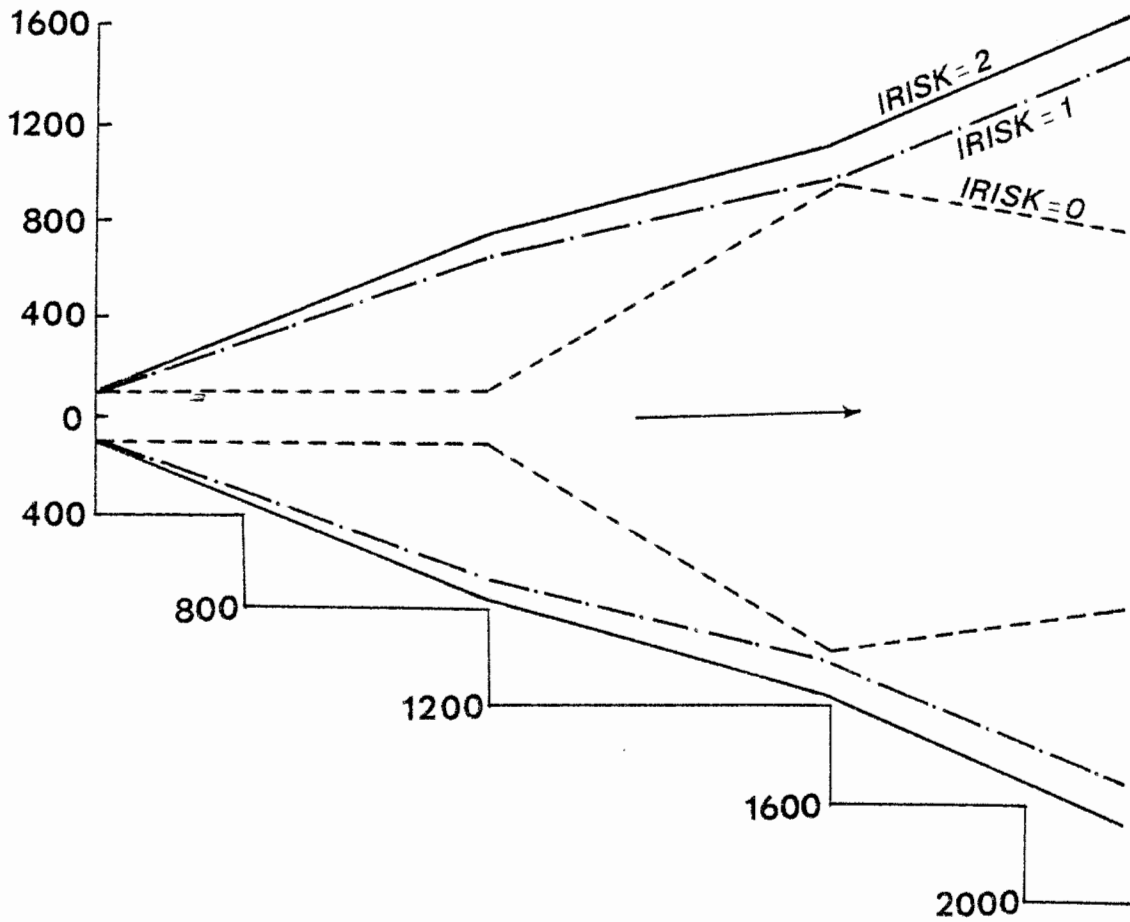
The safety factors associated with the optimal design, resulting from different design philosophies and different state space in the DP and the DDDP, previously described for the log-Pearson type III as loading distribution, are tabulated in Table 6.6. The annual expected damage costs associated with the given optimal design for the other risk options considered are tabulated in Table 6.7. For example, the optimal design obtained by using DDDP without risk consideration, i.e., no damage cost is brought into the trade-off in determining the design, is an annual expected damage cost of \$844,870, computed by Eq. (5.17) considering hydrologic risk only; while using Eq. (5.19) for the case where an overall risk is considered, the annual expected damage cost is \$1,028,322. By comparing the results presented in Tables 6.4 and 6.7 the annual expected damage cost associated with the optimal design, which is obtained under no risk consideration, ranges from 3.5 to 10 times as large as the annual installation cost when the hydrologic risk is considered. The annual expected damage cost computed by considering the overall risk is even larger than that of considering only the hydrologic risk. Based on hydrologic risk only, the annual expected damage cost is significantly underestimated as compared to the case when overall risk is considered. Table 6.7 provides strong evidence that the economic consequences of flood hazards are grossly underestimated if no risk or hydrologic risk only is considered. The procedures of considering an overall risk in the design are recommended. Figure 6.3 shows the optimal layout and design of the levee

Table 6.6 Safety Factor Associated with the Optimal Levee Design in Each Reach for Various Risk Considerations Using Log-Pearson Type III Loading Distribution

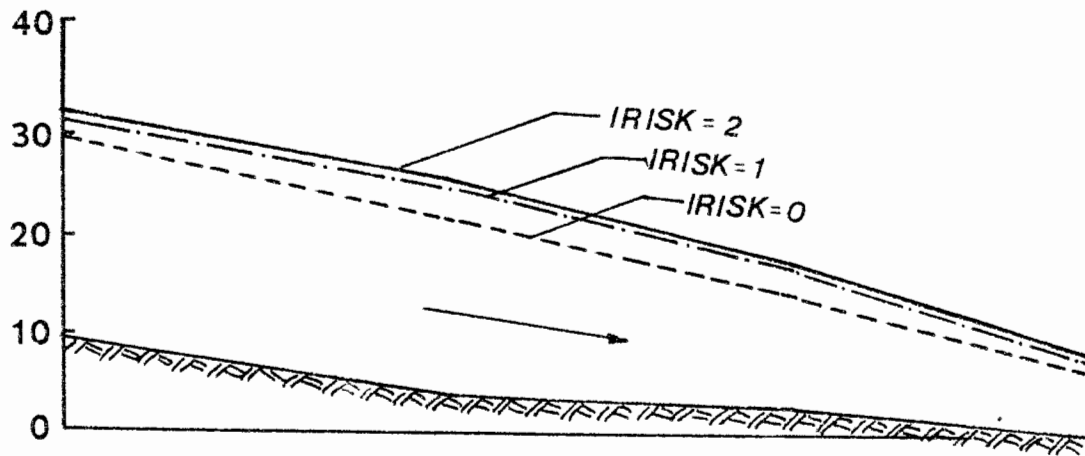
Method Reach IRISK	DP 3 x 3			DP 5 x 5			DP 10 x 10			DDDP 3 x 3		
	1	2	3	1	2	3	1	2	3	1	2	3
	0	1.134	1.471	1.054	1.351	1.183	1.012	1.138	1.000	1.008	1.008	1.003
1	2.561	2.020	2.082	1.938	1.836	1.920	2.033	1.932	1.879	1.867	1.830	1.910
2	2.219	2.920	2.205	2.583	2.655	3.011				2.130	2.119	2.229

Table 6.7 The Annual Expected Damage Costs Associated with the Given Optimal Design for the Other Risk Options Considered When the Log-Pearson III Loading Distribution Is Used

IRISK	Method		DP			DDDP		
	E(D)		3 x 3	5 x 5	10 x 10	3 x 3	5 x 5	10 x 10
0	Eq.(5.17)		449,215	479,112	736,114			844,870
		Eq.(5.19)	572,694	1,055,330	3,733,106			1,028,322
1	Eq.(5.19)		8,767	141,497	863,798			32,581



(a) Layout of Levee Encroachment Width



(b) Profile of Levee Height

Figure 6.3 Optimal Levee Design Using DDDP Technique for Log-Pearson Type III Loading Distribution with Different Design Philosophies

system under different design philosophies when the flood loading distribution is log-Pearson type III. If no flood damage cost is brought into consideration in the design process the resulting design of the levee is significantly different from those if the flood damage cost is considered.

6.4 EFFECT OF LOADING DISTRIBUTION

The above results are based on using the log-Pearson III distribution as the loading probability model. This section examines the effect of different loading distributions on the optimal cost and levee design. The optimal solution and associated levee design by applying DDDP using different loading probability models for various risk options (0, 1, and 2) are presented in Tables 6.8 and 6.9 respectively. The least cost solution and its associated optimal levee design are affected significantly not only by the risk consideration used but also by the loading probability model chosen. For the case when the overall risk is considered, the least cost solutions range from a value of \$84,466 a year for the normal loading model to \$182,986 a year for the log-normal loading model. This is mainly because the magnitudes of the 100-year flow adopted as the basis for levee design are so significantly different, ranging from 79,783 cfs for the normal case to 136,418 cfs for the log-normal case. The optimal design of the levee system, i.e., width of encroachment and height of levee, for various loading probability models considering overall risk are plotted in Figs. 6.4a and b.

A composite model is also considered in the optimization model.

Table 6.8 The Minimum Annual Total Expected Cost and Its Component Costs Using Various Loading Distributions and Different Risk Considerations Obtained by DDDP Approach

IRISK	COST COMPONENT	LOADING DISTRIBUTION							COMPOSITE
		NORMAL	LOGNORMAL	GUMBEL	PEARSON III	LOGPEARSON III			
0	Annual Installation Cost	54,616	94,015	68,681	82,518	82,970			85,403
	Annual Installation Cost	66,403	158,906	94,393	120,017	125,210			158,451
1	Annual Expected Damage Cost	1,117	999	1,183	1,175	3,020			1,685
	Total Annual Expected Cost	67,520	159,904	95,576	121,192	128,230			159,136
2	Annual Installation Cost	80,350	175,112	108,282	134,203	137,203			169,302
	Annual Expected Damage Cost	4,116	7,874	4,666	6,389	7,332			8,157
	Total Annual Expected Cost	84,466	182,986	112,948	140,952	144,535			177,459

Table 6.9 Optimal Levee Layout and Design for Various Risk Considerations and Different Loading Distributions Obtained by DDDP Approach

IRISK	REACH	NORMAL			LOGNORMAL			GUMBEL		
		1	2	3	1	2	3	1	2	3
0	U/S	230.0	235.0	725.0	230.0	235.0	2162.5	230.0	485.0	1037.5
	D/S	235.0	725.0	1100.0	235.0	2162.5	1662.5	485.0	1037.5	1787.5
	U/S	14.2	17.0	10.4	23.1	19.0	12.0	15.5	17.7	10.9
	D/S	17.0	10.4	6.3	19.0	12.0	7.4	17.7	10.9	5.4
1	U/S	230.0	360.0	1162.5	230.0	1860.0	2350.0	230.0	797.5	1475.0
	D/S	360.0	1162.5	1412.5	1860.0	2350.0	3662.5	797.5	1475.0	2162.5
	U/S	15.9	17.2	11.1	25.1	23.6	15.9	19.0	19.4	12.8
	D/S	17.2	11.1	5.8	23.6	15.9	8.7	19.4	12.8	7.2
2	U/S	230.0	672.5	1287.5	230.0	1985.0	2850.0	230.0	985.0	1787.5
	D/S	672.5	1287.5	1850.0	1985.0	2850.0	4287.5	985.0	1787.5	2537.5
	U/S	18.8	18.1	12.0	27.3	24.0	16.1	20.7	20.1	13.3
	D/S	18.1	12.0	6.7	24.0	16.1	8.5	20.1	13.3	7.6

W - Encroachment width (in feet)
H - Levee height (in feet)
U/S - Upstream end of the reach
D/S - Downstream end of the reach

Table 6.9 - continued

IRISK	REACH	PEARSON III			LOGPEARSON III			COMPOSITE		
		1	2	3	1	2	3	1	2	3
0	U/S	230.0	235.0	1912.5	230.0	235.0	1912.5	230.0	235.0	1912.5
	D/S	235.0	1912.5	1600.0	235.0	1912.5	1537.5	610.0	1912.5	1912.5
H	U/S	20.3	18.1	11.3	20.5	18.1	11.5	17.9	17.7	11.3
	D/S	18.1	11.3	6.7	18.1	11.5	6.7	17.7	11.3	6.5
1	U/S	230.0	1235.0	1975.0	230.0	1298.0	1975.0	230.0	1797.5	2662.5
	D/S	1235.0	1975.0	2850.0	1298.0	1975.0	2975.0	1797.5	2662.5	3787.5
H	U/S	21.4	20.7	13.9	22.0	21.2	14.4	25.5	22.9	15.3
	D/S	20.7	13.9	7.4	21.2	14.4	7.8	22.9	15.3	8.0
2	U/S	230.0	1422.5	2287.5	230.0	1485.0	2287.0	230.0	1860.0	2850.0
	D/S	1422.5	2287.5	3289.5	1485.0	2287.0	3350.0	1860.0	2850.0	4100.0
H	U/S	22.9	21.4	14.4	23.1	21.6	14.6	26.8	23.6	15.9
	D/S	21.4	14.4	7.8	21.6	14.6	8.0	23.6	15.9	8.5

W - Encroachment width (in feet)
H - Levee height (in feet)
U/S - Upstream end of the reach
D/S - Downstream end of the reach

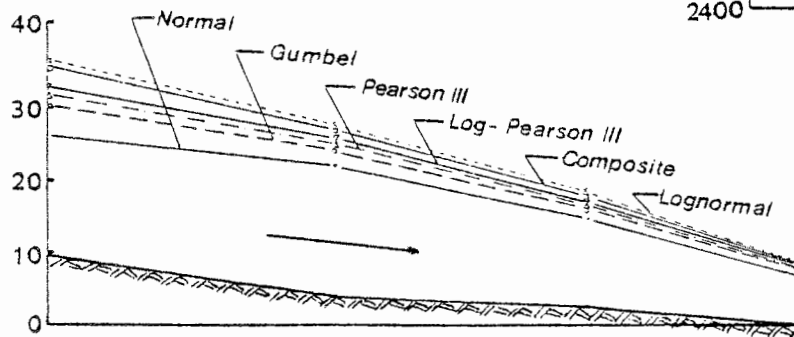
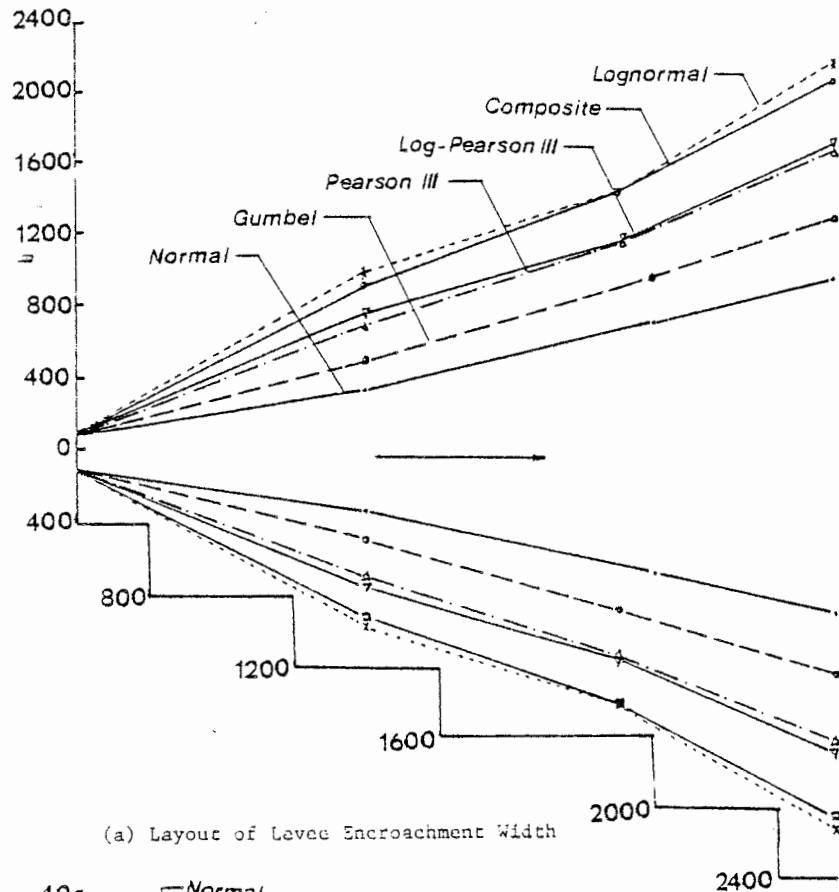


Figure 6.4 Optimal Levee Design Using DDDP for Different Loading Models with IRISK = 2

The procedure of developing a composite model is described in section 3.3. In this example, the composite probability model is developed as Eq. (4.23) or (4.24). This composite model is used to evaluate the annual expected damage cost, $E_c(D)$ in the DP optimization model as follows:

1. hydrologic risk only,

$$E_c(D) = 0.498 \int_{Q_c^*}^{\infty} D(Q_d, Q_c^*) \cdot f_{\ell, LN}(Q_d) \cdot dQ_d \\ + 0.502 \int_{Q_c^*}^{\infty} D(Q_d, Q_c^*) \cdot f_{\ell, LP}(Q_d) \cdot dQ_d \quad (6.4)$$

2. overall risk case,

$$E_c(D) = 0.498 \int_0^{\infty} \left[\int_0^{Q_d} D(Q_c, Q_d) \cdot f_{r, LN}(Q_c) \cdot dQ_c \right] \cdot f_{\ell, LN}(Q_d) \cdot dQ_d \\ + 0.502 \int_0^{\infty} \left[\int_0^{Q_d} D(Q_c, Q_d) \cdot f_{r, LN}(Q_c) \cdot dQ_c \right] \cdot f_{\ell, LP}(Q_d) \cdot dQ_d \quad (6.5)$$

Composite probability model serves as a good alternative model for the cases when the random mechanism of flood loading is not fully understood; and the result of probabilistic analysis is sensitive to the model being chosen because the composite model takes into account the model uncertainty.

CHAPTER 7

SUMMARY AND CONCLUSION

7.1 SUMMARY

In the design and operation of water resources engineering projects there exist many uncertainties relating to the hydrologic, hydraulic, structural, and economic aspects. This study is a theoretical effort to develop procedures which systematically analyze the uncertainties involved in both the hydrologic and hydraulic aspects so that the risk and the reliability of the hydraulic structure can be evaluated. Both static and time-dependent reliability models are developed. Static reliability models consider single application of loading while time dependent models consider the repeated application of loading. In order to define the statistical properties of the flood loading and the structure capacity, the analyses of both hydrologic uncertainty and hydraulic uncertainty are performed.

First-order analysis of uncertainty is especially suitable for analyzing the hydraulic uncertainty in which the capacity of a hydraulic structure is expressed as the function of several variables with uncertainty. Two types of hydraulic structure, box culverts and levees, are considered in this report; however, the methodologies are applicable to other types of hydraulic structures. The first-order analysis is applied to Manning's equation to

estimate the mean and variance (or coefficient of variation) of the hydraulic structure capacity.

For the hydrologic parameter uncertainty, a new methodology is proposed to minimize the variance of the parameter (mean, standard deviation, and skewness) using a weighting procedure which combines a sample parameter estimate and a regional parameter estimate to determine the "best" parameter estimate for the hydrologic loading model. The weight between the sample parameter estimates and the regional parameter estimates depends on the respective variances. The variance of the sample parameter estimate can be computed by two nonparametric statistical techniques, i.e., the jackknife method and the bootstrap method while the variance of the regional parameter estimate can be derived from regression equations. An experimental study is performed to examine the proposed method of estimating the skew coefficient in the log-Pearson type III distribution as opposed to other methods developed. The study shows that the proposed method does the best job in estimating the skewness both in the aspects of stability and accuracy of the estimate. Because the methodology is general enough to be applied to any parameter estimate of hydrologic sequences, it is further extended to minimize the variances of the estimate of the mean and the standard deviation.

A study applied the proposed methodology to five gaging stations in the state of Texas for flood flow frequency analysis with several other approaches, including the currently practiced Water Resources Council's method. The results show that the proposed method is superior, in most

cases, to the other methods tested, indicating that the proposed method provides a better means for estimating the statistical parameters of hydrologic sequences.

The method adopted to treat the hydrologic model uncertainty is to develop a composite hydrologic model by applying a Bayes theorem which depends on the prior probability of the model, sample observations, and parameters involved in the model. Because the true value of parameters are never known, the "best" parameter estimates derived by the above described weighting procedure are used. The composite hydrologic model can be used to derive the composite reliability model for both static and time-dependent cases.

An example of applying the above-described methodologies to analyze the hydraulic as well as hydrologic uncertainties is given to develop the risk and reliability model for a levee system design near Victoria, Texas. A series of risk-safety factor curves for the static as well as for the time-dependent reliability models using various types of loading distributions, normal, lognormal, Gumbel, Pearson III, log-Pearson III and the composite model, are presented. This example demonstrates a systematic and scientific-based procedure which is more meaningful to evaluate the risk-safety factor relationship.

As the final phase of this study, the methods developed to analyze the hydraulic and hydrologic uncertainties are incorporated into an optimization framework. Dynamic programming (DP) and discrete differential dynamic programming (DDDP) are employed to obtain the optimal design of

the levee system. An example application is used to demonstrate the methodology. The economic consequences of using different design philosophies, i.e., (1) considering no risk, (2) considering inherent hydrologic risk, and (3) considering overall risk, are examined. The effect of the choice of hydrologic model used in determining the optimal solution is also examined.

7.2 CONCLUSIONS

Based on the theoretical studies, model development, and model application presented in this report the following general conclusions can be stated:

1. Probabilistic procedures provide a consistent basis for the systematic assessment and analysis of uncertainties.
2. All uncertainties can be assessed in two parts, i.e., as variables due to inherent randomness and as errors of theoretical or empirical equations.
3. The evaluation of risk and reliability through probabilistic measures can be subjected to logical operation by way of the mathematical theory of probability.
4. The probabilistic procedures can be incorporated into optimal design procedures.

A formal approach to the analysis of the performance of a hydraulic structures has been provided resulting in the following conclusions:

1. For prescribed probability distributions for the resistance and loading, the probability of failure (or risk) can be expressed as a function of only the mean values and uncertainties of the loading and resistance, thus the problem of risk evaluation involves essentially the assessment of uncertainties, in addition to the prediction of the mean values of the design variables.
2. A composite risk can be computed as opposed to just the hydrologic risk considered in the conventional return period design methods which tend to underestimate the potential risk.
3. From the standpoint of risk-based design, it is most convenient and practically desirable to describe the loading and resistance in terms of mean values and associated uncertainties.
4. The approach of computing the risk and reliability can be extended quite easily to compute expected damage costs and thereby incorporated into optimal risk-based design procedures.
5. In order to accurately evaluate risk, reliability, and expected damage costs associated with the design a better assessment of uncertainty components (or variables) becomes important. In the analysis of hydraulic uncertainty the first-order analysis is applicable to derive the statistical

properties of the capacity of hydraulic structures which are functions of many hydraulic variables with uncertainty.

Several conclusions can be made concerning evaluation of the hydrologic uncertainty.

1. A generalized skew coefficient can improve the accuracy of determining the frequency factors provided the accuracy of the skew coefficient is evaluated and is taken into account in a weighting procedure.
2. The proposed weighting procedure to compute the generalized hydrologic parameter provides a theoretical basis and minimizes the variance (uncertainty) of generalized parameter estimates which considers the variances resulting from both sample parameter estimates and regional parameter estimates.
3. Consideration should be given to the uncertainty involved in estimating the parameters, mean, standard deviation, and skewness in order to increase the capability of prediction in flood frequency analysis.
4. The methodology proposed for reducing hydrologic parameter uncertainty was found to be superior to the WRC method and others presented. The proposed methodology has a more sound theoretical basis as opposed to the WRC method. This method can be applied to other types of

hydrologic frequency analysis and is applicable for any type of distribution.

5. The risk evaluation is extremely sensitive to the hydrologic loading probability model employed; hence, the loading model used bears important consequence and significant effect on the optimal design. Composite hydrologic probability models are suggested which are a better alternative because the hydrologic model uncertainty is minimized.
6. It has been demonstrated in the levee design that the optimal result differs significantly for different design philosophies adopted. The expected damage costs associated with the resulting levee design is underestimated unless the overall uncertainties are considered.

7.3 SUGGESTIONS FOR FURTHER STUDY

Further extensions of this research effort could include:

1. The risk evaluation procedure can be modified to integrate the variation of generalized parameter estimates which are associated with minimum variance. Under this situation the knowledge of probability distribution function for the weighted parameter estimates is required and the mathematical representation of risk or reliability becomes rather complicated in which multi-dimensional integration is inevitable.

2. The assumption used on sample parameter estimates and regional parameter estimates in determining the weight is that both estimates are unbiased. The unbiased estimate of sample parameters can be derived via a rigorous mathematical statistical analysis while for the regional parameter estimates by regression analysis the priori assumption imposed is that the form of regression model is correct which, in fact, is an uncertainty. This makes the derived weighting factor more restrictive to apply. However, this restriction can be released by allowing one of the parameter estimates to be biased. Under this circumstance, an empirical Bayes procedure can be used.
3. Hydrologic or hydraulic routing technique could be incorporated into the optimal design procedure to properly account for the time lag and attenuation effect of a design flood wave progressing through the levee system. The kinematic wave or the Muskingum models are two routing techniques that can possibly be used in the optimization model. Such techniques require design inflow hydrographs and, consequently, a more sophisticated hydrologic analysis must be used.
4. In the computation of expected flood damage the index variables commonly used are either the flood peak or the

flood volume. The analysis of multivariate relationships between the flood peak and the flood volume (or the time-base of flood hydrographs) can be pursued so that a more realistic model for estimating the expected flood damage can be formulated.

5. The evaluation of the risk of structure safety in water resources engineering projects can be extended by considering the failure mechanisms of the hydraulic structure induced by water such as hydraulic pressure exerted on the structure, reduction of strength due to the erosion and saturation, loss of foundation instability caused by seepage and piping, etc.
6. Economic feasibility is always an important factor in determining whether water resources engineering projects should be undertaken or not. In most economic studies in the water resource field either one of the two measures for the feasibility of the project, i.e., net benefit and benefit-cost ratio, are based on the assumption that the input estimates used to calculate benefits and costs are the "best" or the "most likely" to occur. This procedure may very likely produce a significantly biased picture of the future without considering the uncertainty associated with the input variables in the economic analysis. A probabilistic approach should be used to take into account the uncertainty of the

economic aspect so that a probabilistic statement can be made about the feasibility measure used.

7.4 FINAL COMMENTS

The theoretical concepts of risk and reliability analyses have been available for some time; however, the introduction of these concepts into water resources and hydraulic structure design is only in its infancy. A major concern of this report has been to recognize and illustrate that these concepts can be of significance in water resources design. The implementation of these concepts into the practice of engineering is inevitable, but will take place on a rather slow time scale. In any case, the real and significant roles of probability in hydraulic structure design lie in its logical framework for uncertainty analysis and the quantitative basis for risk and safety assessment. The risk which is a consequence of uncertainty is measured by the probability of failure. For this reason, it is important that the concept of failure probability be accepted even if only as a relative measure of safety and performance.

Unlike many theoretical concepts, the practical implementation of reliability theory requires the introduction of certain approximation and assumptions. However, despite certain shortcomings when very small probabilities are involved and the reluctance to accept the possibility of failure, there are significant advantages provided by the probabilistic basis for hydraulic structure design. These have been previously outlined.

The use of statistical and probability models cannot circumvent the difficulties in hydraulic design resulting from the many uncertainties. In the past these uncertainties have been treated subjectively through the exercise of engineering judgment which may be in the form of multiplicative or additive factors. Alternatively, such judgments can be expressed in the form of "judgmental" probabilities. This serves to express the uncertainties in terms of subjective probabilities which are unfamiliar and, in general, confusing to engineers at this time. Nevertheless, such judgmental probabilities may be a suitable alternative to the conventional form of expressing engineering judgment.

LIST OF REFERENCES

- Ang, A. S-H, "Extended Reliability Basis of Structural Design Under Uncertainties," Proceedings, SAE/AIAA/ASME 9th Reliability and Maintainability Conference, Detroit, July 20-23, Annuals of Reliability, Vol. 9, pp. 642-649, 1970.
- Anscombe, F.J. and J.W. Tukey, "The Examination and Analysis of Residuals," Technometrics, Vol. 5, pp. 141-160, 1963.
- Basco, D.R. and K.M.A. Rahman, "Alternative Solutions to Water Resource Development--A Case Study," TR-55, Texas Water Resources Institute, Texas A & M University, May 1974.
- Beard, L.R., "Statistical Methods in Hydrology," U.S. Army Engineer District, Sacramento, California, January 1961.
- Benson, M.A., "Factors Affecting the Occurrence of Floods in the Southwest," U.S. Geological Survey, Water Supply Paper, 1580-D, pp. D1-D72, 1964.
- Bernier, J., "Les Methodes Beyesieness en Hydrologie Statistique", Proceedings, 1st International Hydrology Symposium, Vol. 1, Colorado State University, Fort Collins, Colorado, pp. 459-470, 1967.
- Bobee, B., "The log-Pearson Type 3 Distribution and Its Application in Hydrology," Water Resources Research, Vol. II, No. 5, pp. 681-689, 1975.
- Bodo, B., and T.E. Unny, "Model Uncertainty in Flood Frequency Analysis and Frequency-Based Design," Water Resources Research, Vol. 12, No. 6, pp. 1109-1117, 1976.
- Bogardi, I., L. Duckstein, and E. Castano, "Effect of Stochastic Model Choice on Hydraulic Design," Stochastic Processes in Water Resources Engineering, Ed. by L. Gottschalk, G. Lindh, and L. de Mase, Water Resources Publications, Fort Collins, Colorado, 1977.
- Bogardi, I. and E. Szidarovsky, "Induced Safety Algorithm for Hydrologic Design Under Uncertainty," Water Resources Research, Vol. 10, No. 2, pp. 155-161, 1974.
- Bogardi, I., and M. Zoltan, "Determination of Degree of Protection Offered by Flood Levees and the Economic Improvement Thereof," Department for Flood Control and River Training, National Water Authority, Budapest, Hungary, 1968.

- Box, G.E.P. and D.R. Cox, "An Analysis of Transformation," Journal of the Royal Statistical Society, Series B, No. 2, 1964, pp. 211-252.
- Castano, E., L. Duckstein, and I. Bogardi, "Choice of Distribution Functions for Hydrologic Design," Water Resources Research, Vol. 14, No. 4, pp. 643-652, August, 1978.
- Chow, V.T., Open Channel Hydraulics, McGraw-Hill Book Co., New York, 1959.
- Chow, V.T., ed., Handbook of Applied Hydrology, McGraw-Hill Book Co., New York, 1964.
- Chow, V.T., and D.D. Meredith, "Water Resources Systems Analysis, Part IV. Review of Programming Techniques," Civil Engineering Studies, Hydraulic Engineering Series, No. 22, University of Illinois at Urbana-Champaign, Illinois, July 1969.
- Chow, V.T., D.R. Maidment, and G.W. Tauxe, "Computer Time and Memory Requirements for DP and DDDP in Water Resources Systems Analysis," Water Resources Research, Vol. 11, No. 5, pp. 621-628, October 1975.
- Conover, W.J., Practical Nonparametric Statistics, John Wiley & Sons, Inc., 1971.
- Conover, W.J., "Introduction to Bayesian Methods Using the Thomas-Fiering Model," Water Resources Research, Vol. 7, No. 2, pp. 406-409, 1971.
- Cook, R.D., "Detection of Influential Observation in Linear Regression," Technometrics, Vol. 19, No. 1, pp. 15-18, Feb. 1977.
- Cornell, C.A., "First-Order Analysis of Model and Parameter Uncertainty," Proceedings, International Symposium on Uncertainties on Hydrologic and Water Resources Systems, Vol. 3, pp. 1245-1274, Tucson, Arizona, 1972.
- Crutcher, H.L., "A Note on the Possible Misuse of Kolmogorov-Smirnov Test," Journal of Applied Meteorology, Vol. 14, pp. 1600-1603, 1975.
- Daniel, C. and F.S. Wood, Fitting Equations to Data, Wiley Interscience, 1971.
- Davis, D.R., C.C. Kiesiel, and L. Duckstein, "Bayesian Decision Theory Applied to Design in Hydrology," Water Resources Research, Vol. 8, No. 1, pp. 33-41, 1972.
- Davis, C.V., and K.E. Sorenson, Handbook of Applied Hydraulics, McGraw-Hill Book Company, 1969.

- DeGroot, M.H., Probability and Statistics, Addison Wesley Publishing Company, 1975.
- Draper, N.R., and H. Smith, Applied Regression Analysis, John Wiley and Sons, Inc., N.Y., 1966.
- Efron, B., "Bootstrap Methods: Another Look at the Jackknife," Technical Report No. 32, Division of Biostatistics, Stanford University, Stanford, California, July, 1977.
- Efron, B., "Computers and the Theory of Statistics: Thinking the Unthinkable," Technical Report No. 39, Division of Biostatistics, Stanford University, Stanford, California, June, 1978.
- Fisher, R.A., "The Moments of the Distribution for Normal Samples of Measures of Departure from Normality," Proc. Royal Society London, (A), Vol. 130, pp. 16-28, 1931.
- Gumbel, E.J., "The Calculated Risk in Flood Control," Applied Science Research, The Hague, Vol. 5A, pp. 272-280, 1955.
- Haan, C.T., Statistical Methods in Hydrology, The Iowa State University Press, 1977.
- Hardison, C.H., "Generalized Skew Coefficients of Annual Floods in the United States and Their Application," Water Resources Research, Vol. 10, No. 4, pp. 745-752, April 1974.
- Heidari, M., "A Differential Dynamic Programming Approach to Water Resources Systems," Ph.D. thesis, Department of Civil Engineering, University of Illinois at Urbana-Champaign, Urbana, Illinois, 1970.
- Heidari, M., V.T. Chow, P.V. Kokotovic, and D.D. Meredith, "Discrete Differential Dynamic Programming Approach to Water Resources Systems Optimization," Water Resources Research, 7(2), pp. 273-282, 1971.
- Hogben, D., S.T. Peavy, and R.N. Varner, OMNITAB II, User's Reference Manual, NBS Technical Note 552, U.S. Department of Commerce, 1971.
- Kapur, K.C. and L.R. Lamberson, Reliability in Engineering Design, John Wiley and Sons, Inc., New York, 1977.
- Kiesiel, C.C., "Stochastic Hydraulics in Relation to Hydrology and Decision Theory," Stochastic Hydraulics, 1st International Symposium on Stochastic Hydraulics, pp. 710-728, 1971.

- Kite, G.W., Frequency and Risk Analysis in Hydrology, Water Resources Publications, Fort Collins, Colorado, 1977.
- Lilliefors, H.W., "On the Kolmogorov-Smirnov Test for Normality with Mean and Variance Unknown," Journal of American Statistical Association, Vol. 62, pp. 399-402, 1967.
- Lilliefors, H.W., "On the Kolmogorov-Smirnov Test for the Exponential Distribution with Mean Unknown," Journal of American Statistical Association, Vol. 64, pp. 387-389, 1969.
- Lilliefors, H.W., "The Kolmogorov-Smirnov and Other Distance Test for the Gamma Distribution and for the Extreme-Value Distribution When Parameters Must be Estimated," George Washington University, Supported in part by U.S. Department of Commerce Contract 1-35214.
- McCuen, R.H., "Map Skew," Journal of the Water Resources Planning and Management Division, ASCE, Vol. 105, WR2, pp. 269-278, September, 1979.
- Mallows, C.L., "Choosing Variables in a Linear Regression: A Graphical Aid," Paper presented at the Central Regional Meeting of the Institute of Mathematical Statistics, Manhattan, Kansas, May 7-9, 1964.
- Matalas, N.C. and Benson, M.A., "Note on the Standard Error of the Coefficient of Skewness," Water Resources Research, Vol. 4, No. 1, 1968.
- Matalas, N.C., J.R. Wallis, "Regional Skew in Search of a Parent," Water Resources Research, Vol. 11, No. 6, pp. 815-826, 1975.
- Mays, L.W., "Optimal Design of Culverts Under Uncertainties," Journal of the Hydraulics Division, ASCE, Vol. 105, No. 5, May 1979.
- Mays, L.W., "Optimal Risk Based Design of Water Resource Projects," Proceedings, International Symposium on Risk and Reliability in Water Resources, University of Waterloo, Waterloo, Ontario, Canada, June 1978.
- Mays, L.W., and B.C. Yen, "Optimal Cost Design of Branched Sewer Systems," Water Resources Research, Vol. 11, No. 1, pp. 37-47, February 1975.
- Miller, R.G., "The Jackknife—A Review," Biometrika, Vol. 6, No. 1, pp. 1-17, 1974.
- Nemhauser, G.L., Introduction to Dynamic Programming, John Wiley and Sons, Inc., 1966.

- Tang, W.H., L.W. Mays, and H.G. Wenzel, "Discounted Flood Risks in Least-Cost Design of Storm Sewer Networks," Proceedings, Second International IAHR Symposium on Stochastic Hydraulics, Lund, Sweden, August 1976.
- Tang, W.H., L.W. Mays, and B.C. Yen, "Optimal Risk-Based Design of Storm Sewer Networks," Journal of the Environmental Engineering Division, ASCE, Vol. 101, No. EE3, pp. 381-398, June 1975.
- Tang, W.H. and B.C. Yen, "Hydrologic and Hydraulic Design Under Uncertainties," Proceedings, International Symposium on Uncertainties in Hydrologic and Water Resources Systems, Vol. 2, pp. 868-882, Tucson, Arizona, 1972.
- Tasker, F.D., "Flood Frequency Analysis with a Generalized Skew Coefficient," Water Resources Research Vol. 14, No. 2, pp. 373-376, April, 1978.
- U.S. Water Resources Council, Hydrology Committee, "A Uniform Technique for Determining Flood Flow Frequencies," Bulletin 15, Washington, D.C., 1967.
- U.S. Water Resources Council, Hydrology Committee, "Guidelines for Determining Flood Flow Frequency," Bulletin 17, Washington, D.C., 1976.
- Vicens, G.J., I. Rodriguez-Iturbe, and J.C. Schaake, Jr., "A Bayesian Framework for the Use of Regional Information in Hydrology," Water Resources Research, Vol. 11, No. 3, pp. 405-414, 1975.
- Wallis, J.R., N.C. Matalas, and J.R. Slack, "Just a Moment!," Water Resources Research, Vol. 10, No. 2, pp. 211-219, August 1974.
- Watt, W.E., and K.C. Wilson, "Allowance for Risk and Uncertainty in the Optimal Design of Hydraulic Structures," Proceedings, International Symposium on Risk and Reliability in Water Resources, University of Waterloo, Waterloo, Ontario, Canada, June 1978.
- Wood, E.F., and I. Rodriguez-Iturbe, "Bayesian Inference and Decision Making for Extreme Hydrologic Events," Water Resources Research, Vol. II, No. 4, pp. 533-542, 1975a.
- Wood, E.F., and I. Rodriguez-Iturbe, "A Bayesian Approach to Analysing Uncertainty Among Flood Frequency Models," Water Resources Research, Vol. II, No. 6, pp. 839-843, 1975b.
- Wood, E.F., "An Analysis of Flood Levee Reliability," Water Resources Research, Vol. 13, No. 3, pp. 665-671, 1977.

- Yeh, W.W-G, and H. Asfur, "An Annotated Bibliography on the Design of Water Resources Systems," Contribution No. 134, Water Resources Center, University of California, Los Angeles, March 1971.
- Yen, B.C., "Risks in Hydrologic Design of Engineering Projects," Journal of the Hydraulics Division, ASCE, Vol. 96, No. HY1, pp. 223-252, January 1970.
- Yen, B.C., "Safety Factor in Hydrologic and Hydraulic Engineering Design," Proceedings, International Symposium on Risk and Reliability in Water Resources, University of Waterloos, Waterloo, Ontario, Canada, June 1978.
- Yen, B.C. and A.H-S Ang, "Risk Analysis in Design of Hydraulic Projects," Stochastic Hydraulics, 1st International Symposium on Stochastic Hydraulics, pp. 694-709, 1971.
- Yevjevish, V., "Risk and Uncertainty in Design of Hydraulic Structures," Stochastic Processes in Water Resources Engineering, Ed. by L. Gottschalk, G. Lindh, and L. deMare, Water Resources Publications, Fort Collins, Colorado, 1977.
- Young, G.K., Childrey, M.R., and Trent, R.E., "Optimal Design of Highway Drainage Culverts," Journal of the Hydraulics Division, ASCE, Vol. 100, No. HY7, pp. 971-993, July 1974.
- Zelenhasiz, E., "Theoretical Probability Distributions for Flood Peaks," Hydrology Paper No. 42, Colorado State University, Fort Collins, Colorado, November 1970.

APPENDIX A

REGRESSION ANALYSIS FOR REGIONAL STREAMFLOW CHARACTERISTICS IN THE CENTRAL AND EAST PART OF TEXAS

A.1 INTRODUCTION

In this appendix regression analysis is applied to define the regional streamflow characteristics and their variances. Hydrologic data for the Southwestern part of the United States (Fig. 3.8) is used. This region comprises most of Texas and New Mexico, and small parts of Louisiana and Colorado. Benson (1964) applied regression analysis for this region to relate the flood magnitudes of specified return periods to meteorological and physiographical characteristics. The region was divided into two subregions based on the mechanism as to how the floods are generated. Based on Benson's study the floods in the northwestern corner of the region are produced by snowmelt and in the remaining portion of the region the floods are caused by local thunderstorms or widespread tropical storms. Benson related the flood magnitudes for each of the two subregions to a different set of meteorological and physiographic characteristics. The regression equations are for the subregion in which the floods are produced by the rain storms. Gaging stations having a minimum of 30 years of streamflow records were selected. The locations of the gaging stations used are shown in Fig. 3.8 and are listed in Table A.1.

Table A.1 List of Streamflow Gaging Stations in Southwestern
United States Used for Regression Study

STA. NO.	LOCATION	NO. RECORD
8010000	RAYOU DES CANNES NEAR FUNICE, LA.	39
8012000	RAYOU NEZPIQUE NEAR BASILE, LA.	39
8013000	CALCASTEU RIVER NEAR GLENMORA, LA.	34
8013500	CALCASTEU RIVER NEAR OBERLIN, LA.	41
8014500	WHISKY CHITTO CREEK NEAR OBERLIN, LA.	38
8015000	RUNDICK CREEK NEAR DRY CREEK, LA.	31
8016400	BECKWITH CREEK NEAR DEQUINCY, LA.	32
8019000	LAKE FORK CREEK NEAR QUITMAN, TEX.	40
8019500	BIG SANDY CREEK NEAR BIG SANDY, TEX.	39
8020000	SABINE RIVER NEAR GLADEWATER, TEX.	48
8022500	SABINE RIVER AT LOGANSPORT, LA.	64
8030500	SABINE RIVER NEAR RULIFF, TEX.	66
8032000	NECHES RIVER NEAR NECHES, TEX.	39
8032500	NECHES RIVER NEAR ALTO, TEX.	35
8033000	NECHES RIVER NEAR DIROLL, TEX.	45
8033500	NECHES RIVER NEAR ROCKLAND, TEX.	75
8034500	MUD CREEK NEAR JACKSONVILLE, TEX.	39
8037000	ANGELINA RIVER NEAR LUFKIN, TEX.	49
8041000	NECHES RIVER AT EVADALE, TEX.	61
8041500	VILLAGE CREEK NEAR KOUNTZE, TEX.	42
8044000	BIG SANDY CREEK NEAR BRIDGEPORT, TEX.	41
8047500	CLEAR FORK TRINITY R AT FORT WORTH TEX.	55
8048000	WEST FORK TRINITY R AT FORT WORTH TEX.	57
8057000	TRINITY RIVER AT DALLAS, TEX.	73
8061500	EAST FORK TRINITY RIVER NR ROCKWALL, TEX.	30
8063500	RICHLAND CREEK NEAR RICHLAND, TEX.	39
8064500	CHAMBERS CREEK NEAR CORSTICANA, TEX.	40
8065000	TRINITY RIVER NEAR OAKWOOD, TEX.	55
8066500	TRINITY RIVER AT ROMAYOR, TEX.	54
8068000	WEST FORK SAN JACINTO R NR CONROE, TEX.	45
8068500	SPRING CREEK NEAR SPRING, TEX.	38
8069000	CYPRESS CREEK NEAR WESTFIELD, TEX.	35
8070000	EAST FK SAN JACINTO RIVER NR CLEVELAND TEX.	37
8070500	CANEY CREEK NEAR SPLENDORA, TEX.	32
8074500	WHITEOAK BAYOU AT HOUSTON, TEX.	43
8075000	BRAYS BAYOU AT HOUSTON, TEX.	43
8080500	DOUBLE MT FORK BRAZOS R NR ASPERMONT, TEX.	49
8082500	BRAZOS RIVER AT SEYMOUR, TEX.	47
8084000	CLEAR FORK BRAZOS RIVER AT NUGENT, TEX.	54
8089000	BRAZOS RIVER NEAR PALO PINTO, TEX.	54
8091500	PALUXY RIVER AT GLEN ROSE, TEX.	31
8093500	AQUILLA CREEK NEAR AQUILLA, TEX.	38
8095000	NORTH BOSQUE RIVER NEAR CLIFTON, TEX.	47
8096500	BRAZOS RIVER AT WACO, TEX.	79

Table A.1 - continued

Sta. No.	Location	No. Record
R109500	LEON RIVER NEAR HASSE, TEX.	39
R1102500	LEON RIVER NEAR BELTON, TEX.	33
R1104000	LAMPASAS RIVER AT YOUNGSPORT, TEX.	48
R1105000	SAN GABRIEL RIVER AT GEORGETOWN, TEX.	41
R1106500	LITTLE RIVER AT CAMERON, TEX.	54
R1110000	YEGUA CREEK NEAR SOMERVILLE, TEX.	53
R1110500	NAVASOTA RIVER NEAR EASTERLY, TEX.	47
R1114000	BRAZOS RIVER AT RICHMOND, TEX.	59
R1126500	COLORADO RIVER AT BALLINGER, TEX.	63
R1127000	ELM CREEK AT BALLINGER, TEX.	43
R1128000	SOUTH CONCHO RIVER AT CHRISTOVAL, TEX.	44
R1128500	MIDDLE CONCHO RIVER NEAR TANKERSLY, TEX.	31
R1131000	SPRING CREEK NEAR TANKERSLY, TEX.	30
R1133500	NORTH CONCHO RIVER AT STERLING CITY, TEX.	36
R1134000	NORTH CONCHO RIVER NR CARLSBAD, TEX.	51
R1136000	CONCHO RIVER NEAR SAN ANGELO, TEX.	63
R1136500	CONCHO RIVER AT PAINTROCK, TEX.	64
R1138000	COLORADO RIVER AT WINCHELL, TEX.	50
R1144500	SAN SARA RIVER AT MENARD, TEX.	57
R1145000	BRADY CREEK AT BRADY, TEX.	40
R1146000	SAN SARA RIVER AT SAN SABA, TEX.	39
R1147000	COLORADO RIVER NEAR SAN SABA, TEX.	62
R1148500	NORTH LLANO RIVER NEAR JUNCTION, TEX.	61
R1150000	LLANO RIVER NEAR JUNCTION, TEX.	60
R1151500	LLANO RIVER AT LLANO, TEX.	36
R1153500	PERDERNALES RIVER NEAR JOHNSON CITY, TEX.	31
R1158000	COLORADO RIVER AT AUSTIN, TEX.	73
R1163500	LAVACA RIVER AT HALLETTSVILLE, TEX.	39
R1164000	LAVACA RIVER NEAR EDNA, TEX.	38
R1164500	NAVIDAD RIVER NEAR GANADO, TEX.	35
R1167000	GUADALUPE RIVER AT COMFORT, TEX.	51
R1168500	GUADALUPE R AB COMAL R AT NEW BRAUNFELS TEX.	43
R1171000	BLANCO RIVER AT WIMMERLEY, TEX.	51
R1172000	SAN MARCOS RIVER AT LULING, TEX.	38
R1173000	PLUM CREEK NEAR LULING, TEX.	41
R1176500	GUADALUPE RIVER AT VICTORIA, TEX.	44
R1179000	MEDINA RIVER NEAR PIPE CREEK, TEX.	35
R1185000	CIRILO CREEK AT SELMA, TEX.	30
R1186000	CIRILO CR NR FALLS CITY TEX.	43
R1188500	SAN ANTONIO RIVER AT GOLIAD, TEX.	46
R1189500	MISSION RIVER AT REFUGIO TEX.	38
R1190000	MUECES RIVER AT LAGUNA, TEX.	54
R1192000	MUECES RIVER BELOW UVALDE, TEX.	38
R1193000	MUECES RIVER NEAR ASHERTON, TEX.	38
R1194000	MUECES RIVER AT COTUILLA, TEX.	49
R1194500	MUECES RIVER NEAR TILDEN, TEX.	37
R1195000	FRIO RIVER AT CONCAN, TEX.	51
R1198000	SABINAL RIVER NEAR SABINAL, TEX.	33
R205500	FRIO RIVER NEAR DERRY, TEX.	59
R207000	FRIO RIVER AT CALLIHAM, TEX.	38
R208000	ATASCOSA RIVER AT WHITSETT, TEX.	42

The basin and meteorological characteristics used as independent variables are as follows:

1. A_d : contributing drainage area, in square miles;
2. S_{ℓ} : main channel slope (85 to 10 percent point), in feet per mile;
3. S_t : Percentage of area in lakes and ponds, increased by 1 percent;
4. L : total length of main channel, in miles;
5. I : 10-yr., 24-hr. rainfall intensity, in inches;
6. N_t : Mean annual number of thunderstorm days;
7. R_t : ratio of runoff to precipitation during months when annual peak discharge occur.

The above seven variables were adopted from Benson (1964) and the respective values of these variables for each gaging station are tabulated in Table A.2.

The application of regression analysis to the regional streamflow characteristics serves two purposes. One is to estimate the value of streamflow characteristics on a regional basis. The other is to determine the variance of corresponding regional estimates. The principles of linear regression analysis such as testing the validity of the model, analysis of residuals, detection of influence points, selection of "best" model, etc., discussed in Chapter 3 were used. The regional streamflow characteristics computed are \bar{Z}_r , S_{Z_r} , G_{Z_r} , which are the mean, standard deviation, and skewness, respectively, of the stream flow of original scale and \bar{Y}_r , S_{Y_r} , G_{Y_r}

Table A.2 Basin Characteristics for Each Streamflow Gaging Station in Southwestern United States Used for Regression Study

Sta. No.	A _d	S _p	S _t	L	I	N _T	R _T
801100	131.0	1.61	1.66	30.7	7.49	70	.860
801200	527.0	2.16	2.39	48.4	7.39	70	.960
801300	499.0	3.36	1.07	49.5	7.01	67	.810
801350	753.0	2.52	1.06	82.0	7.10	68	.730
801450	510.0	5.11	1.02	48.0	7.19	70	.680
801500	238.0	4.58	1.03	41.7	7.36	70	.680
801640	148.0	4.67	1.04	34.6	7.54	70	.910
801900	585.0	4.18	1.02	41.2	6.10	50	.770
801950	231.0	6.57	1.11	36.5	6.26	50	.640
802000	2791.0	2.20	1.21	127.0	6.14	50	.620
802250	4839.0	1.25	1.27	235.0	6.33	49	.650
803050	9329.0	.96	1.18	427.0	6.78	57	.690
803200	1145.0	2.29	1.21	88.6	6.30	47	.650
803250	1945.0	1.57	1.17	146.0	6.37	48	.620
803300	2724.0	1.25	1.16	214.0	6.50	50	.620
803350	3637.0	1.29	1.13	253.0	6.61	52	.630
803450	376.0	4.27	2.16	36.6	6.37	48	.560
803700	1600.0	1.80	1.33	114.0	6.62	50	.640
804100	7951.0	1.07	1.49	350.0	6.82	54	.670
804150	861.0	3.86	1.09	71.2	7.46	64	.560
804400	333.0	5.34	1.00	42.5	5.51	52	.500
804750	518.0	11.10	1.00	55.4	5.65	47	.400
804800	2615.0	3.58	1.85	140.0	5.61	50	.380
805700	6106.0	3.67	1.72	188.0	5.68	52	.430
806150	840.0	7.20	1.01	50.5	5.84	53	.540
806350	730.0	8.40	1.01	50.0	6.10	42	.650
806450	963.0	5.60	1.02	75.0	6.01	45	.580
806500	12833.0	2.56	1.40	339.0	5.92	49	.480

Table A.2 - continued

Sta. No.	A _d	S _g	S _L	L	I	N _L	R _L
806650	17186.0	1.67	1.31	530.0	6.19	50	.520
806800	809.0	3.53	1.06	52.0	7.10	56	.540
806850	409.0	5.97	1.00	41.1	7.25	57	.460
806900	285.0	3.47	1.08	48.2	7.33	58	.320
807000	325.0	4.74	1.00	42.5	7.28	60	.660
807050	105.0	8.14	1.00	28.8	7.53	61	.480
807450	92.0	5.56	1.00	22.5	7.65	57	.570
807500	88.4	3.18	1.00	19.8	7.70	56	.430
808050	1864.0	7.45	1.05	175.0	4.52	40	.130
808250	5250.0	5.24	1.03	281.0	4.64	43	.190
808400	2199.0	2.33	1.10	110.0	4.92	40	.170
808900	14245.0	3.76	1.07	451.0	4.92	43	.200
809150	410.0	11.50	1.00	47.7	5.60	41	.220
809350	306.0	9.88	1.00	32.3	5.92	41	.460
809500	972.0	9.76	1.01	84.3	5.70	39	.380
809650	20007.0	2.77	1.23	706.0	5.14	43	.380
809950	1261.0	6.70	1.02	86.0	5.46	39	.180
810250	3572.0	4.35	1.02	250.0	5.69	38	.280
810400	1244.0	8.82	1.00	89.0	5.79	38	.200
810500	399.0	16.00	1.00	48.0	5.48	39	.320
810650	7088.0	3.98	1.01	315.0	5.86	39	.300
811000	1008.0	4.63	1.11	59.3	6.37	47	.320
811050	940.0	4.95	1.12	65.5	6.30	45	.400
811400	35041.0	2.11	1.14	1010.0	5.69	43	.450
812650	5240.0	3.52	1.42	245.0	4.41	39	.160
812700	471.0	14.00	1.15	41.5	5.03	30	.230
812800	344.0	11.90	1.08	30.5	4.92	33	.170
812850	2509.0	7.78	1.16	109.0	4.62	34	.110
813100	734.0	13.90	1.24	58.0	4.78	34	.120
813350	539.0	10.90	1.12	40.3	4.54	37	.060
813400	1144.0	9.46	1.14	70.5	4.60	36	.160
813600	4094.0	7.86	1.21	127.0	4.74	35	.120

TABLE A-12 CONTINUED

Sta. No.	A _d	S _q	S _e	L	I	U	N _e	R _e
813650	5132.0	7.33	1.17	167.0	4.78		35	.120
813800	11700.0	3.65	1.25	337.0	4.70		37	.130
814450	1151.0	7.98	1.08	60.0	5.05		32	.080
814500	575.0	11.00	1.01	52.5	5.24		34	.210
814600	3042.0	8.66	1.03	144.0	5.24		33	.190
814700	17720.0	3.31	1.36	416.0	4.83		37	.180
814850	914.0	13.20	1.03	52.0	5.10		31	.180
815000	1874.0	10.00	1.02	66.6	5.12		30	.170
815150	4233.0	8.84	1.01	147.0	5.38		32	.190
815350	947.0	12.80	1.00	73.0	5.69		35	.180
815800	26500.0	3.47	1.33	587.0	5.01		36	.200
816350	108.0	9.14	1.00	24.0	6.74		50	.610
816400	826.0	3.29	1.00	80.7	6.71		49	.470
816450	1063.0	3.24	1.00	80.0	6.90		51	.420
816700	838.0	13.30	1.00	64.0	5.53		32	.120
816850	1518.0	8.68	1.00	170.0	5.69		36	.210
817100	355.0	17.20	1.00	54.0	5.88		38	.240
817200	830.0	11.40	1.00	110.0	6.04		40	.190
817300	309.0	9.49	1.00	37.2	6.24		43	.390
817650	5198.0	5.23	1.03	351.0	6.14		41	.320
817900	474.0	18.10	1.01	59.0	5.57		33	.190
818500	274.0	13.20	1.00	59.3	5.90		38	.130
818600	827.0	9.93	1.00	122.0	6.02		40	.210
818850	3921.0	5.86	1.07	258.0	6.05		39	.240
818950	690.0	5.36	1.00	73.1	6.55		42	.190
819000	764.0	14.80	1.00	61.0	5.22		29	.420
819200	1947.0	10.40	1.00	116.0	5.17		29	.140
819300	4062.0	8.32	1.06	188.0	5.20		29	.140
819400	5260.0	7.27	1.08	222.0	5.34		30	.150
819450	8192.0	6.01	1.09	282.0	5.55		32	.150
819500	405.0	20.00	1.00	43.5	5.35		30	.610
819800	206.0	22.50	1.00	32.8	5.46		31	.120
820550	3493.0	11.50	1.02	129.0	5.50		32	.170
820700	5091.0	7.80	1.03	203.0	5.69		39	.170
820800	1171.0	5.29	1.01	86.0	6.05		39	.210

representing the mean, standard deviation, and skewness of log-transformed streamflows, respectively. The corresponding value of the above six streamflow characteristics for the gaging stations are listed in Table A.3. The computer package OMNITAB developed by Hogben, et al. (1971) was used because of its flexibility for computing statistics such as the studentized residual, moment arm, Cook's distance, etc., which other packages do not provide. The following subsections provide a brief description of the regression analysis performed to determine the mean and variance of the statistical parameters.

A.2 REGRESSION EQUATION FOR MEAN OF STREAMFLOWS

Regression equations for the mean and the variance of the mean of the streamflows (\bar{Z}_r) as a function of the independent variables were developed. The first attempt was made relating \bar{Z}_r with the seven hydrological variables (A_d , S_ℓ , S_t , L , I , N_t , and R_t) in linear form as

$$\begin{aligned} \bar{Z}_r = & \beta_0 + \beta_1 A_d + \beta_2 S_\ell + \beta_3 S_t + \beta_4 L + \\ & \beta_5 I + \beta_6 N_t + \beta_7 R_t + \epsilon_1 \end{aligned} \quad (\text{A.1})$$

where the β 's are the regression parameters to be determined and ϵ_1 is the random error.

The estimators of the β 's, $\hat{\beta}$, and their associated t-statistics, $r^2(\bar{r}^2)$, and $\hat{\sigma}$ are listed in Table A.4. The normality assumption can be justified since the probability plot shown in Fig. A.1 is approximately linear. The plot of the standardized residual, i.e., $e_{1,i}/\hat{\sigma}$, vs. the predicted dependent vari-

Table A.3 Streamflow Characteristics for Each Gaging Station in Southwestern United States Used for Regression

Sta. No.	\bar{Z}_r	S_{Z_r}	G_{Z_r}	\bar{Y}_r	S_{Y_r}	G_{Y_r}
801100	4932.8	2675.2	.9188	2.3496	.5973	-.7655
801200	8723.3	5542.8	2.9528	8.9149	.5154	1.1688
801300	16267.9	12548.5	1.7295	9.4118	.9121	-.4424
801350	17158.1	12455.5	2.4583	9.5352	.6778	-.2389
801450	15619.2	23451.8	4.9255	9.2193	.8753	.3751
801500	8619.6	3363.1	1.8644	8.6176	.9883	.2157
801600	4624.9	3175.3	1.5759	8.2395	.6382	.1873
801900	16753.8	14801.3	2.1453	9.3857	.8771	-.3332
801950	3514.2	4145.7	3.6075	7.7362	.9468	-.1714
802000	26934.1	26263.7	2.4347	9.7778	.9513	.2647
802250	21885.2	16226.7	1.8997	9.7489	.7186	.0556
803050	41772.7	22865.0	1.3860	10.5116	.5052	.2046
803200	9239.3	8996.1	2.1003	8.7014	.9873	-.2437
803250	11573.1	11826.3	1.7732	8.8925	.9986	.2757
803300	18299.3	24978.5	2.6793	9.3027	1.0637	-.1608
803350	17047.7	12615.9	1.1601	9.4526	.8104	-.3792
803450	5838.5	5840.9	2.3296	3.2732	.9433	-.2918
803700	14232.9	8395.1	1.4996	8.9026	.8694	-.3702
804100	34046.6	25515.7	1.5590	10.1934	.6965	.1556
804150	12990.2	14680.1	2.3649	9.2274	.9188	.4775
804400	6681.4	9731.4	3.3134	3.1291	1.2075	-.1108
804750	10444.2	16928.7	4.5088	5.7840	.9297	.5129
804800	11471.1	13725.4	3.9252	8.9853	.8093	.3258
805700	30736.0	28709.2	2.6778	9.9985	.8285	.1599
806150	24523.4	16565.9	.8941	9.8322	.8234	-.5747
806350	19896.5	16253.1	.9018	9.4240	1.2377	-1.7126
806450	18303.3	13260.7	.8869	9.4857	.9241	-.7708
806500	46603.5	37251.2	1.6142	10.4461	.8190	-.2406
806650	44014.4	23616.1	.9636	10.5281	.6404	-1.4057
806800	21262.4	25811.3	2.1741	9.3494	1.1802	-.1931
806850	9098.3	11022.7	2.2528	8.4546	1.2646	-.2756
806900	5846.5	5581.2	2.2647	8.2984	.9248	-.4149
807000	11561.6	14688.4	2.0618	8.6546	1.2469	.4582
807050	4675.1	6419.8	3.7195	7.9453	.9579	.5696
807450	5273.5	3899.0	1.2044	8.2652	.8624	-.6053
807500	7379.9	5874.2	1.9267	8.6187	.8077	-.4089
808050	22905.9	18580.8	1.8390	9.7222	.8739	-.7342
808250	31463.6	22313.7	1.1206	10.1068	.7389	-.1799
808400	5679.9	7087.1	4.1514	8.2278	.8841	.2797
808900	28021.1	20452.9	1.1733	9.9376	.8599	-.6173
809150	19462.9	18134.0	1.0321	9.4376	.9694	.2074
809350	13758.4	13195.9	3.0440	9.2423	.7330	.4076
809500	22324.4	15333.9	2.8892	9.7813	.7362	-.5761
809650	56537.0	44494.9	1.8911	10.6828	.7266	.2664
809950	8155.5	10395.2	1.5588	8.0965	1.4620	.8643

Table A.3 - continued

Sta. No.	\bar{z}_r	S_{z_r}	G_{z_r}	\bar{v}_r	S_{v_r}	G_{v_r}
810250	21617.6	14300.8	1.1572	9.7671	.9911	-.3349
810400	21903.3	19256.4	2.0264	9.6497	.9140	-.8696
810500	22993.0	33537.1	3.4069	9.4336	1.1313	-.1947
810650	47970.2	88826.9	6.1113	10.1952	.9923	.5543
811000	9143.2	11240.7	2.3284	8.3341	1.5414	-1.1181
811050	18699.3	18791.1	1.7209	9.2441	1.2726	-.7494
811400	58646.2	28240.1	.1686	10.8311	.5957	-.3181
812650	18823.2	12876.5	1.2183	9.6261	.6923	-.3861
812700	9786.6	10890.6	2.2056	8.7298	.9584	.2975
812800	14943.5	28569.2	2.4968	7.7729	2.4036	-.4599
812850	11285.9	8438.1	.5912	8.8869	1.2494	-1.9952
813100	12925.2	15416.2	3.3420	8.8029	1.4461	-1.2341
813350	3817.3	4519.8	1.7325	7.4373	1.5522	-.8476
813400	15743.7	21671.2	1.9158	8.5311	2.1150	-1.7037
813600	28897.1	46345.2	3.2844	9.1770	1.7304	-.4420
813650	29863.7	50321.2	3.6463	9.4271	1.4198	-.3945
813800	27970.2	17288.3	.9329	10.0318	.6929	-.5577
814450	16212.0	25036.9	2.6902	8.5501	1.7326	-.2782
814500	9894.8	16543.9	3.3180	7.9409	1.7724	-.6107
814600	22476.5	35796.6	3.7250	9.2820	1.2007	.2814
814700	41624.0	42665.3	2.7010	10.3213	.7392	.7316
814850	22120.2	27399.9	1.3122	8.9182	1.7878	-.5044
815000	32971.5	53062.0	3.2380	9.2635	1.7020	-.2243
815150	48980.8	74115.0	3.1837	10.0290	1.3030	-.1091
815350	42027.2	81687.0	4.2266	9.7571	1.4017	-.6830
815800	55478.4	89290.2	4.1012	10.2171	1.1984	.0614
816350	12767.2	15620.0	3.8057	9.0094	.9356	.2011
816400	17445.2	18717.8	2.3735	9.3488	.9519	-.3526
816450	20821.3	22693.6	2.1826	9.4946	.9910	-.3206
816700	33240.6	47403.8	1.9633	9.5244	1.3669	.2657
816850	16495.7	23739.8	2.4331	8.9062	1.3374	-.1018
817100	16746.1	24666.4	2.6821	8.7993	1.6036	-.8160
817200	16721.1	14516.2	1.0428	9.3009	1.2047	-.3139
817300	11891.1	14413.6	2.8338	8.8341	1.2674	.1583
817650	30020.5	30912.2	2.8303	9.8910	.9533	-.1328
817900	16612.4	17409.2	1.7998	9.1823	1.1488	-.5051
818500	11111.0	17834.3	1.9132	7.3132	2.6584	-.4242
818600	11290.6	9373.5	1.2962	8.9726	.9381	-.6731
818850	14390.7	20679.2	4.9811	9.1179	.9138	.2802
818950	12443.1	17490.3	2.3418	8.5506	1.5133	-.6620
819000	42395.3	68271.8	2.2184	9.2031	2.0663	-.4590
819200	50141.6	108326.3	4.2031	8.8826	2.5601	-.5810
819300	7994.8	7180.5	1.3954	8.5592	1.0918	-1.4451
819400	11688.1	14777.2	3.1130	8.8487	1.0286	-.8900
819450	17474.9	19236.4	1.5922	9.0577	1.4153	-.8388
819500	19731.3	33755.7	2.6833	8.5357	1.8639	-.1337
819800	8727.9	11720.7	2.5467	8.1949	1.5537	-.4986
820550	12618.5	30845.5	5.3430	8.5404	1.2780	.1708
820700	11846.1	13399.0	3.8409	9.0316	.7978	.4524
820800	13616.1	24556.6	3.5112	8.6854	1.2131	.6006

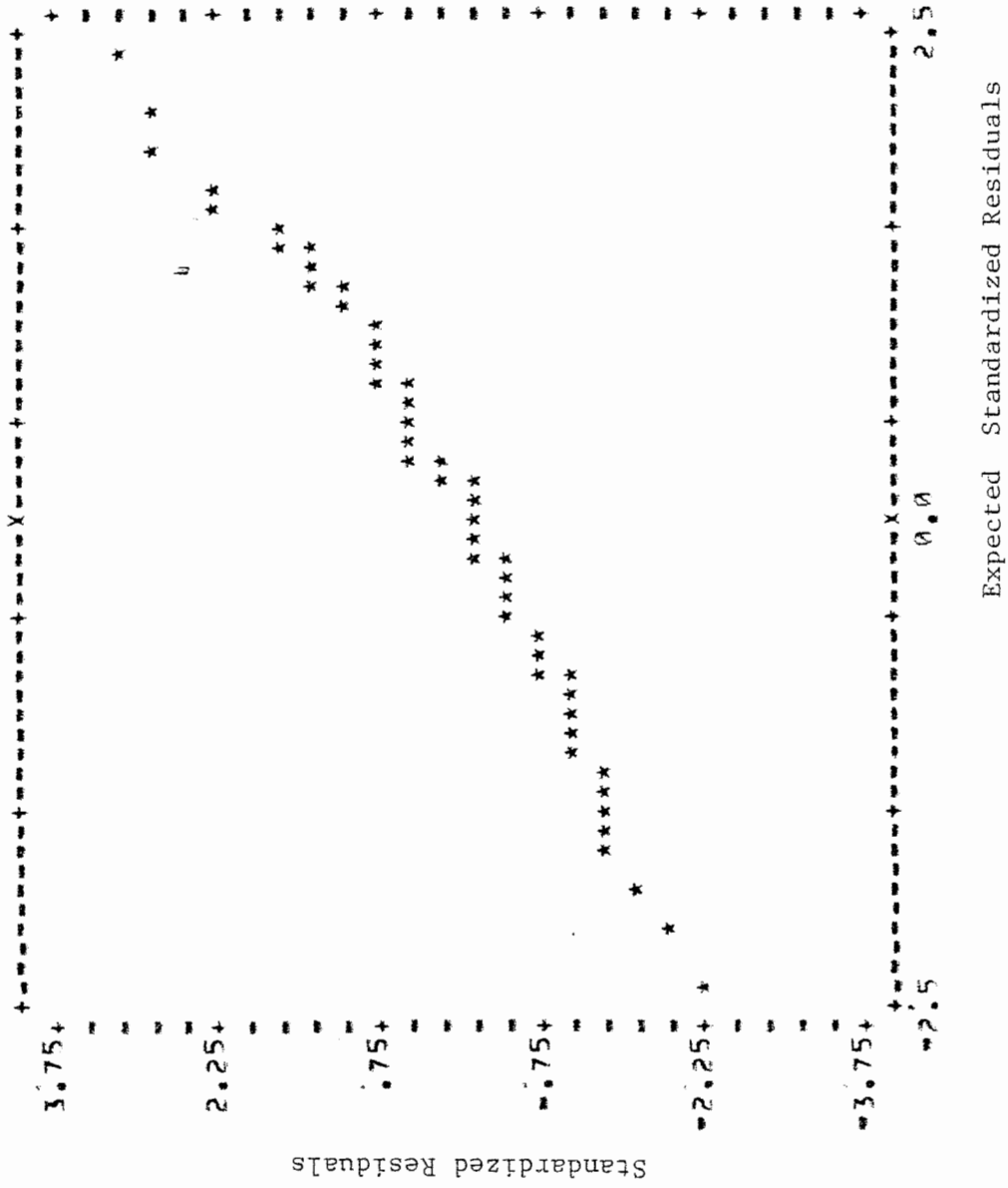


Figure A.1 Probability Plot of Standardized Residuals

Table A.4 Regression Results for Mean of Streamflows, \bar{Z}_T .

	$\hat{\beta}_0$	$\hat{\beta}_1$	$\hat{\beta}_2$	$\hat{\beta}_3$	$\hat{\beta}_4$	$\hat{\beta}_5$	$\hat{\beta}_6$	$\hat{\beta}_7$	R^2 (\bar{R}^2)	$\hat{\sigma}$
Run 1 Eq. (A.1)	33280.51 (2.50)	0.98 (1.72)	193.29 (0.60)	-4669.66 (-1.01)	24.43 (1.16)	-1215.14 (-0.56)	-341.13 (-1.66)	16216.19 (2.11)	0.5654 (0.5330)	8983.44
Run 2 Eq. (A.2)	7.224 (3.34)	0.552 (3.90)	0.373 (2.80)	-0.573 (-1.75)	-0.144 (-0.71)	0.119 (0.19)	-0.286 (-0.68)	0.413 (3.70)	0.6101 (0.5811)	0.5015
Run 3 Eq. (A.5)	5.382 (2.42)	0.670 (4.62)	0.070 (3.70)	-0.734 (-2.42)	-0.289 (-1.45)	0.146 (0.24)	0.157 (0.35)	0.362 (3.05)	0.6328 (0.6055)	0.4115
Run 4 Eq. (A.5)	6.442 (21.54)	0.634 (5.18)	0.064 (4.74)	-0.740 (-2.51)	-0.259 (-1.39)			0.399 (4.56)	0.6318 (0.6122)	0.4074

able, \bar{Z}_r showed an uneven distribution in the data (Fig. A.2) where $e_{1,i}$ is the estimate of the residual, ϵ_1 for the i -th data. The right most point has the largest Cook's distance which is several times larger in magnitude than the rest of the points. This indicates that this data point has a significant influence on the regression result.

The scatter plots, shown in Fig. A.3 are typical for the residual (e_1) vs. A_d , S_t , and L . Fig. A.4, which is a plot of residual (e_1) vs. main channel slope (S_ρ), shows that the scatter is more or less uniformly distributed over the range of data as desired. Other scatter plots for the residual (e_1) vs. I , N_t , and R_t , showed that the variance of residuals decreases as the value of the independent variable increases. The scatter plot for e_1 vs. N_t shown in Fig. A.5 is typical for this case. This dependence of scatter on the level of variables indicates that the assumption of constant variance is not satisfied.

A second attempt modified Eq. (A.1) to the multiplicative form as

$$\bar{Z}_r = e^{\beta_0} A_d^{\beta_1} S_\rho^{\beta_2} S_t^{\beta_3} L^{\beta_4} I^{\beta_5} N_t^{\beta_6} R_t^{\beta_7} e^{\epsilon_2} \quad (\text{A.2})$$

The logarithmic transformation of the above equation is linear so an OLS analysis was applied. The regression parameters estimated are shown in Table A.4. The square of the correlation coefficient r^2 and the adjusted correlation coefficient \bar{r}^2 , are higher than those for the previous model, (Eq. A.1). The standard error of estimates, $\hat{\sigma}$, for models, Eqs. (A.1) and (A.2) are not comparable because of the different model form. The probability plot of standardized residuals in Fig. A.6, indicates that the normality assumption

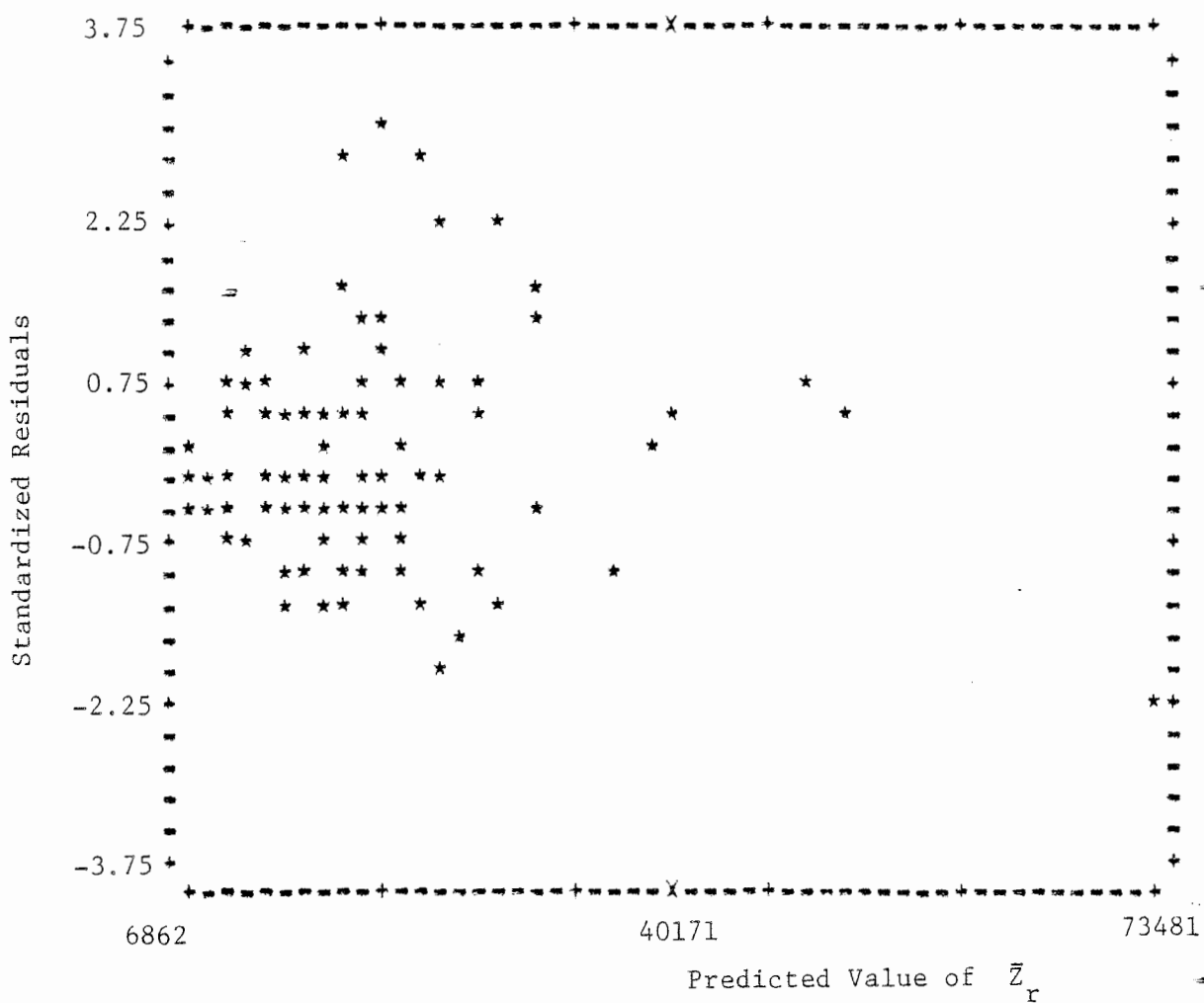


Figure A.2 Standardized Residuals vs. Predicted \bar{Z}_r

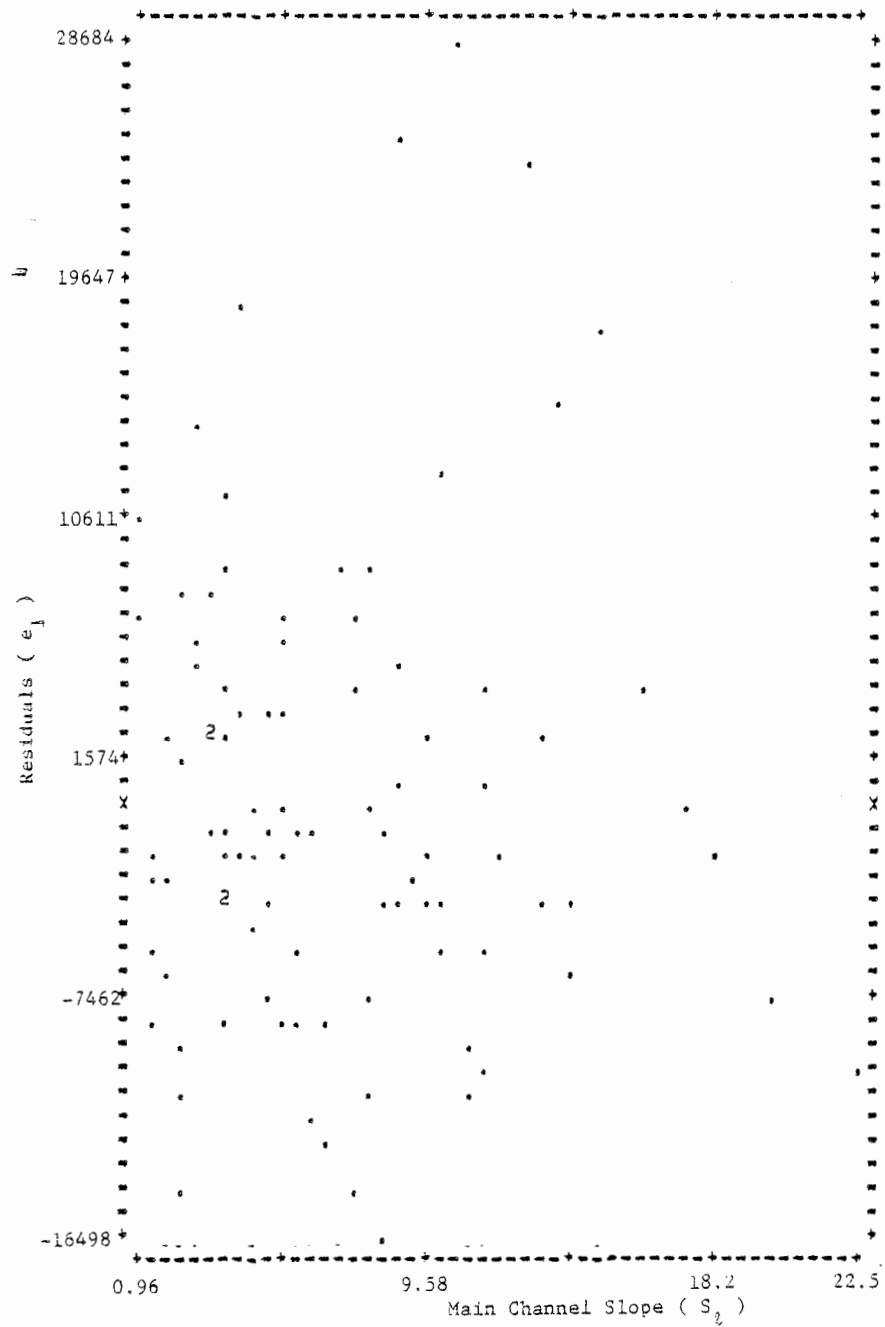


Figure A.4 Residuals (e_1) vs. Main Channel Slope (S_2)

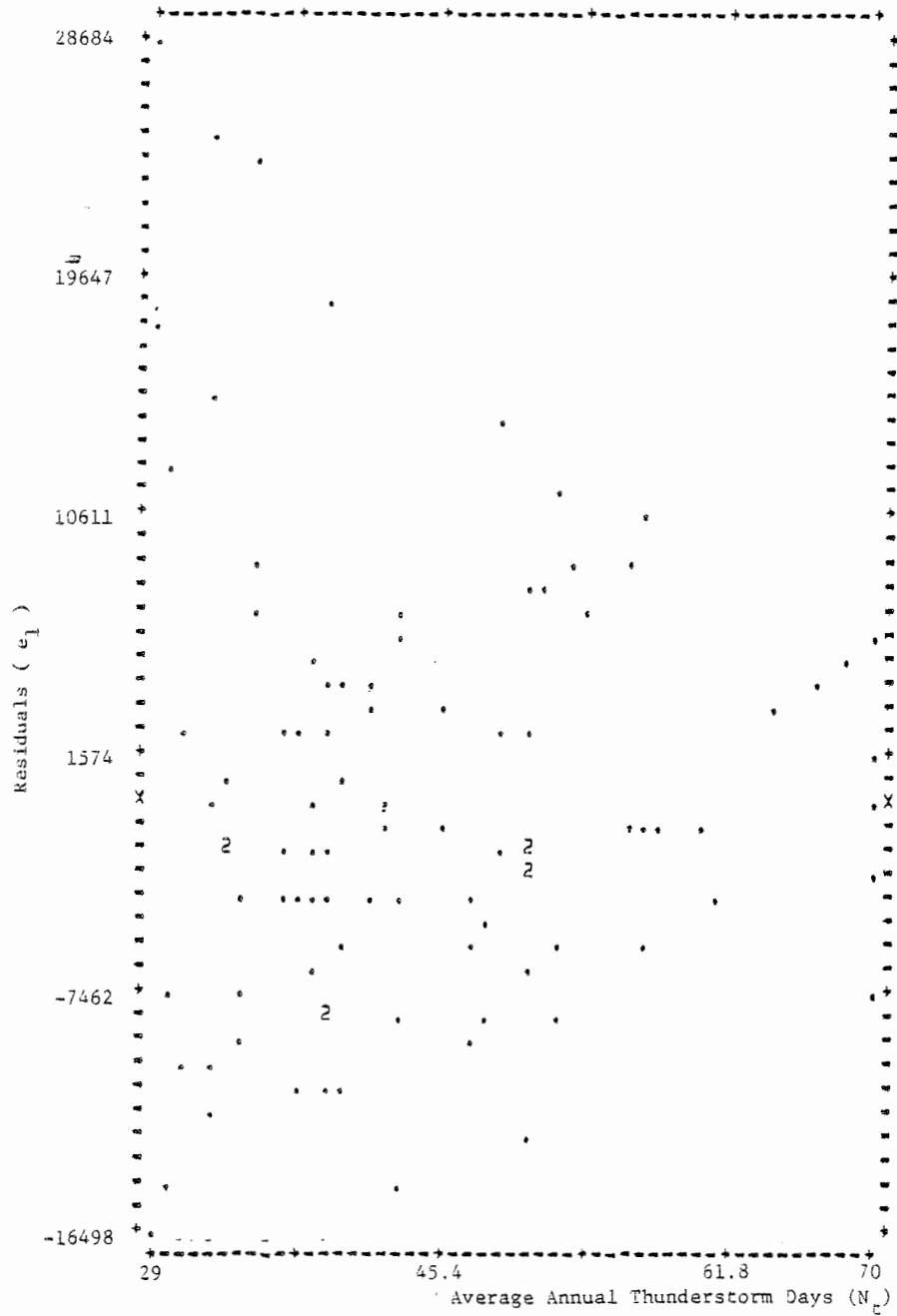


Figure A.5 Residuals (e_1) vs. Average Annual Thunderstorm Days (N_c)

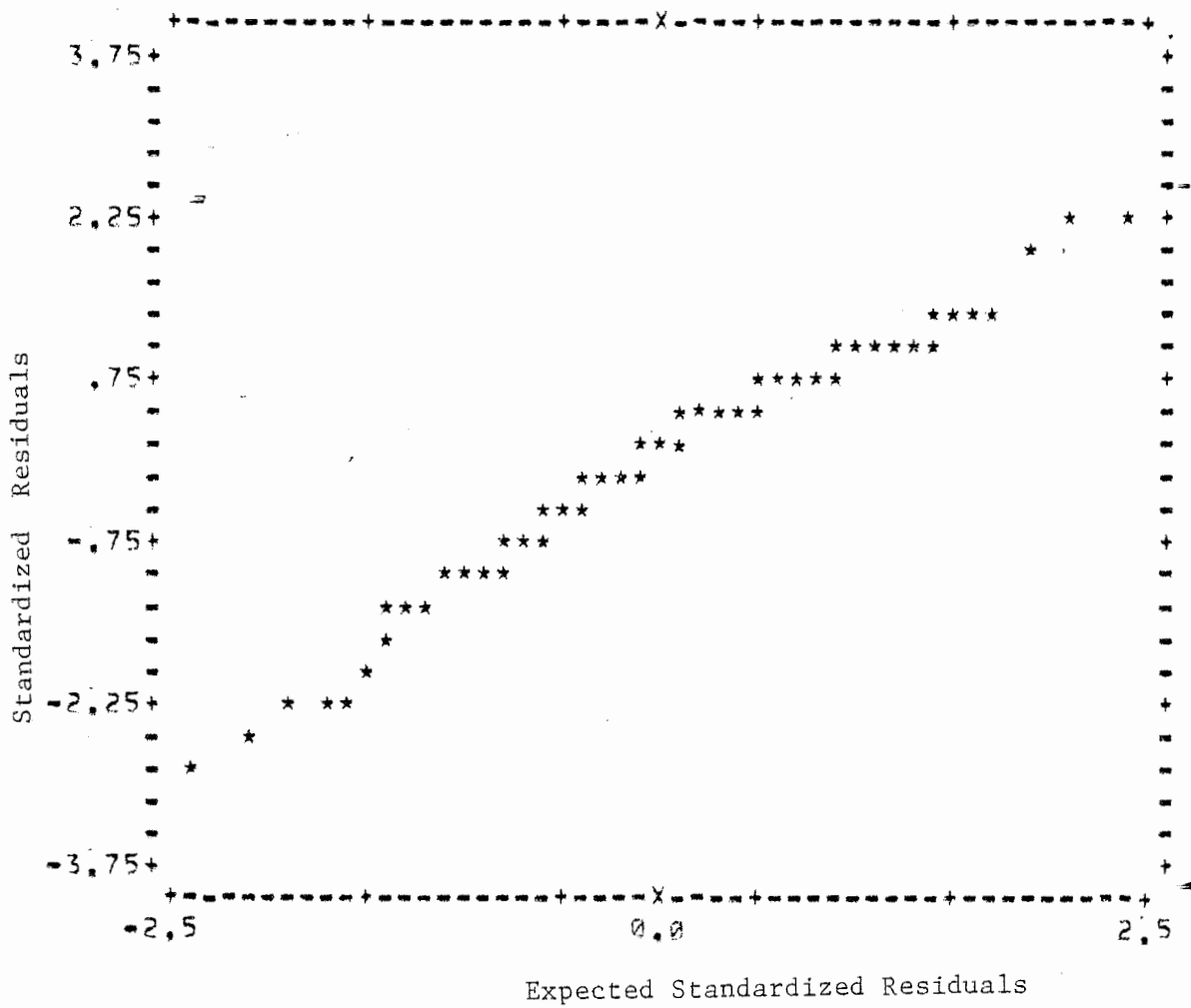


Figure A.6 Probability Plot of Standardized Residuals

for dispersion of ε_2 or $\ln(\bar{Z}_r)$ for given independent variables is satisfied. Hence, the distribution function of \bar{Z}_r is log-normal. The mean and the variance of \bar{Z}_r for a given independent variable \underline{x}^* can be calculated using the following equations:

$$E(\bar{Z}_r | \underline{x}^*) = \exp.(M' + \hat{\sigma}^2/2) \quad (\text{A.3})$$

$$\text{Var}(\bar{Z}_r | \underline{x}^*) = E^2(\bar{Z}_r | \underline{x}^*) \cdot (e^{\hat{\sigma}^2} - 1) \quad (\text{A.4})$$

where $E(\bar{Z}_r | \underline{x}^*)$ is the mean of \bar{Z}_r for an independent variable given \underline{x}^* , M' is the mean of $\ln(\bar{Z}_r)$ for a given \underline{x}^* , $\hat{\sigma}^2$ is the variance of $\ln(\bar{Z}_r)$ provided by the regression equation and $\text{Var}(\bar{Z}_r | \underline{x}^*)$ is the variance of \bar{Z}_r . For the second model (Eq. A.2), the variance of \bar{Z}_r for the \underline{X} is no longer constant. The scatter plot of standardized residual, vs. the predicted value of $\widehat{\ln(\bar{Z}_r)}$, has an approximate uniform spread as shown in Fig. A.7. This indicates that the assumption of constant variance of $\ln(\bar{Z}_r)$ is satisfied. The scatter plot of e_2 vs. $\ln(A_d)$ shown in Fig. A.8 is acceptable. Scatter plots for $\ln(L)$, $\ln(I)$, $\ln(N_t)$, and $\ln(R_t)$ are similar to Fig. A.8. However, the scatter plot for $\ln(S_\ell)$, Fig. A.9, clearly shows the existence of a wedged shape of spreading, indicating that the variance of $\ln(\bar{Z}_r)$ with respect to $\ln(S_\ell)$ is not constant. Since it has been shown in Fig. A.4 that the residual plot of e_1 vs. S_ℓ presents a fairly uniform spreading, the model was then modified to

$$\begin{aligned} \ln(\bar{Z}_r) = & \beta_0 + \beta_1 \ln(A_d) + \beta_2 S_\ell + \beta_3 \ln(S_t) + \beta_4 \ln(L) \\ & + \beta_5 \ln(I) + \beta_6 \ln(N_t) + \beta_7 \ln(R_t) + \varepsilon_3 \end{aligned} \quad (\text{A.5})$$

The result of the OLS analysis for this third attempt is shown in Table A.4.

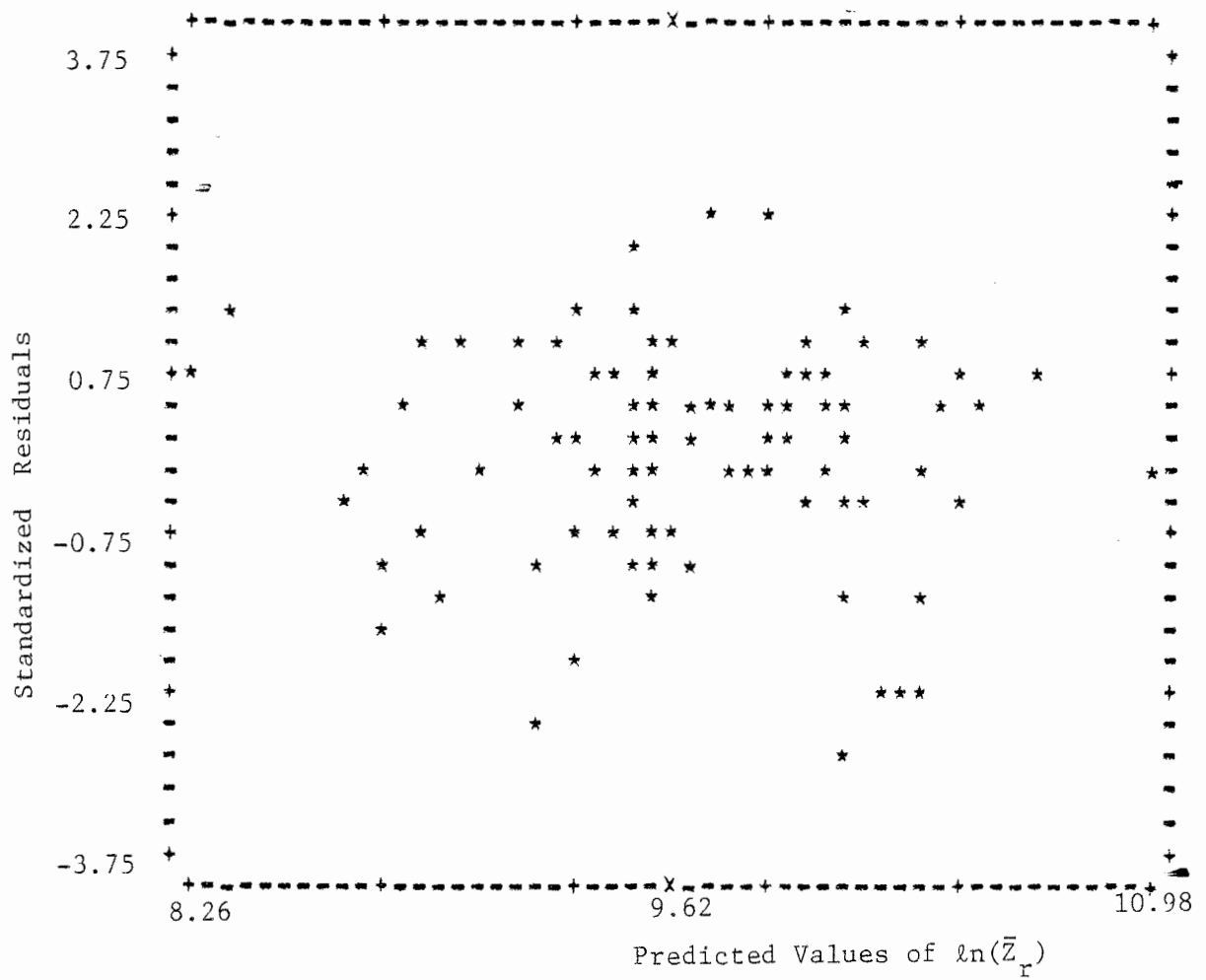


Figure A.7 Standardized Residuals vs. Predicted $\ln(\bar{Z}_r)$

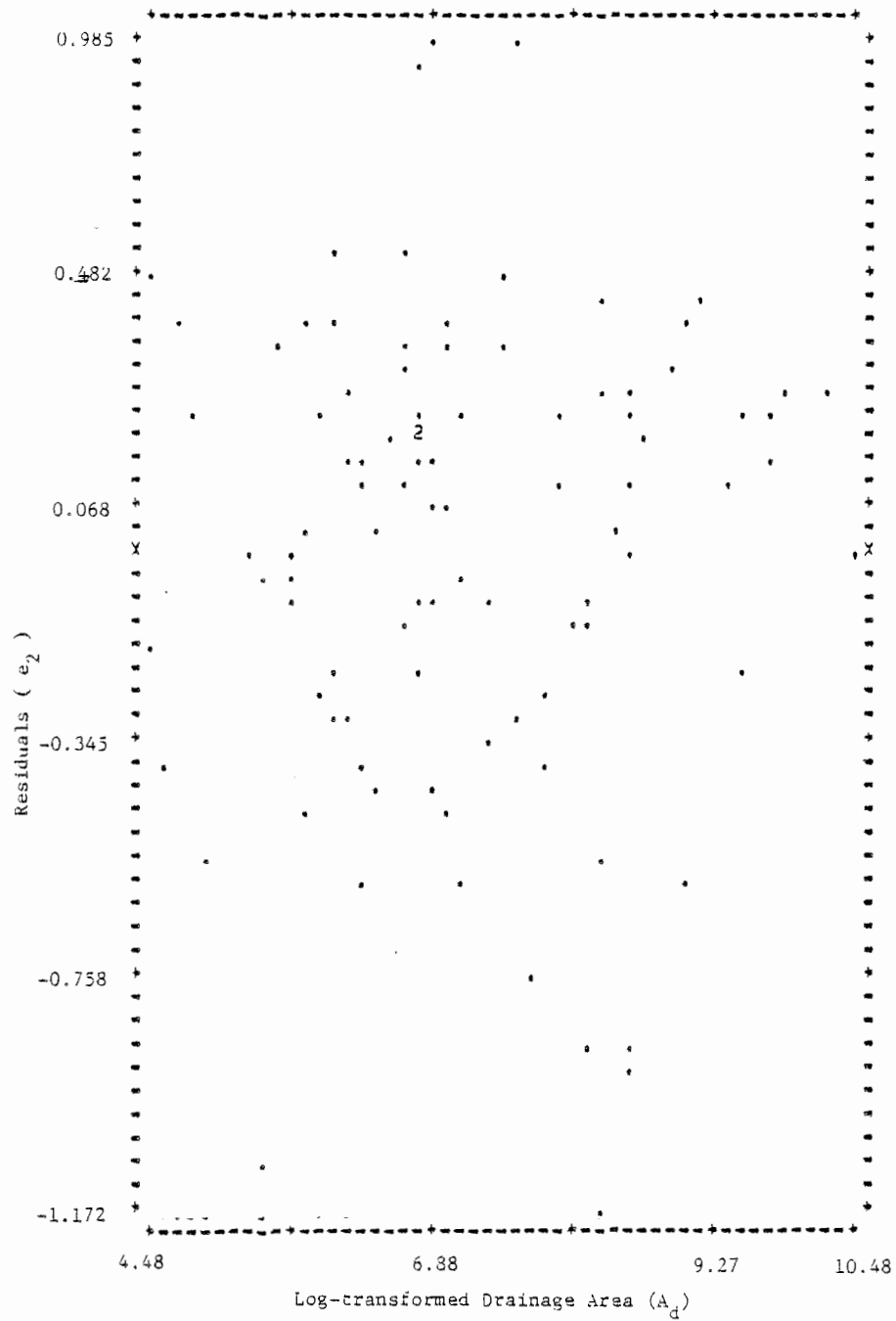


Figure A.8 Residuals (e_2) vs. Log-transformed Drainage Area, $\ln(A_d)$

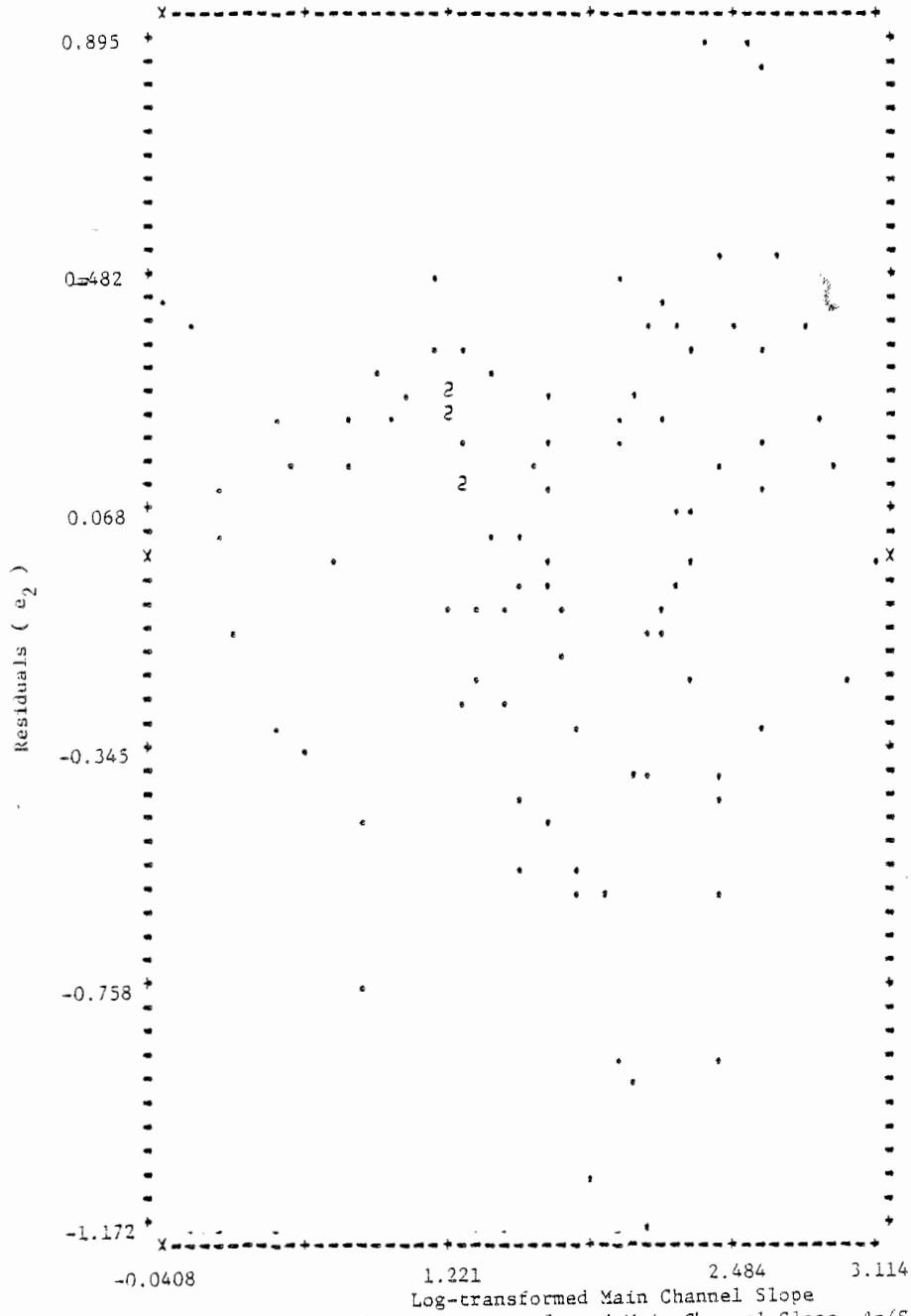


Figure A.9 Residuals (e_2) vs. Log-transformed Main Channel Slope, $\ln(S_2)$

As can be seen the values of r^2 , \bar{r}^2 , and $\hat{\sigma}$ have been improved. This evidence shows that the model of Eq. (A.5) is "superior" to Eq. (A.2). Based on the principle of parsimony the independent variables having little contribution were then deleted from the model.

In a fourth attempt the independent variables I and N_t were deleted, because their t -statistics indicate that they are not statistically significant. The deletion of I and N_t results in decreasing a value of r^2 and an increasing value of \bar{r}^2 . All the residual plots, except e_3 vs. $\ln(S_t)$, present desirable features. The scatter plot of e_3 vs. $\ln(S_t)$, shown in Fig. A.10, indicates that the variance decreases as $\ln(S_t)$ increases. This situation can partly be explained as follows. The uneven positioned data with most of the points clustering on the left side indicates that a large proportion of the river basins have little surface storage, which is typical in semi-arid regions. For the run associated with regression model, Eq. (A.5) there is very little variation in the Cook's distance for all the data points for the 95 gaging stations, implying there exists no point that has large influence on the parameter estimation. Mallows C_p value corresponding to each model is plotted in Fig. A.11. The regression model for the fourth attempt relates the mean of streamflows (\bar{Z}_r) and the hydrologic variables are given as:

$$\begin{aligned} \ln(\bar{Z}_r) = & 6.442 + 0.634 \ln(A_d) + 0.064 S_\ell - 0.730 \ln(S_t) \\ & - 0.259 \ln(L) + 0.400 \ln(R_t) \end{aligned} \quad (\text{A.6})$$

The mean and variance of \bar{Z}_r can be computed using Eqs. (A.3) and (A.4). The procedure used was first to determine the "correct" form of the model by

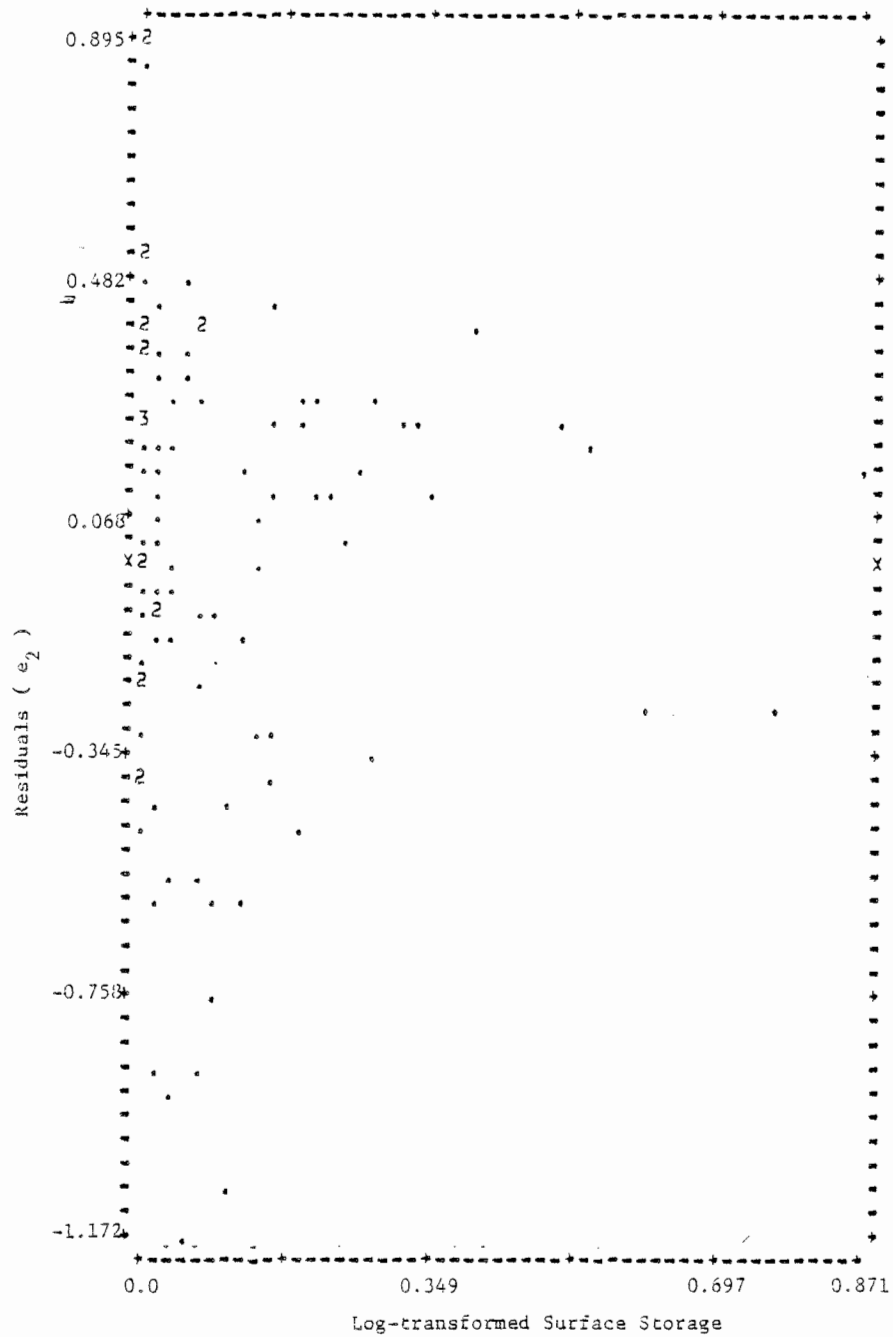


Figure A.10 Residuals (e_2) vs. Log-transformed Surface Storage, $\ln(S_c)$

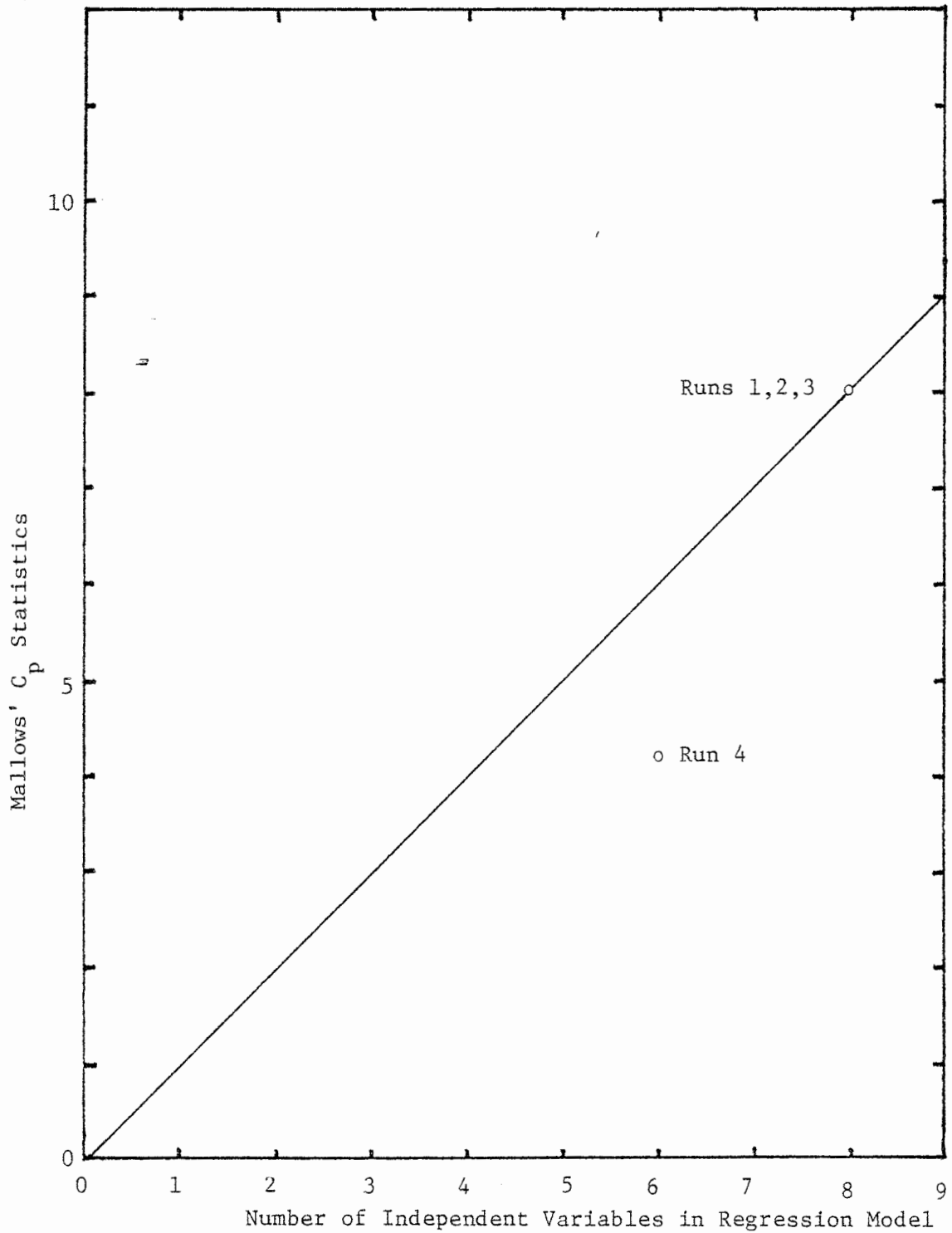


Figure A.11 Mallows' C_p Statistic vs. Number of Independent Variables in Regression Model

examining the validity of assumptions, then choose the "best" subset of independent variables in the model.

A.3 REGRESSION EQUATION FOR STANDARD DEVIATION OF STREAMFLOWS

Regression equations for the mean and variance of the standard deviation of streamflows (S_{Z_r}) as a function of the hydrologic variables are now considered. The first model considered to relate S_{Z_r} to the seven hydrological variables had the same form as Eq. (A.1). The OLS estimators, the t-statistics, r^2 , \bar{r}^2 and $\hat{\sigma}$, are listed in Table A.5. The normality plot and scatter plot of residual vs. predicted dependent variable, S_{Z_r} , illustrated that the assumptions of normality and constant variance are violated. Other scatter plots of e_1 vs. the independent variables showed that the data are either unevenly positioned or had a wedged-shaped dispersion. Based on these scatter plots for the dependent and independent variables, a transformation of variables to the form of Eq. (A.2) was considered. The results of the OLS analysis for this model are listed in Table A.5 on run 2. Obviously, this model of multiplicative form showed significant improvement over the first additive model because the value of r^2 for the second is 0.5573 as compared to 0.288 for the first model. Furthermore, the probability plot of this regression model showed that the normality assumption holds. Scatter plots of the residual e_2 vs. the independent variables (except for S_{Z_r}) showed the desired feature of the data behavior, i.e., the residual is uniformly spread over the range of the independent variables. The scatter plot of the residual vs.

Table A.5 Regression Results for Standard Deviation of Streamflows, S_z

	F_0	$\hat{\beta}_1$	$\hat{\beta}_2$	$\hat{\beta}_3$	$\hat{\beta}_4$	$\hat{\beta}_5$	$\hat{\beta}_6$	$\hat{\beta}_7$	R^2 (R^2)	F
Run 1 Eq. (A.1)	54749.45 (2.14)	2.337 (2.14)	2.882 (0)	-5279.40 (-0.60)	-46.86 (-1.16)	2586.03 (0.62)	-1070.72 (-2.72)	13956.31 (0.92)	0.288 (0.235)	1737.91
Run 2 Eq. (A.2)	7.900 (3.05)	0.7476 (4.40)	0.4950 (3.10)	-0.6734 (-1.72)	-0.4897 (-2.00)	1.038 (1.38)	-0.9227 (-1.83)	0.3622 (2.47)	0.5573 (0.524)	0.3081
Run 3 Eq. (A.5)	6.5210 (2.41)	0.8685 (4.91)	0.0808 (3.51)	-0.9079 (-2.45)	-0.6650 (-2.75)	1.0232 (1.37)	-0.5108 (-0.93)	0.2469 (1.72)	0.5691 (0.5370)	0.5012
Run 4 Eq. (A.7)	4.5529 (2.68)	0.9217 (5.51)	0.0938 (5.12)	-0.9751 (-2.69)	-0.7020 (-2.94)	0.8473 (1.17)		0.1973 (1.48)	0.5648 (0.5370)	0.5008
Run 5	4.598x10 ⁻⁴ (2.97)	-7.387x10 ⁻⁵ (-4.94)	-6.804x10 ⁻⁶ (-3.62)	1.070x10 ⁻⁴ (3.34)	5.585x10 ⁻⁵ (2.70)	-6.497x10 ⁻⁵ (-0.99)	5.39x10 ⁻⁷ (0.55)	-2.242x10 ⁻⁵ (-1.84)	0.5640 (0.532)	4.22x10 ⁻⁵
Run 6	3.678x10 ⁻⁴ (3.23)	-1.80x10 ⁻⁵ (-5.14)	-5.532x10 ⁻⁶ (-3.90)	8.095x10 ⁻⁵ (3.35)	4.316x10 ⁻⁵ (2.77)	-5.111x10 ⁻⁵ (-1.03)	3.776x10 ⁻⁷ (0.51)	-1.787x10 ⁻⁵ (-1.94)	0.584 (0.553)	3.25x10 ⁻⁵
Run 7	3.013x10 ⁻⁴ (3.73)	-4.496x10 ⁻⁵ (-5.65)	-4.57x10 ⁻⁶ (-5.26)	6.031x10 ⁻⁵ (3.50)	3.215x10 ⁻⁵ (2.90)	-3.414x10 ⁻⁵ (-0.99)		-1.236x10 ⁻⁵ (-1.95)	0.5964 (0.5702)	2.56x10 ⁻⁵
Run 8	2.231x10 ⁻⁴ (12.77)	-4.15x10 ⁻⁵ (-5.81)	-4.21x10 ⁻⁶ (-5.35)	6.32x10 ⁻⁵ (3.72)	9.98x10 ⁻⁵ (2.74)			-1.61x10 ⁻⁵ (-3.16)	0.5960 (0.5745)	2.37x10 ⁻⁵
Run 9 Eq. (A.8)	2.157x10 ⁻⁴ (17.74)	-4.165x10 ⁻⁵ (-6.08)	-3.90x10 ⁻⁶ (-5.12)	5.99x10 ⁻⁵ (3.67)	3.23x10 ⁻⁵ (3.09)			-1.14x10 ⁻⁵ (-2.21)	0.6065 (0.5855)	2.25x10 ⁻⁵

$\widehat{\ln(S_{Z_r})}$ showed a wedge-shaped plot that indicated that the variance of the dependent variable depends on the value of $\ln(S_{Z_r})$. The plot of residual vs. $\ln(S_{Z_r})$ gave the same indication. Thus, the assumption of constant variance is violated. Modifying the model to the form of Eq. (A.5) corrects the wedge shape. The results of the OLS analysis for runs 3 and 4 are listed in Table A.5.

Each of the first four runs showed improvement; however, there still existed the dependence of variance on the value of $\ln(S_{Z_r})$ for the third model. This suggests that the log-transformation of S_{Z_r} is not adequate because the shape of dispersion shows some outward curvature in the wedge expansion. The Box-Cox transformation (Box and Cox, 1964) is then applied to stabilize the variance of the dependent variable S_{Z_r} . The transformed model is given as:

$$\frac{1}{S_{Z_r}} = \beta_0 + \beta_1 \ln(A_d) + \beta_2 S_{Z_r} + \beta_3 \ln(S_t) + \beta_4 \ln(L) + \beta_5 \ln(I) + \beta_6 \ln(N_t) + \beta_7 \ln(R_t) + \varepsilon_4 \quad (\text{A.7})$$

Results of the OLS analysis for this model (run 5) are listed in Table A.5. The plot of residual e_4 vs. $(1/S_{Z_r})$ showed an improvement, but was not satisfactory. Further modification of $1/S_{Z_r}$ to $1/(S_{Z_r} + 2500)$ caused the expansion of spreading on the left and suppression of spreading on the right of the scatter plot of the residual (e_4) vs. the dependent variable $1/(S_{Z_r} + 2500)$. Runs 6, 7, and 8 used a model of the form of Eq. (A.7) except that $1/S_{Z_r}$ was replaced by $1/(S_{Z_r} + 2500)$. The model showed its "superiority" to other

models previously proposed by having a larger value of r^2 and a smaller value of $\hat{\sigma}$. Run 8 dropped the two independent variables, I and N_t because of their little contribution to the model. It was found that station 813350 had the largest value of Cook's distance which was twice the value as the second largest. By examining the data, they showed that the value of S_{Z_r} at station 813550 was considerably smaller as compared with those stations with similar magnitudes of hydrological variables. The data for station 813350 were then dropped out of the data set and OLS was applied. The t-statistics of regressors I and N_t were less than unity, therefore were deleted from the model. The regression model and estimates corresponding to run 9 were proposed as a desired model for predicting S_{Z_r} for given independent variables. The probability plot showed that the assumption of normality holds. The model (run 9) found to be the most representative is

$$\frac{1}{S_{Z_r} + 2500} = 2.16 \times 10^{-4} - 4.16 \times 10^{-5} \ln(A_d) - 3.90 \times 10^{-6} S_{\rho} + 5.99 \\ \times 10^{-5} \ln(S_t) + 3.24 \times 10^{-5} \ln(L) - 1.14 \times 10^{-5} \ln(R_t) \quad (\text{A.8})$$

$$\text{Let } S'_{Z_r} = \frac{1}{S_{Z_r} + 2500}.$$

It is justified that S'_{Z_r} for given \underline{x}^* is normally distributed with mean given by Eq. (A.8) and standard deviation $\hat{\sigma} = 2.28 \times 10^{-5}$ given in Table A.5. The mean of S_{Z_r} for given \underline{x}^* can be expressed as

$$E(S_{Z_r} | \underline{x}^*) = \int_{-\infty}^{\infty} \frac{(1 - 2500S'_{Z_r})}{\sqrt{2\pi} S'_{Z_r} \hat{\sigma}} \cdot e^{-\frac{1}{2} \left(\frac{S'_{Z_r} - \underline{x}^* \hat{\beta}}{\hat{\sigma}} \right)^2} \cdot dS'_{Z_r} \quad (\text{A.9})$$

and the variance can be expressed as

$$\text{Var}(S_{Z_r} | \underline{x}^*) = E(S_{Z_r}^2 | \underline{x}^*) - E^2(S_{Z_r} | \underline{x}^*) \quad (\text{A.10})$$

where

$$E(S_{Z_r} | \underline{x}^*) = \int_{-\infty}^{\infty} \frac{(1 - 2500S_{Z_r}')^2}{\sqrt{2\pi} \hat{\sigma} (S_{Z_r}')^2} \cdot e^{-\frac{1}{2} \left(\frac{S_{Z_r}' - \underline{x}^* \hat{\beta}}{\hat{\sigma}} \right)^2} \cdot dS_{Z_r}' \quad (\text{A.11})$$

A.4 REGRESSION EQUATION FOR SKEW OF STREAMFLOWS

Regression equations for the mean and variance of the skew of the streamflows (G_{Z_r}) as a function of the hydrologic variables are now considered. The first run was made for the regression relation among G_{Z_r} and seven hydrological variables considering the form of Eq. (A.1). The results of the OLS are shown in Table A.6. It is observed that the coefficient of determination r^2 is so small that the adjusted value of \bar{r}^2 is less than zero. Most of the t-statistics of the independent variables are less than unity indicating their minor statistical significance. The probability plot of the residual of the regression model indicates the existence of skewness in the distribution of residual which implies that the normality assumption does not hold. The plot of the residual e_1 vs. G_{Z_r} showed a certain degree of expansion of scatter as the value of G_{Z_r} increases. Most scatter plots of residual e_1 vs. independent variables such as A_d , S_t , L , and S_ℓ , turned out to be less desirable, which showed the uneven position of data points and dependence of spreading on the level of the independent variables. Fewer

Table A.6 Regression Results for Skewness of Streamflow, G_{Z_r}

	$\hat{\beta}_0$	$\hat{\beta}_1$	$\hat{\beta}_2$	$\hat{\beta}_3$	$\hat{\beta}_4$	$\hat{\beta}_5$	$\hat{\beta}_6$	$\hat{\beta}_7$	R^2 (\bar{R}^2)	$\hat{\sigma}$
Run 1	2.04 (1.18)	4.72×10^{-5} (0.64)	0.00616 (0.15)	0.345 (0.58)	-0.00272 (-0.99)	0.2047 (0.73)	-0.0149 (-0.56)	-1.00 (-1.00)	0.00734	1.1682
Run 2	-0.831 (-0.3)	0.230 (1.27)	0.204 (1.20)	0.392 (.94)	-0.370 (-1.43)	1.199 (1.48)	-0.266 (-0.50)	-0.103 (-0.66)	0.1123 (0.0462)	0.5385
Run 3		0.194 (1.23)	0.205 (2.50)	0.260 (.66)	-0.341 (-1.34)	0.304 (1.87)			0.2085 (0.1748)	0.5338
Run 4		0.223 (1.48)	0.179 (2.49)		-0.381 (-1.55)	0.328 (2.07)			0.2047 (0.1793)	0.5321
Run 5	-1.281 (-.51)	0.208 (1.29)	0.246 (1.62)	0.315 (.85)	-0.231 (-0.99)	1.178 (1.62)	0.253 (-0.53)	-0.028 (-0.20)	0.0888 (0.0209)	0.4823
Run 6	-0.904 (-.42)	0.227 (1.44)	0.210 (1.48)		-0.264 (-1.16)	0.986 (1.52)	-0.224 (-0.50)		0.0810 (0.0320)	0.4788
Run 7	-1.678 (-1.1)	0.240 (1.56)	0.255 (2.33)		-0.263 (-1.17)	0.845 (1.46)			0.0780 (0.0384)	0.4768
Run 8		0.172 (1.20)	0.187 (2.52)	0.296 (.81)	-0.217 (-0.94)	1.023 (1.62)	-0.433 (-1.33)		0.1737 (0.1293)	0.4776
Run 9		0.197 (1.41)	0.158 (2.44)		-0.254 (-1.13)	0.905 (1.47)	-0.358 (-1.14)		0.1674 (0.1317)	0.4766

scatter plots of residual against independent variable, such as R_t , I and N_t , however, showed the desirable feature, i.e., uniform spreading of residuals.

The model was modified to the form of Eq. (A.2). Comparing the value of r^2 an improvement was made which was also apparent because of the linearity of the probability plot and the residual plot of the predicted dependent variable $\ln(G_{Z_r})$. Runs 3 and 4 in Table A.6 have the same form as Eq. (A.2) but some of the less important independent variables were deleted. Some of the residual plots for the independent variables, e.g.

$\ln(A_d)$ and $\ln(L)$, showed the wedged-shaped dispersion. Other plots such as e_2 vs. $\ln(S_t)$ were more or less satisfactory. It is interesting to note that by examining the normality plots and other residual plots it is found that there is an isolated point having the largest negative residual value. The isolated point is associated with gaging station 811400 which has the largest drainage area and channel length. Cook's distance for the station 811400 data is 0.359, which is 5 times larger than the second largest, 0.074. This implies that the point has great influence on the parameter estimation.

Using the same model (Eq. A.2), the information for station 811400 is deleted and the parameters of the regression equation are reestimated and listed as run 5 in Table A.6. Runs 6, 7, 8, and 9 were all based on the results obtained by run 5. Runs 6 and 7 were made by deleting three independent variables, i.e., S_t , N_t , and R_t , and keeping the regression constant β_0 in the regression model. Runs 8 and 9 deleted two independent variables, S_t , R_t as well as the regression constant. The final results of deleting the two variables are listed in Table A.6 for runs 7 and 9. It can be seen that the

value of r^2 for run 9 is as twice as that of for run 7. The resulting residual plots with respect to A_d and L associated with runs 5 through run 9 are shown more desirable than those of in runs 2 through 4. Therefore, the model suggested is

$$\begin{aligned} \ln(G_{Z_r}) = & 0.197 \ln(A_d) + 0.158 \ln(S_\rho) - 0.254 \ln(L) + \\ & 0.905 \ln(I) - 0.358 \ln(N_t) \end{aligned} \quad (\text{A.12})$$

The mean and variance of G_{Z_r} for given hydrological variables can be computed by Eqs. (A.3) and (A.4) respectively.

A.5 REGRESSION EQUATION FOR MEAN OF LOG-TRANSFORMED STREAMFLOWS

Regression equations for the mean and variance of the mean of log-transformed streamflows (\bar{Y}_r) as a function of the hydrological variables is now considered. The same procedures presented for previous three streamflow characteristics are used. \bar{Y}_r is first regressed on the seven hydrological variables in the form of Eq. (A.1), and the results of the OLS analysis are presented as run 1 in Table A.7. It is interesting to point out that the regression coefficient corresponding to the drainage area is negative, which means the larger the contributing area the smaller the mean streamflow magnitude. This contradicts the results observed by hydrologists for years, and is physically unexplainable. Regardless of this fact, the regression model is less desirable because the scatter plots of residual against \bar{Y}_r , and independent variables such as A_d do not provide evidence of satisfying the

Table A.7 Regression Results for Mean of Log-transformed Streamflow, \bar{Y}_T .

	$\hat{\beta}_0$	$\hat{\beta}_1$	$\hat{\beta}_2$	$\hat{\beta}_3$	$\hat{\beta}_4$	$\hat{\beta}_5$	$\hat{\beta}_6$	$\hat{\beta}_7$	R^2 (\bar{R}^2)	$\hat{\sigma}$
Run 1	9.823 (12.35)	-0.000022 (-0.64)	-0.0104 (-0.54)	-0.256 (-0.93)	0.0037 (2.92)	-0.1787 (-1.39)	-0.0027 (-0.22)	1.005 (2.19)	0.5063 (0.4695)	0.5360
Run 2	1.488 (5.84)	0.059 (3.54)	0.045 (2.85)	-0.054 (-1.40)	0.0046 (0.19)	-0.027 (-0.36)	0.086 (1.73)	0.059 (4.09)	0.6490 (0.6229)	0.050
Run 3	1.407 (5.50)	0.062 (9.72)	0.0071 (3.27)	-0.073 (-2.03)		-0.0384 (-0.54)	0.117 (2.21)	0.0495 (3.50)	0.6549 (0.6329)	0.04918
Run 4	1.358 (5.71)	0.063 (10.46)	0.0072 (3.27)	-0.068 (-1.96)			0.109 (2.16)	0.046 (3.62)	0.6538 (0.6354)	0.4898
Run 5	1.491 (5.86)	0.063 (9.98)	0.0081 (3.58)	-0.071 (-2.01)		-0.051 (-0.72)	0.102 (1.94)	0.062 (4.08)	0.6682 (0.6468)	0.04831
Run 6	1.424 (6.03)	0.064 (10.76)	0.0083 (3.71)	-0.064 (-1.89)			0.091 (1.81)	0.057 (4.18)	0.6667 (0.6488)	0.04817

assumptions of OLS. However, some of the plots such as probability plot and residual vs. slope, S_{ℓ} , are acceptable.

The model was modified to have the form of Eq. (A.2) and the results of regression analysis are presented in Table A.7 as run 2. This model is an improvement over the first because of the larger value of r^2 , since the value of $\hat{\sigma}$ is not comparable on the two models. However, by examining its probability plot the validity of normality assumption is justified. The variance of \bar{Y}_r for the regression model associated with run 2 can be calculated by Eq. (A.4), and the range for all 95 data points is between 0.2820 and 0.3690. This provides evidence that the second model is preferred to the previous regression model with $\text{Var}(\bar{Y}_r | \underline{X}) = 0.536$. The plot of residual vs. $\ln(\bar{Y}_r)$ indicates that assumption of constant variance is satisfied. Other residual plots for the drainage area, $\ln(A_d)$ in the present regression model, while the residual plots for $\ln(S_{\ell})$ was less desirable because of its wedged dispersion.

The modification of the model to the form of Eq. (A.5) can eliminate this problem and the results are presented as run 3 in Table A.7. Although the residual plot of rainfall intensity I , with L deleted, shows the trend of decreasing variance as I increases, I is deleted from the model because it is of lesser importance, (listed as run 4 in Table A.7). Runs 5 and 6 are made with the same model using 94 data points because the one provided by station 819500 has a significantly larger value of Cook's distance than the others. The plots appear to show their desired feature and the model proposed is

$$\begin{aligned} \ln(\bar{Y}_r) = & 1.424 + 0.064 \ln(A_d) + 0.0083 S_\ell - 0.064 \ln(S_t) \\ & + 0.091 \ln(N_t) + 0.057 \ln(R_t) \end{aligned} \quad (\text{A.13})$$

A.6 REGRESSION EQUATION FOR STANDARD DEVIATION OF LOG-TRANSFORMED STREAMFLOWS

Regression equations for the mean and variance of the standard deviation of log-transformed streamflows (S_{Y_r}) as a function of the hydrological variables is now considered. First, a model in the form of Eq. (A.1) is tested with the parameters, r^2 and $\hat{\sigma}$, listed in Table A.8. The probability plot showed the existence of skewness, and the scatter plot of e_1 vs. S_{Y_r} indicated the dependence of dispersion on S_{Y_r} . The assumptions of normality distribution and constant variance in OLS do not hold. Plots of residual vs. the independent variables such as the area, A_d , and the rainfall intensity, I , showed an uneven positioned data. A certain degree of dependence of spreading of residual on the level of the independent variable was typical.

However, the model was improved as far as the validity of the assumptions being satisfied are concerned, by modifying the model to have the form of Eq. (A.2). Run 2 in Table A.8 presents the results of the OLS. Run 3 is based on the same regression model as run 2 except that the deletion of station 819500 is made because of extraordinarily large values of Cook's distance for the data. This value of Cook's distance is three times as large as that of the second largest one because of its high value of studentized residual. The data show that the value of S_{Y_r} of this station is very large as

Table A.8 Regression Results for Standard Deviation of Log-Transformed Streamflow, S_{Y_r} .

	$\hat{\beta}_0$	$\hat{\beta}_1$	$\hat{\beta}_2$	$\hat{\beta}_3$	$\hat{\beta}_4$	$\hat{\beta}_5$	$\hat{\beta}_6$	$\hat{\beta}_7$	R^2 (\bar{R}^2)	$\hat{\sigma}$
Run 1	1.94 (4.11)	3.24×10^{-7} (1.60)	0.0138 (1.21)	-0.113 (-0.69)	-0.00191 (-2.56)	0.0519 (0.68)	-0.0199 (-2.74)	-0.128 (-0.47)	0.4934 (0.4557)	0.3185
Run 2	3.430 (2.94)	0.107 (1.40)	-0.020 (-0.27)	-0.240 (-1.36)	-0.326 (-2.97)	0.456 (1.33)	-0.939 (-4.15)	-0.106 (-1.60)	0.6019 (0.5723)	0.2284
Run 3	3.537 (3.23)	0.171 (2.32)	-0.026 (-0.83)	-0.283 (-1.71)	-0.418 (-3.94)	0.385 (1.19)	-0.932 (-4.39)	-0.068 (-1.08)	0.6250 (0.5968)	0.2142
Run 4	3.243 (4.21)	0.178 (2.47)		-0.263 (-1.68)	-0.414 (-3.94)	0.411 (1.31)	-0.894 (-4.83)	-0.065 (-1.05)	0.6244 (0.6002)	0.2131

compared with the value of S_{Y_r} for other basins having similar values of the hydrological variables. This leads to a substantial under-estimation of S_{Y_r} for station 819500 by the regression model. The results of deleting the station changes the value of the estimated parameters β_1 by 60%, and β_7 by 36%. Run 4 deletes the independent variable $\ln(S_d)$ because of its small contribution. The model finally proposed for relating S_{Y_r} to hydrological variables is =

$$\begin{aligned} \ln(S_{Y_r}) = & 3.24 + 0.178 \ln(A_d) - 0.263 \ln(S_t) - 0.414 \\ & \ln(L) + 0.411 \ln(I) - 0.894 \ln(N_t) - 0.065 \ln(R_t) \end{aligned} \quad (\text{A.14})$$

Other than the higher value of r^2 the multiplicative form is preferred over the additive one because of the range of the standard errors. The standard errors for each station in run 2 ranged from 0.2962 to 0.1020, using Eq. (A.2).

A.7 REGRESSION EQUATIONS FOR SKEW OF LOG-TRANSFORMED STREAMFLOWS

Regression equations for the mean and variance of the skew of the log-transformed streamflows (G_{Y_r}) as a function of the hydrological variables is now considered. First, a model of the form of Eq. (A.1) was used and parameters are estimated by OLS, presented as run 1 in Table A.9. The normality assumption of the residual can be justified because the probability plot is close to a straight line. The residual plot of G_{Y_r} showed the uniform variation over the range of G_{Y_r} which indicates the assumption of constant

Table A.9 Regression Results for Skewness of Log-transformed Streamflow, y_T^G

	$\hat{\beta}_0$	$\hat{\beta}_1$	$\hat{\beta}_2$	$\hat{\beta}_3$	$\hat{\beta}_4$	$\hat{\beta}_5$	$\hat{\beta}_6$	$\hat{\beta}_7$	R^2 (R^2)	$\hat{\sigma}$
Run 1	-1.752 (-2.20)	-0.000009 (-0.26)	0.0081 (0.42)	0.353 (1.28)	0.0053 (0.42)	0.107 (0.83)	0.0090 (0.73)	-0.141 (-.31)	0.0759 (0.0078)	0.5378
Run 2	-4.879 (-1.79)	0.074 (0.41)	0.215 (1.28)	0.453 (1.1)	0.051 (0.20)	0.934 (1.16)	0.494 (0.94)	0.065 (0.42)	0.1103 (0.044)	0.5328
Run 3	-5.449 (-2.29)	0.106 (1.48)	0.204 (1.25)	0.448 (1.13)		1.082 (1.49)	0.562 (1.12)		0.1090 (0.062)	0.5275
Run 4	-4.183 (-1.55)	0.065 (0.37)	0.161 (0.97)	-0.021 (-.05)	0.061 (0.24)	0.685 (0.86)	0.467 (.90)	0.071 (.47)	0.0800 (0.011)	0.5241
Run 5	-4.012 (-1.68)	0.114 (1.63)	0.034 (0.19)	-2.392 (-2.0)	3.910 (2.47)	0.373 (.49)	0.616 (1.3)		0.1659 (0.113)	0.5130
Run 6	-3.601 (-3.23)	0.102 (2.03)		-2.654 (-2.6)	4.201 (3.02)		0.724 (2.9)		0.1637 (0.128)	0.5080

variance is satisfied. The residual plot of drainage area, A_d , showing the data points clustering on the left hand side of the graph, suggested the log-transformation of corresponding independent variable might produce desirable arrangement of the data points. The residual plot of N_t showed the satisfactory feature. The residual plot with respect to the predicted dependent variable presented the pattern as desired while some others do not. The model is modified to have the following form:

$$G_{Y_r} = \beta_0 + \beta_1 \ln(A_d) + \beta_2 \ln(S_\ell) + \beta_3 \ln(S_t) + \beta_4 \ln(L) + \beta_5 \ln(I) + \beta_6 \ln(N_t) + \beta_7 \ln(R_t) + \varepsilon_5 \quad (\text{A.15})$$

The estimated parameters, r^2 , and $\hat{\sigma}$, for the model of Eq. (A.15) are listed as run 2 in Table A.9. Some improvement is observable in run 2 and run 3 in which the deletion of unimportant variables, L and R_t is made. For run 2 and 3 the probability plot indicates the normality assumption hold and the scatter plots such as e_5 vs. G_{Y_r} and e_5 vs. $\ln(A_d)$ were even more desirable than that of the previous regression model formulation. The value of Cook's distance associated with station 801200 significantly larger than that of any other station. Run 4 was made without the station 801200 data. It is noted that the deletion of 801200 reduces the value of $\hat{\beta}_3$ in run 4 by factor 22 to that of in run 2 when 801200 is included. This indicates that station 801200 is highly influential in determining the value of β_3 , which implies that there is an inadequacy in the form of corresponding variable S_t . Careful examination of the residual plot of $\ln(S_t)$ showed the presence of curvature in the plot. This led to including the term $(\ln(S_t))^2$ in the model as

$$G_{Y_r} = \beta_0 + \beta_1 \ln(A_d) + \beta_2 \ln(S_\ell) + \beta_3 \ln(S_t) + \beta_4 (\ln(S_t))^2 + \beta_5 \ln(I) \\ + \beta_6 \ln(N_t) + \beta_7 \ln(R_t) + \varepsilon_6 \quad (\text{A.16})$$

Notice that β_4 in run 5 and 6 is no longer the regression coefficient for channel length, L , which was found not to be statistically different from zero and therefore discarded. The model of Eq. (A.16) is substantially better than the two previous models which can be justified easily by comparing results of the runs in Table A.9. In the residual plot of G_{Y_r} there is a single isolated point on the right end of the graph. The value of Cook's distance associated is not of any larger than others implying that the parameters estimated will not be sensitive to the presence of the data point in OLS analysis. Moreover, the presence of curvature in the residual plot of $\ln(S_t)$ for the previous regression model, Eq. (A.15) vanishes. The final regression equation suggested for G_{Y_r} is

$$G_{Y_r} = -3.601 + 0.102 \ln(A_d) - 2.564 \ln(S_t) + 4.201 (\ln(S_t))^2 \\ + 0.724 \ln(N_t) \quad (\text{A.17})$$

The mean of G_{Y_r} for given independent variable can be obtained from Eq. (A.17) and corresponding variance is 0.5080.

APPENDIX B

FIRST-ORDER ANALYSIS TO DETERMINE THE MEAN AND COEFFICIENT OF VARIATION OF THE LEVEE CAPACITY BY THE AREA-SLOPE METHOD

B.1 AREA-SLOPE METHOD

The determination of the capacity of a channel reach or levee system using Manning's equation requires knowledge of the surface roughness, flow cross-sectional geometry, and the energy slope. It is understood that Manning's equation assumes the uniform flow condition where the energy slope, S_f , is equal to the slope of the longitudinal water-surface profile and also to the channel bottom slope, S_o . However, because of the irregular channel condition and varying levee encroachment widths on both ends of the reach, the velocity may vary appreciably within the reach. Hence, the channel bottom slope, S_o , is not used as an approximation for the energy slope, S_f . Under such circumstances the capacity of the levee system with different encroachment widths on both ends of the reach can be determined by the area-slope method.

The area-slope method is an iterative procedure that can be described as follows (Chow, 1959):

1. From the known values of flow cross-sectional geometry and surface roughness, the conveyance K_u and K_d , respectively, of the upstream and downstream sections of the reach are computed using

$$K_u = \frac{1.49}{N_c} A_{c,u}^{5/3} P_{c,u}^{-2/3} + \frac{2.98}{N_b} A_{b,u}^{5/3} P_{b,u}^{-2/3} \quad (\text{B.1})$$

$$K_d = \frac{1.49}{N_c} A_{c,d}^{5/3} P_{c,d}^{-2/3} + \frac{2.98}{N_b} A_{b,d}^{5/3} P_{b,d}^{-2/3} \quad (\text{B.2})$$

where N is the surface roughness; A is the flow cross-sectional area; P is the wetted perimeter; subscripts c and b represent the channel section and flood plain section, respectively; and subscripts u and d represent the upstream and downstream ends of the reach, respectively.

2. The average conveyance K of the reach as the geometric mean of K_u and K_d is computed using

$$K = \sqrt{K_u \cdot K_d} \quad (\text{B.3})$$

3. Assuming zero velocity head, the energy slope, S_f , is equal to the fall, F , of water surface elevation in the reach divided by the length of the reach, L , or

$$S_f = \frac{F}{L} \quad (\text{B.4})$$

in which

$$F = (h_u - h_d) + S_b L + S_o L \quad (\text{B.5})$$

where h_u and h_d are the levee heights on the upstream and downstream end of the reach, respectively; and S_b and S_o are the longitudinal slopes of the flood plain and channel bottom, respectively.

4. The levee capacity, Q_c , is computed using the following

equation

$$Q_c = \lambda_m K \sqrt{S_f} \quad (\text{B.6})$$

where λ_m is the model correction factor defined in Chapter 2. Equation (B.6) is the first approximation of the levee capacity with the energy slope defined by Eqs. (B.4) and (B.5).

5. Assuming the levee capacity equal to the first approximation, the velocity heads at the upstream and downstream end, $\alpha_u V_u^2/2g$ and $\alpha_d V_d^2/2g$ are computed. The energy slope is

$$S_f = \frac{h_f}{L} \quad (\text{B.7})$$

where

$$h_f = F + k \left(\alpha_u \frac{V_u^2}{2g} - \alpha_d \frac{V_d^2}{2g} \right) \quad (\text{B.8})$$

and h_f is the total energy loss; k is a factor; α_u and α_d are the energy coefficients for the upstream and downstream section; and V_u and V_d are the mean velocities at the upstream and downstream end of the reach. When the reach is expanding ($V_u > V_d$), $k = 0.5$ and for a contracting reach ($V_u < V_d$), $k = 1.0$. The values of the energy coefficients depend on the geometry of the channel and flow condition. Experimental data indicate that the energy coefficient varies from 1.03 to 1.36 for fairly straight prismatic channels. However, for simplification, the energy coefficients are taken to be unity without error. The corresponding levee capacity is then computed by Eq. (B.6) using the revised energy slope obtained by Eq. (B.8). This gives the

second approximation of the levee capacity.

6. Steps 4) and 5) are repeated for the successive approximations until the assumed and computed levee capacities are approximately equal.

B.2 APPLICATION OF FIRST-ORDER ANALYSIS OF UNCERTAINTY TO THE AREA-SLOPE METHOD

First-order analysis of uncertainty, described in Chapter 2, is used to determine the mean and coefficient of variation of the levee capacity computed by the area-slope method. Equation (B.6) indicates that the variables with uncertainty are the conveyance, K , energy slope, S_f , and λ_m , which are functions of other random variables such as surface roughness, flow cross-sectional area, wetted perimeter, and longitudinal slope of flood plain as well as the channel bottom. Because the computation of levee capacity using the area-slope method is an iterative procedure, first-order analysis of uncertainty is applied when the final convergence of the result is reached. The derivation of the mean and coefficient of variation of the levee capacity is given in the following paragraphs.

The mean of the levee capacity, \bar{Q}_C , and the coefficient of variation, Ω_{Q_C} , based on Eq. (B.6) can be expressed as

$$\bar{Q}_C = \bar{\lambda}_m \bar{K} \bar{S}_f^{1/2} \quad (\text{B.9})$$

and

$$\Omega_{Q_C} = \left[\Omega_{\lambda_m}^2 + \Omega_K^2 + \frac{1}{4} \Omega_{S_f}^2 \right]^{1/2} \quad (\text{B.10})$$

Because the conveyance K and the energy slope S_f used above are functions of other variables with uncertainty, first-order analysis is used to estimate their statistical properties. For the conveyance, K , and mean, \bar{K} , and coefficient of variation, Ω_K , based on Eq. (B.3), are

$$\bar{K} = (\bar{K}_u \cdot \bar{K}_d)^{1/2} \quad (B.11)$$

and

$$\Omega_K = \frac{1}{2} \left(\Omega_{K_u}^2 + \Omega_{K_d}^2 \right)^{1/2} \quad (B.12)$$

where \bar{K}_u and Ω_{K_u} can be estimated by first-order analysis, based on Eq. (B.1), as

$$\bar{K}_u = \frac{1.49}{\bar{N}_c} \bar{A}_{c,u}^{5/3} \bar{P}_{c,u}^{-2/3} + \frac{2.98}{\bar{N}_b} \bar{A}_{b,u}^{-5/3} \bar{P}_{b,u}^{-2/3} \quad (B.13)$$

and

$$\Omega_{K_u}^2 = \frac{1}{\psi^2} \left[\Omega_{N_c}^2 + \frac{25}{9} \Omega_{A_{c,u}}^2 + \frac{4}{9} \Omega_{P_{c,u}}^2 \right] + \frac{1}{\phi^2} \left[\Omega_{N_b}^2 + \frac{25}{9} \Omega_{A_{b,u}}^2 + \frac{4}{9} \Omega_{P_{b,u}}^2 \right] \quad (B.14)$$

where the values of $\bar{A}_{c,u}$, $\Omega_{A_{c,u}}$, $\bar{P}_{c,u}$, $\Omega_{P_{c,u}}$, ψ and ϕ for a given levee cross section, Fig. 4.2, are defined, respectively, in Eqs. (4.6), (4.7), (4.12), and (4.13).

In order to compute S_f and Ω_{S_f} based on Eq. (B.8) the values of the mean velocity at both ends of the reach are required. The average velocity at the upstream end of the reach can be computed as

$$V_u = Q_c / A_u \quad (B.15)$$

where A_u is the total cross sectional area of flow encroached by the levee at

the upstream end; or

$$A_u = A_{c,u} + 2A_{b,u} \quad (\text{B.16})$$

The mean of V_u , \bar{V}_u , and the coefficient of variation Ω_{V_u} can be expressed respectively, as

$$\bar{V}_u = \bar{Q}_c / \bar{A}_u \quad (\text{B.17})$$

and

$$\Omega_{V_u} = \left(\Omega_{Q_c}^2 + \Omega_{A_u}^2 \right)^{1/2} \quad (\text{B.18})$$

where

$$\bar{A}_u = \bar{A}_{c,u} + \bar{A}_{b,u} \quad (\text{B.19})$$

and

$$\Omega_{A_u} = \left(\bar{A}_{c,u}^2 \Omega_{A_{c,u}}^2 + 4\bar{A}_{b,u}^2 \Omega_{A_{b,u}}^2 \right)^{1/2} / \bar{A}_u \quad (\text{B.20})$$

Letting $U_u = V_u^2$, then the mean of U_u , \bar{U}_u , and its coefficient of variation, Ω_{U_u} , can be expressed as

$$\bar{U}_u = \bar{V}_u^2 \quad (\text{B.21})$$

and

$$\Omega_{U_u} = 2 \Omega_{V_u} \quad (\text{B.22})$$

The mathematical expressions, Eqs. (B.13) through (B.22) are identically applicable to compute the mean of the conveyance and average velocity and their corresponding coefficients of variation at the downstream end of the reach, except that the subscript u is replaced by the subscript d .

The mean and coefficient of variation of the energy slope through a first-order analysis of Eqs. (B.5) and (B.8) can be expressed as

$$\bar{S}_f = \bar{S}_o + \bar{S}_b + \frac{h_u - h_d}{L} + \frac{k}{2gL} (\bar{U}_u - \bar{U}_d) \quad (\text{B.23})$$

and

$$\Omega_{S_f} = \left[\bar{S}_o^2 \Omega_{S_o}^2 + \bar{S}_b^2 \Omega_{S_b}^2 + \left(\frac{k}{2gL} \right)^2 \bar{U}_u^2 \Omega_{U_u}^2 + \left(\frac{k}{2gL} \right)^2 \bar{U}_d^2 \Omega_{U_d}^2 \right]^{1/2} / \bar{S}_f \quad (\text{B.24})$$

It is noted that from Eq. (B.9) the mean of the levee capacity, \bar{Q}_c , is a function of \bar{S}_f and Ω_{Q_c} is a function of Ω_{S_f} from Eq. (B.10); while from Eqs. (B.15) through (B.24) \bar{S}_f and Ω_{S_f} are expressed in terms of \bar{Q}_c and Ω_{Q_c} through the average velocity V^2 or U . Substituting \bar{S}_f , defined in Eq. (B.23), into Eq. (B.9) the mean levee capacity is expressed as

$$\bar{Q}_c = \bar{\lambda}_m \bar{K} \left[\bar{S}_o + \bar{S}_b + \frac{h_u - h_d}{L} + \frac{k}{2gL} (\bar{U}_u - \bar{U}_d) \right]^{1/2} \quad (\text{B.25})$$

or

$$\bar{Q}_c^2 = \bar{\lambda}_m^2 \bar{K}^2 \left[\bar{S}_o + \bar{S}_b + \frac{h_u - h_d}{L} + \frac{k}{2gL} \left(\frac{\bar{Q}_c^2}{\bar{A}_u^2} - \frac{\bar{Q}_c^2}{\bar{A}_d^2} \right) \right] \quad (\text{B.26})$$

Solving Eq. (B.26) for Q_c results in

$$\bar{Q}_c = \bar{\lambda}_m \bar{K} \left[\frac{\bar{S}_o + \bar{S}_b + \frac{\Delta h}{L}}{1 - \frac{\bar{\lambda}_m^2 \bar{K}^2 k}{2gL} \left(\frac{1}{A_u^2} - \frac{1}{A_d^2} \right)} \right]^{1/2} \quad (\text{B.27})$$

where $\Delta h = h_u^2 - h_d^2$.

The coefficient of variation of the levee capacity Ω_{Q_c} can be solved in the same manner by substituting Ω_{S_f} , defined in Eq. (B.24), into Eq. (B.10) as

$$\Omega_{Q_c}^2 = \Omega_{\lambda_m}^2 + \Omega_K^2 + \frac{1}{4\bar{S}_f^2} \left(\bar{S}_o \Omega_{S_o}^2 + \bar{S}_b \Omega_{S_b}^2 + \omega_u^2 \Omega_{U_u}^2 + \omega_d^2 \Omega_{U_d}^2 \right) \quad (\text{B.28})$$

where

$$\omega_u = \frac{kU_u}{2gL} \quad ; \quad \omega_d = \frac{kU_d}{2gL}$$

or

$$\begin{aligned} \Omega_{Q_c}^2 = & \Omega_{\lambda_m}^2 + \Omega_K^2 + \frac{1}{4\bar{S}_f^2} \left(\bar{S}_o^2 \Omega_{S_o}^2 + \bar{S}_b^2 \Omega_{S_b}^2 + 4\omega_u^2 \Omega_{A_u}^2 + 4\omega_d^2 \Omega_{A_d}^2 \right) \\ & + \frac{\Omega_{Q_c}^2}{\bar{S}_f^2} (\omega_u^2 + \omega_d^2) \end{aligned} \quad (\text{B.29})$$

Then solving Eq. (B.29) for Ω_{Q_c} , the coefficient of variation of the levee

capacity is

$$\Omega_{Q_c}^2 = \left[\Omega_{\lambda_m}^2 + \Omega_K^2 + \frac{1}{4\bar{S}_F^2} \left(\bar{S}_o^2 \Omega_o^2 + \bar{S}_b^2 \Omega_b^2 + 4\omega_u^2 \Omega_{A_u}^2 + 4\omega_d^2 \Omega_{A_d}^2 \right) \right] \\ / \left[1 - \frac{1}{\bar{S}_F^2} (\omega_u^2 + \omega_d^2) \right] \quad (\text{B.30})$$

APPENDIX C

VARIOUS STATIC RELIABILITY MODELS

In order to evaluate the risk and reliability of the design the probability density function of the loading and the resistance are required. In this report the probability density function for the resistance (capacity of the hydraulic structures) is assumed to be log-normal, Eq. (2.15). The loading probability distribution models used in water resources engineering are normal, log-normal, Gumbel, Pearson type III, and log-Pearson type III distributions. The mathematical representation of the static reliability model with log-normal resistance and various types of loading distributions, except Gumbel described in Section 2.3, are described as follows.

C.1 Normally Distributed Loading and Log-normally Distributed Resistance

In this case the normal probability density function (PDF) for loading is

$$f_l(l') = \frac{1}{\sqrt{2\pi} \sigma_l} \cdot \exp\left[-\frac{1}{2} \left(\frac{l' - \mu_l}{\sigma_l}\right)^2\right] \quad (C.1)$$

and the cumulative density function (CDF) is

$$F_{\ell}(\ell) = \int_{-\infty}^{\ell} \frac{1}{\sqrt{2\pi} \sigma_{\ell}} \cdot \exp \left[-\frac{1}{2} \left(\frac{\ell' - \mu_{\ell}}{\sigma_{\ell}} \right)^2 \right] d\ell' \quad (C.2)$$

where μ_{ℓ} and σ_{ℓ} are the mean and standard deviation of the loading. Since the PDF of the resistance is log-normal, Eq. (2.15) the reliability model can be expressed explicitly as

$$R = \int_0^{\infty} \frac{1}{\sqrt{2\pi} r' \sigma_{\ell n r}} \cdot \exp \left[-\frac{1}{2} \left(\frac{\ln r' - \mu_{\ell n r}}{\sigma_{\ell n r}} \right)^2 \right] \cdot \left\{ \int_{-\infty}^{r'} \frac{1}{\sqrt{2\pi} \sigma_{\ell}} \cdot \exp \left[-\frac{1}{2} \left(\frac{\ell' - \mu_{\ell}}{\sigma_{\ell}} \right)^2 \right] \cdot d\ell' \right\} dr' \quad (C.3)$$

C.2 Log-normally Distributed Loading and Log-normally Distributed Resistance

The PDF of the loading has the same functional form as resistance,

$$f_{\ell}(\ell') = \frac{1}{\sqrt{2\pi} \ell' \sigma_{\ell n \ell}} \cdot \exp \left[-\frac{1}{2} \left(\frac{\ln \ell' - \mu_{\ell n \ell}}{\sigma_{\ell n \ell}} \right)^2 \right] \quad (C.4)$$

and its CDF is

$$F_{\ell}(\ell) = \int^{\ell} \frac{1}{\sqrt{2\pi} \ell' \sigma_{\ell n \ell}} \cdot \exp \left[-\frac{1}{2} \left(\frac{\ln \ell' - \mu_{\ell n \ell}}{\sigma_{\ell n \ell}} \right)^2 \right] d\ell' \quad (C.5)$$

where $\mu_{\ell n \ell}$ and $\sigma_{\ell n \ell}$ are the mean and standard deviation of log-transformed loading. The reliability model can be expressed as

$$R = \int_0^{\infty} \frac{1}{\sqrt{2\pi} r' \sigma_{\ln r}} \cdot \exp \left[-\frac{1}{2} \left(\frac{\ln r' - \mu_{\ln r}}{\sigma_{\ln r}} \right)^2 \right] \cdot \left(\int_0^{r'} \frac{1}{\sqrt{2\pi} \ell' \sigma_{\ln \ell}} \exp \left[-\frac{1}{2} \left(\frac{\ln \ell' - \mu_{\ln \ell}}{\sigma_{\ln \ell}} \right)^2 \right] d\ell' \right) dr' \quad (C.6)$$

In this case the computation of reliability can be simplified by defining $q = r/\ell$. Based on the definition of reliability, Eq. (1.1), the reliability can be expressed as

$$R = P_r \left(\frac{r}{\ell} > 1 \right) \quad (C.7a)$$

$$R = P_r \left(\ln r - \ln \ell > 0 \right) \quad (C.7b)$$

$$R = P_r \left(\ln q > 0 \right) \quad (C.7c)$$

Since r and ℓ are log-normally distributed, then $\ln q$ is normally distributed with mean $(\mu_{\ln r} - \mu_{\ln \ell})$ and variance $(\sigma_{\ln r}^2 + \sigma_{\ln \ell}^2)$. Hence, the reliability can be expressed as

$$R = \int_a^{\infty} \phi(q') \cdot dq' = 1 - \Phi(a) \quad (C.8)$$

where $a = -\frac{\mu_{\ln r} - \mu_{\ln \ell}}{\sqrt{\sigma_{\ln r}^2 + \sigma_{\ln \ell}^2}}$, and $\phi(\cdot)$ and $\Phi(\cdot)$ are, respectively, the

PDF and CDF for the standard normal variate q' .

C.3. Pearson Type III Distributed Loading and Log-normally Distributed Resistance

The probability density function for the Pearson type III distribution is

$$f_{\ell}(\ell') = \frac{1}{\beta_1 \Gamma(\beta_2)} \cdot \left(\frac{\ell' - \beta_3}{\beta_1} \right)^{\beta_2 - 1} \cdot \exp \left[- \left(\frac{\ell' - \beta_3}{\beta_1} \right) \right] \quad (C.9)$$

where β_1 , β_2 and β_3 are parameters which can be estimated by the method of moments as

$$\beta_2 = (2/\gamma_{\ell})^2 \quad (C.10)$$

$$\beta_1 = \sigma_{\ell} / \sqrt{\beta_2} \quad (C.11)$$

$$\beta_3 = \mu_{\ell} - \frac{\sigma_{\ell}}{\sqrt{\beta_2}} \quad (C.12)$$

where μ_{ℓ} , σ_{ℓ} and γ_{ℓ} are the mean, standard deviation, and skew coefficient of loading. The CDF is

$$F_{\ell}(\ell) = \int_{\beta_3}^{\ell} \frac{1}{\beta_1 \Gamma(\beta_2)} \cdot \left(\frac{\ell' - \beta_3}{\beta_1} \right)^{\beta_2 - 1} \cdot \exp \left[- \left(\frac{\ell' - \beta_3}{\beta_1} \right) \right] d\ell' \quad (C.13)$$

By letting $s = (\ell - \beta_3) / \beta_1$, the Pearson type III distribution becomes a one parameter Gamma distribution. The CDF of the one parameter gamma distribution is called the incomplete gamma function.

The static reliability of the hydraulic structure under these loading and resistance conditions is expressed as

$$R = \int_0^{\infty} \frac{1}{\sqrt{2\pi} r' \sigma_{\ln r}} \cdot \exp \left[-\frac{1}{2} \left(\frac{\ln r' - \mu_{\ln r}}{\sigma_{\ln r}} \right)^2 \right] \cdot \left\{ \int_0^{r'} \frac{1}{\beta_1 \Gamma(\beta_2)} \cdot \left(\frac{r' - \beta_3}{\beta_1} \right)^{\beta_2 - 1} \cdot \exp \left[-\left(\frac{r' - \beta_3}{\beta_1} \right) \right] d r' \right\} dr' \quad (C.14)$$

C.4. Log-Pearson Type III Distributed Loading and Log-normally Distributed Resistance

The probability density function for the log-Pearson type III is

$$f_{\ell}(\ell') = \frac{1}{\beta_1 \cdot \ell' \cdot \Gamma(\beta_2)} \cdot \left(\frac{\ln \ell' - \beta_3}{\beta_1} \right)^{\beta_2 - 1} \cdot \exp \left[-\left(\frac{\ln \ell' - \beta_3}{\beta_1} \right) \right] \quad (C.15)$$

where β_1 , β_2 and β_3 are the parameters which can be determined by Eq. (C.10), (C.11) (C.12) except that μ_{ℓ} , σ_{ℓ} , and γ_{ℓ} are replaced by $\mu_{\ln \ell}$, $\sigma_{\ln \ell}$, and $\gamma_{\ln \ell}$, respectively.

The corresponding static reliability can be expressed as

$$R = \int_0^{\infty} \frac{1}{\sqrt{2\pi} r' \sigma_{\ln r}} \cdot \exp \left[-\frac{1}{2} \left(\frac{\ln r' - \mu_{\ln r}}{\sigma_{\ln r}} \right)^2 \right] \cdot F_{\ell}(r') \cdot dr' \quad (C.16)$$

where $F_{\ell}(r')$ is the CDF of log-Pearson type III distribution,

$$F_{\ell}(r) = \int_{\beta_3}^{r'} \frac{1}{\beta_3 \cdot \ell' \cdot \Gamma(\beta_2)} \cdot \left(\frac{\ln \ell' - \beta_3}{\beta_1} \right)^{\beta_2 - 1} \cdot \exp \left[- \left(\frac{\ln \ell' - \beta_3}{\beta_1} \right) \right] d\ell'$$

(C.17)

APPENDIX D

USER'S MANUAL FOR COMPUTER PROGRAM "RECVLVT"

The main function of this program, RECVLVT, is to generate the risk-safety factor relationships for highway culverts. Two types of culverts, i.e., circular and box, are considered. Options for treating hydrologic parameter uncertainty and various loading distributions commonly used in hydrological analysis are included. In addition to the hydrologic uncertainty, the variables with uncertainty in computing the capacity of the culvert are the width and depth of box culverts, the diameter of circular culverts, length of the barrel, longitudinal slope of the culvert, surface roughness, and maximum permissible head water elevation. The regression equations for the regional parameter estimates are valid only for the state of Texas.

In this computer program the field length of all input variable is 8, i.e., field 1 is columns 1-8, field 2 is columns 9-16 and so on. The arrangement and descriptions of the input cards are given as follows.

<u>Card Number</u>	<u>Variables</u>
A	ID, XID
B	XA, XSL, XST, XL, XI, XNN, XR
C	MODEL, METHOD, ITYPE, LDIST, NSIZE, MBOOT
D	XLENH, XLNTOL, XLDIST, CLN
E	BSLOPE, BSLPTOL, BSLDIST, CBS
F	AN, ANTOL, ANDIST, CAN
G	HDWTR, HDWTOL, HDWDIST, CHD
H	DIATOL, DIADIST, CDIA
I	WIDTOL, WIDIST, CWD
J	DEPTOL, DPDIST, CDP
K	COVM, XLAM
L	QFLOW(1), QFLOW(2), . . . QFLOW(NSIZE)

M PRIOPN, PRIOPLN, PIORPET, PRIOPP, PRIOPLP
 N NPROB, TRET(1), TRET(2), . . . , TRET(NPROB)
 O NLIFE, SLIFE(1), SLIFE(2), . . . , SLIFE(NLIFE)

The A card gives the gaging station identification for the stream-flow data.

<u>Field</u>	<u>Variable</u>	<u>Value</u>	<u>Description</u>
1	ID	+	Streamflow gaging station number
2	XID	+	Alphabetical characters for the location of gaging station (maximum 50 characters)

The B card contains physiographic and meteorologic characteristics of the drainage basin associated with the gaging station.

<u>Field</u>	<u>Variable</u>	<u>Value</u>	<u>Description</u>
1	XA	+	Contributing drainage area, in sq. miles
2	XSL	+	Main channel slope (85 to 10 percent points), in feet per mile
3	XST	+	Percentage of surface storage area, increased by 1 percent.
4	XL	+	Total length of main channel, in miles.
5	XI	+	10-year, 24-hour rainfall intensity, in inches.
6	XNN	+	Mean annual number of thunder-storm days.
7	XR	+	Ratio of runoff to precipitation during months when annual peak discharges occur in in/in.

The C card is the job option card specifying various options provided in the program.

<u>Field</u>	<u>Variable</u>	<u>Value</u>	<u>Description</u>
1	MODEL	1	Static reliability model
		2	Time-dependent reliability model
2	METHOD	0	Method used to compute the parameter estimates in the hydrologic loading probability model; Sample statistics only
		1	Weighting procedure using jackknife and regression analysis
		2	Weighting procedure using bootstrap and regression analysis
3	ITYPE	0	Type of culvert considered; Circular culvert
		1	Box culvert
4	LDIST	1	Loading probability distribution of flood sequences; Normal distribution
		2	Log-normal distribution
		3	Gumbel distribution
		4	Pearson type III distribution
		5	Log-Pearson type III distribution
		6	Composite distribution of above five individual distributions
5	NSIZE	+	Number of streamflow records
6	MBOOT	+	Number of bootstrap samples to be generated (required only when METHOD = 2).

The D card contains the nominal value, tolerance, type of simple distribution (Fig. 4.3) and the mode for the length of culvert barrel, L.

<u>Field</u>	<u>Variable</u>	<u>Value</u>	<u>Description</u>
1	XLENH	+	The nominal value of L
2	XLNTOL	+	Tolerance of L
3	XLDIST		Type of distribution for L;
		1	Rectangular distribution, Fig. 4.3a
		2	Symmetric triangular distribution, Fig. 4.3b
		3	Triangular distribution with mode at w_u , Fig. 4.3c.
		4	Triangular distribution with mode at w_l , Fig. 4.3d.
		5	Triangular distribution with mode w_c , Fig. 4.3e.
4	CLN	+	Mode of the distribution of L (required only when XLDIST = 5; otherwise, 0)

Cards E, F and G have the same input form as D card. The E card contains the nominal value (BSLOPE), tolerance (BSLPTOL), type of distribution (BSLDIST), Fig. 4.3, and mode (CBS) for the longitudinal slope of the culvert barrel. The F card contains the nominal value (AN), tolerance (ANTOL), type of simple distribution (ANDIST), Fig. 4.3, and mode (CAN) for the surface roughness of the culvert, n , in Eq. (2.8). The G card contains the nominal value (HDWTR), tolerance (HDWTOL), type of simple distribution (HDWDIST), Fig. 4.3, and mode (CHD) for the permissible head water elevation, Y_u in eq. (2.42).

The G card contains the tolerance, type of distribution, Fig. 4.3, and mode for the culvert diameter (required when ITYPE = 0). Nominal

value of diameter is set in the program, ranging from one foot to three feet while the number of barrels ranges from one to seven.

<u>Field</u>	<u>Variable</u>	<u>Value</u>	<u>Description</u>
1	DIATOL	+	Tolerance of culvert diameter
2	DIADIST	+	Type of distribution used (integer-valued)
3	CDIA	+	Mode of culvert diameter.

The next two cards, I and J, are required when ITYPE = 1. The I card contains the tolerance, type of distribution, Fig. 4.3, and mode for the width of culvert barrel.

<u>Field</u>	<u>Variable</u>	<u>Value</u>	<u>Description</u>
1	WIDTOL	+	Tolerance of culvert width
2	WIDIST	+	Type of distribution (integer-valued).
3	CWID	+	Mode of culvert width

The J card contains the tolerance (DEPTOL), type of distribution (DPDIST) Fig. 4.3, and mode (CDP) for the depth of culvert barrel. It has the same form of input as I card.

The K card contains the coefficient of variation and mean of the hydraulic model correction factor, λ_m .

<u>Field</u>	<u>Variable</u>	<u>Value</u>	<u>Description</u>
1	COVM	+	Coefficient of variation of λ_m
2	XLAM	+	Mean of λ_m .

The L cards input the stream flow record.

<u>Field</u>	<u>Variable</u>	<u>Value</u>	<u>Description</u>
1	QFLOW(1)	+	Flow magnitude of 1st record
2	QFLOW(2)	+	Flow magnitude of 2nd record
⋮	⋮	⋮	⋮
10	QFLOW(10)	+	Flow magnitude of 10th record.

Each card contains ten flow records. Continue using additional cards until total length of record, NSIZE, are read.

The M card contains the prior probability for the flood loading distribution (required only when LDIST=6).

<u>Field</u>	<u>Variable</u>	<u>Value</u>	<u>Description</u>
1	PRIOPN	+	Prior probability for normal distribution
2	PRIOPLN	+	Prior probability for lognormal distribution
3	PRIOPET	+	Prior Probability for Gumbel distribution
4	PRIOPP	+	Prior probability for Pearson III distribution
5	PRIOPLP	+	Prior probability for log-Pearson III distribution

The N card contains the design return periods to be considered in developing the risk-safety factor curves. It is required for considering both the static case and the time-dependent case.

<u>Field</u>	<u>Variable</u>	<u>Value</u>	<u>Description</u>
1	NPROB	+	Number of design return periods to be considered.
2	TRET(1)	+	Design return period 1
.	.	.	.
.	.	.	.
.	.	.	.
7	TRET(2)	+	Design return period 7

Maximum number of design return periods considered is seven in each run.

The last card, O card, is required only when time-dependent risk model is desired, i.e., MODEL = 2.

<u>Field</u>	<u>Variable</u>	<u>Value</u>	<u>Description</u>
1	NLIFE	+	Number of service life of structure considered.
2	SLIFE(1)	+	Service life 1
.	.	.	.
.	.	.	.
.	.	.	.
8	SLIFE(7)	+	Service life 7.

Maximum value of NLIFE is seven in each run.

APPENDIX E

LISTING OF COMPUTER PROGRAM FOR GENERATING
RISK-SAFETY FACTOR RELATIONSHIPS FOR HIGHWAY CULVERTS

- " RECVLT "


```

COMMON/HRK KZAMIDTH,ADOPFN,AKLENH,ANSLOPE,AIN,ANDHTD,AFSLOPE,ADIAN
COMPUTE THE MEAN AND THE C.O.V. OF DIAMETER OF CULVERT, AND
HEADWATER ELEVATION RESPECT TO THE TOLERANCE AND TYPE OF
DISTRIBUTION SPECIFIED.
ADIAN = DIAH
C2 = P
A3 = 0
A4 = 0
A5 = 0
CALL STATIS,ADIAN,P,AY,AN,AS,DIATOL,0,0,0,0,DIADIST,9,9,9,9,9
ADIAN,ADIAN
DOFFX3)
COMPUTE THE AREA OF CULVERT
AREA = 0.7854X9A*ADIAN*ADIAN*HRARS
COMPUTE THE HYDRAULIC RADIUS
HYDR = ADIAN/4.
FIND THE HEADWATER ELEVATION BY UTILIZING THE VOLUME-STAGE
RELATIONSHIP OF STORED WATER BEHIND THE CULVERT.
ASSUMPTION IS MADE BY CONSIDERING THAT WHEN HEADWATER ELEVATION
EXCEEDS THE DEPTH OF CULVERT THE FLOW IS FULL FLOW OTHERWISE
FRICTION SLOPE IS EQUALLED TO BOTTOM SLOPE.
DMS = 1.486*AFR*AHYDR*AD,AD7*SBOTR(SLOPE)/AN*XI*AN
QWATTO = Q1/ZORS
IF(QWATTO .GT. 0.1) GO TO 109
IF(QWATTO .GT. 1.1) OR, QWATTO .LT. 0.3) GO TO 111
109 JTYPE=0
CALL COMPFITTYPE,HRARS,AREA,HYDR)
QCM1,0RS,AN,AFR*AHYDR*AD,AD7*SBOTR(SLOPE)/AN*XI*AN
SAFETY FACTOR GREATER THAN UNITY IS DESIRED
IF(COEF1 .GT. 0.1) GO TO 110
IF(COEF1 .LT. 0.1) GO TO 111
COMPUTE THE COEFFICIENT OF VARIATION OF QC
110 COVOC = SQRT((COV1*COV1+0.35*(COV1*COV1+COV1*COV1)*.11*COV1A*
-COV1A3)
CALCULATE THE VALUE OF SAFETY FACTOR
SF=QCM/QT1
CALL RELSIA(MOD1,LOI1,IRISK,OLMH,OLSD,OLSK,XMIN,QCM,COVOC,IRET,
-SLIFE,RELIAN)

```

```

RELIAN = 1.0 - RELIAN
GO TO 112
111 FTYPE=0
112 CONTINUE
DEFIN
----- RELIAX
THIS SUBROUTINE COMPUTE THE RISK OR RELIABILITY OF HYDRAULIC
STRUCTURE. ( THE DISTRIBUTION OF RESISTANCE IS TAKEN TO BE
LOG-NORMAL.)
FORMSIE
MODEL = (1) STATIC, OR (2) TIME-DEPENDENT.
LOI1 = DISTRIBUTION OF LOADINGS, (1) NORMAL, (2) LOG-NORMAL,
(3) GUMBEL, (4) PEARSON III, (5) LOG-PEARSON III, OR
(6) COMPOSITE.
IRISK = (1) HYDROLOGIC RISK CONSIDERED, OR (2) OVERALL RISK
CONSIDERED.
OPFN = MEAN OF THE LOADING
OLSD = STAN. DEV. OF THE LOADING
OLSK = SAFTESS OF THE LOADING
XMIN = MIN. VALUE OF LOADING CONSIDERED ( REQUIRED ONLY WHEN
LOI1=0,5,00 6)
QCM = MEAN OF STRUCTURE CAPACITY
COVOC = C.O.V. OF CAPACITY
THEY = RETURN PERIOD OF DESIGN FLOOD ( FOR MODEL=2)
SLIFE = SERVICE LIFE OF STRUCTURE (FOR MODEL=2)
OUTPRT=
RELI = RELIABILITY OF STRUCTURE
RELI = 1.0 - RELI
SUBROUTINE SUBROUTINE OF
SUBROUTINE RELSTAT(MOD1,LOI1,IRISK,OLMH,OLSD,OLSK,XMIN,QCM,COVOC,
,RET,SLIFE,RELI)
RELI = 0.0
DEFIN .(0, 1) GO TO 540
COMPUTE THE STANDARD DEVIATION OF LOGS OF QC
QCLSD = SQRTALOG(COVOC+COVOC * 1.1)
COMPUTE THE MEAN OF LOGS OF QC
XX = SQRT(2.3*1.015)*QCLSD
DEFIN UPPER BOUND OF QC FOR NUMERICAL INTEGRATION
QCLP = QCLSD*Y
QCM = FPDF(QCLP+QCLM)
DEFIN QCM/50
QC = -R.9994DF1(QC
DO 555 1131,51
QC = QCM*DF1(QC
FPRM1 = /LOG(XKX)
FPRM2 = /LOG(QC)-DF1(X)/QCLSD
FPRM3 = X*(-0.5*FPRM2+EXP12)
CALL DEFIN(IRET,OC,OLPM,OLSD,OLSK,XMIN,IFRM3)

```

```

IF(MODEL,FO,1) GO TO 528
P=SLIFEZ/REI
TERMSXP=(PPA(1)-TERM3)
528 RELIEXP=TERMSXP/REI;DQ=OC
IF(1,FO,1,OP,11,FO,51) RFL=REL/2.
555 CONTINUE
GO TO 560
560 CALL COP(LEIAT,OCM,OLMN,OLSD,OLSK,XMIN,RELI)
C
C COMPUTE THE RELIABILITY OF THE STRUCTURE OVER THE PERIOD
C (O,SLIFE) WITH THE RATE OF OCCURRENCE OF DESIGN EVENT OF 1/TP
C
IF(MODEL,FO,1) GO TO 578
OLSK1=RELI
RELI=SP(-SLIFE*OLSK/TP)
578 CONTINUE
RETURN
END
----- CDF
THIS SUBROUTINE INTEGRATES THE PROBABILITY FUNCTION
INPUTS I - PROBABILITY DENSITY FUNCTION I (1)NORMAL, (2) LOG-
NORMAL, (3) GUMBEL, (4) PEARSON III, OR (5) LOG-
PEARSON III.
OX - ARGUMENT TO WHICH IS TO BE INTEGRATED
OLMN - THE MEAN IN THE PROBABILITY FUNCTION
OLSD - THE STANDARD DEVIATION
OLSK - THE SKEW COEFFICIENT
OUTPUT I - CUMULATIVE PROBABILITY
CUMPROR - CUMULATIVE PROBABILITY
REQUIRED SUBROUTINES - HOGAN,ALGAMA
SUBROUTINE COP(LEIAT,OX,OLMN,OLSD,OLSK,XMIN,CUMPROR)
IF(LEIAT,FO,3) GO TO 288
IF(LEIAT,FO,4) GO TO 388
IF(LEIAT,FO,5) GO TO 388
C
C COMPUTE C.D.F. OF NORMAL OR LOG-NORMAL DISTRIBUTION
C
IF(LEIAT,FO,2) OX=ALG(OX)
Z=OX-OLMN/OLSD
IF7,FO,0.1 CUMPROR=0.5
IF7,FO,0.3 GO TO 500
IF7,FO,0.5 GO TO 500
IF7,FO,1.0,1.09,11,FO,21) TERM=1/ERF(Z)
CUMPROR=CUMPROR+TERM
IF7,FO,0.3 CUMPROR=0.5+CUMPROR
IF7,FO,0.5 CUMPROR=0.5+CUMPROR
IF(LEIAT,FO,2) OX=EXP(OX)

```

1
1
1
1
1

```

GO TO 588
C
C COMPUTE C.D.F. OF GUMBEL DISTRIBUTION
C
288 ALPHA1,2A3/OLSD
RELIEXP=0.5772/ALPHA
CUMPROR=EXP(-EXP(-ALPHA))
GO TO 588
C
C COMPUTE C.D.F. OF PEARSON TYPE III AND LOG-PEARSON TYPE III
C DISTRIBUTION
C
388 IF(LEIAT,FO,5) OX=ALG(OX)
XMIN=MIN(OLSK*(1-Z/OLSK)
PAR=101.50/SBL(1,PAR)2
PAR=OLSK*OLSD/OLMN/PAR2
IF(LEIAT,FO,5) XMIN=ALG(XMIN)
IF(PAR,GT,5) PAR=5
PAR=0.94*PAR
IF(OX,LT,PAR) GO TO 555
OX=(OX-PAR)/PAR
CALL HOGAN(OCM,PAR2,CUMPROR,IF)
C
C
IF(LEIAT,FO,5) OX=EXP(OX)
GO TO 588
555 CUMPROR=0
588 CONTINUE
RETURN
END
SUBROUTINE STAT(OL,X1,X2,X3,X4,X5,Y1,Y2,Y3,Y4,Y5,Z1,Z2,Z3,Z4,
Z5,C1,C2,C3,C4,C5,COVX1,COVX2,COVX3,COVX4,COVX5)
INTEGER Z1,Z2,Z3,Z4,Z5,Z7,Z0
DIMENSION XX(10),YY(10),ZZ(10),CC(10),XX(10),XCOV(10)
XX(1) = X1
XX(2) = X2
XX(3) = X3
XX(4) = X4
XX(5) = X5
YY(1) = Y1
YY(2) = Y2
YY(3) = Y3
YY(4) = Y4
YY(5) = Y5
ZZ(1) = Z1
ZZ(2) = Z2
ZZ(3) = Z3
ZZ(4) = Z4
ZZ(5) = Z5
CC(1) = C1
CC(2) = C2
CC(3) = C3
CC(4) = C4
CC(5) = C5
DO 11 I=1,N1

```



```

SIGN = 1.0
IF (AMOD(2.0) .EQ. 0.0) SIGN = -1.0
N = 1-N
IF (0.0E+00) GO TO 15
ALGAMA = TIME
GO TO 0000
15 N = PI/SIN(0.0PI)*SIGN
  Y = 1.0/N
  R = LOG(CABS(R))
20 IF (1.0E+12.0) GO TO 10
  IF (1.0E+00) GO TO 00
  IF (1.0E+53) GO TO 50
  IF (1.0E+00.5) GO TO 35
  R = -ALOG(1.0)
  Y = 1.0/N
  IF (A.G.F.FP8) GO TO 00
  ALGAMA = R
  GO TO 0005
35 TOP = 1-0.5
  R = 0.0
  A = TOP-0.5
40 TOP = PI*(1.0E+11)+PI*(1.0E+00)
  DEN = 1.0E+11.0E+00
  GO 05 1.0E+11.0E+00
  TOP = TOP+PI*(1.0E+11)
  DEN = DEN+PI*(1.0E+11)
45 CONTINUE
  Y = (TOP/DEN)*A+B
  IF (FLAG) Y = B-Y
  ALGAMA = Y
  GO TO 0005
50 R = 1-1.0
  A = B-1.0
  TOP = PI*(1.0E+11)+PI*(1.0E+00)
  DEN = 1.0E+11.0E+00
  GO 55 1.0E+11.0E+00
  TOP = TOP+PI*(1.0E+11)
  DEN = DEN+PI*(1.0E+11)
55 CONTINUE
  Y = (TOP/DEN)*A
  IF (FLAG) Y = B-Y
  ALGAMA = Y
  GO TO 0005
60 TOP = PI*(1.0E+11)+PI*(1.0E+00)
  DEN = 1.0E+11.0E+00
  GO 65 1.0E+11.0E+00
  TOP = TOP+PI*(1.0E+11)
  DEN = DEN+PI*(1.0E+11)
65 CONTINUE
  Y = (TOP/DEN)
  IF (FLAG) Y = B-Y
  ALGAMA = Y
  GO TO 0005

```

```

70 TOP = ALOG(1.0)
TOP = (1-1.5)*(TOP-1.0)+TOP-1.5
  Y = 1.0/1
  IF (1.0E+12.0) GO TO 75
  B = 1.0
  TOP = ((PI*(1.0E+11)+PI*(1.0E+00))*TOP-1.0)+TOP
  IF (FLAG) Y = B-Y
  ALGAMA = Y
  GO TO 0005
0000 CONTINUE
  IF (1.0E+12.0) PRINT 00
  IF (1.0E+12.0) PRINT 05
  GO FORW(1.0E+12.0), THE INPUT ARGUMENT X TO ALGAMA WAS SPECIFIED G
  AFTER THIS FOR F001 TO 0005. THE ALGAMA IS SET TO MACHINE INFINIT
  Y.
  IF (1.0E+12.0) PRINT 00
  IF (1.0E+12.0) PRINT 05
  GO FORW(1.0E+12.0), THE INPUT ARGUMENT X TO ALGAMA WAS SPECIFIED A
  NEGATIVE INTEGER. THE ALGAMA IS SET TO MACHINE INFINIT
  Y.
0005 RETURN
END

```

```

75 Y = TOP/0.001
  IF (FLAG) Y = B-Y
  ALGAMA = Y
  GO TO 0005

```

```

75 Y = TOP/0.001
  IF (FLAG) Y = B-Y
  ALGAMA = Y
  GO TO 0005

```

APPENDIX F

USER'S MANUAL FOR COMPUTER PROGRAM "RELEVEE"

The main function of this program is to generate the risk and safety factor relationship for flood levees. The assumptions and hydraulic model used to compute the levee capacity are described in detail in chapter 4. The variables with uncertainty in computing the levee capacity are identified in chapter 4. Note that the regression equations used in the program are only valid for the State of Texas, which are derived in Eqs. (3.27) through (3.32). Basically the sequence of input cards follow very much the same as those of previous program, Appendix C. The field length of all input variables is also 8. The arrangement and descriptions of the input cards are presented as follows.

<u>Card Number</u>	<u>Variables</u>
A	ID, XID
B	XA, XSL, XST, XL, XI, XNN, XR
C	MODEL, METHOD, LDIST, NSIZE, MBOOT
D	ZSLOPE
E	XLAM, XLAMTOL, LAMDIST, CXLAM
F	WDCH, WDCHTOL, WDCHDST, CWDCH
G	SCH, SCHTOL, SCHDIST, CSCH
H	NCH, NCHTOL, NCHDIST, CNCH
I	ACH, ACHTOL, ACHDIST, CACH
J	ANG, ANGTOL, ANGDIST, CANG
K	SBK, SBKTOL, SBKDIST, CSBK
L	NBK, NBKTOL, NBKDIST, CNBK
M	QFLOW(1), QFLOW(2), . . . , QFLOW(NSIZE)
N	PRIOPN, PRIOPLN, PRIOPET, PRIOPP, PRIOPLP
O	NPROB, TRET(1), . . . , TRET(NPROB)
P	NLIFE, SLIFE(1), . . . , SLIFE(NLIFE)

The A card is for station identification.

<u>Field</u>	<u>Variable</u>	<u>Value</u>	<u>Description</u>
1	ID	+	Streamflow gaging station number
2-7	XID	+	Alphabetic character for the location of gaging station (maximum 50 characters)

B card contains physiographic and meteorologic characteristics for the drainage basin associated with the gaging station investigated.

<u>Field</u>	<u>Variable</u>	<u>Value</u>	<u>Description</u>
1	XA	+	Contributing drainage area, in sq. miles.
2	XSL	+	Main channel slope (85 to 10 percent points) in feet per mile.
3	XST	+	Percentage of surface storage area, increased by 1 percent.
4	XL	+	Total length of main channel, in miles.
5	XI	+	10-year, 24-hour rainfall intensity, in inches.
6	XNN	+	Mean annual number of thunderstorm days
7	XR	+	Ratio of runoff to precipitation during months when annual peak discharges occur in in/in.

The C card is the job option card specifying various options provided in the program.

<u>Field</u>	<u>Variable</u>	<u>Value</u>	<u>Description</u>
1	MODEL	1	Static reliability model
		2	Time-dependent reliability model
2	METHOD	0	Method used to compute the parameter estimates in hydrologic loading probability model; Sample statistics only
		1	Weighting procedure using jackknife and regression analysis,
		2	Weighting procedure using bootstrap and regression analysis
3	LDIST	1	Loading probability distribution of flood magnitudes; Normal distribution,
		2	Log-normal distribution,
		3	Gumbel distribution,
		4	Pearson type III distribution,
		5	Log-Pearson type III distribution, and
		6	Composite distribution of above five individual distribution
4	NSIZE	+	Number of streamflow records
5	MBOOT	+	Number of bootstrap samples to be generated (required only when METHOD=2)

The D card contains only one variable, ZSLOPE, the side slope of the levee embankment on the river face.

<u>Field</u>	<u>Variable</u>	<u>Value</u>	<u>Description</u>
1	ZSLOPE	+	Side slope of the levee embankment on the river side, ft/ft.

The E card contains the nominal value, tolerance, type of distribution (Fig. 4.3) and mode of hydraulic model correction factor, λ_m , in Eq. (4.1).

<u>Field</u>	<u>Variable</u>	<u>Value</u>	<u>Description</u>
1	XLAM	+	The nominal value of λ_m .
2	XLAMTOL	+	Tolerance of λ_m .
3	LAMDIST	1	Type of distribution for λ_m . Rectangular distribution, Fig. 4.3a,
		2	Symmetric triangular distribution, Fig. 4.3b,
		3	Triangular distribution with mode at w_u , Fig. 4.3c,
		4	Triangular distribution with mode at w_l , Fig. 4.3d,
		5	Triangular distribution with mode at w_c , Fig. 4.3e.
4	CXLAM	+	Mode of λ_m (required only when LAMDIST = 5; otherwise, 0)

The F card contains the nominal value, tolerance, type of distribution (Fig. 4.3) and mode for the top width of the channel.

<u>Field</u>	<u>Variable</u>	<u>Value</u>	<u>Description</u>
1	WDCH	+	Nominal value of channel top width
2	WDCHTOL	+	Tolerance of channel top width
3	WDCHDST	+	Type of distribution of channel top width (integer-valued)
4	CWDCH	+	Mode of channel top width

The G card contains the nominal value, tolerance, type of distribution (Fig. 4.3) and mode for the longitudinal channel bottom slope, S_o .

<u>Field</u>	<u>Variable</u>	<u>Value</u>	<u>Description</u>
1	SCH	+	Nominal value of S_o
2	SCHTOL	+	Tolerance of S_o
3	SCHDIST	+	Type of distribution of S_o (integer-valued)
4	CSCH	+	Mode of S_o

The H card contains the nominal value, tolerance, type of distribution (Fig. 4.3) and mode for Manning's roughness of the channel, N_c .

<u>Field</u>	<u>Variable</u>	<u>Value</u>	<u>Description</u>
1	NCH	+	Nominal value of N_c (real-valued)
2	NCHTOL	+	Tolerance of N_c (real-valued)
3	NCHDIST	+	Type of distribution of N_c
4	CNCH	+	Mode of N_c

The I card contains the nominal value, tolerance, type of distribution (Fig. 4.3) and mode for full bank flow cross sectional area, A_{fb} .

<u>Field</u>	<u>Variable</u>	<u>Value</u>	<u>Description</u>
1	ACH	+	Nominal value of A_{fb}
2	ACHTOL	+	Tolerance of A_{fb}
3	ACHDIST	+	Distribution of A_{fb} (interger-valued)
4	CACH	+	Mode of A_{bf}

The J card contains the nominal value, tolerance, type of distribution (Fig. 4.3) and mode for the traverse slope of the flood plain, τ .

<u>Field</u>	<u>Variable</u>	<u>Value</u>	<u>Description</u>
1	ANG	+	Nominal value of τ
2	ANGTOL	+	Tolerance of τ
3	ANGDIST	+	Distribution of τ (integer-valued)
4	CANG	+	Mode of τ

The K card contains the nominal value, tolerance, type of distribution (Fig. 4.3) and mode for the longitudinal slope of flood plain, S_b .

<u>Field</u>	<u>Variable</u>	<u>Value</u>	<u>Description</u>
1	SBK	+	Nominal value of S_b
2	SBKTOL	+	Tolerance of S_b
3	SBKDIST	+	Distribution of S_b (integer-valued)
4	CSBK	+	Mode of S_b

The L card contains the nominal value, tolerance, type of distribution (Fig. 4.3) and mode of the Manning's roughness in the flood plain, N_b .

<u>Field</u>	<u>Variable</u>	<u>Value</u>	<u>Description</u>
1	NBK	+	Nominal value of N_b
2	NBKTOL	+	Tolerance of N_b
3	NBKDIST	+	Distribution of N_b (integer-valued)
4	CNBK	+	Mode of N_b

The M cards input the stream flow record.

344

<u>Field</u>	<u>Variable</u>	<u>Value</u>	<u>Description</u>
1	QFLOW(1)	+	Flow magnitude of 1st record
2	QFLOW(2)	+	Flow magnitude of 2nd record
.	.	.	.
.	.	.	.
.	.	.	.
10	QFLOW(10)	+	Flow magnitude of 10th record

Each card contains ten flow records. Continue using additional cards until total length of record, NSIZE, are read.

The N card contains the prior probability for the flood loading distribution (required only when LDIST = 6).

<u>Field</u>	<u>Variable</u>	<u>Value</u>	<u>Description</u>
1	PRIOPN	+	Prior probability for normal distribution
2	PRIOPLN	+	Prior probability for lognormal distribution
3	PRIOPET	+	Prior probability for Gumbel distribution
4	PRIOPP	+	Prior probability for Pearson III distribution
5	PRIOPLP	+	Prior probability for log-Pearson III distribution

The O card contains the design return periods to be considered in developing the risk-safety factor curves. It is required for considering both static case and time-dependent case.

<u>Field</u>	<u>Variable</u>	<u>Value</u>	<u>Description</u>
1	NPROB	+	Number of design return periods to be considered
2	TRET(1)	+	Design return period 1
.	.	.	.
.	.	.	.
.	.	.	.
8	TRET(7)	+	Design return period 7

Maximum number of design return periods considered is seven in each run.

The last card, P card, is required only when time-dependent risk model is desired, i.e., MODEL=2.

<u>Field</u>	<u>Variable</u>	<u>Value</u>	<u>Description</u>
1	NLIFE	+	Number of service life of structure considered
2	SLIFE(1)	+	Service life 1
.	.	.	.
.	.	.	.
.	.	.	.
8	SLIFE(7)	+	Service life 7

Maximum value of NLIFE is seven in each run.

APPENDIX G

LISTING OF COMPUTER PROGRAM FOR GENERATING
RISK-SAFETY FACTOR RELATIONSHIP FOR FLOOD LEVEES

- " RELEVVEE "


```

15 REMARK
16 PRTOP
17 PRC
18 INSL ROUTINE NAME - MCGAM
19 -----
20 PURPOSE - GAMMA PROBABILITY DISTRIBUTION FUNCTION
21 USAGE - CALL MCGAM (X,P,PROB,IFR)
22 ARGUMENTS X - INPUT VALUE TO WHICH GAMMA IS TO BE INTEGRATED
23 P - INPUT GAMMA PARAMETER
24 PROB - OUTPUT PROBABILITY THAT A RANDOM VARIABLE
25 HAVING A GAMMA DISTRIBUTION WITH PARAMETER P
26 WILL BE LESS THAN OR EQUAL TO X.
27 IFR - ERROR PARAMETER. (OUTPUT)
28 TERMINAL ERROR
29 IFR = 129 INDICATES Y IS LESS THAN ZERO.
30 IFR = 130 INDICATES P IS LESS THAN OR EQUAL
31 TO ZERO.
32 PRECISION/HARDWARE - SINGLE/ALL
33 MCGAM, INSL ROUTINES - MCGAM=ALGAMA, MERTIN, MGT10
34 NOTATION - INDICATION ON SPECIAL NOTATION AND
35 CONVENTIONS IS AVAILABLE IN THE MANUAL
36 INTRODUCTION OR THROUGH E-PSL ROUTINE UNFLP
37 WARRANTY - E-PSL HARDWARE ONLY THAT LOCAL TESTING HAS BEEN
38 APPLIED TO THIS CODE, NO OTHER WARRANTY,
39 EXPRESSED OR IMPLIED, IS APPLICABLE.
40 -----
41 SUBROUTINE MCGAM (X,P,PROB,IFR)
42 INPUT
43 X,P,PROB
44 REAL
45 V(6),V(14),PHI,G,CMT,VCNT,X-IN,X-R,PIC,CUT,
46 Y,Z,RATIO,REDUC
47 I(3),V(11)
48 DATA
49 XMIN=-678,65701986/
50 IFR = 0
51 IF (X .GT. 0) GO TO 5
52 IFR = 129
53 GO TO 9000
54 IF (P .GT. 0) GO TO 10
55 IFR = 130
56 GO TO 9000
57 IF (V .EQ. 0) GO TO 9000
58 IF (V .GT. 0) GO TO 9000
59 OFFLINE LOG-GAMMA AND INITIALIZE
60 PHIG = ALGAM(PT)
61 CMT = P * ALGOC(3)
62 VCNT = X * PHIG
63 -----
64 IF (CMT .EQ. 0) GO TO 15
65 AX = MCGAM
66 GO TO 20
67 IS AX * EXP(CMT-VCNT)
68 20 01G * 1.535
69 CUT * 1.5-A
70 -----
71 IF (CMT .EQ. 1.0) .OP. (Y .11. P 3) GO TO 40
72 CHOOSE ALGORITHMIC METHOD
73 CONTINUED FRACTION EXPANSION
74 Y = 1.0 - P
75 Z = X * Y * 1.0
76 CMT = 0.0
77 V(1) = 1.0
78 V(2) = X
79 V(3) = X * 1.0
80 V(4) = X * 7 * X
81 PHIG = VC(1)/VC(3)
82 Y = Y * 1.0
83 Z = Z * 2.0
84 YCMT = Y * CMT
85 V(5) = V(1) * Z - V(1) * YCMT
86 V(6) = V(2) * Z - V(2) * YCMT
87 V(7) = V(3) * Z - V(3) * YCMT
88 V(8) = V(4) * Z - V(4) * YCMT
89 RATIO = V(5)/V(6)
90 PHIG = PHIG * RATIO
91 REDUC = V(6)/V(8)
92 IF (REDUC .GT. 1.0) GO TO 10
93 IF (REDUC .LT. 1.0) GO TO 10
94 GO TO 50
95 PHOR = 1.0 - PHOR * 47
96 GO TO 9000
97 -----
98 RATIO = P
99 CMT = 1.0
100 PHOR = 1.0
101 RATIO = RATIO * 1.0
102 CMT = PHOR * CMT
103 IF (CMT .GT. 0) GO TO 95
104 PHOR = PHOR * 47
105 GO TO 9000
106 GO 50 5A 1.1.4
107 V(1) = V(1)
108 IF (ABS(V(5)) .LT. 1E-10) GO TO 25
109 SCALE TERMS DOWN TO PREVENT OVERFLOW
110 GO 50 1.1.0
111 V(1) = V(1)/PIC
112 CONTINUE
113 GO TO 25
114 CONTINUE
115 IFR = 129 PRINT 70
116 IFR = 130 PRINT 75
117 FOR (FOR, PHIG) INPUT VALUE X IN MCGAM TO WHICH GAMMA IS TO BE
118 INTEGRATED IS LESS THAN ZERO
119 FOR (FOR, PHIG) THE PARAMETER P IN GAMMA DISTRIBUTION IS LESS
120 THAN OR EQUAL TO ZERO
121 GIVE RETURN
122 END
123 -----
124 INSL ROUTINE NAME - MCGAM=ALGAMA
125 END

```



```

DATA
  IEND=0, IEND=1, IEND=2, IEND=3, IEND=4, IEND=5, IEND=6, IEND=7
  X1=1/3, X2=1/5, X3=1/7, X4=1/11, X5=1/13, X6=1/17, X7=1/19, X8=1/23, X9=1/29, X10=1/31, X11=1/37, X12=1/41, X13=1/43, X14=1/47, X15=1/53, X16=1/59, X17=1/61, X18=1/67, X19=1/71, X20=1/73, X21=1/79, X22=1/83, X23=1/89, X24=1/97, X25=1/101, X26=1/103, X27=1/107, X28=1/109, X29=1/113, X30=1/119, X31=1/127, X32=1/131, X33=1/137, X34=1/139, X35=1/143, X36=1/149, X37=1/151, X38=1/157, X39=1/163, X40=1/167, X41=1/173, X42=1/179, X43=1/181, X44=1/187, X45=1/191, X46=1/193, X47=1/197, X48=1/199, X49=1/211, X50=1/217, X51=1/223, X52=1/227, X53=1/229, X54=1/233, X55=1/239, X56=1/241, X57=1/247, X58=1/251, X59=1/257, X60=1/263, X61=1/269, X62=1/271, X63=1/277, X64=1/281, X65=1/283, X66=1/287, X67=1/293, X68=1/299, X69=1/307, X70=1/311, X71=1/313, X72=1/317, X73=1/323, X74=1/329, X75=1/331, X76=1/337, X77=1/341, X78=1/347, X79=1/353, X80=1/359, X81=1/367, X82=1/371, X83=1/373, X84=1/379, X85=1/383, X86=1/389, X87=1/397, X88=1/401, X89=1/403, X90=1/407, X91=1/409, X92=1/413, X93=1/419, X94=1/421, X95=1/427, X96=1/431, X97=1/433, X98=1/437, X99=1/439, X100=1/443, X101=1/449, X102=1/451, X103=1/457, X104=1/461, X105=1/463, X106=1/467, X107=1/471, X108=1/473, X109=1/479, X110=1/481, X111=1/483, X112=1/487, X113=1/491, X114=1/493, X115=1/497, X116=1/499, X117=1/503, X118=1/509, X119=1/511, X120=1/517, X121=1/521, X122=1/523, X123=1/527, X124=1/531, X125=1/533, X126=1/537, X127=1/541, X128=1/547, X129=1/551, X130=1/553, X131=1/557, X132=1/561, X133=1/563, X134=1/567, X135=1/571, X136=1/573, X137=1/577, X138=1/581, X139=1/583, X140=1/587, X141=1/591, X142=1/593, X143=1/597, X144=1/599, X145=1/603, X146=1/607, X147=1/609, X148=1/613, X149=1/617, X150=1/619, X151=1/623, X152=1/627, X153=1/631, X154=1/633, X155=1/637, X156=1/641, X157=1/643, X158=1/647, X159=1/649, X160=1/653, X161=1/657, X162=1/659, X163=1/663, X164=1/667, X165=1/671, X166=1/673, X167=1/677, X168=1/681, X169=1/683, X170=1/687, X171=1/691, X172=1/693, X173=1/697, X174=1/699, X175=1/703, X176=1/707, X177=1/709, X178=1/713, X179=1/717, X180=1/719, X181=1/723, X182=1/727, X183=1/731, X184=1/733, X185=1/737, X186=1/741, X187=1/743, X188=1/747, X189=1/749, X190=1/753, X191=1/757, X192=1/759, X193=1/763, X194=1/767, X195=1/769, X196=1/773, X197=1/777, X198=1/779, X199=1/783, X200=1/787, X201=1/789, X202=1/793, X203=1/797, X204=1/799, X205=1/803, X206=1/807, X207=1/809, X208=1/813, X209=1/817, X210=1/819, X211=1/823, X212=1/827, X213=1/831, X214=1/833, X215=1/837, X216=1/841, X217=1/843, X218=1/847, X219=1/849, X220=1/853, X221=1/857, X222=1/859, X223=1/863, X224=1/867, X225=1/869, X226=1/873, X227=1/877, X228=1/879, X229=1/883, X230=1/887, X231=1/889, X232=1/893, X233=1/897, X234=1/899, X235=1/903, X236=1/907, X237=1/909, X238=1/913, X239=1/917, X240=1/919, X241=1/923, X242=1/927, X243=1/931, X244=1/933, X245=1/937, X246=1/941, X247=1/943, X248=1/947, X249=1/949, X250=1/953, X251=1/957, X252=1/959, X253=1/963, X254=1/967, X255=1/969, X256=1/973, X257=1/977, X258=1/979, X259=1/983, X260=1/987, X261=1/989, X262=1/993, X263=1/997, X264=1/999, X265=1/1003, X266=1/1007, X267=1/1009, X268=1/1013, X269=1/1017, X270=1/1019, X271=1/1023, X272=1/1027, X273=1/1031, X274=1/1033, X275=1/1037, X276=1/1041, X277=1/1043, X278=1/1047, X279=1/1049, X280=1/1053, X281=1/1057, X282=1/1059, X283=1/1063, X284=1/1067, X285=1/1069, X286=1/1073, X287=1/1077, X288=1/1079, X289=1/1083, X290=1/1087, X291=1/1089, X292=1/1093, X293=1/1097, X294=1/1099, X295=1/1103, X296=1/1107, X297=1/1109, X298=1/1113, X299=1/1117, X300=1/1119, X301=1/1123, X302=1/1127, X303=1/1131, X304=1/1133, X305=1/1137, X306=1/1141, X307=1/1143, X308=1/1147, X309=1/1149, X310=1/1153, X311=1/1157, X312=1/1159, X313=1/1163, X314=1/1167, X315=1/1169, X316=1/1173, X317=1/1177, X318=1/1179, X319=1/1183, X320=1/1187, X321=1/1189, X322=1/1193, X323=1/1197, X324=1/1199, X325=1/1203, X326=1/1207, X327=1/1209, X328=1/1213, X329=1/1217, X330=1/1219, X331=1/1223, X332=1/1227, X333=1/1231, X334=1/1233, X335=1/1237, X336=1/1241, X337=1/1243, X338=1/1247, X339=1/1249, X340=1/1253, X341=1/1257, X342=1/1259, X343=1/1263, X344=1/1267, X345=1/1269, X346=1/1273, X347=1/1277, X348=1/1279, X349=1/1283, X350=1/1287, X351=1/1289, X352=1/1293, X353=1/1297, X354=1/1299, X355=1/1303, X356=1/1307, X357=1/1309, X358=1/1313, X359=1/1317, X360=1/1319, X361=1/1323, X362=1/1327, X363=1/1331, X364=1/1333, X365=1/1337, X366=1/1341, X367=1/1343, X368=1/1347, X369=1/1349, X370=1/1353, X371=1/1357, X372=1/1359, X373=1/1363, X374=1/1367, X375=1/1369, X376=1/1373, X377=1/1377, X378=1/1379, X379=1/1383, X380=1/1387, X381=1/1389, X382=1/1393, X383=1/1397, X384=1/1399, X385=1/1403, X386=1/1407, X387=1/1409, X388=1/1413, X389=1/1417, X390=1/1419, X391=1/1423, X392=1/1427, X393=1/1431, X394=1/1433, X395=1/1437, X396=1/1441, X397=1/1443, X398=1/1447, X399=1/1449, X400=1/1453, X401=1/1457, X402=1/1459, X403=1/1463, X404=1/1467, X405=1/1469, X406=1/1473, X407=1/1477, X408=1/1479, X409=1/1483, X410=1/1487, X411=1/1489, X412=1/1493, X413=1/1497, X414=1/1499, X415=1/1503, X416=1/1507, X417=1/1509, X418=1/1513, X419=1/1517, X420=1/1519, X421=1/1523, X422=1/1527, X423=1/1531, X424=1/1533, X425=1/1537, X426=1/1541, X427=1/1543, X428=1/1547, X429=1/1549, X430=1/1553, X431=1/1557, X432=1/1559, X433=1/1563, X434=1/1567, X435=1/1569, X436=1/1573, X437=1/1577, X438=1/1579, X439=1/1583, X440=1/1587, X441=1/1589, X442=1/1593, X443=1/1597, X444=1/1599, X445=1/1603, X446=1/1607, X447=1/1609, X448=1/1613, X449=1/1617, X450=1/1619, X451=1/1623, X452=1/1627, X453=1/1631, X454=1/1633, X455=1/1637, X456=1/1641, X457=1/1643, X458=1/1647, X459=1/1649, X460=1/1653, X461=1/1657, X462=1/1659, X463=1/1663, X464=1/1667, X465=1/1669, X466=1/1673, X467=1/1677, X468=1/1679, X469=1/1683, X470=1/1687, X471=1/1689, X472=1/1693, X473=1/1697, X474=1/1699, X475=1/1703, X476=1/1707, X477=1/1709, X478=1/1713, X479=1/1717, X480=1/1719, X481=1/1723, X482=1/1727, X483=1/1731, X484=1/1733, X485=1/1737, X486=1/1741, X487=1/1743, X488=1/1747, X489=1/1749, X490=1/1753, X491=1/1757, X492=1/1759, X493=1/1763, X494=1/1767, X495=1/1769, X496=1/1773, X497=1/1777, X498=1/1779, X499=1/1783, X500=1/1787, X501=1/1789, X502=1/1793, X503=1/1797, X504=1/1799, X505=1/1803, X506=1/1807, X507=1/1809, X508=1/1813, X509=1/1817, X510=1/1819, X511=1/1823, X512=1/1827, X513=1/1831, X514=1/1833, X515=1/1837, X516=1/1841, X517=1/1843, X518=1/1847, X519=1/1849, X520=1/1853, X521=1/1857, X522=1/1859, X523=1/1863, X524=1/1867, X525=1/1869, X526=1/1873, X527=1/1877, X528=1/1879, X529=1/1883, X530=1/1887, X531=1/1889, X532=1/1893, X533=1/1897, X534=1/1899, X535=1/1903, X536=1/1907, X537=1/1909, X538=1/1913, X539=1/1917, X540=1/1919, X541=1/1923, X542=1/1927, X543=1/1931, X544=1/1933, X545=1/1937, X546=1/1941, X547=1/1943, X548=1/1947, X549=1/1949, X550=1/1953, X551=1/1957, X552=1/1959, X553=1/1963, X554=1/1967, X555=1/1969, X556=1/1973, X557=1/1977, X558=1/1979, X559=1/1983, X560=1/1987, X561=1/1989, X562=1/1993, X563=1/1997, X564=1/1999, X565=1/2003, X566=1/2007, X567=1/2009, X568=1/2013, X569=1/2017, X570=1/2019, X571=1/2023, X572=1/2027, X573=1/2031, X574=1/2033, X575=1/2037, X576=1/2041, X577=1/2043, X578=1/2047, X579=1/2049, X580=1/2053, X581=1/2057, X582=1/2059, X583=1/2063, X584=1/2067, X585=1/2069, X586=1/2073, X587=1/2077, X588=1/2079, X589=1/2083, X590=1/2087, X591=1/2089, X592=1/2093, X593=1/2097, X594=1/2099, X595=1/2103, X596=1/2107, X597=1/2109, X598=1/2113, X599=1/2117, X600=1/2119, X601=1/2123, X602=1/2127, X603=1/2131, X604=1/2133, X605=1/2137, X606=1/2141, X607=1/2143, X608=1/2147, X609=1/2149, X610=1/2153, X611=1/2157, X612=1/2159, X613=1/2163, X614=1/2167, X615=1/2169, X616=1/2173, X617=1/2177, X618=1/2179, X619=1/2183, X620=1/2187, X621=1/2189, X622=1/2193, X623=1/2197, X624=1/2199, X625=1/2203, X626=1/2207, X627=1/2209, X628=1/2213, X629=1/2217, X630=1/2219, X631=1/2223, X632=1/2227, X633=1/2231, X634=1/2233, X635=1/2237, X636=1/2241, X637=1/2243, X638=1/2247, X639=1/2249, X640=1/2253, X641=1/2257, X642=1/2259, X643=1/2263, X644=1/2267, X645=1/2269, X646=1/2273, X647=1/2277, X648=1/2279, X649=1/2283, X650=1/2287, X651=1/2289, X652=1/2293, X653=1/2297, X654=1/2299, X655=1/2303, X656=1/2307, X657=1/2309, X658=1/2313, X659=1/2317, X660=1/2319, X661=1/2323, X662=1/2327, X663=1/2331, X664=1/2333, X665=1/2337, X666=1/2341, X667=1/2343, X668=1/2347, X669=1/2349, X670=1/2353, X671=1/2357, X672=1/2359, X673=1/2363, X674=1/2367, X675=1/2369, X676=1/2373, X677=1/2377, X678=1/2379, X679=1/2383, X680=1/2387, X681=1/2389, X682=1/2393, X683=1/2397, X684=1/2399, X685=1/2403, X686=1/2407, X687=1/2409, X688=1/2413, X689=1/2417, X690=1/2419, X691=1/2423, X692=1/2427, X693=1/2431, X694=1/2433, X695=1/2437, X696=1/2441, X697=1/2443, X698=1/2447, X699=1/2449, X700=1/2453, X701=1/2457, X702=1/2459, X703=1/2463, X704=1/2467, X705=1/2469, X706=1/2473, X707=1/2477, X708=1/2479, X709=1/2483, X710=1/2487, X711=1/2489, X712=1/2493, X713=1/2497, X714=1/2499, X715=1/2503, X716=1/2507, X717=1/2509, X718=1/2513, X719=1/2517, X720=1/2519, X721=1/2523, X722=1/2527, X723=1/2531, X724=1/2533, X725=1/2537, X726=1/2541, X727=1/2543, X728=1/2547, X729=1/2549, X730=1/2553, X731=1/2557, X732=1/2559, X733=1/2563, X734=1/2567, X735=1/2569, X736=1/2573, X737=1/2577, X738=1/2579, X739=1/2583, X740=1/2587, X741=1/2589, X742=1/2593, X743=1/2597, X744=1/2599, X745=1/2603, X746=1/2607, X747=1/2609, X748=1/2613, X749=1/2617, X750=1/2619, X751=1/2623, X752=1/2627, X753=1/2631, X754=1/2633, X755=1/2637, X756=1/2641, X757=1/2643, X758=1/2647, X759=1/2649, X760=1/2653, X761=1/2657, X762=1/2659, X763=1/2663, X764=1/2667, X765=1/2669, X766=1/2673, X767=1/2677, X768=1/2679, X769=1/2683, X770=1/2687, X771=1/2689, X772=1/2693, X773=1/2697, X774=1/2699, X775=1/2703, X776=1/2707, X777=1/2709, X778=1/2713, X779=1/2717, X780=1/2719, X781=1/2723, X782=1/2727, X783=1/2731, X784=1/2733, X785=1/2737, X786=1/2741, X787=1/2743, X788=1/2747, X789=1/2749, X790=1/2753, X791=1/2757, X792=1/2759, X793=1/2763, X794=1/2767, X795=1/2769, X796=1/2773, X797=1/2777, X798=1/2779, X799=1/2783, X800=1/2787, X801=1/2789, X802=1/2793, X803=1/2797, X804=1/2799, X805=1/2803, X806=1/2807, X807=1/2809, X808=1/2813, X809=1/2817, X810=1/2819, X811=1/2823, X812=1/2827, X813=1/2831, X814=1/2833, X815=1/2837, X816=1/2841, X817=1/2843, X818=1/2847, X819=1/2849, X820=1/2853, X821=1/2857, X822=1/2859, X823=1/2863, X824=1/2867, X825=1/2869, X826=1/2873, X827=1/2877, X828=1/2879, X829=1/2883, X830=1/2887, X831=1/2889, X832=1/2893, X833=1/2897, X834=1/2899, X835=1/2903, X836=1/2907, X837=1/2909, X838=1/2913, X839=1/2917, X840=1/2919, X841=1/2923, X842=1/2927, X843=1/2931, X844=1/2933, X845=1/2937, X846=1/2941, X847=1/2943, X848=1/2947, X849=1/2949, X850=1/2953, X851=1/2957, X852=1/2959, X853=1/2963, X854=1/2967, X855=1/2969, X856=1/2973, X857=1/2977, X858=1/2979, X859=1/2983, X860=1/2987, X861=1/2989, X862=1/2993, X863=1/2997, X864=1/2999, X865=1/3003, X866=1/3007, X867=1/3009, X868=1/3013, X869=1/3017, X870=1/3019, X871=1/3023, X872=1/3027, X873=1/3031, X874=1/3033, X875=1/3037, X876=1/3041, X877=1/3043, X878=1/3047, X879=1/3049, X880=1/3053, X881=1/3057, X882=1/3059, X883=1/3063, X884=1/3067, X885=1/3069, X886=1/3073, X887=1/3077, X888=1/3079, X889=1/3083, X890=1/3087, X891=1/3089, X892=1/3093, X893=1/3097, X894=1/3099, X895=1/3103, X896=1/3107, X897=1/3109, X898=1/3113, X899=1/3117, X900=1/3119, X901=1/3123, X902=1/3127, X903=1/3131, X904=1/3133, X905=1/3137, X906=1/3141, X907=1/3143, X908=1/3147, X909=1/3149, X910=1/3153, X911=1/3157, X912=1/3159, X913=1/3163, X914=1/3167, X915=1/3169, X916=1/3173, X917=1/3177, X918=1/3179, X919=1/3183, X920=1/3187, X921=1/3189, X922=1/3193, X923=1/3197, X924=1/3199, X925=1/3203, X926=1/3207, X927=1/3209, X928=1/3213, X929=1/3217, X930=1/3219, X931=1/3223, X932=1/3227, X933=1/3231, X934=1/3233, X935=1/3237, X936=1/3241, X937=1/3243, X938=1/3247, X939=1/3249, X940=1/3253, X941=1/3257, X942=1/3259, X943=1/3263, X944=1/3267, X945=1/3269, X946=1/3273, X947=1/3277, X948=1/3279, X949=1/3283, X950=1/3287, X951=1/3289, X952=1/3293, X953=1/3297, X954=1/3299, X955=1/3303, X956=1/3307, X957=1/3309, X958=1/3313, X959=1/3317, X960=1/3319, X961=1/3323, X962=1/3327, X963=1/3331, X964=1/3333, X965=1/3337, X966=1/3341, X967=1/3343, X968=1/3347, X969=1/3349, X970=1/3353, X971=1/3357, X972=1/3359, X973=1/3363, X974=1/3367, X975=1/3369, X976=1/3373, X977=1/3377, X978=1/3379, X979=1/3383, X980=1/3387, X981=1/3389, X982=1/3393, X983=1/3397, X984=1/3399, X985=1/3403, X986=1/3407, X987=1/3409, X988=1/3413, X989=1/3417, X990=1/3419, X991=1/3423, X992=1/3427, X993=1/3431, X994=1/3433, X995=1/3437, X996=1/3441, X997=1/3443, X998=1/3447, X999=1/3449, X1000=1/3453, X1001=1/3457, X1002=1/3459, X1003=1/3463, X1004=1/3467, X1005=1/3469, X1006=1/3473, X1007=1/3477, X1008=1/3479, X1009=1/3483, X1010=1/3487, X1011=1/3489, X1012=1/3493, X1013=1/3497, X1014=1/3499, X1015=1/3503, X1016=1/3507, X1017=1/3509, X1018=1/3513, X1019=1/3517, X1020=1/3519, X1021=1/3523, X1022=1/3527, X1023=1/3531, X1024=1/3533, X1025=1/3537, X1026=1/3541, X1027=1/3543, X1028=1/3547, X1029=1/3549, X1030=1/3553, X1031=1/3557, X1032=1/3559, X1033=1/3563, X1034=1/3567, X1035=1/3569, X1036=1/3573, X1037=1/3577, X1038=1/3579, X1039=1/3583, X1040=1/3587, X1041=1/3589, X1042=1/3593, X1043=1/3597, X1044=1/3599, X1045=1/3603, X1046=1/3607, X1047=1/3609, X1048=1/3613, X1049=1/3617, X1050=1/3619, X1051=1/3623, X10
```

APPENDIX H
USER'S MANUAL FOR COMPUTER PROGRAM "LEVOPT"

The main function of computer program "LEVOPT" is for the optimal risk-based design of levee system. The program uses DP and DDDP techniques to compute optimal levee heights and encroachment widths for a levee system. The basic assumptions and constraints in this model are described in Chapter 5. The objective function is to minimize the total cost that depends on the different design philosophies adopted. The options for taking into account the analysis of hydraulic uncertainty and hydrologic uncertainty, assessment of reliability based on the static case or the time-dependent case, using method of jackknife or bootstrap for reducing hydrologic parameters uncertainty, and defining the composite hydrologic loading model are provided. The basic theories of those options are described in the text.

Subroutines REGION, XMNR, XSDR, and XSKR are used to compute the regional mean, standard deviation, and skewness and their respective variance corresponding to the regression equations developed in Chapter 3 for the Southwestern U.S. If other areas are studied, users have to substitute these subroutines and supply their own regression equations. In computing the cost of a project the land purchasing cost and construction cost are considered deterministic. The basic variables with uncertainty in computing the levee capacity are identified in Chapter 4. In the computer program the

field length of all input variables is 8, field 1 is columns 1-8, field 2 is columns 9-16, field 3 is columns 17-24, etc.

The arrangement of data cards are described as follows.

<u>Card Number</u>	<u>Variables</u>
A	ID, XID
B	XA, XSL, XST, XL, XI, NXX, XR
C	MODEL, METHOD, IRISK, NSEGMNT, LDIST, NSIZE, MBOOT, IOPT
D	ZSLPRVR, ZSLPLND, WDCRWN, FREBORD, UCLEVE
E	XLAM(I), XLAMTOL(I), LAMDIST(I), CXLAM(I); I=1, .. ., NSEGMNT
F	WDCH(I), WDCHTOL(I), WDCHDST(I), CWDCH(I); I=1, . . . , NSEGMNT
G	SCH(I), SCHTOL(I), SCHDIST(I), CSCH(I); I=1, . . . , NSEGMNT
H	NCH(I), NCHTOL(I), NCHDIST(I), CNCH(I); I=1, . . . , NSEGMNT
I	ACH(I), ACHTOL(I), ACHDIST(I), CACH(I); I=1, . . . , NSEGMNT
J	ANG(I), ANGTOL(I), ANGDIST(I), CACH(I); I=1, . . . , NSEGMNT
K	SBK(I), SBKTOL(I), SBKDIST(I), CSBK(I); I=1; . . . , NSEGMNT
L	NBK(I), NBKTOL(I), NBKDIST(I), CNBK(I); I=1, . . . , NSEGMNT
M	UCLND(I), XLEN(I); I=1, . . . , NSEGMNT
N	QFLOW(1), QFLOW(2), . . . , QFLOW(NSIZE)
O	TRET, SLIFE, RATEINT, TBASE, NPOIT
P	VOLUM(I), DAMAG(I), HD(I); I=1, . . . , NPOIT
Q	NWID, NHGT, ITMAX, NKAT, IPRINT
R	DELWD, DELHT, EPS, SHRINKF
S	PRIOPN, PRIOPLN, PRIOPET, PRIOPP, PRIOPLP

The A card is for station identification.

<u>Field</u>	<u>Variable</u>	<u>Value</u>	<u>Description</u>
1	ID	+	Stream gaging station number
2-6	XID		Alphabetical characters for the location of gaging station

The B card contains the physiographic and meteorologic characteristics of the river basin where the stream gaging station is located. A B card is not required if the variable METHOD=0 in the C card.

<u>Field</u>	<u>Variable</u>	<u>Value</u>	<u>Description</u>
1	<u>X</u> A	+	Contributing drainage area in sq. miles
2	XSL	+	Main channel slope (85 to 10 percent point), in feet per mile.
3	XST	+	Percentage of surface storage area, increased by 1 percent
4	XL	+	Total length of main channel in miles
5	XI	+	10-year, 24-hour rainfall intensity, in inches.
6	XNN	+	Mean annual number of thunderstorm day
7	XR	+	Ratio of runoff to precipitation during months when annual peak discharges occur, in in/in.

The C card is the job option card specifying various options in the program.

<u>Field</u>	<u>Variable</u>	<u>Value</u>	<u>Description</u>
1	MODEL	1 2	Static reliability model; Time-dependent reliability model
2	METHOD	0	Method used to compute the parameter estimates in hydrologic loading probability model Sample statistics only;

		1	Weighting procedure using jack-knife method and regression analysis;
		2	Weighting procedure using bootstrap method and regression analysis.
3	IRISK		Risk issue considered in optimization
		0	No risk;
		1	Hydrologic risk only;
		2	Include both hydrologic and hydraulic uncertainty.
4	NSEGMENT	+	Number of levee reaches considered in optimization
5	LDIST		Loading probability distribution of flood magnitudes
		1	Normal distribution;
		2	Log-normal distribution;
		3	Gumbel distribution;
		4	Pearson type III distribution;
		5	Log-Pearson type III distribution;
		6	Composite distribution of above five individual distributions.
6	NSIZE	+	Number of streamflow records
7	MBOOT	+	Number of bootstrap samples to be generated (required only when METHOD=2).
8	IOPT		Option for optimization technique used
		1	DP technique;
		2	DDDP technique

D cards contain information about the levee.

<u>Field</u>	<u>Variable</u>	<u>Value</u>	<u>Description</u>
1	ZSLPRVR	+	Side slope of that levee on the river face, in ft/ft
2	ZSLPLND	+	Side slope of the levee on the land face, in ft/ft.
3	WDCRWN	+	Crown width of the levee, in feet
4	FREBORD	+	Freeboard of the levee, in feet
5	UCLEVE	+	Construction cost of the levee, in \$/cu. yard of compaction.

The E cards contain the nominal value, tolerance (\pm something), types of distribution (simple distribution presented in Fig. 4.3, and the mode for the correction factor of the hydraulic model, λ_m , for each reach $i, i=1, \dots, NSEGMENT$. There are a total of NSEGMENT E cards that follow the D cards.

<u>Field</u>	<u>Variable</u>	<u>Value</u>	<u>Description</u>
1	XLAM(I)	+	Nominal value of λ_m for reach I
2	XLAMTOL(I)	+	Tolerance of λ_m for each I.
3	LAMDIST(I)		Types of distribution for λ_m for reach I
		1	Rectangular distribution, Fig. 4.3a
		2	Symmetric triangular distribution, Fig. 4.3b
		3	Triangular distribution with mode at w_u , Fig. 4.3c
		4	Triangular distribution with mode at w_l Fig. 4.3d

		5	Triangular distribution with mode w_c , Fig. 4.3e
4	CXLAM(I)	+	Mode of the distribution of λ_m for reach I (required only when LAMDIST(I)=5; otherwise, 0)

The F cards provide the nominal value, tolerance, type of distribution, Fig. 4.3, and mode of channel top width, B, for each reach I, $I=1, \dots, NSEGMNT$.

<u>Field</u>	<u>Variable</u>	<u>Value</u>	<u>Description</u>
1	WDCH(I)	+	Nominal value of B for reach I
2	WDCHTOL(I)	+	Tolerance of B for reach I
3	WDCHDST(I)	+	Type of simple distribution of B for reach I (integer-valued)
4	CWDH(I)	+	Mode of B for reach I

These are a total of NSEGMNT F cards that follow the E cards.

The G cards provide the nominal value, tolerance, type of distribution (Fig. 4.3) and mean of longitudinal channel bottom slope, S_o , for each reach I, $I=1, \dots, NSEGMNT$.

<u>Field</u>	<u>Variable</u>	<u>Value</u>	<u>Description</u>
1	SCH(I)	+	Nominal value of S_o for reach I
2	SCHTOL(I)	+	Tolerance of S_o for reach I
3	SCHDIST(I)	+	Type of distribution of S_o for reach I (integer-valued,
4	CSCH(I)	+	Mode of S_o for reach I

There are a total of NSEGMNT G cards that follow the F cards.

The H cards give the nominal value, tolerance, type of distribution, Fig. 4.3, and mode of channel surface roughness, N_c , for each reach I, $I=1, \dots, NSEGMNT$.

<u>Field</u>	<u>Variable</u>	<u>Value</u>	<u>Description</u>
1	NCH(I)	+	Nominal value of N_c for reach I (real-valued)
2	NCHTOL(I)	+	Tolerance of N_c for reach I (real-valued)
3	NCHDIST(I)	+	Type of distribution of N_c for reach I
4	CNCH(I)	+	Mode of N_c for reach I (real-valued)

There are a total of NSEGMNT H cards that follow the G cards.

The I cards provide the nominal value, tolerance, type of distribution, Fig. 4.3, and mode of the full bank flow cross sectional area of channel, A_{fb} , for each reach I, $I=1, \dots, NSEGMNT$.

<u>Field</u>	<u>Variable</u>	<u>Value</u>	<u>Description</u>
1	ACH(I)	+	Nominal value of A_{fb} for reach I.
2	ACHTOL(I)	+	Tolerance of A_{fb} for reach I.
3	ACHDIST(I)	+	Type of distribution of A_{fb} for reach I (integer-valued).
4	CACH(I)	+	Mode of A_{fb} for reach I.

There are a total of NSEGMNT I cards that follow H Cards.

The J cards provide the nominal value, tolerance, type of distribution (Fig. 4.3), and mode of transverse flood plain slope, τ , for each reach I, $I=1, \dots, NSEGMNT$.

<u>Field</u>	<u>Variable</u>	<u>Value</u>	<u>Description</u>
1	ANG(I)	+	Nominal value of τ for reach I.
2	ANGTOL(I)	+	Tolerance of τ for reach I.
3	ANGDIST(I)	+	Type of distribution of τ for reach I (integer-valued)
4	CANG(I)	+	Mode of τ for reach I.

There are a total of NSEGMNT J cards that follow the I cards.

The K cards provide the nominal value, tolerance, type of distribution (Fig. 4.3), and mode of the longitudinal flood plain slope, S_b , for each reach I, $I=1, \dots, N$ SEGMNT.

<u>Field</u>	<u>Variable</u>	<u>Value</u>	<u>Description</u>
1	SBK(I)	+	Nominal value of S_b for reach I
2	SBKTOL(I)	+	Tolerance of S_b for reach I.
3	SBKDIST(I)	+	Type of distribution of S_b for reach I (integer-valued)
4	CSBK(I)	+	Mode of S_b for reach I.

There are a total of NSEGMNT K cards that follow the J cards.

The L cards provide the nominal value, tolerance, type of distribution (Fig. 4.3), and mode of Manning's roughness for the flood plain, N_b , for each reach I, $I=1, \dots, N$ SEGMNT.

<u>Field</u>	<u>Variable</u>	<u>Value</u>	<u>Description</u>
1	NBK(I)	+	Nominal value of N_b for reach I (real-valued)
2	NBKTOL(I)	+	Tolerance of N_b for reach I (real-valued)
3	NBKDIST(I)	+	Type of distribution of N_b for reach I

4 CNBK(I) + Mode of N_b for reach I.

There are a total of NSEGMNT L cards that follow the K cards.

The M cards provide the unit land purchasing cost, C_{LND} , in \$/acre, and length of channel reach, L, in feet, for each reach I, $I=1, \dots, NSEGMNT$.

<u>Field</u>	<u>Variable</u>	<u>Value</u>	<u>Description</u>
1	QFLOW(1)	+	Flow magnitude of first record
2	QFLOW(2)	+	Flow magnitude of 2nd record
.	.	.	.
.	.	.	.
.	.	.	.
10	QFLOW(10)	+	Flow magnitude of 10th record.

Each M card contains ten flow records. Continue using additional cards until total length of record, NSIZE, are read.

The O cards have five variables.

<u>Field</u>	<u>Variable</u>	<u>Value</u>	<u>Description</u>
1	TRET	+	Design return period of flood flow, in years
2	SLIFE	+	Service life of the levee
3	RATEINT	+	Interest rate, in percent
4	TBASE	+	Time base of flood hydrograph, in hours
5	NPOIT	+	Number of points describing the damage-discharge relationship.

The P cards describe the damage-flood volume-stage relationship.

<u>Field</u>	<u>Variable</u>	<u>Value</u>	<u>Description</u>
1	VOLUM	+	Volume of water, in acre-feet
2	DAMAG	+	Flood damage cost, in dollars
3	HD	+	Stage height, in feet.

There are a total of NPOIT P cards that follow the O cards.

The Q cards and R cards provide information for the state space, etc. for DP and/or DDDP techniques. The Q cards have five variables.

<u>Field</u>	<u>Variable</u>	<u>Value</u>	<u>Description</u>
1	NWID	+	Number of lattice points for the encroachment width in state space
2	NHGT	+	Number of lattice points for levee height in state space
3	ITMAX	+	Maximum number of iterations in DDDP
4	NKAT	+	Maximum number of times the size of the state space is being reduced
5	IPRINT		Printing control for DDDP only
		0	Print final result
		1	Print result for an iteration only when the objective function is improved
		2	Print every iteration

The R card consists of four variables.

<u>Field</u>	<u>Variable</u>	<u>Value</u>	<u>Description</u>
1	DELWD	+	Incremental encroachment width in state space

2	DELHT	+	Incremental levee height in state space
3	EPS	+	Criterion for state space reduction
4	SHRINKF	+	Shrinking factor for state space, ($0 < \text{SHRINKF} < 1$)

The final card (S card) is required if a composite probability model is desired.

<u>Field</u>	<u>Variable</u>	<u>Value</u>	<u>Description</u>
1	PRIOPN	+	Prior probability for normal distribution
2	PRIOPLN	+	Prior probability for log normal distribution
3	PRIOPET	+	Prior probability for Gumbel distribution
4	PRIOPP	+	Prior probability for Pearson III distribution
5	PRIOPLP	+	Prior probability for log-Pearson III distribution

APPENDIX I

LISTING OF COMPUTER PROGRAM FOR
OPTIMAL RISK-BASED FLOOD LEVEE DESIGN

- "LEVOPT"


```

C 182 CONTINUE
C 183 RETURN
C 195 FORMAT(1H8,5X,SHADPCH,4X,WHIACH,5X,SHAMPCH,4X,SHAKCH,5X,SHAMPBK,
C 5X,SHAKONV,5X,SHADTOL,4X,THCOVDPEM,4X,SHCOVLCM,5X,THCOVMPCH,4X,
C 4X,SHCOVABK,5X,THCOVMPBK,5X,THCOVKNV,5X,THCOVATOL)
C 196 FORMAT(1X,7F10.2,1X,7F10.2)
C 197 FORMAT(1H8,3X,THAKONV,4F10.2,2X,9HCOVKNV,4F10.2)
C 198 FORMAT(1H8,2H4,13,5H 01,4F10.2,5H VUS,1F10.2,5H VO,1F10.2,
C 4H F82,1F10.2,5H 02,4F10.2,4H 8,5F10.2)
C 199 FORMAT(1H8,5X,SHQCH,4F10.2,3X,THCOVOC,4F10.2)
C 200 FORMAT(1H8,47H+2A AREADLP DOES NOT CONVERGE IN 50 ITERATIONS/
C 4X,THRATED,4E11.5,2X,SHQCM,4E11.4)
C 201 END
C 202 ***** COMPONT
C 203 COMPUTE THE MEAN AND C.O.V. OF LEVEE CAPACITY FOR
C 204 GIVEN HEIGHT OF LEVEE AND WIDTH BETWEEN THE EMBROCHMENT
C 205
C 206 SUBROUTINE COMPUTE(WIDTH,HEIGHT,TSLOPE,ADPCH,ADPCH,ADPCH,ALPHA,
C 207 COVACH,COVMPCH,COVABK,COVMPBK)
C 208 CL=WIDTH*HEIGHT/2.
C 209 C2=TSLOPE*HEIGHT
C 210
C 211 THE MEAN AND C.O.V. OF WATER DEPTH IN CHANNEL SECTION
C 212
C 213 ADPCH=HEIGHT+ALPHA*(CL+ADPCH)
C 214 COVACH=SOR((LADCH+ALPHA*COVACH)/2.)*2.9*(ALPHA*(CL+ADPCH)+2.)/
C 215 *(ADPCH+COVMPBK)*2.23/(ADPCH+ADPCH)
C 216
C 217 THE MEAN AND C.O.V. OF FLOW AREA IN CHANNEL SECTION
C 218
C 219 LACH=ADPCH*ADPCH
C 220 COVACH=SOR((LADCH+COVACH+COVMPCH)/2.)*2.9*(LADCH+COVMPCH)+2.)/
C 221 *(LACH+ADPCH)
C 222
C 223 THE MEAN AND C.O.V. OF FLOW AREA IN ONE SIDE OF BANK AREA
C 224
C 225 C2=(LADPCH+ADPCH*HEIGHT)/2.
C 226 LACH=C2*HEIGHT/2.4C=CL
C 227 COVACH=SOR((CL+2A*(LADPCH+COVMPCH)+2.)*2.9*(LADPCH+COVMPCH)
C 228 +2.1*(LADCH+COVMPCH)+2.)/2.4C*(LACH+LACH)
C 229
C 230 THE MEAN AND C.O.V. OF WETTED PERIMETER IN ONE SIDE
C 231 OF BANK AREA
C 232
C 233 C2=SOR((TSLOPE+TSLOPE)
C 234 C2=SOR((1.-ALPHA+ALPHA)
C 235 AMPH=HEIGHT+ES+CL/2
C 236 COVMPBK=SOR((LADCH+COVMPCH)/2.)*2.9*(LADPCH+ADPCH)+2.1*(LADCH+
C 237 COVMPCH)+2.1*(LADCH+COVMPCH)
C 238
C 239 RETURN
C 240 END
C 241 ***** OLEVEE
C 242
C 243 THIS SUBROUTINE COMPUTES THE MAGNITUDE OF DESIGN FLOOD FOR
C 244 THE LEVEE SYSTEM BASED ON THE LOADING DISTRIBUTION SPECIFIED.
C 245
C 246 INPUTS:
C 247 LOIST - DISTRIBUTION OF LOADING I (1) NORMAL, (2) LOG-NORMAL,
C 248 (3) GUMBEL, (4) PEARSON III, (5) LOG-PEARSON III, AND
C 249 (6) COMPOSITE
C 250 NY(1) - WEIGHTING FACTOR FOR THE LOADING DISTRIBUTION (ONLY
C 251 FOR LOIST=6)
C 252 TRET - RETURN PERIOD FOR DESIGN FLOOD
C 253
C 254 OUTPUT:
C 255 QLT - MAGNITUDE OF DESIGN FLOOD
C 256
C 257 REQUIRED SUBROUTINE I/OLOAD
C 258
C 259 SUBROUTINE OLEVEE(LOIST,MT,TRET,OLT)
C 260 DIMENSION MT(5)
C 261 COMMON/BLK G,YMN,YSD,YBK,YMNL,YBDL,YSKL,CONST,AMIN
C 262 IOIST=LOIST
C 263 IF(LOIST.NE.4) GO TO 134
C 264 ZOL=YMN
C 265 IOIST=6
C 266
C 267 133 IOIST=IOIST+1
C 268 KOIST=IOIST
C 269 IF(MT(KOIST).LT.0.801.AND.KOIST.LT.5) GO TO 133
C 270 IF(MT(KOIST).LT.0.801.AND.KOIST.EQ.5) GO
C 271 TO 518
C 272 134 IF(LOIST.EQ.2.OR.IOIST.EQ.5) GO TO 135
C 273 OLM=NY
C 274 OLSO=YSD
C 275 OLSK=YBK
C 276 GO TO 134
C 277
C 278 135 OLM=NYMN
C 279 OLSO=YSDI
C 280 OLSK=YSKI
C 281
C 282 134 CONTINUE
C 283 CALL OLOAD(IOIST,OLMH,OLSD,OLBK,CONST,FRET,OLT)
C 284
C 285 IF(OLT.NE.6) GO TO 520
C 286 MOLT=MT(KOIST)*OLT
C 287 ZOLT=ZOL+MOLT
C 288 OLT=ZOLT
C 289
C 290 520 CONTINUE
C 291 IF(KOIST.LT.5) GO TO 133
C 292
C 293 WRITE(6,25) LOIST,TRET,OLT
C 294 FORMATTING=10X,7HLDIST,13,2X,8HTRET,4F6.1,5X,4HOLT,4F10.2)
C 295 RETURN
C 296 END
C 297 ***** 3FTRK

```



```

108. FORMAT(2HINDIRECT METHOD OPT 1,3X,3HP=,E11.4,2X,3HP=,E11.4,2X,
3HP=,E11.4)
204. FORMAT(1H0,3X,2AHVALUE OF PRIOR PROBABILITY/2,4HNORMAL,7X,1BH00=
NORMAL,7X,THEXTREME,3X,THEPEARSON,6X,THELOGP=,E15,9)
206. FORMAT(1H0,3X,2AHVALUE OF LIKELIHOOD FUNCTION/2,4HNORMAL,7X,1BH00=
G-NORMAL,7X,THEXTREME,3X,THEPEARSON,6X,THELOGP=,E15,9)
208. FORMAT(1H0,3X,3AHVALUE OF POSTERIOR PROBABILITY/2,4HNORMAL,7X,1BH0
LOG-NORMAL,7X,THEXTREME,3X,THEPEARSON,6X,THELOGP=,E15,9)
212. RETURN
END
SUBROUTINE DAMAGE(LR1X,LO1I,MT,YMH,YSD,YRK,YMNL,YBOL,YBKL,
CONST,DCM,COVQC,COVCC+COVCC+I,1)
C
C THIS SUBROUTINE COMPUTES THE EXPECTED FLOOD
C DAMAGE COST FOR GIVEN SIZE OF STRUCTURE UNDER
C SPECIFIED LOADING CONDITION.
C
C DIMENSION TPT(20)
C DIMENSION VOLUM(15),DAMAG(15),HO(15)
C DIMENSION PHOB(20),OAH(20)
C DIMENSION MI(5)
C COMMON/ALC 1/MPOTT,VOLUM,DAMAG,HO
C
C EPI = SORT(2,-5,1015)
C EPI WRITE(7,3) YMH,YSD,YRK,YMNL,YBOL,YBKL
C
C 3. FORMAT(1H,4(2X,E11.4))
C
C *****
C QIT = PEAK DISCHARGE OF HYDROGRAPHS OF RETURN PERIOD T
C VOL = VOLUME OR STORAGE OF FLOODING IN ELUIC FEET
C DAMC = DAMAGE COST OF VOL
C OCH = MEAN OF QC
C QCLM = MEAN OF THE LOGS OF QC
C QCLSD = STANDARD DEVIATION OF LOGS OF QC
C QO3D = STANDARD DEVIATION OF QC
C COVQC = COEFFICIENT OF VARIATION OF QC
C
C COMPUTE STANDARD DEVIATION OF LOGS OF QC
C
C OCLSD = SORT(ALOG(COVQC+COVCC+I,1))
C
C COMPUTE MEAN OF LOGS OF QC
C
C OCLM = ALOG(OCH) - 0.5*OCLSD+OCLBO
C
C IDISTH0101
C IF(COIN1,NEC. 8) GO TO 134
C ZAREA=0.8
C IDISTH0101
C IDISTH0101+1
C 133. KOIST=IDISTH0101
C IF(COIN1,NEC. 8) GO TO 133
C IF(COIN1,NEC. 8) GO TO 133
C IF(COIN1,NEC. 8) GO TO 133
C *****

```

```

C
C COMPUTE THE LOGARITHMIC VALUE OF LIKELIHOOD
C
C 00 231. I=1,N
C IF(LG .EQ. 1) GO TO 225
C C1=AE*(Z08A1)-BE
C XIP=XTRM-EI-EXPI-EI1
C 225. SNO=7083(1)-ZNN
C XOML=XOML+8NOASNO
C IF(LG .EQ. 1) YNL=XNL-Z08B(1)
C PNI=Z08B(1)+G
C PSHPSU=PNI/AP;BP(1)=LOG(PNI)
C IF(PNT .EQ. 1 AND LG .EQ. 1) WRITE(6,187) XOML,PON
C IF(PNT .EQ. 1 AND LG .EQ. 8) WRITE(6,184) XOML,PEN,XTRM
C 231. CONTINUE
C IF(LG .EQ. 1) GO TO 242
C XLMNL=XOML/12.47SD+ZSD1+INI+ZNL
C XLPNS=PNS+TPI
C GO TO 278
C 242. XLLNML=XOML/12.47SD+ZSD1+INI+ZNL
C XLLPNS=PNS+TPI
C 278. CONTINUE
C L=ALD41
C IF(LG .EQ. 1) GO TO 199
C IF(LG .EQ. 1) GO TO 199
C PRINT 212,XLMNL,XLLNML,XLXTRM,XLPEN,XLLPEN
C
C RESCALING OF LIKELIHOOD
C
C BASE=ABS(XLMNL)
C XLMNL=XLMNL/BASE
C XLLNML=XLLNML/BASE
C XLXTRM=XLXTRM/BASE
C XLPEN=XLPEN/BASE
C XLLPNS=XLLPNS/BASE
C XPN=EXP(XLMNL)*PRIOPN
C XPLN=EXP(XLLNML)*PRIOPLN
C XPT=EXP(XLXTRM)*PRIOPET
C XPP=EXP(XLPEN)*PRIOPP
C XPLP=EXP(XLLPNS)*PRIOPLP
C SUML=EXP(XPLN)+EXP(XPP)+XPLP
C
C COMPUTE THE POSTERIOR PROBABILITY
C
C PSTPN=EXPN/SUML
C PSTPLN=EXPLN/SUML
C PSTPT=EXPT/SUML
C PSTPP=EXPP/SUML
C PSTPLP=EXPLP/SUML
C PRINT 206
C PRINT 212,PRIOPN,PRIOPLN,PRIOPET,PRIOPP,PRIOPLP
C PRINT 209
C PRINT 212. PSTPN,PSTPLN,PSTPT,PSTPP,PSTPLP
C 101. FORMAT(1H0,22HPLOM OF ORIGINAL SCALE/1X,6HMETHOD,14,5X,5HYMH 2,
2,11.4,3X,SHYSD =,E11.4,3X,SHVSK =,E11.4/1X,SHINI =,E11.4,3X,SHI2
=,E11.4)
C 102. FORMAT(1H0,20HPLOG-TRANSFORMED FLOM/1X,6HMETHOD,14,5X,5HYMH =,E11.4,3X
=,SHYSD =,E11.4,3X,SHVSK =,E11.4/1X,SHINI =,E11.4,3X,SHI2 =,E11.4)
C 103. FORMAT(1H0,24HPLOM OF ORIGINAL SCALE/1X,6HMETHOD,14,5X,5HYMH 2,
2,11.4,3X,SHYSD =,E11.4,3X,SHVSK =,E11.4,3X,SHI1 =,E11.4)
C 104. FORMAT(1H0,24HPLOM OF ORIGINAL SCALE/1X,6HMETHOD,14,5X,5HYMH 2,
2,11.4,3X,SHYSD =,E11.4,3X,SHVSK =,E11.4,3X,SHI2 =,E11.4)
C 105. FORMAT(1H0,24HPLOM OF ORIGINAL SCALE/1X,6HMETHOD,14,5X,5HYMH 2,
2,11.4,3X,SHYSD =,E11.4,3X,SHVSK =,E11.4,3X,SHI1 =,E11.4)
C 106. FORMAT(1H0,24HPLOM OF ORIGINAL SCALE/1X,6HMETHOD,14,5X,5HYMH 2,
2,11.4,3X,SHYSD =,E11.4,3X,SHVSK =,E11.4,3X,SHI2 =,E11.4)

```



```

IF(MODEL, EQ, 1) GO TO 570
ASK1 = RELI
REL = EXP(-ALTFEABK/TRET)
570 CONTINUE
RETURN
----- COF
C THIS SUBROUTINE INTEGRATES THE PROBABILITY FUNCTION
C INPUTS I
C LDIST = PROBABILITY DENSITY FUNCTION I (NORMAL), (2) LOG-
C NORMAL, (3) GUMMEL, (4) PEARSON TYPE III, OR (5) LOG-
C OX ARGUMENT TO WHICH IS TO BE INTEGRATED
C OLN = THE MEAN OF THE PROBABILITY FUNCTION
C QLD = THE STANDARD DEVIATION
C QLSK = THE SKEW COEFFICIENT
C OUTPUT I
C CUMPROB = CUMULATIVE PROBABILITY
C REQUIRED SUBROUTINES = NORMAN, ALGAMA
C SUBROUTINE COF(LDST, OX, OLN, QLD, QLSK, XMIN, CUMPROB)
IF(LDST, EQ, 1) GO TO 200
IF(LDST, EQ, 3) GO TO 200
IF(LDST, EQ, 4) GO TO 300
IF(LDST, EQ, 5) GO TO 300
C COMPUTE C.O.F. OF NORMAL OR LOG-NORMAL DISTRIBUTION
IF(LDST, EQ, 2) OX = LOG(OX)
Z = (OX - OLN) / QLD
IF(Z, EQ, 0) CUMPROB = 0.5
IF(Z, EQ, 0) GO TO 500
TERML = 1. / SQRT(1. - 1.1547 * Z)
DELZ = Z / 20
CUMPROB = 0
DO 100 JI = 1, 21
QZ = DELZ
QZ = QZ * DELZ
TERML = EXP(-0.5 * QZ * QZ)
TERML = TERML * (1 + 0.1423 * QZ)
IF(JI, EQ, 1) OR JI, EQ, 21) TERML = TERML * Z
CUMPROB = CUMPROB + TERML
100 CONTINUE
IF(Z, LT, 0) CUMPROB = 0.5 - CUMPROB
IF(Z, GT, 0) CUMPROB = 0.5 + CUMPROB
IF(LDST, EQ, 2) OX = EXP(OX)
GO TO 500
C COMPUTE C.O.F. OF GUMMEL DISTRIBUTION
200 ALPHA1 = 203 / QLSK
RETS = QLN - 0.5772 / ALPHA
CUMPROB = EXP(-EXP(-ALPHA * (RETS - OLN)))
GO TO 500
C COMPUTE C.O.F. OF PEARSON TYPE III AND LOG-PEARSON TYPE III
C DISTRIBUTION
300 IF(LDST, EQ, 5) OX = LOG(OX)

```

```

VMIN = XMIN
PARM2 = (Z - QLSK) * (Z - QLSK)
PARM3 = QLSK / SQRT(PARM2)
PARM4 = OLN - OLSK + SQRT(PARM2)
IF(LDST, EQ, 5) VMIN = ALG(YMIN)
IF(PARM3, GT, VMIN) PARM3 = 0.
VMAX = VMIN
IF(IX, LT, PARM3) GO TO 555
OX = (OX - PARM3) / PARM1
CALL MDGHT(DXM, PARM2, CUMPROP, IER)
IF(LDST, EQ, 5) OX = EXP(OX)
GO TO 500
555 CUMPROP = 0
560 CONTINUE
RETURN
END
SUBROUTINE STATIS(MI, XI, X2, X3, X4, X5, Y1, Y2, Y3, Y4, Y5, Z1, Z2, Z3, Z4,
Z5, C1, C2, C3, C4, C5, COV12, COV13, COV14, COV15, COV23, COV24,
COV25, Z1, Z2, Z3, Z4, Z5, Z12, Z13, Z14,
DIMENSION X(1:5), Y(1:5), Z(1:5), C(1:5), YH(1:5), XCOV(1:5))
X(1) = X1
X(2) = X2
X(3) = X3
X(4) = X4
X(5) = X5
Y(1) = Y1
Y(2) = Y2
Y(3) = Y3
Y(4) = Y4
Y(5) = Y5
Z(1) = Z1
Z(2) = Z2
Z(3) = Z3
Z(4) = Z4
Z(5) = Z5
C(1) = C1
C(2) = C2
C(3) = C3
C(4) = C4
C(5) = C5
DO 11 I = 1, 5
XA = X(I) - Y(I)
XB = X(I) + Y(I)
XC = C(I)
ZD = Z(I)
IF(XA, EQ, 0) .AND. XB, EQ, 0) .AND. XC, EQ, 0) .AND. ZD, EQ,
0) GO TO 10
C COMPUTE THE MEAN AND C.O.V. OF PARAMETER CONSIDERED.
CALL DISTR(XA, XB, XC, ZD, XH, COV)
YH(I) = XH
XCOV(I) = COV

```



```

Y2=V1*Y1
V1=V2*P1
V3D=(Y-X*AD1)/AD01
T2=EXP(-Y*AO*AD0/2.)
INFATV1=I2
IF(I .EQ. 1 .OR. I .EQ. 51) TMR=TH2/Z2.
15 CONTINUE
X3D=1./X3D1-2500.
X3D2=V2*20L
V3D=X3D2-X3D*X3D
28 CONTINUE
RETURN
END
----- XSKA
C
C COMPUTE THE MEAN AND VARIANCE OF REGIONAL SKEWNESS
C
SUBROUTINE XSKV(XSK1,XSK1/LG,XSK,VSK)
  I=LG / GO, I GO, I+1
  V3=V3+XSK1*(XSK1/LG)
  XSK=EXP(XSK1/LG)
  V4=XSK*(XSK*(EXP(V3*2.)-1.))
  GO TO 12
11 XSK=XSK+V4
12 CONTINUE
RETURN
END
----- BOO1
C
C APPLY BOOTSTRAP METHOD DERIVING STANDARD DEVIATION FOR THE
C SAMPLE STATISTICS
C
SUBROUTINE BOO1(N,ISD,ISET,ORG,SEEM,ASED,SESK)
  DIMENSION ORG(100),XSK(100),XNN(100),XSD(100)
  IS=B
  ISEEN=1870
203 IS=IS+1
  IF(IS .GT. ISEY) GO TO 205
  C
  C GENERATE N PSEUDO RANDOM NUMBERS BETWEEN (P,1)
  C
  CALL GCRUTSEED,N,RANDOM1
  C
  C COMPUTE THE STATISTICS FOR BOOTSTRAP SIMPLE
  C
  DO 204 I=1,N
    RANERANDRM(I),N
    XANN=I
    ROBJIT=ORSEK
204 CONTINUE
    XANN(I)=XANN(N,ROBS,B)
    XSKANN(I)=XANN(N,XMEAN,B)
    XSDANN(I)=XANN(N,XMEAN,B)
    XSD1=XSD(I)+XSD(N)-XSD(I)
    XSK1=XSK(I)+XSK(N)-XSK(I)
  END

```

```

285 CONTINUE
  AVGMN=MEAN(1SET,XNN,B)
  AVGSD=SDRT(1SEV(1SET,XNN,AVGMN,B))
  AVGXSD=MEAN(1SET,XSD,B)
  ROZSD=SDRT(1SEV(1SET,XSD,AVGXSD,B))
  AVGSK=MEAN(1SET,XSK,B)
  ROZSK=SDRT(1SEV(1SET,XSK,AVGSK,B))
  RETURN
END
----- JACK
C
C APPLY JACKKNIFE METHOD ESTIMATING
C THE ACCURACY OF SIMPLE STATISTICS
C
SUBROUTINE JACK(MSIZE,ORG,VHEANJ,VSD1,XSKJ1,VHEANJ,XSD1,XSKJ1)
  DIMENSION ORG(100),XSK(100),XNN(100),XSD(100)
C
C COMPUTE THE SAMPLE STATISTICS WITH THE K-TH OBSERVATION
C DELETED.
C
  XMSIZE=MSIZE
  DO 32 K=1,MSIZE
    XNN(K)=MEAN(MSIZE,ORG,K)
    SK=XNN(K)
    XVR=VAR(MSIZE,ORG,BH,K)
    XSD(K)=SDRT(EVA)
    XSK(K)=XSK(MSIZE,ORG,K)
  32 CONTINUE
  XHEANJ=MEAN(MSIZE,ORG,BH,XSD1,K)
  XSDJ=SD
  XSKKJ=XSK
  C
  C WITH RIAS CORRECTION,
  C
  XHEANKB=
  XSDKB=
  XSKKB=XSK
  DO 35 K=1,MSIZE
    XHEANB=XHEAN(XSKKB,K)
    XSDKB=XSD(K)-XSD(K)
    XSKKB=XSK(XSKKB,K)
  35 CONTINUE
  XHEANJ=XHEAN(XSKKJ,XMSIZE)
  XSDJ=XSD(XSDJ,XMSIZE)
  XSKJ=XSK(XSKKJ,XMSIZE)
  DO 36 K=1,MSIZE
    XHEANJ=XHEAN(XSKJ,XMSIZE)
    XSD1=XSD(1)+XSD(K)-XSD1
    XSK1=XSK(1)+XSK(K)-XSK1
  36 CONTINUE
  C
  C COMPUTE THE VARIANCE AND STAN. DEV. OF SIMPLE STATISTICS
  C
  CONST=(XMSIZE-1.)/XMSIZE
  VHEANJ=CONST*XHEANJ
  VSDJ=CONST*XSDJ
  VSKJ=CONST*XSKKJ
  RETURN
END

```